Identifying novel drug therapies for acute myeloid leukaemia by targeting the interactions between leukaemia cells and bone marrow microenvironment

A thesis submitted to the National University of Ireland in fulfilment of the requirement for the degree of

Doctor of Philosophy

by

Sukhraj Pal Singh Dhami

Apoptosis Research Centre, Department of Biochemistry

School of Natural Sciences,

National University of Ireland, Galway

PhD supervisor: Dr Eva Szegezdi

September 2019

Table of Contents

Declaration

This thesis comprises of two published articles and two unpublished manuscripts. My specific contribution to each chapter has been explicitly mentioned in the preamble of respective chapters.

I certify that the thesis is all my work and I have not obtained a degree in this university or elsewhere, on the basis of this work.

Sukhraj Pal Singh Dhami

Galway, September 2019

Acknowledgements

Undertaking this research work has been a learning, challenging and rewarding experience. However, the journey embarked upon would not have been complete without the care and support of the people who have been an integral part of this journey.

Firstly, I am sincerely grateful to my supervisor Dr Eva Szegezdi for providing me the opportunity to pursue PhD in her lab. I have achieved invaluable experience working in her lab and she has provided me great opportunities for my career advancement. I sincerely thank her for consistently supporting me, guiding me and encouraging me to bring out the best in me.

Secondly, I would like to thank my graduate research committee (GRC) members for all the advice and support during this tenure.

I would like to acknowledge College of Science, NUI, Galway for awarding me College of Science scholarship (2014-2018) to carry out my PhD. Additionally, I am grateful to Thomas Crawford Hayes research awards (2015 & 2017) for supporting my research work.

My sincere thanks to all the co-authors, collaborators and participants of the studies who took out time from their busy schedules to make this research possible.

My heartfelt thanks to all the lab members past and present, Dr Denis Baev, Dr Mairead Reidy, Dr Sharon S. Kappala, Dr Delphine O'hayon, Eimear O'Reilly, Hojjat Alizadeh Zeinabad, Margaret Twohig, Tatiana Cichoka, Pramath Kakodkar, Andrea Tirincsi, Sanket More, Mark Watters, Sachin Chauhan, Cian Darcy, Rafael Saraiva, Caoimhe Nolan and Cait Simpson for creating a friendly and learning environment in the lab. I really enjoyed being part of this group. Also, big thanks to everyone from Prof. Afshin Samali and Dr Adriene Gorman's group for helping me with lab resources from time to time. I also appreciate the support of members of Apoptosis Research Centre (ARC) for their valuable suggestions and discussions during department seminars and presentations. I am thankful to the members of NCBES core facilities, Dr Shirley Hanley and Dr Enda O'Connell for providing training and access to equipment's.

A special mention to PD Dr Philippe Krebs, Regula Stuber Roos, Coline Nydegger, Kristyna Hlavackova, Lester Thoo, Vivian Vu, Jeremy Yeoh and Patrick van Delden at Institute of Pathology, University of Bern, Switzerland. It was an excellent opportunity to work along these wonderful people and using their facilities. What an amazing place to work!

Big thanks to Dr Shashank Sharma and Dr Satbir Gill for introducing me to NUI Galway, Ireland and helping me whenever the need arises. I am also very thankful to my friend Dr Shivakumar Basavaraju for being there for me through the thick and thins of this journey. A big thanks to my friends in Galway- Dr Abhigyan Satyam, Dr Rajesh Sharma, Dr Arindam Haldar, Malancha Karmarkar, Yashpal Rawat, Dr Vijay K. Kannala, Vaishali, Vaibhav, Dr Vijay Kumar, Heena, Sravanthi, Sam Batra, Ashish Gumber, Dr Subashish Sarkar and Mango – for

the fun-filled parties, dinners, festival celebrations and making sure I feel at home! There is a long list of friends to mention, both in and out of the lab, who kindly helped me and supported me throughout this journey but I could not name them all, Thank you!

A big thanks to my Mom, Dad, brother and my extended family members without them this endeavour would not have been possible. Thank you for all your love and support during this journey. Thank you for always being there for me!

Finally, and most importantly, I would like to thank my wife Navneet for supporting me in every step of the way and for always being so positive. Thanks for being a good listener, planner and for providing an endless supply of love and support. You helped me enjoy this phase of my life!

-Sukhraj Dhami

Abstract

Acute myeloid leukaemia (AML) is a malignancy caused by a block in differentiation in which aberrant leukemic stem cells drive the production of undifferentiated or partially differentiated leukemic blast cell clones. Between 10-40% of patients, however, have refractory disease or undergo relapse. The impact of the bone marrow microenvironment (BMM) is increasingly recognised as a reason for this. Hence, this thesis is aimed at understanding the interactions between leukemic cells and the BMM and to devise a therapeutic strategy to target these interactions. We have developed a functional, drug testing system that can incorporate the impact of BMM while rapidly and faithfully predicting the clinical response of the patient to cytarabine+daunorubicin (AraC+Dnr) therapy. We have developed and characterised a layered co-culture system consisting of primary AML blasts with immortalised bone marrow stromal cells (BMSCs). This BMSC-AML co-culture can predict the clinical response of AraC+Dnr therapy with very high accuracy [area under the curve (AUC=0.94)]. The advantage of this model over more complex pre-clinical AML models is its suitability to be developed into a laboratory diagnostic tool, which could greatly advance the clinical decision on treatment choice. Having established the model that mimics the BMM, we have studied its role in protecting the AML cells against cytotoxic agents such as BH_3-mimetics, cytarabine and daunorubicin. We found that BMSCs induce Mcl-1 expression over Bcl-2 and/or Bcl-X_L in AML cells and that inhibition of Mcl-1 with a small-molecule inhibitor, A1210477, or through repression of its expression with the cell division cycle-7 kinase/ cyclin dependent kinase 9 (CDC7/CDK9) dual-inhibitor, PHA-767491, restores sensitivity to chemotherapeutics. Importantly, the $CD34^+/CD38^-$ leukemic stem cell-encompassing population was equally sensitive to this combination. These results highlight the potential of Mcl-1-repression to revert BMM-mediated drug resistance thus preventing disease relapse and ultimately improving patient survival. Next, we investigated the mechanism through which the BMM protects the FLT3-ITD mutated AML cells against tyrosine kinase inhibitors (TKIs). We found that FLT3-ITD cells do not depend on intrinsic, FLT3-driven survival signalling pathways in BMM. We also observed that exposure of BMSCs to a mild, proteostatic stress revert its ability to protect AML cells against chemotherapeutics. Importantly, we also found that proteostatic stress-conditioned BMSCs themselves trigger an anti-leukemic effect, which is mediated through secreted lipids or non-protein moieties. In summary, the results presented in this thesis illustrate the role of microenvironment interactions in providing chemoresistance to malignantly transformed cells. We have also presented strategies to target these interactions for effective and novel therapies that could improve patient outcome.

List of Figures

List of Tables

List of Supplementary Figures

List of Supplementary Tables

List of Abbreviations

2-HG	2-hydroxyglutarate
3D	3-dimension
4-HNE	4-hyroxynonenal
5-BPSA	3-bromo-5-phenylsalicyclic acid
α-KG	alpha-ketoglutarate
AKR1C	Aldo-keto reductase family C
AKRs	Aldo-keto reductases
ALL	Acute lymphoblastic leukemia
AML	Acute myeloid leukemia
AML-1	Acute myeloid leukemia 1 protein
APC	Allophycocyanine
AraC	Cytarabine
ATCC	American type culture collection
ATP	Adenosine triphosphate
AUC	Area under the curve
BAD	Bcl-2 associated agonist of death domain
BCBI	Blood cancer biobank ireland
Bcl-2	B-cell lymphoma 2
BCR-ABL1	Breakpoint cluster region-abelson murine leukemia viral oncogene homolog 1
BET	Bromodomain and extraterminal
BH3	Bcl-2 homology domains
BM	Bone marrow
BMM	Bone marrow microenvironment
BMP	Bone morphogenic protein
BMP2	Bone morphogenetic protein 2
BMP4	Bone morphogenetic protein 4
BMSC	Bone marrow stromal cells
BRD4	BET protein 4
BSA	Bovine serum albumin
CAR-T cells	Chimeric antigen receptor-T cells
CBF	Core binding factor
CCL5	C-C motif chemokine ligand 5
CDC7	Cell division cycle 7
CDK9	Cyclin-dependent kinase 9
CEBPA	CCAAT/enhancer-binding protein alpha
CFC	Colony forming cells
cFLIP	FLICE-like inhibitory protein
CFSE	5-(and 6)-Carboxyfluorescein diacetate succinimidyl ester)
CI	Combination index
CLL	Chronic lymphocytic leukemia
CLP	Common lymphoid progenitors
CM	Conditioned medium
CMP	Common myeloid progenitors
CR	Complete remission
CRISPR	Clustered regularly interspaced short palindromic repeats
CRL	Cullin-RING ligases
CXCL10	C-X-C motif chemokine ligand 10
CXCL12	C-X-C motif chemokine ligand 12
CYP3A	cytochrome P450 A4
DAPI	4,6-diamidino-2-phenylindole dihydrochloride
DFS	Disease free survival
DNA	Deoxyribose nucleic acid
DNMT	DNA methyltransferase
DNMT3A	DNA methyltransferase 3A
Dnr	Daunorubicin
DOT1L	Disruptor of telomeric silencing 1-like
DR	Death receptors
eBM	engineered Bone Marrow
EC	Endothelial cells
ECM	Extracellular matrix
EFS	Event free survival

ELN	European LeukemiaNet
EMC	ER membrane protein complex subunit
EPO	Erythropoetin
ER	Endoplasmic reticulum
ERG	ETS-related gene
Erk	Extracellular-signal-regulated kinase
ETS	Erythroblast transformation-specific
EWS	Ewing's sarcoma
FAB	French-American-British
FACS	Flourescence activated cell sorting
FBS	Fetal bovine serum
FCS	Fetal calf serum
FDA	Food and Drug Administration
FDR	False discovery rate
FGF-1	Fibroblast growth factor-1
FGF2	Fibroblast growth factor 2
FISH	Flourescence insitu hybridisation
FITC	Fluorescein isothiocyanate
FL	FLT3 ligand
FLT3	Fms like tyrosine kinase 3
FLT3-L	Fms-like tyrosine kinase 3 ligand
FMS	Feline McDonough Sarcoma
Fn	Fibronectin
FSC	Forward scatter
GATA-1	GATA-binding factor 1
G-CSF	Granulocyte colony stimulating factor
G-CSF	Granulocyte-colony stimulating factor
GDF15	Growth differentiation factor 15
GEMM	Genetically engineered mouse models
GFP	Green flourescent protein
GM-CSF	Granulocyte-macrophage colony stimulating factor
GO	Gemtuzumab ozogamicin
GPI	Glucose-6-phosphate isomerase
HA	Hyaluronic acid
HDAC	Histone deacetylase
HD-pBMSC	Healthy donor derived bone marrow stromal cell
HI-FBS	Heat-inactivated fetal bovine serum
HMA	Hypomethylating agents
Hox	Homeobox genes
HOXA9	Homeobox A9
HSC	Haematopoietic stem cell
HSCT	Haematopoietic stem cell transplant
hTERT	Human telomerase
HUVEC	Human umbilical vein endothelial cells
IDH	Isocitrate dehydrogenase
IGFBP2	Insulin-like growth factor binding protein-2
IgG	Immunoglobulin G
IL-1	Interleukin-1
IL-11	Interleukin-11
IL-1β	interleukin 1β
IL-3	Interleukin-3
IL-6	Interleukin-6
IL-8	Interleukin-8
iMSC	Immortalised healthy donor primary bone marrow stromal cells
IPA	Ingenuity pathway analysis
ITD	Internal tandem duplication
Jag-1	Jagged-1
Jag-2	Jagged-2
KRAS	Kirsten rat sarcoma viral oncogene homolog
LEPR+	Leptin receptor expressing
LSCs	Leukemic stem cells
LTC	Long term culture
LTC-IC	Long term culture initialing cell
LT-HSC	Long term- haematopoietic stem cell

MAPK	Mitogen activated protein kinase
MDS	Myelodysplastic syndromes
MFI	Mean fluorescence intensity
MK	Megakaryocytes
MLL	Mixed lineage leukemia
MM	Multiple myeloma
MNC	Mononuclear cell
MPA	Medroxyprogesterone
MPN	Myeloproliferative neoplasm
MRD	Minimal residual disease
mRNA	Messenger RNA
MSC	Mesenchymal stromal cells
MuLV	Murine leukemia viruses
NAC	N-acetyl cysteine
NAE	Nedd-8 activating enzyme
Nes+	Nestin-expressing
nGEMMs	Non-germline genetically engineered mouse models
NGS	Next generation sequencing
NK	Normal karyotype
NOD/SCID	Non-obese diabetic mice with severe combined immunodeficiency
NPM1	Nucleophosmin-1
NPMc+ AML	AML bearing cytoplasmic nucleophosmin
NRAS	Neuroblastoma RAS viral oncogene homolog
NSG	NOD SCIDγ mouse
OB	Osteoblasts
OC	Osteoclasts
ORR	Overall response rate
OS	Overall survival
PB	Peripheral blood
pBMSC	Primary human bone marrow mesenchymal stromal cell
PBS	Phosphate buffer saline
PDGFRβ	Platelet derived growth factor receptor beta
PDMS	Polydimethylsiloxane
PE	Phycoerythrin
PEG	Polyethylene glycol
PET	Polyethylene terephythlate
PFA	Paraformaldehyde
PGA	Poly (glycolic acid)
PGE2	Prostaglanin E2
PGJ2	Prostaglanin J2
PI	Propidium iodide
PI3K	Phosphoinositide 3-kinase
PLGA	Poly (L-lactic-glycolic acid)
PLLA	Poly (L-lactic acid)
PML-RARα	Promyelocytic leukemia- retinoic acid receptor alpha
PMMA	Poly (methyl-methacrylate)
PPARγ	Peroxisome proliferator-activated receptor gamma
PR	Partial response
PSMB2	Proteasome subunit beta 2
PTEFb	Positive transcription elongation factor b
PU	Polyurethane
PU.1	Spi-1 proto-oncogene
PVF	Polyvinyl formaldehyde
qRT-PCR	Quantitative real time polymerase chain reaction
Qtb	Quizartinib
RFP	Red flourescent protein
RFS	Relapse free survival
RNA	Ribonucleic acid
ROC	Receiver operating characteristics
ROS	Reactive oxygen species
rpm	Revolutions per minute
RT	Room temperature
RTK	Receptor tyrosine kinase
RUNX1	Runt-related transcription factor 1

s.e.m.	Standard error mean
sAML	Secondary acute myeloid leukemia
SC	Schwann cells
SCF	Stem cell factor
SCGF	Stem cell growth factor
SDF1α	Stromal derived factor 1α
Sfb	Sorafenib
sgRNA	Small guide RNA
siRNA	Small interfering RNA
SN	Sympathetic neurons
SOCS	Supressor of cytokine signaling
SPR	Surface plasmon resonance
SSC	Side scatter
STAT	Signal transducer and activator of transcription
tAML	Therapy-related acute myeloid leukemia
TET2	Tet methylcytosine dioxygenase 2
TGFβ	Transforming growth factor beta
TKD	Tyrosine kinase domain
TKI	Tyrosine kinase inhibitor
TMRE	Tetramethylrhodamine ethyl ester perchlorate
TNF	Tumour necrosis factor
TPO	Thrombopoietin
TRAIL	Tumour necrosis factor-related apoptosis-inducing ligand
TRITC	Tetramethylrhodamine
UC	Umbilical cord
USFDA	United states food and drug administration
VCAM-1	Vascular cell adhesion molecule-1
VEGF	Vascular endothelial growth factor
WHO	World health organisation
WT	Wild type

CHAPTER 1: *Introduction*

Preamble to Chapter 1: Statement of Contribution

This chapter includes the background and relevant literature review of the thesis topic. Part of this chapter (section 1.10)-has been published in Drug Discovery Today (Dhami et al, 2016). I have written the manuscript and generated tables and figures. There is also a contribution of other co-authors in writing and editing of this manuscript.

Three-dimensional ex vivo co-culture models of the leukemic bone marrow niche for functional drug testing

Sukhraj Pal S. Dhami[1], Shanthi S. Kappala[1], Alexander Thompson[2] and Eva Szegezdi[1]

[1]Apoptosis Research Centre, School of Natural Sciences, National University of Ireland, Galway, Ireland

[2]Centre for Cancer Research and Cell Biology, Queen's University, Belfast, United Kingdom

Drug Discovery Today, 2016 Sep;21(9):1464-1471.

1.1 Overview of Leukaemia

Leukaemia (from Greek word *leukos*- white, and *haima*- blood) is widely known as cancer of blood-forming cells, usually white blood cells in the bone marrow. In leukaemia, there is a block in the differentiation of early progenitor cells leading to an accumulation of abnormal and undifferentiated cells [1]. Bone marrow (BM) is a thick, spongy tissue present inside the bones; it is also the place where haematopoiesis occurs [2]. In 1845, Rudolf Virchow was the first to describe white blood cells in blood cancer and called the disease "*leukemiahe*".

There are four types of leukaemia depending on the type of cells involved: acute lymphoblastic leukaemia (ALL), acute myeloid leukaemia (AML), chronic lymphocytic leukaemia (CLL) and chronic myeloid leukaemia (CML). Lymphocytic or lymphoblastic leukaemia can occur when lymphoid stem cells are involved and leads to accumulation of B-cells or T-cells and myeloid leukaemia occurs when myeloid stem cells are involved. Leukaemia can be further sub-classified into two categories: acute leukaemia when the disease progresses aggressively and chronic leukaemia when the disease progresses slowly. However, the genetic aberrations, disease progression and therapies used for treatment of leukaemia is different for each type.

Haematopoiesis is a process of formation of blood cells, which occurs in the bone marrow. It is a hierarchical and steady state process of production of nearly $10x10^8$ cells/day. Pluripotent hematopoietic stem cells (HSCs) give rise to all the lineages of blood cells. They possess the self-renewal ability and can differentiate into multiple hematopoietic lineages throughout life [3,4]. HSCs can differentiate into two progenitor cells- common lymphoid progenitors (CLPs) or common myeloid progenitors (CMPs). CLPs can differentiate further into pro-B, pro-T, pro-NK and dendritic cells, which can then give rise to mature T-cells, B-cells and natural killer (NK) cells. CMPs can differentiate into granulocyte-macrophage progenitors (GMPs) or megakaryocytes-erythrocytes progenitors (MEPs). GMPs give rise to granulocytes, macrophages and dendritic cells whereas MEPs give rise to mature erythroid lineage forming red blood cells (RBCs), and platelets (Figure 1.1).

1.2 Acute myeloid leukaemia

Acute myeloid leukaemia (AML) is characterised as an aggressive form of cancer consisting of partially or undifferentiated myeloid progenitor cells [5,6]. To date many different aberrations have been described in AML [7]. Therapy related AML or AML arising from myelodysplastic syndrome (MDS) or myeloproliferative syndrome are more resistant to treatment as compared to *de novo* malignancy arising in healthy individual. Pathogenesis of AML involves block in the myeloid differentiation, characterised by rapid clonal proliferation of immature myeloid cells in the bone marrow that impairs the normal haematopoiesis. Signs and symptoms of AML include fever, bone pain, fatigue, frequent infection, easy bruising, unusual bleeding, pale skin and shortness of breath. If left untreated, death ensues within months of diagnosis. AML is diagnosed by presence of 20% or more blast cells in the bone marrow or peripheral blood [7].

AML is further diagnosed by testing for myeloperoxidase activity, immunophenotyping or presence of Auer rods (needle shaped cytoplasmic inclusion bodies).

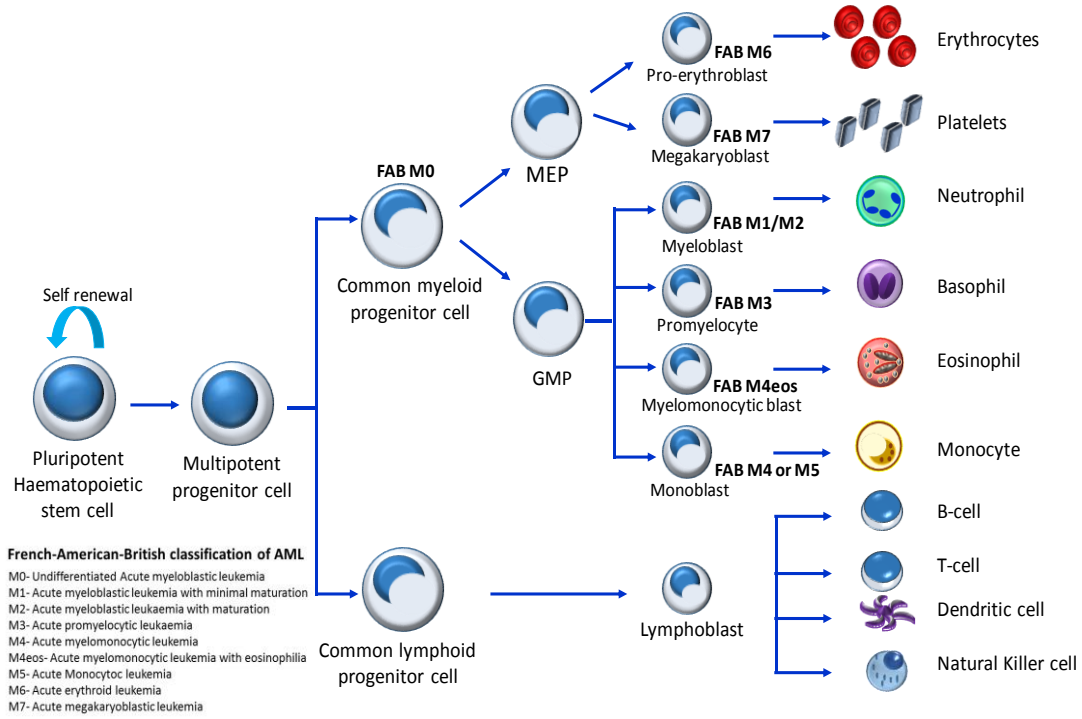

Figure 1.1: Haematopoietic hierarchy
Haematopoiesis is organised in a hierarchical order showing multiple lineages of the haematopoietic system, with rare long-term pluripotent HSCs at the top that give rise to myeloid and lymphoid progenitor cells through various intermediate stages. Which then proliferates extensively, generating mature blood cells. Multipotent progenitor cell (MPP) lacks self-renewal capacity and has vigorous replication power. Common myeloid progenitors (CMPs) are the first committed myeloid progenitor cells and differentiate into mature cells through megakaryoblast/erythroblast and myeloblast. Common lymphoid progenitors (CLPs) differentiate into lymphoblasts, which then segregate into B cell, T cell, dendritic cell and Natural Killer (NK) cell. French American British classification of AML is used to define the stage of AML based upon level of maturity and blast cells from which leukaemia developed. AML is subtyped into eight classifications; M0 to M5 starts in the precursor of white blood cells while M6-M7 developed from early forms of red blood cells and platelets.

AML is the second most common leukaemia in adults with approximately 21,000 new cases in USA alone in 2019 [8,9] and accounts for approximately 30% of all adult leukaemia, affecting mostly elderly people and its incidence increases with age [10]. Treatment of AML consists of 2 types of chemotherapy- induction and consolidation therapy. The current 5-year survival rate in patients under the age of 60 is 35-40% and 5-15% in patients over the age of 60. Patients who are not suitable for intensive chemotherapy have a much poorer outcome, with the median overall survival of 5-10 months [11]. Older patients who receive intensive chemotherapy have a worse prognosis with 5-year survival rate at 15%. The reasons for this poor outcome in older patients are chemotherapy related toxicity, poor risk cytogenetic abnormalities and overexpression of drug resistance associated genes (Table 1.2) [12]. Aside from all these factors, age itself is an independent prognostic factor in AML [12]. Patients who

had relapse undergo hematopoietic stem cell transplantation (HSCT). Recent advances in AML therapies now include a combination therapy (e.g. non-cytotoxic agent and standard chemotherapy) [13].

Classification of AML has changed a lot over years, it has moved from a system based on the cellular morphology to a system based on the molecular genetic data, clinical features and immunophenotyping. The original, French-American-British (FAB) classification is based upon the morphology to define immunotypes [14] and divides AML into 8 subtypes from M0-M7 based upon the type of cells from which leukaemia develops – as it is indicated in Figure 1.1. FAB classification system is useful but does not consider factors known to affect prognosis. World Health Organisation (WHO) classification (2016) is based upon chromosomal translocations and molecular profile [15] and includes factors affecting prognosis to better classify AML (Table 1.1).

Table 1.1: WHO classification of acute myeloid leukemia

	Inversion and/or translocation	**Gene**
AML with genetic abnormalities		
AML with	t(8;21)(q22;q22.1)	*RUNX1-RUNX1T1*
AML with	inv(16)(p13.1q22) or t(16;16)(p13.1;q22)	*CBFB-MYH11*
APL with	t(15;17)	*PML-RARA*
AML with	t(9;11)(p21.3;q23.3)	*MLLT3-KMT2A*
AML with	t(6;9)(p23;q34.1) or t(3;3)(q21.3;q26.2)	*GATA2, MECOM*
AML with	t(6;9)(p23;q34.1)	*DEK-NUP214*
AML with	inv(3)(q21.3q26.2) or t(3;3)(q21.3;q26.2)	*GATA2, MECOM*
AML (megakaryoblastic)	t(1;22)(p13.3;q13.3)	*RBM15-MKL1*
AML with		*BCR-ABL1*
AML with		mutated *NPM1*
AML with		Biallelic mutations of *CEBPA*
AML with		Mutated *RUNX1*

AML with myelodysplasia-related changes		
Therapy related myeloid neoplasms		
AML, not otherwise specified (NOS)		
AML with minimal differentiation		
AML without maturation		
AML with maturation		
Acute myelomonocytic leukaemia		
Acute monoblastic/monocytic leukaemia		
Pure erythroid leukaemia		
Acute megakaryoblastic leukaemia		
Acute basophilic leukaemia		
Acute panmyelosis with myelofibrosis		
Myeloid Sarcoma		
Myeloid proliferation related to Down syndrome		
Blastic plasmacytoid dendritic cell neoplasm		
Acute leukaemia of ambiguous lineage		
Acute undifferentiated leukaemia		
Mixed phenotype acute leukemia (MPAL) with	t(9;22)(q34.1;q11.2)	*BCR-ABL1*
MPAL with	t(v;11q23.3)	*KMT2A* rearranged
MPAL, B/myeloid, NOS		
MPAL, T/myeloid, NOS		

The modern advances in the next-generation sequencing technology has revealed marked heterogeneity and genomic complexity within AML, based upon the presence or absence of cooperating mutations within functional categories such as epigenetic regulators, cell signalling and proliferation pathways, and master hematopoietic transcription factors [16]. With the current knowledge of mutations in AML patients it is important to understand their role as a driver and passenger mutations. Driver mutations directly affect the cells by providing the fitness advantage to the mutated AML cell while passenger mutations have no effect on

these cells. Mutations that are in isolation have a no effect or even negative effect on long-term clonogenicity of cancer cells (passengers). These mutations might be 'selected' if they co-occur with a fitness-conferring mutation (drivers) or are advantageous in the context of other mutations (epistatic effect) [17]. The resolution of passenger mutations in tumour cells is similar to genetic draft or the 'hitchhiking' effect seen in population genetics. These mutations are only detected in the final tumour because they exist in a cell at the time of acquisition of the first or subsequent driver mutations [18]. The highly variable number of passenger lesions both between and within subtypes of cancer affects the dynamics of clonal evolution [19,20]. Initiation mutations exist within the founding clone and are found in all AML cells. Progression mutations which emerge later in leukaemia evolution tree, can be found in sub clones, and exist in only a fraction of AML blast cells. Selection pressure, in the form of chemotherapy treatment, can eliminate or outgrow different branches within the AML clonal evolutionary tree. Sub clonal mutations can be gained or lost over time, whereas founding mutations exist in all leukemic cells at all-time [21]. Thus, paired sample analysis taken at the time of diagnosis and at relapse may help identify mutations that were present at diagnosis and lost at relapse, and these must have existed in a sub clone that was eliminated. Similarly, mutations that are not present at diagnosis and were present at relapse must have existed in a resistant sub clone. It may have been acquired by the leukemic cell that escaped chemotherapy treatment, thus forming a new sub clone which can eventually lead to disease relapse [22].

The current hypothesis for the development of AML is a multi-step model, which means that multiple mutations need to occur for the onset of AML. This current model has recently been expanded from an older version of 2-hit model proposed by Gilliland and Griffin in 2002 (Figure 1.2) [23]. Firstly, chromosomal translocations or mutations (loss of function mutation) (class II mutations) in transcription factors required for differentiation of normal haematopoietic stem cells or myeloid precursor cells take place, causing impaired or halted differentiation. Mutations of such transcription factors commonly include promyelocytic leukaemia/retinoic acid receptor alpha (PML-RARα), Runt related transcription factor 1/Runt related X1 transcription factor 1 fusion protein (AML1/ETO [t(8;21)]), Breakpoint cluster region protein-Abelson murine leukaemia viral oncogene homolog 1 (BCR-ABL1) gene fusion. In addition, mutations in the transcription factors like CCAAT enhancer binding protein alpha (*CEBPA),* GATA Binding Protein 1 *(GATA-1), PU.1,* Runt-related transcription factor 1 *(RUNX1)* is strongly associated with AML. These types of mutations will result in a differentiation block, leading to the production of immature, non-functional blasts [24,25]. The second mutation, or second hit is a gain of function mutation (class I mutations), which leads to activation of pro-proliferative pathways. These mutations usually occur in the kinases like Fms-like tyrosine kinase 3 (*FLT3)*, KIT proto-oncogene receptor tyrosine kinase (*c-KIT)*, Kirsten RAt Sarcoma virus (*KRAS)* and Neuroblastoma Rat Sarcoma virus oncogene (*NRAS)* (Table 1.2). This type of mutation will confer a proliferation advantage for the AML blasts [26]. A gain of function mutations works in conjunction with loss of function mutation leading to development of AML

phenotype. Alterations in genes involved in epigenetic regulation are now considered as third hit mutations (class III mutations), which affects both the cellular proliferation and differentiation. These include mutations in DNA methyl transferase 3A (*DNMT3A)*, Additional sex combs like 1 (*ASXL1)*, Enhancer of zeste homolog 2 (*EZH2)*, Tet methylcytosine dioxygenase 2 (*TET2)*, Isocitrate dehydrogenase 1 (*IDH1)* and Isocitrate dehydrogenase 2 (*IDH2)*. Class III mutations have been associated with worse patient outcome and is most frequently present in older AML patients [27]. Supporting this multistep development, AML is characterised by clonal heterogeneity at the time of diagnosis with the existence of at least one subclone in addition to the founding clone [26]. Other studies have shown the existence of pre-leukemic stem cells and the pattern of mutation acquisition. Mutations in the epigenetic regulator genes like *IDH1*, *IDH2*, *DNMT3A*, *ASXL1* and *TET2* (Table 1.2) are present in pre-leukemic HSCs and occur early in the evolution of AML. These mutations alone do not lead to AML development, demonstrating the need for subsequent mutations. These mutations in epigenetic regulators are also found in relapse samples, indicating that they are resistant to chemotherapeutics [28,29].

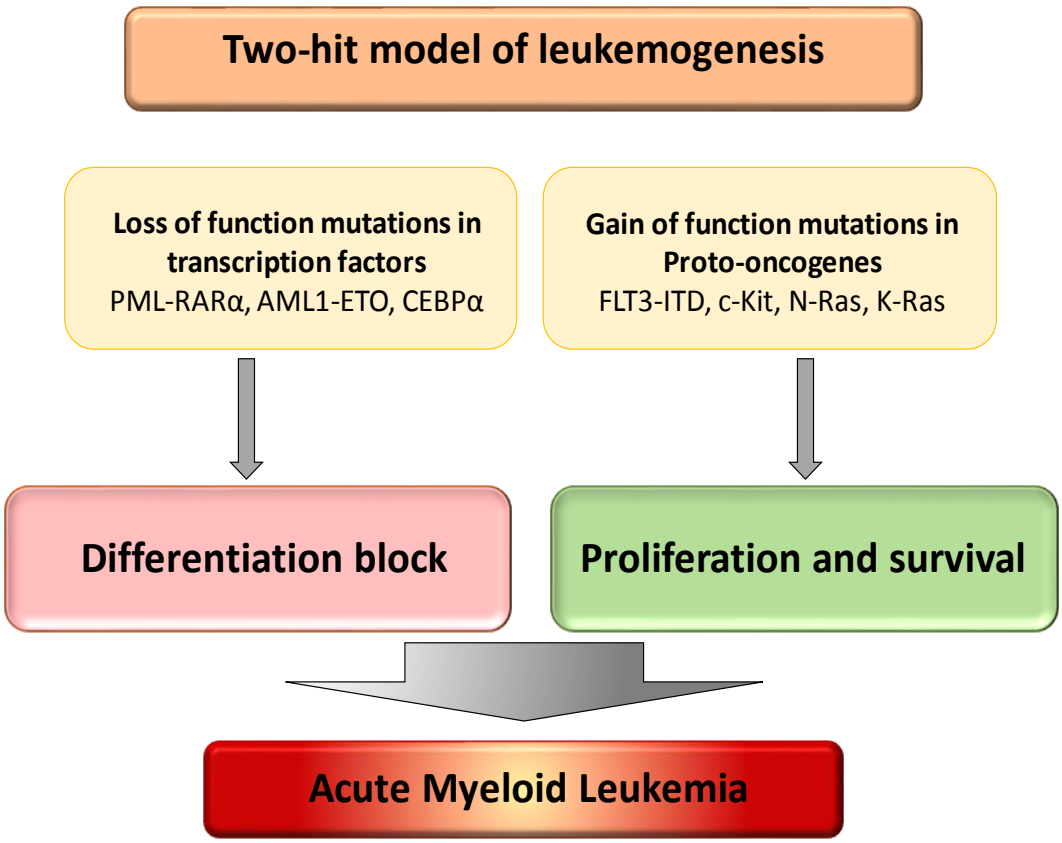

Figure 1.2: Two hit model of leukemogenesis.
The development of acute myeloid leukemia depends on at least two mutations to occur as proposed by Gilliland and Griffin (2002). Class II mutations (loss of function) involving transcription factors occurs early in HSCs leading to block in differentiation and class I mutations (gain of function) promotes proliferation and survival of these undifferentiated myeloid cells.

Table 1.2: Recurrent gene mutation frequency and its clinical significance in AML.

Gene	Frequency	Clinical significance	References
		Cell signalling	
c-KIT	<5%	25-30% in core-binding factor AML, unfavourable prognosis with t(8;21)	[30-33]
FLT3-ITD	20-25 %	30-35% in cytogenetically normal AML. High blast count, Poor prognosis in cases with high mutant to WT allelic ratio	[34-38]
FLT3-TKD	5-7%	10-14% in normal karyotype, Prognostic impact unknown	[37,39]
NRAS	15%	Enriched for core-binding factor AML, AML with inv(16)/t(16;16) and inv(3)/t(3;3), Prognosis unknown	[40-43]
PTEN	<2%	Prognosis unknown	[44,45]
		Transcription factors	
CEBPA	5-10%	10-19% in normal karyotype, favourable prognosis with biallelic mutation	[25,46,47]
NPM1	25-35%	40-65% in normal karyotype, M4 FAB morphology, Hox upregulated, favourable prognosis in presence of FLT3	[48-52]
RUNX1	5-15%	Increased incidence with older age, enriched for trisomy 13, M0 FAB, poor prognosis	[53-57]
WT1	10%	Associated with M0 FAB, poor prognosis	[58-60]
TP53	4-8%	Predominant in complex karyotype AML, associated with -5 or del(5q), -7 or del(7q), monosomy karyotype and genomic complexity, very poor prognosis	[25,61-63]
		Epigenetic modifiers	
DNMT3A	20-25%	Early events in leukemogenesis, incidence increases with older age, associated with normal karyotype, NPM1 and FLT3-ITD mutations. Poor prognosis in normal karyotype AML	[25,54]
IDH1/IDH2	12-22%	Mutant IDH1/IDH2 are mutually exclusive, IDH1 mutations are enriched with patients with NPM1 mutation. $IDH1^{R132}$ and $IDH2^{R172}$ are associated with adverse effect and $IDH2^{R140}$ with a favourable effect	[54,64-66]
TET2	10-15%	Mutually exclusive to IDH1/IDH2 mutations, More common in secondary AML-MPN. Associated with the inferior outcome with cytogenetically normal karyotype AML	[25,54,67]
ASXL1	3%	Poor prognosis	[54,68]
EZH2	<2%	Enriched for MDS/MPN, prognosis unknown	[16,69,70]
KMT2A (MLL)-PTD	<2%	2-5% in Normal karyotype AML, enriched in trisomy 11	[25,34,71]
		Overexpress	
EVI-1		Deregulated in inv(3)(q21q26); Poor prognosis	[72,73]
MN1		Correlated with WT-NPM1 and high BAALC expression, poor prognosis	[74,75]
BAALC		High expression in NK and +8, poor prognosis	[76,77]
ERG		Occurs with complex karyotype and normal karyotype AML, poor prognosis	[76,78]
miR-181		Increased in FAB M1/M2, $CEBPA^{mut}$, favourable prognosis	[76,79,80]

Pre-leukemic clones contain the leukemogenic mutations arise in multipotent hematopoietic stem cells (HSCs). First mutation must occur either in a cell with self-renewal capacity or confer self-renewal upon the cell [81]. These initial observations were enabled by the identification of cell surface markers T-cell immunoglobulin and mucin-domain containing-3 (TIM3) and CD99 molecule (Xg blood group) (CD99) which allows separation of normal HSCs from leukemic HSCs [82-84]. Targeted deep sequencing studies on HSCs were able to identify some but not all the leukaemia specific mutations suggesting the existence of pre-leukemic HSCs in AML [85]. Earliest mutation that occurs predominantly in genes that regulate the epigenome, while the latest mutation occurs in genes that lead to activated signal transduction and proliferation pathways [86]. The common pre-leukemic mutation occurs in DNA methyltransferase 3A (DNMT3A) and ten- eleven translocated 2 (TET2) genes [29] [87]. Additional mutation that is known to exist in pre-leukemic clones is IDH1/IDH2 [29] [88]. These pre-leukemic clones present at diagnosis in AML patient can develop the entire hematopoietic hierarchy while possessing repopulation advantage over non-leukemic HSCs leading to clonal expansion. Unlike AML blast cells, pre-leukemic clone survives induction chemotherapy and persists in bone marrow at remission, providing a reservoir for leukaemia relapse and progression [89].

In a large study, the existence of clonal haematopoiesis harbouring mutations in epigenetic modifiers was discovered in group with no history of haematological malignancies [90,91]. Clonal haematopoiesis of indetermined potential (CHIP) was associated with increased risk of progression to haematological malignancy [92]. The prevalence of CHIP increases with age of the population. This age-dependent clonal haematopoiesis is driven by the accumulation of mutations throughout an individual's lifetime [93]. The term age related clonal haematopoiesis (ARCH) was proposed [91] and is associated with poor outcome. Patients with CHIP are at high risk of developing leukaemia, atherosclerosis and related cardiovascular disorders, however in subset of patients with CHIP/ARCH no malignancy or disease develops [91]. In AML, CHIP like mutations are indicative of a good prognosis regarding clonal stability [94]. However, CHIP like mutations with multiple mutations are expressed or CHIP like mutations are accompanied by clonal haematopoiesis of oncogenic potential (CHOP) or loss of tumour suppressor gene leading to poor prognosis [94-97]. CHOP-related mutants have also been accepted as promising targets of therapy in acute myeloid leukaemia. However, for complete suppression and eradication of leukaemia requires the elimination of all pre-leukemic and leukemic stem cells.

1.3 AML prognosis and risk stratification

Accurate assessment of AML prognosis is the key to disease management. Based on the prognostic factors, patient stratification is done, and the treatment regime is designed. Morphological assessment of bone marrow blasts, cell surface marker expression, identifying chromosomal abnormalities and genetic lesions are used to determine the AML subtype

[11,98]. AML is then stratified into favourable, intermediate and poor/adverse prognostic risk groups (Table 1.3 [98]). Cytogenetic abnormalities are the single strongest prognostic factor in determining complete remission (CR) and overall survival (OS) in AML [99]. Gene mutations have further helped in refining the prognostic risk stratification [98]. Conventional cytogenetics along with mutational screening for *NPM1*, *FLT3, RUNX1* and *CEBPA* is routinely used in the clinic. While genetic markers are good prognostic markers, they show limited power in predicting treatment outcome and relapse [100]. Thus, monitoring of minimal residual disease (MRD) by quantitative reverse-transcriptase-polymerase chain reaction (qRT-PCR) assay as well as multiparametric flow cytometry to detect leukaemia-specific gene signatures or cell surface markers/phenotypes is the current best practice to monitor treatment outcome and predict relapse [101]. MRD monitoring in AML with core-binding factor (CBF) or with *NPM1* mutation is already being integrated to monitor AML. Among clinical factor, age and poor performance status are associated with lower rate of complete remission (CR) and decreased overall survival (OS).

Table 1.3: AML prognostic groups according to ELN2017 risk stratification by genetics.

Prognostic risk category	Genetic abnormality
Favourable	t(8;21)(q22;q22.1);RUNX1-RUNX1T1
	Inv(16)(p13.1q220 or t(16;16)(p13.1;q22);CBFB-MYH11
	Mutated NPM1 without FLT3-ITD
	Mutated NPM1 with FLT3-ITD $^{\text{low allelic ratio <0.5}}$
	Biallelic mutated C/EBPα
Intermediate	Mutated NPM1 with FLT3-ITD $^{\text{high allelic ratio>0.5}}$
	WT NPM1 without FLT3-ITD
	WT-NPM1 with FLT3-ITD^{low} (without adverse risk genetic lesions)
	t(9;11)(p21.3;q23.3); MLLT3-KMT2A
	Cytogenetic abnormalities not classified as favourable or adverse
Unfavourable/Adverse	t(6;9)(p23;q34.1); *DEK-NUP214*
	t(v;11q23.3); *KMT2A* rearranged
	t(9;22)(q34.1;q11.2); *BCR-ABL1*
	Inv(3)(q21.3q26.2)or t(3;3)(q21.3;q26.2); *GATA2*,*MECOM(EVI1)*
	−5 or del(5q); −7; −17/abn(17p)
	Complex karyotype monosomal karyotype

	WT-*NPM1* and *FLT3*-ITD^{high}
	Mutated RUNX1, ASXL1, TP53

1.4 Current treatment/therapeutics for AML

Over recent years, new diagnostic techniques have contributed to better disease prognosis; however, the treatment strategies have not improved [98]. Regardless of better understanding and recent advances in AML, therapies for most patients have remained unchanged. Patients first receive induction chemotherapy to achieve CR, AML patients usually show heterogeneous response with standard of care therapy due to minimal residual disease (MRD) which eventually leads to relapse. Therefore, to achieve a longer remission, induction therapy is followed by consolidation therapy to eradicate any residual disease [24]. Initial remission can be achieved in 50-70% of patients using a 7+3 regimen of cytarabine (AraC) and anthracyclines (daunorubicin or idarubicin) [102]. Cytarabine (100-200 mg/m^2) is infused continuously for 7 days while daunorubicin (60 or 90 mg/m^2) is administered for 3 days. Patients with favourable to intermediate-risk group are generally treated with this combination [102]. High dose daunorubicin is usually administered to patients with poor prognosis group [54]. Combination of fludarabine, cytarabine, granulocyte-colony stimulating factor (G-CSF) and Idarubicin (FLAG-IDA) is administered in treating relapse patients [103]. Elderly patients (over 65 years of age) do not respond to induction chemotherapy and represent the adverse cytogenetic risk group. However, induction therapy is superior and leads to higher overall survival (OS) in comparison to supportive care and palliative chemotherapy [104]. Patients that achieve remission then undergo consolidation therapy to eradicate residual disease to reduce the chance of relapse [24]. Standard post-remission consolidation therapy includes high dose chemotherapy and allogeneic hematopoietic stem cell transplant (allo-HSCT) [105]. Intensive chemotherapy is the first-line choice for the patients with favourable prognosis and consists of intermediate doses of cytarabine at 1-3 mg/m^2 for two to four cycles and is found to be as effective as high dose cytarabine [103,106]. Intermediate risk prognosis group is difficult to treat with consolidation therapy and only beneficial option they have is allo-HSCT; high-risk group has shown prolonged OS with this treatment option and thus should be offered as first-line consolidation therapy to these patients [105,107,108].

A relapse in AML is a major challenge. Factors responsible for relapse are the cytogenetic characteristics of the AML and detection of residual leukaemia. Factors increasing the risk of relapse in AML patients are high-risk cytogenetics, therapy-related AML, AML after myelodysplastic syndrome (MDS) or myeloproliferative neoplasm (MPN). Presence of residual leukaemia before transplantation also increases the risk of relapse in AML patients [109]. The survival rate after relapse is poor with no standard treatment for relapsed or primary refractory AML. Limiting the risk of relapse and newer treatment options are being explored including targeting mutated genes like FLT3 inhibitors, post-transplantation maintenance

therapy like azacytidine, therapy targeting immunotoxins such as gemtuzumab ozogamicin (GO), chimeric antigen receptor T-cells (CAR-T cells), bispecific T-cell engagers or vaccines targeting leukaemia-associated antigens like Wilms' tumour 1 (WT1) or HLA-A2 restricted peptide of proteinase 3 and neutrophil elastase (PR1) [11].

1.5 New therapies targeting AML

New therapies for the treatment of AML include a variety of targets of cellular processes like cell cycle and signalling through kinases or other pathways, epigenetic regulations of chromatin, anti-apoptotic proteins, nuclear export of proteins and antigens expressed on the leukemic cells or leukemic stem cells [110,111].

1.5.1 FLT3 inhibitors

Feline McDonough Sarcoma (fms)-like tyrosine kinase 3 (FLT3) is a class III receptor tyrosine kinase [112,113]. It plays a role in the development of early hematopoietic stem and progenitor cells and its expression diminishes during maturation [112]. There are two modes of FLT3 receptor activation that can cause changes in its signalling. Overexpression of FLT3 (wild type) can promote constitutive activation of receptor in malignant cells and is associated with worse prognosis [114,115]. Second reason for abnormal activation of FLT3 signalling is mutations (internal tandem duplication-ITD or tyrosine kinase domain mutation-TKD) in this receptor, which also leads to constitutive activation of receptor and is associated with worse prognosis. When FLT3 ligand binds to the extracellular immunoglobulin-like domains of FLT3, the receptor dimerises, leading to autophosphorylation of tyrosine residues and receptor activation [112]. The activated receptor triggers three main downstream signalling pathways: phosphoinositide 3-kinase/AKT serine/threonine kinase (PI3K/AKT), mitogen activated protein kinase/extracellular signal-regulated kinase (MAPK/ERK) and signal transducer and activator of transcription-3 and 5 (STAT3/STAT5) signalling [112]. Activation of FLT3 signalling promotes cell survival, proliferation and differentiation (Figure 1.3) [26,40].

FLT3 is one of the most frequently mutated genes in AML (30% in adult and 15% in paediatric AML patients) [5,11,24]. There are two types of mutations in FLT3 associated with AML: internal tandem duplication (ITD), which occurs due to a replicated sequence within the juxta-membrane domain and tyrosine kinase domain (TKD) mutations, which are typically point mutations [26,40]. The size of insert in ITD mutation varies from 3 to 400 base pairs. ITDs are in-frame mutations caused by duplication of various in length fragments of juxta-membrane domain of FLT3 receptor [116]. Different size of ITDs leads to variation in length duplication within juxta-membrane domain of receptor thereby determining which downstream effectors can bind to the receptor [116,117]. Arginine 595 (R595) is the most frequently duplicated amino acid in ITD and plays a critical role in activation of FLT3-ITD mutants and ligand dependent activation of WT-FLT3 [114]. In long ITD forms, tyrosine phosphorylation sites such as Y589 and Y591 which serves as a docking site for Src family kinases. This leads to stronger

activation of Ras/ERK pathway and PI3K/AKT pathway. ITD mutation leads to constitutive activation of receptor in a ligand-independent manner [118-120].

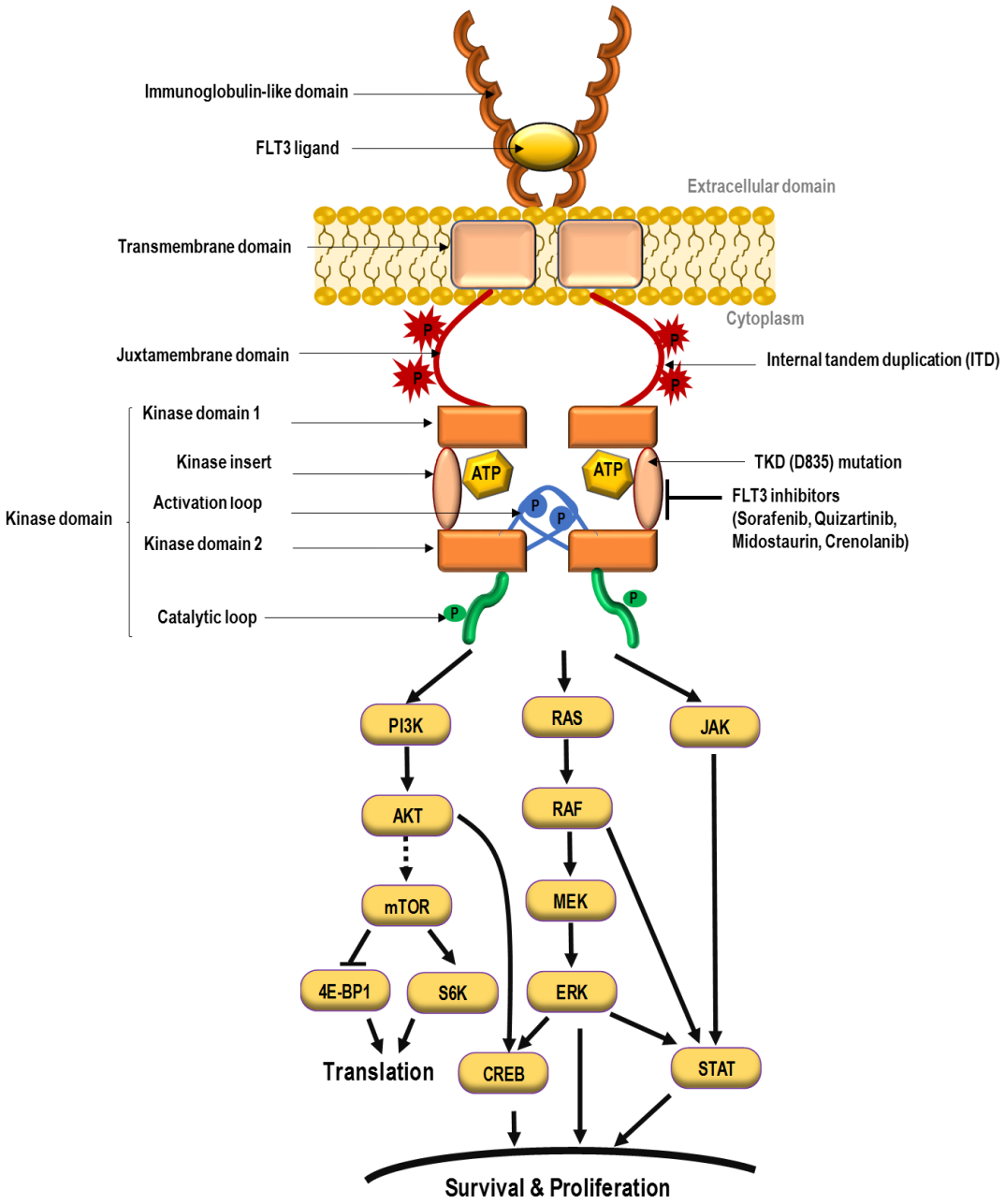

Figure 1.3: FLT3 signalling pathway in AML.
Activation of FLT3 occurs when FLT3 ligand (FL) bind to extracellular Immunoglobulin-like domains and dimerises FLT3 receptors in proximity. It then trans-phosphorylate the tyrosine residues of the juxta membrane domain allowing activation of the kinase domain by unfolding the activation loop into open conformation. This open conformation then allows the binding of ATP and phosphorylation of the kinase domain and subsequently the downstream pathways. Type I FLT3 inhibitors (Crenolanib, Midostaurin) binds the receptor near the activation loop or the ATP binding site in active conformation and can target ITD and TKD mutations. Type II FLT3 inhibitors (Quizartinib, Sorafenib) bind to the region adjacent to ATP binding domain in inactive conformation and can only target the ITD mutations (Modified from Grafone T. and colleagues, [112].

A point mutation in FLT3 receptor at aspartate 835 (D835) position is most frequent, where aspartate is exchanged with tyrosine (Y) or histidine (H) [121,122]. TKD point mutation at D835

is found in nearly 7% of AML patients [122]. Other FLT3 mutations include deletion or substitution at I836 and insertion of glycine and serine at S840 and N841 [123]. These mutations can also lead to constitutive and ligand–independent activation of FLT3 without receptor dimerization by phosphorylation of receptor. TKD and ITD mutations interrupt the auto-inhibitory mechanism of FLT3 receptor [124]. So far, no AML patient has been reported which carries both the ITD and TKD (D835) mutations, suggesting different underlying mechanism and downstream signalling [122].

Depending upon the ITD location, FLT3 can activate different signalling pathways. It has been shown that FLT3-ITD can activate STAT3 and STAT5 signalling by upregulating proto-oncogenic serine /threonine kinases (Pim1 and Pim2), but not the PI3K and MAPK signalling when localised to endoplasmic reticulum (ER) [125,126]. FLT3-ITD when localised to the membrane can strongly activate the PI3K and MAPK signalling pathways but not the STAT3/5 [126]. Activation of STAT5 signalling by mutated FLT3 receptor differentiates it from the wild type FLT3 receptor [120,127]. Activation of STAT5 leads to higher expression of downstream targets such as Pim-1, cell division cycle 25A (Cdc25A), Bcl-2 associated agonist of cell death (BAD) and B-cell lymphoma 2 (Bcl-2) [128]. This activation of anti-apoptotic proteins by FLT3-ITD mutation is associated with worse outcome. FLT3-ITD can also activate AKT signalling, which in turn blocks the Forkhead box O (FOXO) transcription activity leading to increased cell proliferation, survival and leukemic transformation [129]. Activation of FLT3 receptor has been associated with upregulation of suppressors of cytokine signalling (*SOCS2 and SOCS3*), myeloid cell leukaemia sequence -1 (*MCL-1*), V-Myc avian myelocytomatosis viral oncogene homolog (*MYC)* and cyclin D3 (*CCND3*) providing activation of cell proliferation, survival, cell cycle regulation and inhibits apoptosis [130-133].

Given the high rate of FLT3 mutations and its prognostic impact, FLT3 emerged as a potential therapeutic target. FLT3-ITD mutation is strongly associated with high leukemic burden, poor prognosis and has negative impact on the maintenance of AML patients [134-136].

This has generated a lot of interest in developing inhibitors against it. Small molecule inhibitors can vary in selectivity, competitive with ATP binding site or non-competitive leading to cell cycle arrest and differentiation [137]. Additionally, FLT3 inhibitors also target other tyrosine kinases influencing the tolerability and efficacy of these agents. First-generation inhibitors like sorafenib, lestaurtinib and midostaurin are less specific for FLT3, target broad range of kinases, and have more off target toxicity. Whereas second-generation agents such as quizartinib, gilteritinib and crenolanib are more specific and potent inhibitors of FLT3 with little off target toxicity (Table 1.4). FLT3 inhibitors can be further divided into type I or type II depending upon the mechanism of FLT3 inhibition. Type I inhibitors bind the active form of the kinase that is associated with ‘DFG-in’ conformation (Asp-Phe-Gly-DFG motif at the N-terminus of activation loop) either near the activation loop or near ATP binding site. These inhibitors are active against both the ITD and TKD mutations. On the other hand type II inhibitors bind the ‘DFG-out’ conformation (accessible only when the kinase is inactive) near

ATP-binding domain. As a result, type II inhibitors prevent the activity of ITD mutations but not the TKD mutations [138,139].

Table 1.4: First and second generation FLT3 inhibitors

Inhibitor	Type	Targeted tyrosine kinases
First-generation FLT3 inhibitors		
Sunitinib	I	VEGFR2, PDGFRβ, KIT, RET
Sorafenib	II	RAF, VEGFR1/2/3, PDGFRβ, KIT,
Midostaurin	I	PKC, SYK, FLK-1, AKT, PKA, KIT,
Lestaurtinib	I	JAK2/3, TrkA/B/C
Ponatinib	II	LYN, ABL, PDGFRα, VEGFR2,
Tandutinib	II	KIT, PDGFRβ
KW-2449	I	FGFR1, BCR-ABL, aurora kinase
Second-generation FLT3 inhibitors		
Crenolanib	I	PDGFRβ
Quizartinib	II	KIT, PDGFR
Gilteritinib	I	LTK, ALK, AXL

First generation of FLT3 inhibitors, such as lestaurtinib, sunitinib, sorafenib and midostaurin have activity against FLT3 and are investigated in clinic [139-143]. Studies evaluating these inhibitors as a monotherapy have shown limited anti-leukemic activity, some benefit when combined with chemotherapy and is usually associated with severe toxicity [144,145]. Lestaurtinib when combined with salvage therapy offers no improvement in OS when compared to salvage therapy alone in FLT3-ITD relapse AML patients [146]. Limited single agent activity was reported for sunitinib in phase-I studies with only partial response in relapse or refractory AML patients [147]. Sorafenib has also shown similar efficacy as a single agent in relapse/refractory FLT3-ITD AML with only 10% of patients achieved CR [148]. Conversely, in younger patients (age <60) with newly diagnosed AML when treated with sorafenib and standard of care induction chemotherapy offers significant event free survival (EFS) and relapse free survival (RFS) but not overall survival (OS) when compared to control in phase 2 study [145]. It has also been observed that patients with ITD received no benefit from sorafenib treatment whereas patients with WT-FLT3 had improved EFS and RFS [145]. Similarly, when sorafenib was combined with 7+3 (AraC+Dnr) in elderly patients over 60 years did not show significantly improved survival [149]. Sorafenib when combined with cytarabine and idarubicin has shown higher response rate with CR at 95% in patients with FLT3-ITD mutation and DFS and OS at 13.8 and 29 months respectively [150]. Midostaurin has been approved as first-line treatment of FLT3-ITD patients in combination with induction chemotherapy (cytarabine + daunorubicin) by US food and drug administration (USFDA) for younger patients with newly diagnosed FLT3-ITD AML patients [151]. Overall, these first-generation tyrosine kinase inhibitors (TKIs) lack specificity for FLT3-ITD and this explains their transient activity when used as a monotherapy and may contribute to adverse effects due to targeting of multiple other kinases [152].

To overcome these challenges, second-generation inhibitors, like quizartinib (AC-220), crenolanib (CP-868596) and, gilteritinib have shown higher potency, efficacy and specificity for FLT3. Gilteritinib and crenolanib are type I inhibitors targeting both the active and inactive conformations of FLT3 receptor where as quizartinib is type II inhibitor targeting only inactive conformation [138]. These inhibitors have shown promising single agent activity in early clinical trials. Gilteritinib as a monotherapy has shown response in younger patients with relapsed/refractory AML overall response rate (ORR) at 49% for FLT3-ITD patients and complete remission (CR) at 37% with median duration of response at 17 weeks [153]. Crenolanib has also shown activity against relapse/refractory FLT3-ITD AML as a monotherapy with complete remission with incomplete hematologic recovery (CRi) of 39% and partial response (PR) at 11% for relapse patients with median overall survival (OS) at 33.4 weeks for treatment of naïve patients and 34 weeks for patients with FLT3-ITD mutation [154]. Quizartinib as a monotherapy when compared with salvage therapy has comparable effect on relapse/refractory FLT3-ITD patients [155]. In phase 2 studies, quizartinib has shown composite complete response (CRc) at 46-56% and overall response rate (ORRs) at 74-77% in relapse/refractory disease [156]. Quizartinib in combination with chemotherapy in younger patients and older patients with newly diagnosed AML appears effective [157]. Quizartinib is well tolerated as single agent post allo-HSCT therapy in ITD mutated patients who are in remission [158]. These findings suggest that the targeting FLT3-ITD mutations with highly selective and potent inhibitor is a promising clinical strategy which can help improve clinical outcome in patients.

Gilteritinib has also been recently approved for relapsed or refractory AML with FLT3-ITD mutations [159], while quizartinib was not approved due to the only marginal benefit in overall survival in comparison to choice of traditional chemotherapy [160].

Despite advances in the development of efficient FLT3 inhibitors, emergence of resistance to them poses a significant challenge [138]. It has been shown by Piloto and colleagues that FLT3 inhibitor-resistant cells become independent of FLT3 signalling due to FLT3-independent activation of survival signalling pathways, such as the PI3K/AKT, RAS/ERK and the STAT3/STAT5 pathway, which compensate for the loss of the FLT3-mediated survival signalling [161]. Both inherent and acquired mutations contribute to drug resistance. WT-FLT is sensitive to FLT3 ligand and is usually resistant to FLT3 inhibitors. Therefore, presence of WT-FLT3 in patients with FLT3-ITD mutation contribute to resistance against TKIs. High level of FLT3 ligand (FL) present in bone marrow microenvironment can activate FLT3 signalling leading to survival of leukemic blast even in the presence of FLT3 inhibitors [162,163]. It has to be mentioned that while FLT3 alone does not drive a robust proliferative signal, it strongly synergises with other bone marrow-typical trophic factors, such as interleukin-3 (IL-3) and stem cell factor-V (SCF-V) [164]. Unfortunately, none of these FLT3 targeting tyrosine kinase inhibitors has shown promising results in AML patients [141]. Generally, FLT3-inhibitors effectively kill FLT3-mutant AML cells in the periphery but only cause a transient reduction of AML blasts in the bone marrow [139,165]. It is predicted that the limited clinical efficacy of the

FLT3 inhibitors may be due their inability to elicit the complete and sustained response in the AML patients. The preclinical studies for FLT3 inhibitors did not take into consideration the effect of the bone marrow microenvironment and the synergistic interaction between FLT3, IL-3, SCF and other trophic factors [166]. Inadequate efficacy of FLT3 inhibitors may arise due to suboptimal drug concentration in plasma due to rapid metabolism by cytochrome P450 A4 (CYP3A4) enzymes in the liver [167]. Chang and colleagues have also shown that bone marrow stroma cells express elevated levels of CYP3A, which provides resistance to FLT3-ITD AML cells against sorafenib, quizartinib and gilteritinib. When combined with CYP3A inhibitor clarithromycin, FLT3 inhibitors overcomes the bone marrow microenvironment mediated drug resistance and shows higher efficacy [168]. Yang and colleagues have shown that bone marrow stroma secreted cytokines activate the extracellular regulated kinases (ERK) in AML blasts which mediated the drug resistance against the FLT3 inhibitors [163]. Sung and colleagues have shown that bone marrow secreted cytokines such as granulocyte-macrophage colony-stimulating factor (GM-CSF) and interleukin-3 (IL-3) activates the JAK kinase, STAT5 and proviral integration of moloney murine leukemia virus (PIM) which help to provide the survival signal to FLT3-ITD mutated AML cells. Combining FLT3 inhibitor with JAK inhibitor or PIM kinase inhibitor block the GM-CSF and IL-3 mediated cell survival [169]. In addition, activation of FLT3 signalling in the presence of FLT3 inhibitors by downstream mediators like NRAS through acquisition of mutations may lead to relapse [161,165]. Sexauer and colleagues have shown that quizartinib induces terminal differentiation and cell cycle arrest of myeloid cells in bone marrow rather than apoptosis and C/EBPα mutation prevents the cell from differentiation offering a mechanism of resistance against FLT3 inhibitors [137]. Acquired FLT3 mutations such as TKD mutations can arise from type I and type II inhibitors that can confer resistance [170,171]. These secondary acquired mutations represent a complex mechanism to targeted therapies [172].

A important strategy to overcome the drug resistance to chemotherapy is the use of combination therapy [138]. In current clinical trials, combining FLT3 inhibitors with conventional chemotherapy is an attempt to increase the cytotoxic effect against FLT3-ITD mutated leukaemia cells. Future therapies focusing on the divergent pathways linked to FLT3 signalling will provide improved combination therapy to treat and improve the response rate along with sustained remission in FLT3-mutant AML patients.

1.5.2 IDH1/IDH2

Genes involved in chromatin modifications and DNA methylation are identified in AML in mutated forms. A gain of function mutation in the mutant metabolic enzymes isocitrate dehydrogenases, IDH1 and IDH2, are found in 20% of AML cases [26]. Mutations were found in catalytically active arginine residues at R132 on IDH1, and R140 and R172 on IDH2. Instead of catalysing the conversion of isocitrate to alpha-ketoglutarate (α-KG) [173,174], these mutated enzymes catalyse the conversion of alpha-ketoglutarate (α-KG) to 2-hydroxyglutarate

(2-HG) [175,176]. Intracellular levels of oncometabolite 2-HG lead to hypermethylation of target genes, which causes a block in cellular differentiation [177]. Small molecule inhibitors of mutant IDH1/IDH2 were developed to reduce the levels of 2-HG and to unblock the cellular differentiation. AG-120 and AG-221 are currently in clinical trials against IDH1/IDH2 mutation respectively [178,179]. These inhibitors have shown encouraging results by triggering differentiation of leukemic blasts with IDH mutation. Chan and colleagues have also shown that IDH1/IDH2 mutated blasts are highly dependent upon anti-apoptotic B-cell CLL-lymphoma 2 protein (BCL2) expression. Inhibition of BCL2 with venetoclax (ABT-199), a second-generation BH3 mimetic, induces cell death, thus suggesting a potential combination therapy of IDH1/2 inhibitors with venetoclax in AML [180]. FDA has recently approved the IDH2 inhibitor enasidenib for relapsed/refractory IDH2 mutated AML. Combination of these inhibitors along with induction therapy in the frontline treatment setting is currently ongoing [181].

1.5.3 STAT inhibitors

Signal transducer and activator of transcription (STAT) signalling pathway is shown to be upregulated in AML cases and confers with poor prognosis [182]. Activation of aberrant STAT3 or STAT5 signalling is due to a variety of upstream regulators in leukaemia (FLT3 signalling) [183]. STAT3/STAT5 are activated by paracrine factors such as epidermal growth factor (EGF), transforming growth factor-alpha (TGFα), colony-stimulating factor-1 (CSF-1), and interleukin-6 (IL-6). In addition, epigenetic suppression of suppressor of cytokine signalling (SOCS), protein tyrosine phosphatases or chromosomal translocations like BCR-ABL results in activation of STATs [182,184]. FLT3-ITD activating mutation causes aberrant activation of multiple downstream pathways such as PI3K/AKT, RAS/ERK, STAT3/STAT5. Activation of STAT5 signalling pathway by constitutively active FLT3 leads to development of resistance to FLT3 tyrosine kinase inhibitors [182]. Zhou and colleagues have shown that upregulation of FLT3 ligand and the silencing of SOCS merge to enhance the STAT signalling pathway [183]. Several small-molecule inhibitors to target STATs are currently being tested in pre-clinical studies. STAT3 inhibitors C188-9 or MM-206 have shown to induce cell death in FLT3-ITD AML cells. OPB-31121, small-molecule inhibitor of STAT3 and STAT5 phosphorylation has shown activity against FLT3-ITD AML cell and overcoming the FLT3 mediated resistance to TKI [24,184]. Combination of STAT5 inhibitor AC-4-130 (SH2 domain inhibitor) with JAK1/2 inhibitor ruxolitinib eradicates the primary FLT3-ITD AML blasts both in *in vitro* and *in vivo* studies [185]. These data support the use of combination therapy of FLT3 inhibitors with agents targeting the STAT pathway as treatment for AML patients with FLT3 mutations.

1.5.4 Cytotoxic agents

Cytotoxic drugs like clofarabine, vosaroxin and CPX-351 are developed and approved to treat AML. Clofarabine is a purine nucleoside analogue and administered as a single agent with an overall response rate of 40% [186]. Combination of clofarabine with low dose cytarabine is administered as first line of therapy. Vosaroxin is a quinolone derivative, inhibits DNA topoisomerase II, and induces double-strand breaks in DNA. Enhanced overall survival (OS) and complete remission (CR) rate in vosaroxin plus cytarabine combination trial was observed for relapsed or refractory AML [187]. CPX-351 is a liposomal formulation of cytarabine and daunorubicin at 5:1 molar ratio and has shown better OS, event-free survival (EFS) and CR against cytarabine (100mg/m^2) plus daunorubicin (60mg/m^2) in older patients [188]. Hypomethylating agents targeting DNA-methyltransferase (DNMT) enzymes are also in clinic. In AML epigenetic silencing of genes by DNA methylation leads to leukemogenesis, especially in older patients [111,189]. Hypomethylating agents (HMA) have similar outcome as chemotherapy in older patients with lower toxicity. 5-azacitidine and decitabine (5-aza-2'-deoxycytidine) are DNMT inhibitors which are recommended for low dose therapy for elderly patients. The activity of hypomethylating agents (Decitabine or 5-Aza) is enhanced in combination with histone deacetylase (HDAC) inhibitors like vorinostat, panobinostat, HDACs causes gene silencing by histone deacetylation thus disrupting the gene expression in leukemic cells [111,190].

1.5.5 Immunotherapy

Although chemotherapy with induction and remission phases is the first treatment option, this is usually associated with high toxicity and high risk of relapse [191] because leukemic stem cell (LSC) are resistant to chemotherapy [192-194]. Cancer cells express stress proteins, which is recognised by the immune system through immunosurveillance and are eliminated. Therefore, for AML the best therapeutic option is immunotherapy, where immune cells (T-cells, NK cells) are activated to re-establish the immunosurveillance activity against these cancer cells. Immunotherapy has an activity that is more specific and is well tolerated due to low toxicity [195]. Many AML associated antigens were identified that can be targeted by immunotherapy such as CD33, CD123, CD44, CD30, CD96 and TIM-3 [196]. Treatment of AML using immunotherapy employs various techniques that engage specific immune cells such as monoclonal antibody therapy, T-cell therapy, alloreactive natural killer (NK) cells and therapeutic vaccines [197]. Novel therapies based on antibodies are new in AML treatment [198]. CD33 antigen is expressed on about 80% of AML blasts; this makes it an attractive target for therapy. Gemtuzumab ozogamicin (GO) or Mylotarg is anti-CD33 monoclonal antibody which is expressed during myeloid differentiation. The antibody is conjugated with calicheamicin (DNA cleaving cytotoxic agent) as antibody-drug conjugate [199]. GO has been approved for older AML patients in combination with fludarabine, cytarabine and G-CSF (FLAG) [200]. Bispecific T-cell engager (BiTE) antibody construct targeting tumour antigen

and the T-cell receptor leading to recruitment of T-cell. First BiTE developed in AML is against CD33 (AMG330, CD33/CD3) [201]. CD123 (also known IL-3 receptor alpha) is expressed on leukemic stem cells (LSCs) and blasts. CD123 overexpression drives the cell proliferation and is associated with poor outcome [202,203]. Monoclonal antibodies targeting CD123 have shown poor response in clinical trials and new CD123 antibodies conjugated with drugs (ADCs) are currently being tested, such as SGN-CD123, Anti-CD123-PBD conjugate and SL-401 with diphtheria toxin conjugated with IL-3 ligand [204,205]. Chimeric antigen receptor T-cells (CAR-T cells) are also developed to target CD123 [206]. CAR-T cells developed against FLT3 have also shown good efficacy, both $CD4^+$ T-cells and $CD8^+$ T-cells show potency against WT-FLT3 or FLT3-ITD [207]. CAR-T cell therapy is growing and can provide an alternative therapy to treat patients with relapsed or refractory leukaemia. Immune checkpoint inhibitors against AML appears promising. Cytotoxic T-lymphocytes associated protein 4 (CTLA-4) and programmed cell death protein 1 (PD-1), T-cell immunoglobulin mucin-3 (TIM-3) and lymphocyte activating gene-3 (LAG-3) are investigating targets in AML [208].

Understanding of molecular pathogenesis of AML has not yet been translated into clinical practice. New therapies hold promise to improve treatment outcomes, however, it is improbable that any of these drugs, when used as single agents, will cure the AML patient. Designing of combinatorial therapies based upon the response of specific agents can solve the problem. Although the challenge remains to specifically, target the leukemic cells while sparing the healthy cells. Understanding the reason for AML relapse or refractory disease along with new improved targeted drug development may help in overcoming the shortcomings of the present treatment regimen.

1.6 Causes of drug resistance in AML

Despite the availability of newer treatment options, the first line of therapy in AML is still a combination of cytarabine and daunorubicin or cytarabine with idarubicin. Resistance to intensive chemotherapy is the major obstacle in the treatment of AML. Firstly, in the main, elderly population, intensive chemotherapy can achieve complete remission in 40% of patients, but in over 60% of patients the CR is temporary, and they relapse. Approximately in 85% of these patients the relapsed disease is chemoresistant [7,209], which means that in only 10% of the patients, long-term cure can be achieved.

The primary reason for treatment failure is the existence of blast subpopulations that are resistant to the therapeutic drug. Cells that survive the treatment or are resistant to drugs eventually cause disease relapse. These resistant clones then evolve to become a prominent clone in the relapsed disease, making it even more difficult to treat [134]. Although the low-differentiation-status leukemic stem cells (LSCs) have intrinsic mechanisms which makes them resistant to drugs, such as expression of drug resistance-related proteins (Multidrug resistance-associated protein 1 (MRP1), Protein kinase C (PKC), Topoisomerase II), genetic

alternations (FLT3, WT1, NRAS) driving cell survival signalling pathways (PI3K, autophagy) [210]. It has been proposed that leukemic stem cells (LSCs) preferentially resist chemotherapy treatment, providing a cellular reservoir that is thought to form the basis for relapse [211]. However, this prediction is primarily due to the dormant/quiescent cell-cycle status of LSCs [212], and these ideas have not been rigorously tested by analysing leukemic populations that selectively persist post-therapy. However, the concept of bone marrow microenvironment, where LSCs reside, as a driver of drug resistance has attracted the most attention in recent times. It has been shown that microenvironmental factors contribute to the selection and expansion of malignant LSC clones. Ding and colleagues have shown that dominant clones or less abundant subclones can drive AML relapse [134]. Shlush and colleagues have shown that relapse can originate from rare LSCs with a hematopoietic stem/progenitor cell phenotype, while subclones with immunophenotypically committed LSCs with a strong stemness like transcriptional signature can also initiate relapse in AML [28]. Defining and characterising the cells responsible for relapse is difficult from patients, as the number of residual leukemic cells reduces drastically post-treatment. This is further enhanced by the difficulty to resolve rare primitive AML cells from endogenous normal hematopoietic stem/progenitors within patient bone marrow (BM), due to overlapping molecular and phenotypic properties [213,214]. LSCs, much like HSCs, reside in the bone marrow niche that supports their clonal expansion, survival and subsequently, leading to relapse of leukaemia [215]. Boyd and colleagues have shown that the post chemotherapy the onset of relapse is due to leukemic-regenerating cells (LRCs) [216]. LRCs have a unique molecular profile, are transient, exists only in *in vivo* and are different from therapy resistant LSCs. Molecular profile of LRCs is conserved across various genetically diverse AML patients and identifies a reservoirs of minimal residual disease (MRD) in clinically treated patients who ultimately progress to relapse. LRCs can be therapeutically targeted given the uniquely nature of LRC signatures to inhibit leukaemia relapse and can also act as markers of AML disease recurrence. Despite recent advances, our current understanding of LSCs has been rendered in the absence of chemotherapy treatment, and thus represents properties of “therapy-naive” LSCs/therapy resistant LSCs [213]. This leaves the acute response of AML LSCs to chemotherapy *in vivo* largely unknown. These observations complement recent insights from Ebinger and colleagues and Passaro and colleagues that the bone marrow microenvironment (BMM) contributes to the dynamics of therapy response in human leukaemia [217,218], and mirror previous findings where leukemic cell proliferation could be stimulated *in vitro* by exposure to serum from patients who were recovering from chemotherapy treatment [219]. AML LSCs were shown to reside at the apex of a cellular hierarchy that initiates and maintains the disease, exhibiting properties of self-renewal, cell cycle quiescence, and chemoresistance. This cancer stem cell model offers an explanation for chemotherapy resistance, disease relapse and implies that approaches to treatment must eradicate LSCs for long term disease free survival. Therefore, identifying factors released by bone marrow microenvironment that confers resistance to leukemic cells is crucial to prevent relapse. Thus,

developing the understanding and therapeutic strategies targeting the interactions of leukemic cells and niche cells may lead to improved therapy.

1.7 Bone marrow microenvironment

Hematopoietic stem cells (HSCs) interact with an intricate network of cells in the bone marrow microenvironment (BMM) or niche facilitating their differentiation and expansion into blood cell lineages [215,220]. In the bone marrow (BM), HSCs are tightly regulated in their local microenvironment or niche, which regulates self-renewal, quiescence, proliferation and differentiation of HSCs through mechanisms such as cell-cell interaction or cell-paracrine interactions [221]. Cell types of the BM that are involved in promoting HSC maintenance, including osteoblasts, perivascular stromal cells, macrophages, endothelial cells, adipocytes, CXCL12-abundant reticular cells (CAR cells), non-myelinating schwann cells and sympathetic neurons. Additionally, several paracrine factors relevant to HSCs maintenance like C-X-C motif chemokine ligand 12 (CXCL12), transforming growth factor-beta (TGF-β), angiopoietin 1 (ANGPT1), Notch and Wnt ligand [221,222]. BM niche maintains the HSCs primarily in quiescent state by providing signals to inhibit its proliferation and only upon activating signals these stem cells undergo proliferation [223,224]. Despite the complexity of BMM, bone marrow niche can be divided into two compartments- endosteal niche (near to the trabecular bone region or osteoblasts) and perivascular niche (near to the sinusoidal or arteriolar vascular endothelium) [225,226]. Arterioles run in close proximity to endosteal surface, sympathetic nerve fibres accompanied by non-myelinating Schwann cells, and quiescent HSCs are associated with periarteriolar niche in endosteal BM niche [227]. Sinusoids lines with reticular shaped sinusoidal cells are associated with active HSCs relocating to perisinusoidal niches [227,228]. Hypoxia maintain HSCs in a quiescent and pluripotent state [229]. HSCs residing near vascular niche are actively cycling and regularly replenish the circulating cells (Figure 1.4).

1.7.1. The Endosteal niche

Endosteal niche is localised in the internal bone shell surface [230]. The organisation of BM niche in endosteal niche has been identified through imaging technologies along with functional assays. Endosteal niche consists of bone-forming cells osteoblasts (OB), bone-resorbing cells osteoclasts (OC), fibroblasts, macrophages endothelial cells and adipocytes. Osteoblast (OB) lineage cells line the surface of the endosteum and play an important role in normal haematopoiesis. Osteoblasts produce extracellular matrix proteins (ECM) and form bone while osteoclasts resorb bone and help in bone remodelling [97]. These cells secrete variety of cytokines like C-X-C motif chemokine ligand 12 (CXCL12), angiopoietin-1 and granulocyte colony-stimulating factor (G-CSF) [231-233]. In endosteal niche HSCs interacts with N-cadherin^{+} osteoblasts and are kept in a quiescent state regulating their self-renewal

and protect them from chemotherapeutics [234,235]. It has been shown that HSC number can be expanded by increasing the osteoblast cell in endosteal niche through Jagged-1 dependent activation of Notch-1 [236,237]. HSCs retention and quiescence in the endosteal niche is also regulated by notch-1 and Jagged-1 or δ-like ligand 4 (Dll4) [238]. Osteoblast deficiency reduces the HSC pool by loss of quiescence and self-renewal capacity [239]. Nakamura and colleagues have shown that immature osteoblastic cells express high level of CXCL12 and stem cell factor (SCF) that maintain the HSC pool [240]. HSCs adhere to osteoblasts through angiopoietin receptor-2 (Tie-2), this interaction of Tie-2 with angiopoietin-1 (Angpt-1) promotes quiescence, enhances their survival and protects them from cellular stresses [224]. Endosteal niche also regulates the levels of extra cellular matrix component- osteopontin (OPN) or calcium ions secreted through sympathetic neurons, which were shown to negatively regulate the HSC number [241]. OPN interacts with CD44 and α4 integrins, which are expressed by HSCs, and plays a role in their localization. A defect in calcium-sensing receptor in HSC affects their homing in endosteal niche and reduce their long-term repopulation capacity [241]. Osteoblasts also play a role in regulating the endosteal niche and stem cell mobilization. There is evidence that HSCs regulate the differentiation of mesenchymal stromal cells into osteoid lineage cells, providing a bidirectional control to the endosteal niche. Bone marrow stromal cells (BMSC) are known to constitutively produce CXCL12, which regulates the HSCs mobilization, cell adhesion, survival and proliferation in BM niche [242,243]. CXCL12 expression is negatively regulated by granulocyte-colony stimulating factor (G-CSF) [244,245]. Stem cell factor (SCF) induces differentiation and proliferation in HSCs and its receptor c-kit is essential for maintenance of quiescent HSCs in endosteal niche [4,246,247]. Regulatory signals in the endosteal niche in the form of paracrine factors, bound factors and oxygen gradient (hypoxia) control the HSC quiescence and activation, while in the vascular niche signalling molecules are important to sustain HSC self-renewal and maintenance [221,231,244].

1.7.2 The Perivascular Niche

Perivascular niche is close to sinusoidal endothelium supported by stromal cells. Moreover, HSCs are associated with the vascular structure and around 60% of them are present in this niche. Sinusoids are distributed around draining central sinus and haematopoiesis occurs in the extravascular spaces between them [248,249]. Vascular sinuses are lined with endothelial cells and CXCL12 abundant reticular (CAR) cells. CAR cells along with mesenchymal stromal cells form reticular network that supports the HSC formation [250,251]. Notch signalling by endothelial cells is a critical regulator of HSC niche, by increasing the expression of platelet-derived growth factor receptor beta (PDGFR-β)$^{+}$ perivascular cells, CD31^{+} vessels, production of SCF thus maintaining the niche forming vessels [249]. Kunisaki and colleagues demonstrated that quiescent HSC localises to arteriolar region in endosteal niche, which consists of Nestin^{high}NG2^{+}LEPR^{-} pericytes, CXCL12 abundant reticular (CAR) cells,

endothelial cells, nonmyelinated Schwann cells (SC) and sympathetic nerves (SN) [227]. In the sinusoidal niche, $NG2^-$ mesenchymal stromal cells (MSC) support the actively cycling HSCs [252].

CAR cells play a role in regulation of HSC proliferation and provide resistance against the chemotherapeutics [253]. In a study conducted by Itkins and colleagues, it was shown that lower permeability of arterial vessels along with close proximity of megakaryocytes (MK) provides a metabolically inactive microenvironment, which helps in maintaining the quiescent HSC along with low levels of reactive oxygen species (ROS) [254]. Interaction between CXCR4 and CXCL12 are important for HSC retention and localization. CXCL12 plays an important role in colonization of HSCs in early development [255]. Bone marrow niche, in part, is mediated by circadian rhythms in sympathetic nervous system. During daytime adrenergic inputs downregulates the CXCL12 effecting the stem cell mobilization and up-regulates the CXCR4 in HSCs at night [256].

Megakaryocytes (MKs) regulate osteoblast development in endosteal niche. MKs interact with the sinusoidal endothelial cells through CXCL12 and fibroblast growth factor 4 (FGF4), resulting in higher expression of adhesion molecules like vascular cell adhesion molecule-1 (VCAM-1) and very late antigen-4 (VLA-4) [244,255]. These adhesion molecules retain and localise the HSCs in bone marrow niche. In case of depletion of blood cells or exhaustion of HSC, osteoblastic cells secrete Dickkopf-1 inhibitor of Wnt signalling which leads to loss of stem cell quiescence[257] [257]. The notch ligand, Jagged-1, expressed by endosteal cells leads to clonal expansion of HSCs, increasing their pool size [258] (Figure 1.4). Transforming growth factor-beta (TGF-β) is a negative regulator of HSC proliferation and induces quiescence [259]. Bone morphogenetic proteins (BMPs)-2 and -7 at high concentration inhibits proliferation, while BMP-4 negatively affects their survival whereas at lower concentration they stimulate proliferation and differentiation of HSCs [260]. Endothelial cells and bone marrow stromal cells express CXCL12 while HSCs express CXCR4, which regulates their mobilization and homing. Endothelial cells express P-selectin and E-selectin while HSCs express glycoprotein-1 which helps in transmigration of HSCs into the niche [261]. Migration of HSCs to endosteal niche after transplantation occurs with the help of hyaluronic acid (HA) [262]. Thus, perivascular niche regulates the haematopoiesis and support the self-renewal of HSCs as well as their regulation between two niches deciding the HSCs fate.

1.8 Leukemic niche in haematological malignancies

Leukaemia stem cells (LSCs) give rise to leukemic cells leading to propagation of leukaemia. It has been postulated the normal HSCs are expelled from the bone marrow niche by LSCs and the resulting microenvironment favours leukemogenesis [220]. During leukemogenesis, malignant clones become independent of bone marrow niche mediated physiological control mechanisms. In early disease onset, bone marrow homing and localisation of LSCs or pre-

LSCs is similar to that of normal HSCs [221]. There is also increasing evidence that the microenvironment protects the LSCs from chemotherapeutics [263-265]. Xenograft transplantation assay in mice has revealed the role of microenvironmental factors in LSC engraftment, cell-cycle regulation and chemoresistance. $CD34^{+}/CD38^{-}$ leukemic stem cells engraft to endosteal niche of NOD-SCID mice, these cells were found to be quiescent and resistant to therapy [266-269].

Homing to microenvironment is the most important factor in sustaining AML by LSC survival. Several studies have shown the mounting evidence that LSC hijacks the microenvironment and dictates to its advantage [270,271]. It has been shown that AML generated by MLL-AF9 chromosomal translocation depends on microenvironmental signals or cue for immunophenotypic differentiation. In a study conducted by Wei J and colleagues, it was found that cord blood cells transformed with MLL-AF9 when transplanted into NOD/SCID mice transgenic for cytokine production of SCF, GM-CSF and IL-3 develops into AML [272]. This indicates the role of host microenvironment in determining the lineage fate and immunophenotypic difference [220]. Alteration in phenotype and functional properties were found in the mesenchymal stromal cells (MSCs) derived from AML patient and healthy donor. This corrupted component of leukemic niche co-operates with leukemic initiating cells (LICs) to maintain their dormancy and survival. Mutations in stromal cells have a primary role in AML initiation. Blau and colleagues has found the cytogenetic abnormalities in the stromal cells of AML patients [273]. BMSC from AML and MDS patient's shows chromosomal abnormalities which are not clonal and differ from haematopoietic cells. Suggesting that for leukaemia development genetic alterations are accumulated in BMSC [274]. Despite heterogeneity in AML, BMSCs heterogeneity has been found to be minimal across subtypes, suggesting that BMSCs could be a universal target in AML therapy [275]. Deletion of Dicer 1 (RNA processor and miRNA synthesizer) in osterix expressing osteoprogenitor cells in mouse model causes MDS or occasionally secondary AML [276] suggesting that dysfunctional osteoblast precursors could mediate clonal evolution. Similarly, activation of beta-catenin in osteoblasts results in dysregulated haematopoiesis similar to that in human AML. Suggesting that the altered osteogenic niche could induce damage to long-term haematopoietic stem cells (LT-HSCs) and transform them to pre-leukemic or leukemic cells [277]. Mutant allele of protein tyrosine phosphatase SHP2 (Ptpn11) in osteoprogenitor cells or $Nestin^{+}$ MSC can develop myeloproliferative neoplasm (MPN) which lead to development of AML in animal studies [278]. Collectively it is increasing recognised that genetic aberrations in endosteal compartment could be a key event in AML initiation and disease progression [279]. Bone marrow-derived MSCs from AML patients have altered exosome micro-RNA profiles [280]. Mitochondrial transfer also occur between BMSCs and AML blasts protecting them against chemotherapeutics [281,282]. These modes of cellular or soluble mediator communication between BMSC and AML could alter BMSCs in AML.

Huang and colleagues have shown higher expression of CD146 and CD105 in MSCs found derived from AML patients as compared to healthy control [274]. CD146 is a cell adhesion

molecule and its increased expression helps bone marrow support the cell renewal of LSC. AML derived MSCs have also shown higher expression of CD271, which can help in expansion of leukemic blasts through CXCL12 [283]. It has been shown that bone marrow mesenchymal stromal cells from newly diagnosed AML patients have upregulated cytokine related genes and downregulated cell cycle-related genes [284]. Leukaemia cells remodelled the niche by regulating the cross-talk molecules CXCL12 and Jagged-1 to favour leukemogenesis [284]. Endothelial cells communicate with AML cells through paracrine signalling via Vascular endothelial growth factor (VEGF) leading to AML development and progression [285].

Battula and colleagues illustrated that AML cells induce osteoblastic differentiation of mesenchymal stromal cells through BMP signalling [286] thus favouring the osteoblastic niche to help in AML expansion. IDH1/IDH2 mutated AML produce high levels of oncometabolite 2-hydroxyglutarate (2-HG) which can alter the differentiation of AML cells but also affects the bone marrow stromal cells by upregulating the NF-kB pathway. This higher NF-kB gene signature leads to enhanced proliferation and chemoresistance in AML cells [180,287]. In a study by Ye and colleagues, it was shown that LSCs interact with adipose tissue leading to lipolysis in them, which in turn promote the fatty acid metabolism and chemoresistance in LSC [263]. Differences in BMSCs isolated from AML patients as compared with their healthy donors have highlighted differences in their morphology [288], growth rate [289], altered osteogenic or adipogenic differentiation capacity [286,289,290] [291], altered methylation signatures [289], and altered ability to support normal hematopoietic stem and progenitor cells [288,289].

AML derived exosomes have been indicated to regulate the bone marrow niche by interfering with the function of bone marrow stromal cells by altering the secretion of cytokines [292]. Exosomes are the critical mediators of intercellular signalling by reprogramming the stromal cells to support the leukaemia promoting microenvironment by enhancing the cell proliferation, promoting angiogenesis and secreting cytokines [293]. Lagadinou and colleagues found that AML cells depend on oxidative phosphorylation for survival while normal HSC utilises glycolysis. Therefore, targeting oxidative phosphorylation can selectively affect the leukaemic blasts [294].

The above discussion suggests that leukemic cells create their malignant niche, which favours the LSC over normal HSCs. Leukaemia cells compete with normal HSCs for the niche and inhibit haematopoiesis by deregulating the HSC functions. Targeting these interactions represents a novel and promising therapeutic avenue in treating AML.

1.9 Targeting AML-bone marrow microenvironment interaction

Although there are a large number of targeted therapies to treat AML, yet patient outcome remains poor. This indicates a clear and urgent need for better treatment strategies.

Understanding of the niche-mediated drug resistance is growing which in turn benefits the identification of the interactions within BMM that influences the AML survival and progression to identify novel druggable targets. Translating the knowledge and biological insights into meaningful clinical insights for AML patients is challenging.

One of the major challenges encountered is targeting the interactions between the leukemic cells and their niche to selectively target the LSC as opposed to normal HSCs. Potential targets include cytokine signalling, self-renewal pathways like Notch or Wnt signalling, homing mechanisms, or cell adhesion molecules. Niche regulation of LSC quiescence to allow long-term self-renewal potential indicates the importance of quiescence. Ito and colleagues have shown that targeting the promyelocytic leukaemia protein (PML) by arsenic trioxide (As_2O_3) leads to loss of self-renewal capacity of CML-LSCs by breaking their dormancy [295]. This suggests that uncoupling the LSC from their protective niche can make LSC enter the cell cycle and thus, make them responsive to chemotherapeutics. CXCL12-CXCR4 signalling promotes the localization of LSC into bone marrow niche. Targeting CXCL12-CXCR4 axis can effectively mobilise leukemic cells out of their niche [296] and effectively target them by CXCR4 antagonist, plerixafor (AMD3100) or LY2510924 [297,298]. CD44 (Hyaluronic acid receptor) can mediate localization of LSC in BM niche, making it a promising target [299,300]. Jacamo and colleagues found that interaction between leukemic cells and BMM, mediated through VCAM-1/VLA-4, induces NF-κB activation [301]. Therefore, targeting NF-kB by small molecule inhibitor [302] and VCAM-1 [303] may be useful in targeting the leukemic cells. Proteasome inhibitors are also attractive due to their diverse effect in inhibiting cytokine-signalling pathways. Liesveld and colleagues illustrate the role of bortezomib in inhibiting the migration of leukemic blasts to CXCL12 derived from stromal cells [304]. Epigenetic chromatin modifiers such as histone deacetylase (HDAC) inhibitors have strong effect on leukemic blasts including repression of self-renewal pathway [305].

Although it remains unclear whether these niche targeting therapies mediate their effect through synergistic cytotoxicity, overcoming stromal cell-derived chemoprotection or specific targeting of LSCs by enforced cell cycling and loss of quiescence/dormancy. These therapies must also maintain the homeostasis for HSCs and promotes HSC regeneration. Niche residing leukemic cells may lead to relapse of the disease after the withdrawal of treatment. The role of bone marrow niche in conferring protection to leukemic cells against any type of therapy either through paracrine soluble factors or through direct cell-cell contact has been well established. The BMM is a critical regulatory component in the development and survival of AML *in vivo*. Standard cell line-based assays for cell viability and cell death are not enough to identify the compounds that are able to target LSCs seeded in their soil (BMM). Therefore, a well-designed high-through *in vitro* co-culture system mimicking the BMM is required to better target the bidirectional crosstalk between them and to identify new targets [306]. These systems will enable modelling of the complex BMM consisting of leukemic cells and their counterpart cells (stromal cells, endothelial cells etc), so that potent and efficient molecule can be identified in a high-throughput manner.

Challenges will remain in knowing the effect of targeting the BMM interaction selectively and how it will affect the LSCs or normal HSCs. It should also be noted that perhaps the LSCs might migrate to other niches in the body like spleen if they were mobilised from the bone marrow. Combination with chemotherapy will remain critical in order to target them efficiently along with the sequence of treatment. Therefore, it is important to model the bone marrow microenvironment *in vitro* to study the effect of its components on AML cell survival, differentiation and to develop better drug screens that considers and targets AML in this complexity so that new improved therapeutics will come out to better target leukaemia.

1.10 Experimental tools to model the bone marrow microenvironment

AML is characterised by a hierarchical structure, where a small population of leukemic stem cells or leukemia-initiating cells (LSCs) give rise to the abnormal, partially differentiated AML blast population [6]. LSCs, although malignantly transformed, share many properties with normal hematopoietic stem cells (HSCs): they reside in the bone marrow (BM) and depending on the signals received from their microenvironment, they either lay dormant or actively proliferate, but most importantly, they depend on BM-derived signals for survival [225,307,308](Figure 1.4).

The bone marrow is one of the most complex and dynamic tissue microenvironments in the human body. It co-ordinates the production and fate of over 500 billion blood cells daily by instructing the processes of HSC pool maintenance, HSC clonal expansion and production of all red and white blood cell populations [309]. These processes are regulated by the co-ordinated action of the various cell constituents of the hematopoietic microenvironment (or hematopoietic niche), including arteriolar and sinusoidal endothelial cells, osteoblasts (OB), adipocytes, sympathetic neurons, Schwann cells, mesenchymal stromal cells (MSC) and reticular cells [310]. Modelling this complex microenvironment has been a challenge and thus up to very recently *in vivo* models dominated the pre-clinical stage of drug discovery studies (Figure 1.5A).

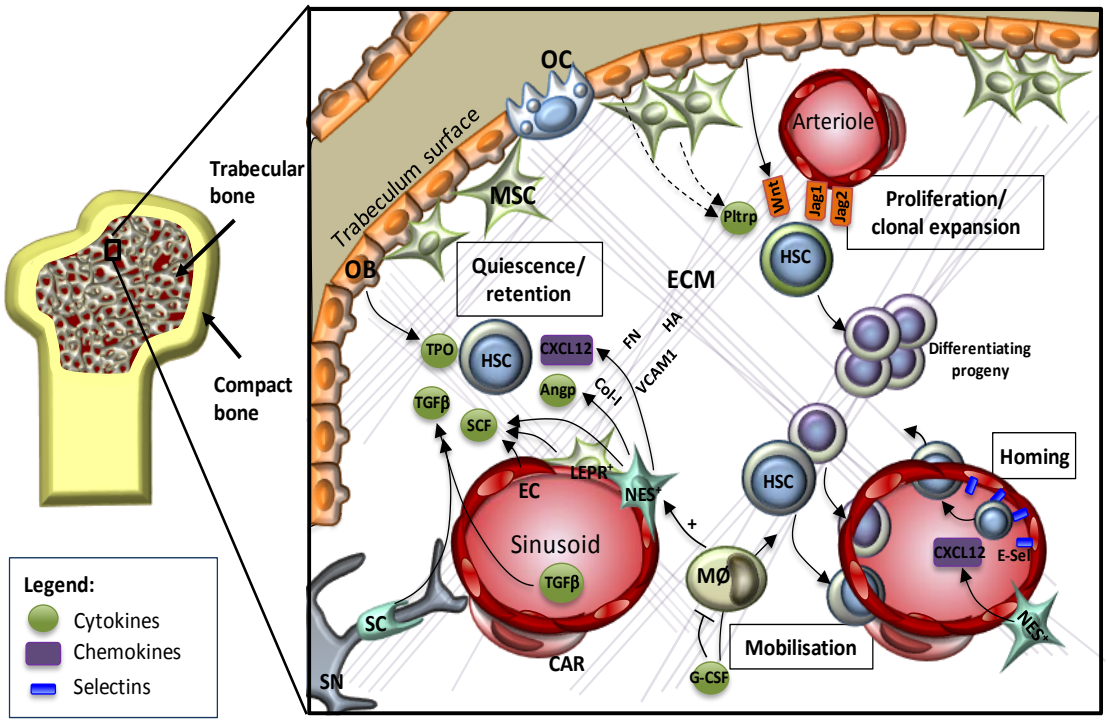

Figure 1.4: The bone marrow hematopoietic niche and its molecular interactions driving quiescence, trafficking and clonal expansion of hematopoietic stem cells (HSC). Trafficking of HSCs involves their homing to the niche and their mobilisation. HSCs traffic in and out of the niche rhythmically, following the circadian cycle signalled by sympathetic neurons (SN). To home to the bone marrow, they follow chemokine gradients, such as that of CXCL-12 secreted by Nestin-expressing (Nes^+) and other bone marrow (BM) stromal cells and bind to the vessel walls by recognising glycan structures, such as E-Selectin on BM-endothelial cells followed by extravasation. Mobilisation of HSCs and their differentiated progeny is triggered by reduced CXCL-12 and other chemokine expression and by increased levels of granulocyte colony stimulating factor (G-CSF). G-CSF triggers mobilisation through a monocyte/macrophage (MØ)-dependent and independent manner, the latter being much less characterised. MØ promote CXCL-12 expression by perivascular stromal cells and endothelial cells (EC). G-CSF depletes MØ and thus reduces CXCL-12 expression. HSCs are retained in the BM niche by multiple signals, including CXCL-12, interaction with ECM components, such as vascular cell adhesion molecule-1 (VCAM-1), fibronectin (Fn), collagen-1 (Col-1) and hyaluronic acid (HA). Long term HSCs are maintained in a quiescent state in the BM by transforming growth factor beta (TGFβ), angiopoietin (Angp), stem cell factor (SCF), thrombopoietin (TPO). TGFβ is produced systemically, mostly by the liver in an inactive form and activated by proteases produced by Schwann cells (SC). SCF is produced by EC, Nes^+ mesenchymal stroma cells (MSC) and leptin receptor expressing (LEPR+) MSCs located in the perivascular region, while TPO is produced by osteoblasts (OB) of the endosteal region. HSCs proliferate in specific pockets of the BM to regenerate the blood cell populations, which is mediated by canonical and non-canonical Wnt signalling, Notch ligands, Jagged-1 (Jag-1) and Jagged-2 (Jag-2) and the cytokine, pleiotropin (pltrp) expressed by BM stromal cells depending on the progeny (erythroid, lymphoid, myeloid etc.). OC: osteoclasts.

1.10.1 *In vivo* models

Zebrafish models of AML: Identification and dissection of normal haematopoiesis and the realisation that its molecular pathways are evolutionarily conserved have paved the way for the development of leukemia models in zebrafish [311]. Of particular importance is that most genes involved in the cancer-relevant cellular signal transduction pathways, such as apoptosis and cell cycle regulation, oncogenes and tumour suppressors as well as critical transcription factors controlling cellular differentiation (e.g. Hox and Pu.1) are conserved between zebrafish and humans [312]. The ability to generate transgenic zebrafish lines and to manipulate single-

cell stage embryos *ex vivo* using morpholinos to introduce mutations or knock genes down has provided a robust platform for generating clinically-relevant models of AML (e.g. AML bearing cytoplasmic nucleophosmin (NPMc+ AML) [313], NUP98-HOXA9 transgenic zebrafish modelling HOXA9 overexpressing AML [314] as well as MYC and FLT3-driven AML [315,316]). These models have been used for high-throughput genetic and chemical screens to identify suppressors and inhibitors of leukemia [317]. The main limitations of the zebrafish models are that the site of haematopoiesis is the kidneys as opposed to the BM, and how the cellular constituents of the zebrafish hematopoietic niche compare to the human hematopoietic system is not well characterised [318,319].

Mouse models of AML: Rodents are the most used *in vivo* study organisms of AML. Similar to humans, adult haematopoiesis in the mouse takes place in the BM and currently the mouse is the best-characterised animal model of the BM niche. Inbred strains of mice have been used to study leukaemia since the 1930's using either inoculation of human leukemic cells [320,321] or mutagene [322] treatment. Several mouse strains, such as the AKR mice [323,324] develop spontaneous leukaemia over time caused by the murine retrovirus MCF 247 they carry in their genome [325]. Although these spontaneous models resemble the human disease and contributed to our understanding of the biology of AML, the inconsistency in time required to disease onset, the low or variable penetrance and overall poor response to therapy meant they were unsuitable for drug discovery studies. Mouse models generated by insertional mutagenesis, primarily using murine leukemia viruses (MuLV) produced more consistent disease onset and more predictable disease progression [326]. Indeed, these models helped to identify over 90 AML-associated genes, including hoxa9 and meis1 and significantly contributed to the current view of the genetic lesions that drive AML.

The landmark technology of genetic engineering (transgenetics) using homologous recombination [327] provided the platform for the design, development and application of a vast array of mouse models of AML. The genetically engineered mouse models (GEMM) of AML include gene knock-in, translocator and invertor-based methods using conditional alleles to investigate chromosomal translocations associated with AML, such as MLL and Ews-ERG gene fusions [328]. Although streamlined, the generation of germline GEMMs is labour intensive and slow process ultimately producing only a small number of offspring with the required genotype. In addition, germline GEMMs often demonstrate heterogeneity in disease penetrance and burden making the interpretation of pre-clinical drug testing difficult.

The increasing demand for *in vivo* models due to the growing number of identified oncogenic mutations led to the development of non-germline GEMMs (nGEMMs), where the genetic modification is introduced only in the HSC population *ex vivo,* which is then transplanted into the mice. Importantly, the first nGEMMs carrying the AML-specific AML1-ETO or the MLL-AF9 fusion protein in mice closely replicated the human risk profile of these mutations [329].

The very recent advance in the nGEMM technology [330] has used CRISPR-Cas9 gene editing to introduce a combination of multiple leukemogenic mutations. A combination of

mutations could be introduced in mouse HSCs by transducing them *ex vivo* with a pool of Cas9 and small guide RNA (sgRNA)-expressing lentiviruses that target AML-associated genes and then re-injecting the HSCs into the mice. It must be noted that the resulting HSC pool is not homogeneous, the individual cells carry mutations in a subset of the targeted genes. Accordingly, not all animals develop AML and it cannot be controlled which mutation combination is present in a given animal, making this approach more an investigational tool for the study of leukemogenesis than a translational tool.

An alternative to genetic models is xenograft models where patient-derived AML cells are transplanted into recipient animals, predominantly zebrafish [331,332] or mouse [333,334]. Whilst the zebrafish is relatively immunologically naïve and thus does not reject the xenotransplant, to achieve AML cell engraftment in mice, immunodeficient recipient mice, such as the Non-obese diabetic mice with severe combined immunodeficiency (NOD/SCID) or NSG mice (NOD-SCID/interleukin-2 receptor γ null (IL2rγ)) have to be used [335]. Even in these mice, engraftment of the AML cells is still partial. Thus, the ability of the engrafted fraction of the AML cells to fully replicate the human disease is debated. To study the chromosomal translocations involving chromosome 17 associated acute promyelocytic leukemia (APML), classical transgenic mouse model was developed to study the myeloid compartment. Expression of exogenous cDNA under the regulation of myeloid-specific sequences using human cathepsin-G (hCG) expression vector for murine models of PML-RARα (t15;17) [336],NPM/RARα (t5;17) [337] were generated.

An alternative xenotransplantation approach that is currently gaining space is the establishment of subcutaneous, extramedullar bone marrow [338]. In these models, bone marrow-derived mesenchymal stromal cells (MSC) are implanted subcutaneously in a scaffold, such as matrigel [339], or calcium phosphate particles [340]. The implanted cells differentiate into a small bone (ossicle) harbouring a trabecular region and marrow with an apparently complete hematopoietic machinery. The advantages of this model are that (1) it is nearly fully human that enhances the engraftment efficacy of human leukemic cells (2) and the fact that both the stromal and the leukemic component can be genetically modified prior to implantation.

One of the well-characterised humanised bone marrow models has been described by Chen and colleagues [339]. They transplanted human MSCs and endothelial colony forming cells in a matrigel scaffold subcutaneously into NSG mice. After 8 weeks, the transplanted cells have differentiated and formed a human bone-like tissue with trabecular structure and marrow providing a fully functional hematopoietic niche into which human AML cells could effectively engraft and developed extensive hypoxic regions, characteristic of the human leukemic bone marrow.

Human immune system and the BMM are the most difficult to be replicate in mouse models because of the differences in the signalling molecules responsible for the maturation of various hematopoietic cell populations [341]. As a result, many malignant hematopoietic disorders do

not successfully engraft in conventional mice models. AML is one of these malignancies that fail to properly graft into the existing strains of mice due to the lack of a proper BMM, homing elements, absence of specific human growth factors and supporting stromal cells [342]. As a result, efforts were made to develop murine models that can faithfully reproduce human haematopoiesis.

Early attempts to increase the support for myelopoiesis involved the use of mice injected with IL-3, GM-CSF, SCF [343], mice producing human thrombopoietin (TPO) [344] or MISTRG mice strain which produces human tumour necrosis factor (TNF) and interleukin-6 (IL-6) [345]. These confirmed that the introduction of human genes into mice led to the production of functional proteins capable of supporting engraftment and proliferation of human grafts. McIntosh and colleagues have developed a mouse model that can support the human AML cells in mouse bone marrow niches via depletion of mouse stroma cells through mutations in c-kit gene. SCF plays an important role in maintenance and differentiation of HSCs [346]. The c-kit mutated mice strain, known as NODB6.SCID Il2rγ$^{-/-}$ Kit (W41/W41) (NBSGW) mice, supports engraftment studies with human HSCs without prior irradiation. W41-NBSGW has higher level of CD45^{+} in bone marrow than non-irradiated NSG mice.

The need for the supporting cytokines for the human myeloid cells was overcome by transgenic expression of hSCF, hGM-SCF and hIL-3 in NOD SCID mice resulting in NSG-SGM3 mouse strain or NOD.Cg-*Prkdc*^{scid}*Il2rg*^{tm1Wjl}Tg(CMV-IL3,CSF2,KITLG)/1Eav) [342]. NSG-SGM3 mouse model can engraft CD34^{+} cells from normal and AML xenografts and has higher rate of engraftment as compared to NSG mice [347]. Klco and colleagues has shown higher rate of bone marrow engraftment and CD34^{+} expression levels in NSG-SGM3 mice as compared to NSG mice [348].

NSG-S mice strain developed by Krevvata and colleagues has a knock-in for human stem cell factor (hSCF), human granulocyte-macrophage colony-stimulating factor (hGM-CSF) and human interleukin-3 (hIL-3) in NSG background mice. 82% of primary AML samples engrafted with higher leukemic burden and shorted survival as compared to NSG mice [349].

Another humanised mice developed by Flavell's team where mice is repopulated with human immune system. MISTRG are immunodeficient mice lacking T and B lymphocytes and NK cells, preventing rejection of human grafts. These mice express human SIRPa protein which protects the human cells phagocytosis. MISTRG has 4 genes encoding human cytokines M-CSF$^{h/h}$ IL-3/GM-CSF$^{h/h}$ hSIRPA^{tg} TPO$^{h/h}$ Rag2$^{-/-}$ Il2rg$^{-/-}$. MISTRG supports the engraftment of HSPCs and supports the maintenance of these cells in serial transplantation assay. This model is unique in supporting the development of functional monocytes and macrophages and natural killer cells [345,350].

AML xenotransplantation into immunodeficient murine models is a valuable tool for the expansion and study of some aspects of the biology of human AML. Xenotransplantation models are still limited by their inability to address the interplay of leukemic blasts with different cells of the immune system and to dissect the cell autonomous from cell non-cell autonomous

aspect of the disease as they tend to develop other spontaneous malignancies. To overcome these limitations, new advances in the fields of bioengineering and synthetic material development to create biological inserts or scaffolds [351]. These scaffolds help in creating a humanised microenvironment in mouse that can efficiently support graft cell expansion and differentiation. Ceramic scaffolds coated with human mesenchymal stromal cells (hMSCs) when implanted subcutaneously in NSG mice were able to support the non-engrafting AML samples. The scaffold supported their proliferation, maintained clonal heterogeneity and LSC self-renewal capacity [352]. To study the AML heterogeneous sub-clones detection patient samples, Chao and colleagues developed an induced pluripotent stem cells (iPSC) techniques to establish AML-iPSC. AML-iPSC do not possess a transformed phenotype; however, these cells retain their leukemic potential upon induced hematopoietic differentiation and are able to induce disease in NSG mice [353]. Interestingly, when stimulated to differentiate towards non-hematopoietic lineage, AML-derived iPSC are able to form non-malignant cells from all three embryonic germ layers.

Extramedullar, humanised or chimeric bone marrow systems are currently being tested for translational models of not only AML, but also for ALL and MM [340,354,355]. While mouse models can recapitulate multiple features of the BMM, they are time and labour intensive requiring several weeks for the establishment of the leukaemia even in the fastest, extramedullar bone marrow models due to which they are not well suited for high throughput drug screens or detailed mechanistic studies. To address this gap, sophisticated *ex vivo* AML culture models are being developed (Figure 1.5A and Table 1.5).

Table 1.5: Cytokine combinations used in *ex vivo* HSC and AML cultures.

Cytokine cocktail	Cell type	Culture media/Stromal support	References
SCF, IL-3, IL-6, FLT-3L, TPO	Cord blood $CD34^+$ cells	IMDM+ FCS/Stroma free culture	[356]
IL-3, G-CSF, TPO	Peripheral blood and bone marrow derived $CD34^+$ cells	LTC medium (Alpha MEM, FCS, Horse serum, β-mercaptoethanol, hydrocortisone/ MS-5 stromal cell support	[357]
FLT-3L, SCF, IL-3	Peripheral blood $CD34^+$ cells	RPMI1640/ BM-MSC stromal cell support	[358]
IL3, TPO, G-CSF	Leukemic stem cells	Myelocult H5100 medium/ MS-5 stromal support	[359]
SCF, TPO, FLT-3L, IL-6	Umbilical cord blood $CD34^+$ cells	Stemspan serum free medium/ BM-MSC or UC-MSC stromal support	[360]
SCF, IL-3, GM-CSF, G-CSF	Cord blood mononuclear cells	IMDM, 10% FBS/ stroma free culture	[361]
SCF, GM-CSF, IL3, TPO, FLT-3L	Cord blood $CD34^+$ cells	IMDM, FCS /Stroma free culture	[362]

SCF, GM-CSF, IL-3, TPO, IL-6	Cord blood $CD34^+$ cells	IMDM, FCS /Stroma free culture	[362]
SCF, TPO, FLT-3L,IL-3, G-CSF, IL-6, GM-CSF, SCGF, IL-11	Cord blood mononuclear cells ($CD34^+CD38^-$, CFC, LTC-IC)	IMDM, BSA, Insulin, Transferrin/ Stroma free culture	[363]
SCF, TPO, FGF1, Angptl-5, IGFBP2	Cord blood $CD34^+$ cells	Stem span serum free medium/ Umbilical cord MSC stromal support	[364]
SCF, TPO, FLT-3L, IL-3, IL-6, GM-CSF, G-CSF, EPO	Cord blood $CD34^+$ cells	Myelocult medium/ BM-MSC stromal support	[365]
SCF, FLT-3L, TPO	Cord blood $CD34^+$ $CD38^-$ cells	BIT 9500 medium/ Stroma free culture	[366]
SCF, FLT-3L, TPO, IL-3, IL-6, G-CSF, GM-CSF	Umbilical cord blood $CD34^+$ cells	Stemspan serum free medium/ Stroma free culture	[367]

SCF- Stem cell factor, GM-CSF- Granulocyte-macrophage colony stimulating factor, G-CSF- Granulocyte colony stimulating factor, FLT-3L- Fms-like tyrosine kinase 3 ligand, TPO- Thrombopoetin, IL-3- Interleukin-3, IL-6- Interleukin-6, EPO- Erythropoetin, FGF-1- Fibroblast growth factor-1, Angptl-5- Angiopoietin like-5, IGFBP2- Insulin-like growth factor binding protein-2.

1.10.2 Layered stroma-AML co-culture models

The first BM stroma-AML culture models were based on *ex vivo* culture models of healthy hematopoietic stem cells developed to study the process of HSC differentiation. One of the first of these models was the Dexter culture model [369] (Figure 1.5 B). The basal cell layer in the Dexter culture consisted of mixed BM stromal cells obtained by flushing out the marrow from mouse femurs and sub-culturing the adherent cell fraction. After establishing the stromal cell layer, HSCs - also isolated from mouse BM - were seeded onto it. The feeder stromal cell layer could maintain prolonged HSC viability and stemness (over 7-12 weeks), especially when the culture medium was supplemented with cytokines [370,371], which could not be achieved in pure HSC cultures. This advantage could be due to the direct cell-cell interaction between HSC and BM stromal cells in addition to the stromal-secreted paracrine factors. The Dexter model still forms the basis of many HSC and AML *ex vivo* culture models. These models vary in the subset of BM cellular components and paracrine factors incorporated and the incorporation of a 3D scaffold or not.

Cytokine-supplemented culture system: A major mechanism by which the BM niche supports HSC function is the secretion of cytokines and chemokines. Soluble factors like CXC motif chemokine ligand 12 (CXCL12, also known as stromal derived factor 1α, SDF1α), interleukin-1 (IL-1), IL-6, IL-8, thrombopoietin (TPO) and Flt3 ligand (FL) are known BM-derived trophic factors that control the survival and expansion of hematopoietic stem cells [356,372-374]. The

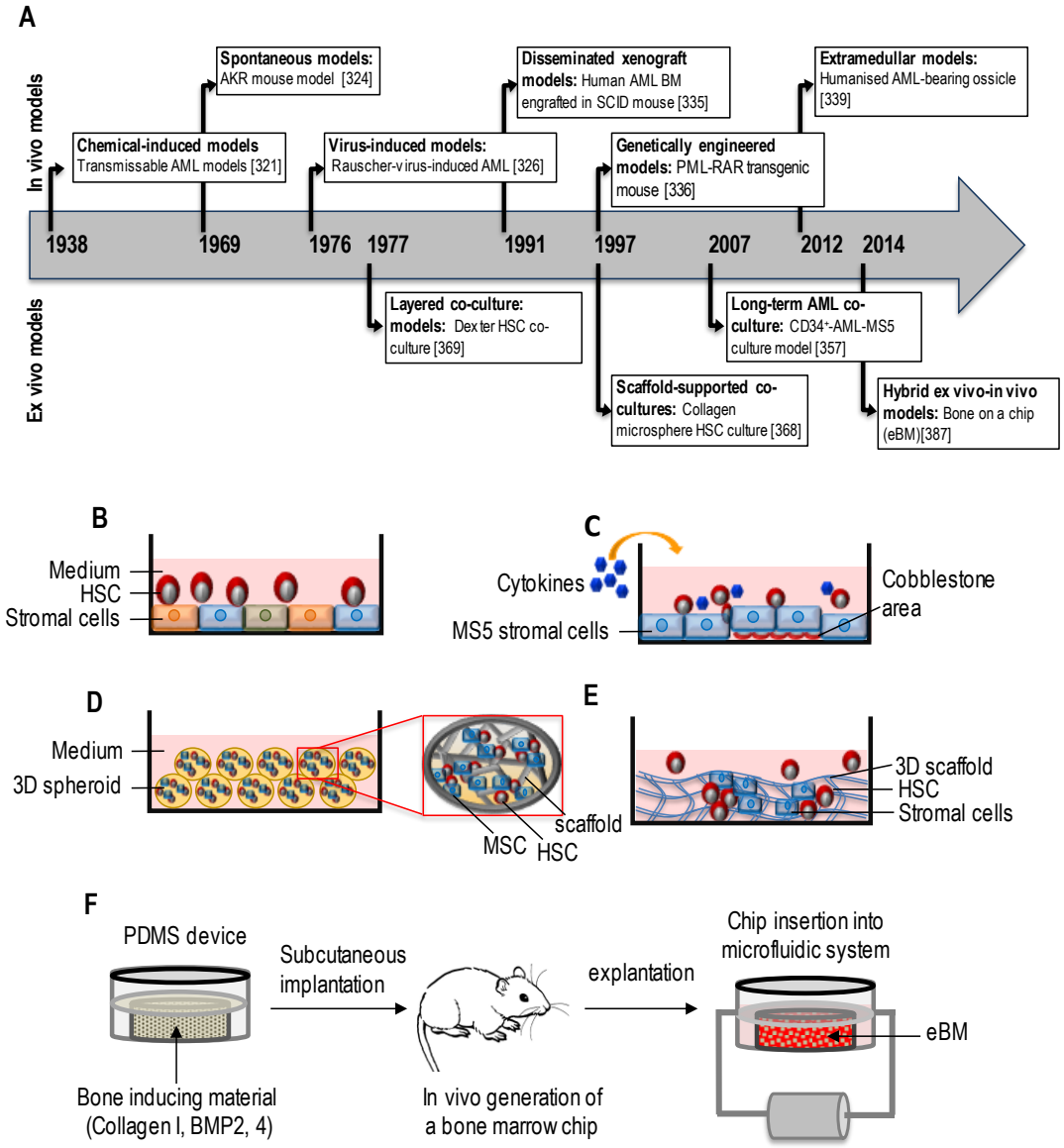

Figure 1.5: *In vivo* and *ex vivo* culture models. (A) The history of in vivo and ex vivo experimental AML model development. The boxes show the year when each model has been developed and the first example published. (B-F) The configuration of the different ex vivo culture models. (B) Dexter culture system where primary HSC cells are co-cultured with the adherent cell fraction of primary bone marrow aspirates. (C) Long-term AML-MSC co-culture developed by Gosliga and colleagues [357]. (D, E) Scaffold-supported 3D culture models. (D) Microspheroid HSC-bone marrow stroma culture developed by the Wu laboratory [368] where a collage scaffold is used to mimic the 3D bone marrow structure. (E) Non –microsphere scaffold culture. The 3D scaffold can derive from decellularised extracellular matrix, collagen, hydrogels, hydroxyapaptite-collagen combinations, synthetic scaffolds etc. (F) Hybrid in vivo-ex vivo models. Bone on a chip recently developed where bone marrow is formed in vivo in a PDMS capsule containing bone-inducing material (BMP: bone morphogenic protein) subcutaneously implanted into mouse. This engineered bone marrow (eBM) implant can then be explanted and maintained ex vivo in using a microfluidic system.

increasing understanding of the paracrine regulation of HSC function and the opportunity to gain a highly reproducible and tightly controllable model, pure HSC cultures have been tested where instead of a stromal feeder layer, the culture medium was supplemented with recombinant cytokines only (for a summary of the cytokine use of the various *ex vivo* models, please refer to Table 1.5). In comparison to the Dexter model, the cytokine cocktail alone could

support HSC viability only for a shorter period of time. Additionally, the increasing recognition of the impact of the direct interactions between the stroma and HSCs on HSC functionality and AML drug resistance deemed this model unsuitable for drug testing studies.

Based on the Dexter culture system, Gosliga and colleagues developed and extensively tested the first long-term co-culture system for the *ex vivo* maintenance of primary AML cells [357,375] (Figure 1.5C). The culture was based on an immortalised mouse BM mesenchymal stromal cell line (MS5) as the feeder layer onto which primary, patient-derived AML cells were seeded. The great advantage of the MS5 cells is that the confluent cell layers can be stably maintained for prolonged periods of time. Many other immortalised MSC cell lines lack this feature (e.g. HS5) that makes them unsuited for long-term cultures. While irradiation can be applied to gain a non-proliferating MSC culture, the irradiation-induced DNA damage and cellular senescence can have unpredictable effects on the AML cells. For example, HS5 cells show variable, inconsistent responsiveness to irradiation with regards to cell cycle arrest and the irradiated cell culture deteriorates within a 3-5 day period (unpublished observations, ES lab). Other modification that the Gosliga culture system included was 12.5% horse serum (in addition to 12.5% foetal calf serum) and exogenous supplement of the cytokines IL-3, granulocyte colony-stimulating factor (G-CSF) and thrombopoietin (TPO).

In this co-culture the $CD34^+$ immature cell population - that includes LSCs - penetrated beneath the MS5 feeder layer and formed little clusters. These clusters appeared as so-called cobblestone areas, which are non-reflectile regions when the culture is visualised by light microscopy (Figure 1.5C). The cobblestone areas of the $CD34^+$ population maintained self-renewal capacity and the ability to generate the more differentiated AML blast progeny, which appeared as the cell fraction floating above or loosely attached to the upper surface of the MS5 feeder layer. The cobblestone-forming cells could be serially re-plated on MS5 feeder for several weeks without losing this hierarchical organisation (LSCs generating more differentiated blast cells). Unfortunately, the feeder-layer generated ECM or the drug responsiveness properties of the AML cells in this culture have not been tested or compared to that of *in vivo* models. A shortcoming of this model is the mouse-origin of the feeder layer that may not mimic the human stromal cell features sufficiently. Finally, the co-culture can only model the BM MSC-AML interactions as no osteoblasts, endothelial cells or other BM stromal cell types are incorporated.

In order to address the species incompatibility, Ito and colleagues have tested a co-culture model where primary human BM stroma was used as a feeder layer [358]. For the co-culture, the feeder layer was generated from the adherent cell fraction of BM aspirates taken from healthy volunteers. Proliferation of the feeder cells was blocked by exposing them to a high dose (50 Gy) of irradiation. This feeder layer could support AML survival between 4-6 weeks. Interestingly, supplementation of the culture with recombinant IL-3, FLT3 ligand and stem cell factor (SCF) led to a rapid and very substantial drop in the $CD34^+/CD38^-$ LSC-harbouring

population, which could be due to the quiescence-promoting effect of SCF highlighting the need for comprehensive testing of the correct cytokine cocktail supplementation.

The Bonnet laboratory further developed the layered co-culture system and compared the drug response of AML cells maintained *ex vivo* to that of *in vivo* using immunodeficient mouse models in a small AML sample cohort [359]. The study found that BM-MSCs had a higher potency to support AML cell survival than HUVEC endothelial cells or the osteoblast-derived SAOS2 osteosarcoma cells and in transplantation assays they found that low O_2 (3%) concentration supports LSC self-renewal over normoxic conditions. The niche-like conditions consisted of MS5 stromal layer supplemented with IL-3, G-CSF and TPO in hypoxic conditions. Importantly, in this *ex vivo* culture primary AML cells displayed a comparable sensitivity profile to cytarabine as *in vivo* in mice, emphasizing that even a relatively simple and easy to control *ex vivo* model system may be sufficient to mimic the effect of the leukemic BMM on drug resistance.

The layered co-culture system has also been applied for specialised high-throughput drug screening [376]. The Golub laboratory screened over 14,700 compounds to identify drugs that could selectively kill LSCs receiving stromal support using layered co-culture. The screen allowed the identification of drugs that eradicated LSCs via a non-cell-autonomous manner by impacting stromal function as well as drugs that directly targeted LSCs. The findings were corroborated with primary AML samples and by *in vivo* transplantation assays.

Overall, the layered co-culture models hold promise because they are cheap, allow tight control over the system components, easy to manipulate and perfectly scalable for both high-throughput testing and mechanistic studies. To determine their true potential, their ability to replicate the *in vivo* drug response of AML cells is essential. These studies would need to comprehensively characterise the culture models with regards the actual cellular composition of the used stromal feeder layer, the stroma-produced ECM and paracrine factors and finally the differences between the different sources of stromal feeders, such as healthy versus leukemic and between individual AML patients.

1.10.3 Scaffold-supported AML-stroma co-culture models

A major question about the layered co-culture models is how faithfully they can represent the spatial, 3-dimensional trabecular bone microenvironment. In the layered co-culture the stromal cells are likely to be polarised as the basal surface of the cells (the one adhering to the culture dish surface) receives a very different set of signals from the apical side (exposed to the culture medium). To overcome these limitations, numerous biomimetic 3D models of HSC expansion and differentiation have been developed [377,378] using a broad range of biomimetic materials as scaffolds, such as collagen microspheres, hydrogels of natural or artificial origin, de-cellularised ECM extracts and synthetic polyacrylates with varying success. It is important that in order to model the 3D BMM the scaffolds need to be designed with properties comparable to that of the *in vivo* BM including pore size, surface area to volume

ratio and surface cell-adhesive features to allow free penetration of cells and establishment of cell-cell and cell-niche associations.

The first well characterised scaffold-supported HSC differentiation model has been described over 20 years ago by the Wu laboratory [368] where mouse BM-MSC and human BM-mononuclear cells (including HSCs) were seeded on microspheres generated from bovine collagen (Figure 1.5D). To simulate blood flow and increase nutrient supply within the microspheres the culture was perfused with Dexter's growth medium. This 3D collagen scaffold model was superior to the layered Dexter culture as it supported the differentiation of multiple blood cell lineages, which also confirms that inclusion of the 3D bone matrix creates a closer model of the BMM. Efforts were made to add more complexity to these models by addition of further ECM components [360], such as fibronectin, laminin and glucoseaminoglycans (heparin sulphate, hyaluronic acid). This avenue however is too complicated with questionable advantages when considering that the ECM is a supra-molecular structure, which is difficult to be replicated by mixing purified ECM components. Currently it is not clear to what level of complexity the BM ECM would need to be replicated in *ex vivo* models although increasing number of BM ECM components are being reported to contribute to AML cell homing, engraftment and consequent drug resistance. Thus, de-cellularised BM matrix or BM-MSC and osteoblast-produced ECM may be better sources of scaffolds [379,380].

Synthetic materials, such as polyethylene glycol derivatives (PEG), poly(glycolic acid), polyurethane (PU) and ploy(dimethylsiloxane) (PDMS) are also gaining attention for their easy to modulate properties and broad range of possible formulations (Figure1.5E). Since to date none of these models have been explored for AML, due to space restrictions, the details of these HSC culture models are not covered here (a summary and references provided in Table 1.6) [381,382].

Table 1.6: Scaffold-supported *ex vivo* AML-stroma culture models.

Source of biomaterial	Culture system	Bone marrow Components	Screened for drug sensitivity	References
Natural	Collagen scaffold	Isolated MSCs, $CD34^+$ HSCs	No	[360,368,383]
	Bone derived/ Decellularised scaffold	Mouse isolated MSCs and MS5 stromal cell derived ECM, $CD34^+$ HSCs	No	[383-385]
Synthetic	PEG hydrogels	Isolated MSCs, CD34+ HSCs	No	[379,386]
	PGA/PLLA/PLGA/ PU/PET/PVF/PMMA	Isolated MSCs, Leukemic cell lines	No	[364,381,382]
Chip	Bone inducing biomaterial	Whole bone marrow	No	[387,388]

PEG- Polyethylene glycol, PGA- Poly (glycolic acid), PLLA- Poly (L-lactic acid), PLGA-Poly (L-lactic-co-glycolic acid), PU- Polyurethane, PET-Polyethylene terephythlate, PVF- Polyvinyl formal, PMMA- Poly (methyl-methacrylate), PDMS- Poly (dimethylsiloxane).

1.10.4 Hybrid *in vivo*-*ex vivo* models

While *ex vivo* models are increasingly used (Figure 1.5A), until the *in vivo* leukemic BMM features are better characterised, there will be an uncertainty to what level and exactly what features of the *in vivo* BMM can be replicated in *ex vivo* conditions. To bridge this gap, the best BMM models incorporate an *in vivo* implantation stage, typically into mice. This allows population of a biomimetic scaffold by mouse MSCs and circulating HSCs and consequent establishment of a self-regulated hematopoietic niche. This niche has close resemblance to the natural BMM, with well-developed/distinguished endosteal and perivascular niches, multiple stromal cell types and ECM [339,387,388].

The first example of the hybrid models - developed by the Martin laboratory [387] - used a bioreactor to create the core unit *ex vivo* by perfusing a hydroxyapatite scaffold first with BM stromal cells to establish a stromal fraction followed by perfusion with HSCs. This core unit was then implanted subcutaneously into nude mice for 8 weeks. The implantation fostered not only haematopoiesis, but also ECM deposition, as well as vessel- and sinusoid formation.

The approach of the second hybrid model (engineered bone marrow; eBM), developed by the Ingber laboratory [388], was opposite to the above bioreactor model in the sense that establishment of the BMM occurred *in vivo* in an implanted scaffold-capsule, which was then removed and maintained *ex vivo* by connecting it to a microfluidic pump (Figure 1.5F). To establish the BMM, demineralised bone powder and bone morphogenetic proteins (BMP2 and BMP4), embedded in a cylindrical hole within a poly(dimethylsiloxane) (PDMS) disc was implanted subcutaneously in mice with the opening of the capsule facing towards the subcutaneous muscle layer. In the implanted unit a BM with blood supply and an outer shell of compact bone developed. Histological comparison of the eBM and bones confirmed that its morphology and cellular composition was nearly identical to that of the natural BM. After a 6-8 week implantation period, the chip could be removed and maintained *ex vivo* for several weeks with steady-state haematopoiesis. This model serves as a proof of concept for the creation of the hematopoietic BM tissue on a chip. This model was able to perform the complex functionalities of the hematopoietic niche and proved to be superior to the solely *ex vivo* models.

Unfortunately, none of the hybrid models have been tested for their ability to harbour and support AML cells, retain LSC functionality and replicate chemotherapy-resistance mediated by the leukemic BMM.

1.10.5 Concluding remarks

Therapeutic outcomes for AML patients have not improved significantly over the past twenty years. With the advance of genomics, new, promising drug targets have been identified. However, inhibitors against these targets have shown limited clinical efficacy. This disparity is a consequence of the current lack of high throughput assays able to model the protective

effect of the BMM. While a broad range of *ex vivo* systems have been developed to model the healthy hematopoietic bone marrow, this capability has not been translated for the development of urgently needed *ex vivo* models of AML. Reasons for this may include scepticism about the feasibility of such models given the complex and dynamic nature of the BMM, the currently limited understanding how AML cells shape this microenvironment and the heterogeneous nature of this microenvironment across AML patients and AML subtypes. While undoubtedly technically challenging, the success of *ex vivo* HSC differentiation models provides proof that complex features of the BMM can be replicated *ex vivo*. Emerging, although small-scale studies that applied HSC co-culture settings to AML cells and tested the drug response profile *ex vivo* found that it could replicate the *in vivo* response. While these results are promising, the number of studies that tested primary AML cells; cells that truly depend on the BMM (as opposed to secondary cell lines) were small-scale studies and tested only one model system. Without doubt the HSC/AML *ex vivo* models have numerous components, ranging from the presence and type of 3D scaffolds, the source and type of stroma cells, the addition of exogenous cytokines and the applied oxygen concentration, all of which makes comparative testing and identification of the best model a real challenge. However, as demonstrated by the Bonnet laboratory [359] a relatively simple, layered co-culture model, can successfully mimic *in vivo* BMM-mediated drug resistance. This suggests that not all features of the BMM may need to be incorporated into *ex vivo* models to suit drug discovery purposes and more widely to AML translational research.

Over the past number of years our understanding of the BMM and its influence on AML development and therapy has exponentially increased. While the field undoubtedly faces technical challenges, this is an exciting time in AML research.

1.11 Aims and Objectives

The overall aim of this thesis is to understand the interactions between leukaemic cells and bone marrow microenvironment and to design novel therapies to target these interactions. This thesis comprises of three studies, which collectively investigate the role of bone marrow microenvironment in protecting the malignant cells against the chemotherapeutics.

Objective 1: To develop an *ex-vivo* co-culture model system that mimics the bone marrow microenvironment for the functional drug testing and to predict the clinical response of AML patient to chemotherapeutic treatment.

Objective 2: To identify a therapeutic strategy that can overcome the drug resistance the bone marrow niche mediates against chemotherapeutics or BH3 mimetics.

Objective 3: To identify the mechanism through which the bone marrow microenvironment mediates resistance against FLT3-targeting tyrosine kinase inhibitors (TKIs) and to identify a therapeutic strategy that can sensitise the niche residing FLT3-ITD AML cells.

CHAPTER 2: *Ex vivo AML cell culture modelling the bone marrow microenvironment can predict the clinical response to chemotherapy*

Preamble to Chapter 2: Statement of Contribution

This chapter includes work which is currently under review. This work has also been presented and published as an American Society of Haematology (ASH) 2018 conference abstract in Blood Supplementary 2018 (Dhami et al, Blood suppl. 2018). I have performed the wet lab experiments except for the ECM studies, which were carried out by Andrea Tirincsi in collaboration with Dr. Dimitrios Zeugolis. I have also generated all the figures, performed statistical analysis, analysed the data and wrote the manuscript along with my supervisor Dr. Eva Szegezdi. Our clinical collaborator from University Hospital Galway, Dr Janusz Krawcyzk and Beaumont Hospital Dublin, Dr John Quinn provided the clinical information on the patient samples. All other authors contributed to editing of the manuscript.

***Ex vivo* AML cell culture modelling the bone marrow microenvironment can predict the clinical response to chemotherapy**

Sukhraj Pal Singh Dhami[1], Andrea Tirincsi[1], Denis Baev[1], Janusz Krawczyk[2], John Quinn[3], Dimitrios Zeugolis[4,5], Eva Szegezdi[1]

[1]Apoptosis Research Centre, School of Natural Sciences, National University of Ireland Galway, Galway, Ireland;

[2]Department of Haematology, Galway University Hospital, Galway, Ireland;

[3]Department of Haematology, Beaumont Hospital, Dublin, Ireland.

[4]Regenerative, Modular & Developmental Engineering Laboratory (REMODEL), Biomedical Sciences Building, National University of Ireland, Galway, Ireland; Science Foundation Ireland,

[5]Centre for Research in Medical Devices (CURAM), Biomedical Sciences Building, National University of Ireland, Galway, Ireland.

(Under review)

2.1 Abstract

Between 10-40% of acute myeloid leukaemia (AML) patients are resistant to induction therapy with cytarabine (AraC) and anthracycline. While the patient outcome could be improved by selecting the right induction therapy, reliable prediction of treatment failure based on cytogenetics, molecular profile or gene expression signatures is still a challenge. The impact of the bone marrow microenvironment (BMM) is increasingly recognised as a reason for this. Thus, the aim of this study was to develop a functional drug test which incorporates the impact of the BMM to predict the clinical response to AraC+daunorubicin (Dnr). We have developed and characterised a 3D co-culture of primary AML blasts with matched bone marrow stromal cells (BMSCs isolated from the same patient) or with immortalised BMSCs. Immortalised BMSCs could closely replicate effect of the patients' own BMSCs with regards to maintaining AML blast viability and driving chemotherapy resistance. With kinome and secretome studies, we show the complex signalling networks triggered by BMSCs driving AML survival and drug resistance. By monitoring the percentage of surviving AML blasts and the $CD34^{+}/CD38^{-}$ sub-population, we show that the BMSC-AML co-culture is superior to AML blast single cultures in predicting clinical response. By calculating a drug efficacy score, we found that the developed BMSC-AML co-culture can predict the clinical response to AraC+Dnr therapy with very high accuracy [area under curve (AUC=0.94)]. The advantage of this model over more complex pre-clinical AML models is its suitability to be developed into a laboratory diagnostic tool to advance the clinical decision on treatment choice.

2.2 Introduction

Acute myeloid leukaemia (AML) is the second most common form of adult leukaemia [73]. The mainstream therapy, which 60-70% of patients receive is intensive chemotherapy based on the nucleoside analogue, cytarabine (AraC) and anthracyclines (typically daunorubicin (Dnr) or idarubicin) [389]. Between 10-40% of patients, however, fail to respond to induction therapy (primary refractory disease defined by not achieving complete remission (CR) after 1 to 2 cycles of treatment) [11]. Treatment of these patients is difficult; they are typically referred to as haematopoietic stem cell transplantation (HSCT) [390].

Currently, the decision to use intensive chemotherapy is based on physical fitness and prognostic markers as no biomarkers or functional test exists to reliably predict treatment failure [391]. It is increasingly accepted that patient outcome would improve if better ways of selecting the induction therapy existed [392]. Early death is also a major concern, affecting between 35-47% of patients, with the rate being the highest in the main, elderly population (age over 65) and in patients with weaker physical fitness [393,394]. Thus, there is a pressing need for a method to predict primary refractory disease to spare patients from the toxic effects of an ineffective treatment. If a patient was predicted to be refractory to AraC+Dnr, alternative therapies such as etoposide, mitoxantrone, CD33-targeting antibodies, isocitrate dehydrogenase (IDH) inhibitors or BH_3 mimetics [395] could be considered. Additionally, an accurate tool to identify primary refractory disease could be an important aid in the selection of this high-risk patient group for clinical trials.

While it is routine clinical practice to isolate mononuclear cells from bone marrow aspirates and there are a number of sophisticated methods to culture AML blasts enabling *ex vivo* drug efficacy testing [381,388,396-398], how closely these systems replicate the actual clinical response of the patient, i.e. the *in vivo* efficacy of the chemotherapy is not known.

The aim of this study was to develop a theranostic drug testing system that can accurately predict the clinical response of the patient. To achieve this aim, we have established and characterised an *ex vivo* 3D, layered co-culture of patient-derived AML cells with bone marrow mesenchymal stromal cells, where the cell-cell, cell-extracellular matrix and paracrine interactions, typical of the bone marrow microenvironment (BMM) could be recapitulated. Here we report that this *ex vivo* co-culture system can be utilised to reliably predict the clinical response of AML patients to induction chemotherapy.

2.3 Materials and Methods

2.3.1 Cell culture

Molm13 AML cells (ATCC) were cultured in RPMI1640 (Gibco), HS-5 human bone marrow stromal cells (ATCC) in DMEM (high glucose, Gibco), healthy donor primary bone marrow stromal cells (HD-pBMSCs) and human telomerase (hTERT) immortalised healthy donor

primary bone marrow stromal cells (iMSC) in αMEM (Sigma). For each cell type the medium was supplemented with 10% Hyclone FBS (Fisher), penicillin (100 U/ml, Sigma), streptomycin (100 µg/ml, Sigma), sodium pyruvate (1 mM, Sigma) and GlutaMAX (2 mM, Gibco).

2.3.2 Patient samples

Mononuclear cells and bone marrow stromal cells (BMSC) isolated from marrow aspirates of newly diagnosed AML patients were provided by Blood Cancer Biobank Ireland (BCBI). BMSCs were isolated and expanded *ex vivo* in αMEM medium. Primary AML mononuclear cells were cultured in RPMI1640 medium (Gibco) containing 10% Hyclone FBS, penicillin (100 U/ml), streptomycin (100 µg/ml) and GlutaMAX (2 mM, Gibco) and sodium pyruvate (1 mM, Sigma). Cell viability was assessed at the time of thawing the cells and only samples that showed a minimum of 75% viability were used for experiments.

2.3.3 Ethical approval

All patients and healthy donors provided written informed consent, in accordance with Research Ethics Board-approved protocols of each BCBI collection sites: University College Hospital, Galway and Beaumont Hospital, Dublin. This study was fully compliant with all relevant ethical regulations regarding human participants.

2.3.4 *Ex vivo* culture of AML mononuclear cells with bone marrow stromal cells

BMSCs were fluorescently labelled either by stable expression of green fluorescent protein (GFP, HS-5 cells) or by loading the cells with the long-term cell tracker, CFSE (5-(and 6)-Carboxyfluorescein diacetate succinimidyl ester) (Biolegend) (HD-pBMSC, iMSC). BMSCs were then seeded in 24 well plates at the density of 50,000 cells/ml and cultured for 48 h in αMEM medium after which the medium was removed and replaced with primary AML cells seeded at the density of 500,000 cells/ml in RPMI-1640 medium. After 24 h of co-culture, the cells were treated with a 3:1 molar ratio of AraC (Sigma) and Dnr (Sigma) for 24 h and 48 h.

2.3.5 AML cell viability and phenotyping

MNCs were pipetted off the stromal cell layer and were blocked with 1%BSA/PBS for 20 min on ice prior to incubation with anti-CD34-PE and anti-CD38-APC-H7 antibodies (BD Bioscience, San Diego, USA) in 1% BSA/PBS (Sigma) for 30 min on ice in the dark. After washing off unbound antibodies, the cells were stained with the viability dye, To-Pro3 (Molecular Probes) by adding it in a final concentration of 1 µM for 15 min on ice in the dark. Stained samples were analysed using BD FACS Canto II flow cytometer (BD Bioscience, San

Diego, USA). A minimum 30,000 events were collected in the AML blast gate (GFP/CFSE negative cells). Detached BMSCs were excluded from the analysis based on their green fluorescence FSC^{high}/GFP^{+} (GFP expression of HS-5 cells and CFSE-labelling of pBMSCs and iMSCs) (Supplementary figure 2.8).

Cell death in the Molm13 AML cell line was quantified with Annexin V-APC staining. Cells were collected and stained with Annexin V-APC in Annexin V buffer (10 mM HEPES/NaOH, pH 7.5, 140 mM NaCl, 2.5 mM $CaCl_2$) for 15 min on ice in the dark. Samples were analysed on a FACS Canto II flow cytometer.

2.3.6 Cytokine secretome analysis

Soluble factors (chemokines and cytokines) secreted by BMSCs were determined with proteome profiling using the Human XL Cytokine Array kit (R&D Systems). Culture medium from BMSCs was collected after 48 h of culture. The medium was cleared by centrifugation at 4000 x rpm for 5 min at 4ºC and then incubated with the antibody array as described in the manufacturer's protocol and developed using X-ray film (Agfa-CP-BU). The X-ray images were analysed using the $HLImage^{++}$ software (Western Vision Software, USA).

2.3.7 Kinome analysis of AML cells

Activation of intracellular kinases (by phosphorylation), receptor tyrosine kinases and mitogen-activated protein kinases (MAPKs) in Molm13 cells were determined using the Human Proteome Profiler Antibody array from R&D systems (43 phospho-kinases, 49 receptor tyrosine kinases and 26 MAPKs). Molm13 cells were cultured in the presence or absence of the immortalised bone marrow stromal cells (iMSC) for 48 h after which the Molm13 cells were harvested, lysed and the arrays probed according to the manufacturer's protocol and developed using X-ray film (Agfa-CP-BU). The X-ray images were analysed using the $HLImage^{++}$ software (Western Vision Software, USA).

2.3.8 Network and pathway analysis

The activated kinases (receptor tyrosine kinases, intracellular kinases and MAPKs) in the Molm13 cells upon co-culturing with bone marrow stromal cells underwent pathway and network analysis using the phospho-proteomic analysis tool of the Ingenuity pathway analysis software (Qiagen).

2.3.9 Immunocytochemistry

iMSCs and primary human bone marrow mesenchymal stromal cells (pMSCs) were cultured in 8-well chamber slides (Lab-tek® II Chamber Slide System) at a density of 50,000 cells/ml

for 7 days. At the end of the culture period, the cells were washed with Hanks' balanced salt solution (Sigma) and fixed with 2% paraformaldehyde (Sigma) for 15 min at room temperature (RT). Unspecific antibody binding sites were blocked with 3% bovine serum albumin (Sigma) in PBS for 30 min at room temperature (RT) followed by incubation of the slides with primary antibodies against collagen I (Abcam, ab34710), IV (Abcam, ab 21295), VI (Abcam, ab6588) and fibronectin (Sigma, F0791) for 90 min at 1:200 dilution, at RT. The signal was developed by adding Alexa Fluor 488-labelled secondary antibodies for 30 min at 1:500 dilution, at RT in the dark (goat anti-mouse IgG (A32723, Thermofisher) for anti-collagen IV, VI, and fibronectin antibodies or anti-rabbit IgG (A-11034, Thermofisher) for anti-collagen I antibody). After washing off excess antibodies, slides were fixed with 2% PFA for 15 mins at RT, the nuclei of the cells were counterstained with 4,6-diamidino-2-phenylindole dihydrochloride (DAPI, Sigma) and slides were mounted with Fluorosave mounting media (Calbiochem). Images were taken with an Olympus IX-51 inverted fluorescence microscope. Images were analysed with ImageJ software.

2.3.10 Decellularisation and Immunostaining

BMSCs were cultured in 8 well chamber slides (Lab-tek® II Chamber Slide System) for 7 days. After 7 days of ECM deposition, cells were washed with HBSS and de-cellularisation was done by treating cells with 0.5% sodium-deoxycholate (Sigma) containing protease inhibitors (Sigma) for 10 min. To remove DNA, 1000U/ml of deoxyribonuclease I (Sigma) was added to chambers for 20 min at 37°C. The slides were gently washed with PBS to remove any cellular debris. Immunostaining of ECM was performed against collagen I (Abcam, ab34710), III (Abcam, ab23746), VI (Abcam, ab6588) and fibronectin (Sigma Aldrich, F0791). Images were taken with Olympus IX-51 inverted fluorescence microscope (Olympus, Waltham, US) and image analysis was performed with ImageJ.

2.3.11 Statistical Analysis

FACS data visualization was performed using FCSExpress (DeNovo Software Inc, USA) and statistical analysis performed using GraphPad Prism (GraphPad Software Inc., La Jolla, USA) software packages. Pearson correlation analysis (two-tail) was performed using GraphPad Prism correlation analysis package (GraphPad Software Inc., La Jolla, USA). Area Under the Curve (AUC) - Receiver Operating Characteristics (ROC) curve for measuring the model's performance was calculated using MedCalc (MedCalc software v18, Ostend, Belgium).

2.4 Results

To develop a functional drug efficacy test that can recapitulate the key features of the BM microenvironment we have established a co-culture model where primary, patient-derived

AML cells were cultured in direct contact on a layer of BMSCs providing ECM, cell-cell contact and paracrine trophic signals, replicating multiple features of the BMM.

Because MSCs in the bone marrow of AML patients have reduced clonogenic potential and proliferative capacity and they also rapidly undergo senescence under *in vitro/ex vivo* culture conditions [284,289,399], we tested whether immortalised BMSCs can be used. Immortalised MSC were immunophenotypically tested for mesenchymal stem cell surface markers as described by International society for cellular therapy (ISCT) [400] and were found to be $CD11b^-$, $CD34^-$, $CD45^-$, $CD73^+$, $CD90^+$, $CD105^+$. iMSCs were also tested for their differentiation potential as shown by Kassem' group [401] into osteoblasts, adipocytes and chondrocytes. To test the suitability of immortalised BMSCs (healthy donor-derived BMSCs immortalised with HPV-16 E6/E7 (HS-5), or with human telomerase (iMSC)) to model primary BMSCs, we compared them to primary (non-immortalised) BMSCs derived from healthy donors (HD-pBMSC) and the patients' own BMSCs (AML-pBMSC). Three main characteristics of the BMSCs were studied: cytokine/chemokine secretion, formation of ECM-BMSC proteo-cellular scaffold and ability to support *ex vivo* AML blast survival.

2.4.1 Immortalised BMSCs have a bone marrow-typical secretome

The secretome of HS-5 cells, iMSCs and HD-pMSCs were determined using the Human XL cytokine array detecting 102 cytokines and chemokines. HS-5 cells, iMSCs and HD-pBMSC secreted 39, 44 and 51 paracrine factors, respectively (Table 2.1, Supplementary Table 2.1) including all key BMM-typical factors reported to contribute to BMM-mediated drug resistance, such as angiopoietin 1, granulocyte-colony stimulating factor (G-CSF), C-X-C motif chemokine 12 (CXCL12), CXCL10, vascular endothelial growth factor (VEGF), fibroblast growth factor, interleukin-6, interleukin-8 (IL-8) etc. 51% of cytokines/chemokines were common between iMSCs and HD-pBMSC, while the HS-5 secretome shared 43% commonality with HD-pBMSC (Supplementary Figure 2.1, Supplementary Table 2.1).

2.4.2 Support for AML survival and drug resistance

To determine the ability of the different BMSC types to support AML blast survival, BM-derived AML blasts from 6 patients were cultured on HS-5 cells, iMSCs or the patient's own BMSCs (matching AML-pBMSCs) over 5 days. Immortalised BMSCs supported the survival of the blast cells to similar extent as the patient's own BMSCs, except in Patient 2, where the AML cells showed better viability in the absence of BMSCs, including the patient's own BMSCs, indicating that these cells may depend on a factor produced by other BMM constituent cells (Figure 2.1) (Supplementary table 2.3).

Table 2.1: Cytokines/chemokines commonly secreted by pBMSC, HS-5 cells and iMSCs.

Gene ID	Gene Symbol	UniProt Protein Name
283	**ANG**	**Angiogenin**
285	**ANGPT2**	**Angiopoietin-2**
627	BDNF	Brain-derived neurotrophic factor
682	**BSG**	**Basigin**
1116	CHI3L1	Chitinase-3-like protein 1
1435	**CSF1**	**Macrophage colony-stimulating factor 1**
2022	ENG	Endoglin
2919	CXCL1	Growth-regulated alpha protein
3569	**IL6**	**Interleukin-6**
3576	**CXCL8**	**Interleukin-8; Multifunctional fusion protein**
3605	**IL17A**	**Interleukin-17A**
3627	**CXCL10**	**C-X-C motif chemokine 10; C-X-C motif chemokine**
3976	**LIF**	**Leukemia inhibitory factor**
4282	**MIF**	**Macrophage migration inhibitory factor**
5054	**SERPINE1**	**Plasminogen activator inhibitor 1**
5329	**PLAUR**	**Urokinase plasminogen activator surface receptor**
5806	PTX3	Pentraxin-related protein PTX3
6347	**CCL2**	**C-C motif chemokine 2**
6387	**CXCL12**	**Stromal cell-derived factor 1**
6696	**SPP1**	**Osteopontin**
7057	**THBS1**	**Thrombospondin-1**
7422	**VEGFA**	**Vascular endothelial growth factor A**
9518	**GDF15**	**Growth/differentiation factor 15**
9965	**FGF19**	**Fibroblast growth factor 19**
22943	DKK1	Dickkopf-related protein 1

Bold indicates cyto/chemokines known to present in the bone marrow microenvironment.

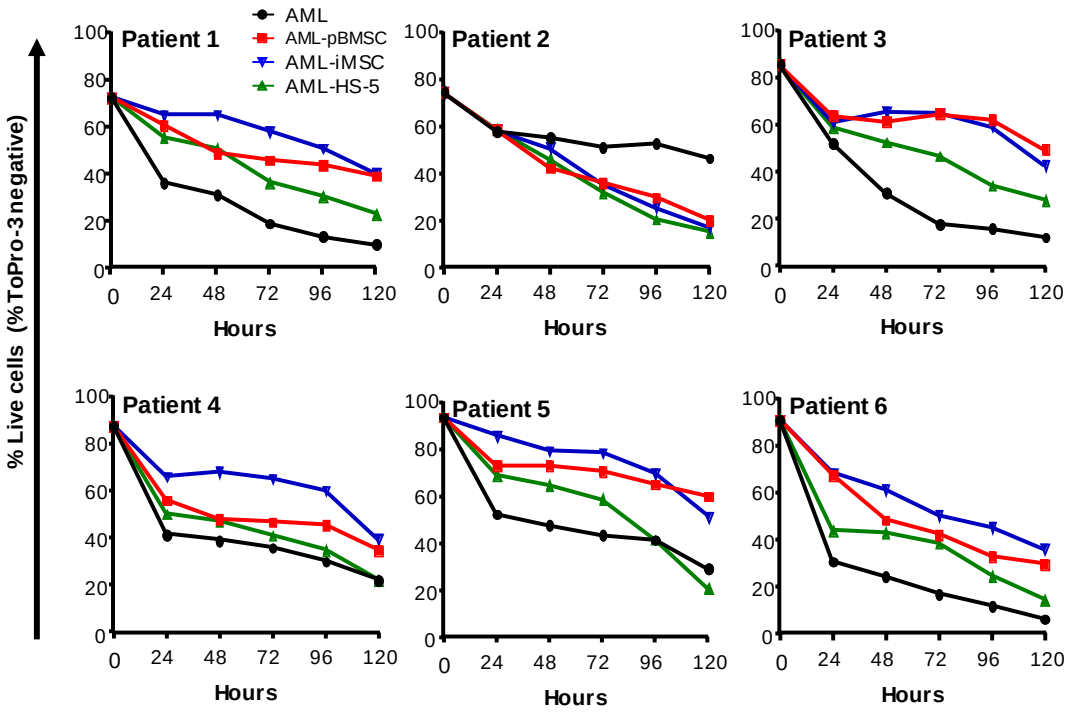

Figure 2.1: BMSCs promote the survival of AML blasts. Bone marrow-derived primary AML cells from 6 patients were cultured on 3 different BMSC layers: HS-5 cells, iMSCs and the patient's own BMSCs (matching AML-pBMSCs). Viability of the AML blasts was followed over 5 days using To-Pro3 cell viability staining by flow cytometry (BMSCs excluded based on their GFP/CFSE positivity).

After confirming that both HS-5 cells and iMSCs were able to give resistance to AML cell lines against chemotherapeutics and targeted agents (cytarabine, sorafenib, quizartinib, (Supplementary Figure 2.2), their ability to protect primary AML blasts against drugs was compared. AML blasts were cultured with HS-5 cells, iMSCs or the patients' own BMSCs (AML-pBMSCs) and treated with BH_3 mimetics (ABT-737 and ABT-199) or with the combination of AraC+Dnr. BMSCs, regardless of their type, gave protection against all drugs and the effect of the immortalised BMSCs was comparable to the matched AML-pBMSCs, except for AraC+Dnr treatment for patient 5 (Figure 2.2). This overall trend was retained after 48 h of treatment (Supplementary Figure 2.3). iMSCs showed a stronger cytoprotective effect compared to HS-5 cells and in some cases higher than the matched AML-pBMSCs, especially after 48 h of treatment (Supplementary Figure 2.3).

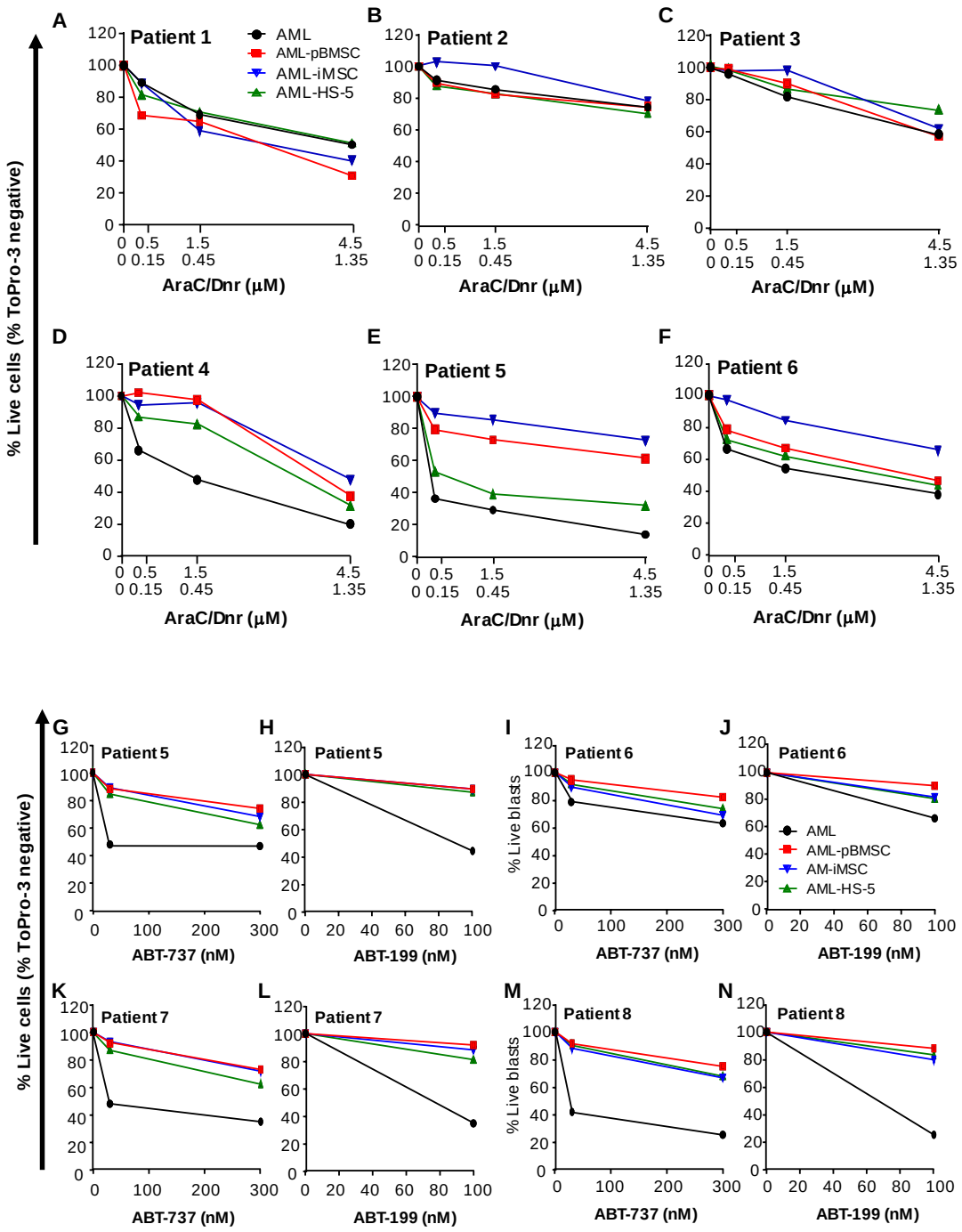

Figure 2.2: Comparison of drug resistance mediated by different BMSCs. AML blasts from 6 patients were cultured alone or with HS-5, iMSC or matched pBMSC feeder layers for 24 h. Cells were then treated with the combination of AraC+Dnr (A-F) or with the BH_3 mimetics, ABT-737 (G, I, K, M) and ABT-199 (H, J, L, N). After 24 h of treatment the mononuclear cells were gently removed from the co-culture and induction of cell death in the AML blasts was determined with flow cytometry in the GFP^-/$CFSE^-$ population with To-Pro-3 staining.

In order to characterise the potential survival signalling pathways driving drug resistance, BMSC-mediated activation of receptor tyrosine kinases and intracellular kinases in AML cells was determined. Contact with iMSCs drove a profound change in kinase activation in AML cells, with 43 kinases activated and 8 inhibited at cutoff of FDR <0.05 and log2 fold change of 1.5 (Figure 2.3A, Supplementary Table 2.2, Supplementary figure 2.5A). Ingenuity signal

transduction network analysis (Qiagen) showed that the activated kinases drive several converging BM-typical pro-survival signalling pathways demonstrating the substantial effect BMSCs have on how AML cells are equipped against cytotoxic drugs (Figure 2.3B, 2.3C, Supplementary figure 2.5).

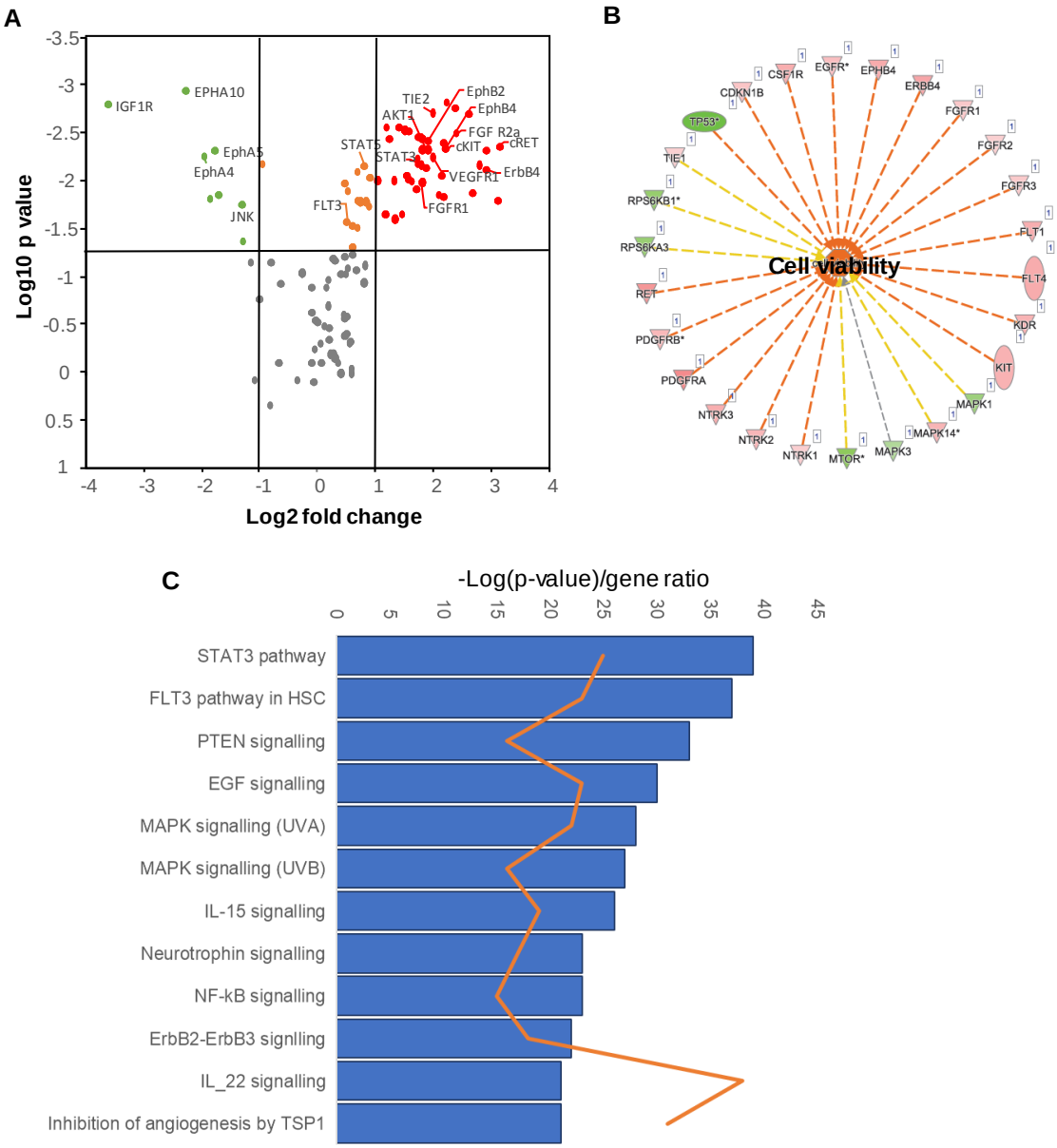

Figure 2.3: Contact with BMSCs drives BM-typical receptor tyrosine kinase activation and survival signalling in AML cells. (A) Volcano plot of BMSC-driven kinase activation. Molm-13 AML cells were cultured with iMSCs for 24 h after which the activation status of receptor tyrosine kinases and intracellular signalling kinases were determined with proteome arrays. Grey: kinases with unchanged activity, red: activated kinases, green: downregulated kinases, orange: kinases with a significant change in activity but below the 2-fold change cut-off. (B) Kinase pathways regulated by BMSCs driving cell survival signalling. Red shading of kinase nodes shows activated kinases, green: inhibited kinases, orange edges: change in activity driving cell survival, yellow edges: changed activity inhibiting survival. (C) Cascade of pro-survival cell signalling pathways activated by BMSCs in residing AML cells.

2.4.3 Characterisation of the extracellular matrix

The core infrastructure of the BM is formed by a proteo-cellular scaffold of ECM fibres and BMSCs [402]. To characterise whether such an ECM-BMSC scaffold is formed *ex vivo*, deposition of key BM ECM proteins by BMSCs was determined using fluorescent immunocytochemistry. Deposition of core ECM microfibers, namely fibronectin, collagen I, IV and VI showed a similar structure between pBMSC and iMSC cultures with a tight association between the ECM fibres and BMSCs, confirming the *in vitro* formation of the BM-like proteo-cellular scaffold (Figure 2.4). Of note, we found that the ECM deposited by iMSCs (Supplementary Figure 2.4A) alone was not sufficient to potentiate drug resistance (Supplementary Figure 2.4B&C). Although, a positive control was required for this experiment showing the effect of iMSC-Molm13 co-culture in protecting the cells against AraC and quizartinib treatment.

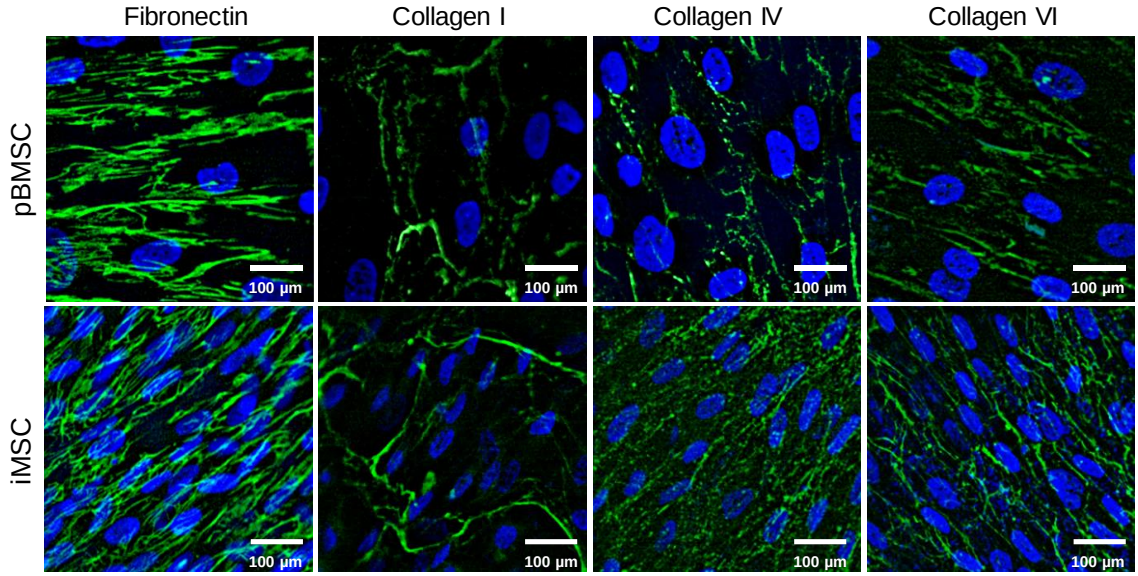

Figure 2.4: Deposition of extracellular matrix proteins is similar in both pBMSCs and iMSCs. pBMSCs and iMSCs were cultured in chamber slides and immunostained for key bone marrow ECM proteins. Representative fluorescent microscopy images for fibronectin, collagen I, IV, and VI shown (BMSC nuclei: blue, deposited ECM proteins: green).

2.4.4 The layered bone marrow stroma-AML co-culture can accurately predict the clinical response to induction chemotherapy

The *ex vivo* co-culture system, while able to replicate key features of the BMM, is a highly simplified model of the BM with many components of the hematopoietic niche missing. To determine how faithfully the BMSC-based co-culture can replicate BMM-mediated drug resistance and the consequent clinical response of patients, primary AML blasts were cultured alone or on an iMSC layer and AraC+Dnr-induced AML cytotoxicity was determined (Supplementary figure 2.6).

A total of 20 patient samples were screened all of whom received 3+10 AraC+Dnr therapy in the clinic. The median age of the patients was 67 years. All patients were analysed by

conventional G-band karyotyping, FISH as part of the clinical routine to identify the AML cytogenetics (Table 2.2).

First, we determined how well AraC+Dnr-induced cytotoxicity correlated between the single culture of AML blasts to AML-BMSC co-culture based on the percentage of surviving AML blasts at the highest drug dose (parallel to the clinical assessment of CR) by calculating Pearson's correlation. The percentage of surviving blasts showed a moderate positive correlation between single and co-cultures ($r = 0.615$, $p = 0.0039$; Supplementary figure 2.7A), with a noticeably weakening correlation with increasing drug resistance. We then compared the drug response determined in the *ex vivo* co-culture (% surviving AML blasts at highest drug dose) to the clinical response of the patients. The single culture showed a poor correlation with the clinical response ($r = 0.399$, $p = 0.0809$; Supplementary figure 2.7B). On the other hand, the co-culture system showed a significant, moderate correlation with clinical response ($r = 0.635$, $p = 0.0026$; Supplementary figure 2.7C).

In order to better capture the variable kinetics of drug sensitivity of individual patient samples, we also quantitated drug response by calculating the area under the curve (AUC) from the plotted cell death – drug dosage graphs using the trapezoid model.

Based on the AUC values calculated from the 48 h viability measurements the samples were segregated into 2 groups, the first where the drug response value was under 35% (drug-resistant sample), and the second above 35% (drug-sensitive, Figure 2.5A). By comparing the *ex vivo* measured drug response to the clinical response, the *ex vivo* tests predicted primary refractory disease in 6 out of the 7 cases tested and complete remission (responders) in 10 out of 11 samples (Table 2.2). Using the drug efficacy score and calculating the area under the ROC curve our model predicted the clinical response of patients with AUC=0.94 (p-value = <0.001, Figure 2.5B). While the assay could not predict the 2 partial responses, the overall accuracy of the *ex vivo* test is still very high (Supplementary figure 2.7D).

The clinical follow-up of the patients showed that 54.4% (6/11) of the CR patients relapsed. Relapse has been correlated to the leukaemia-initiating cells [266,403-405], broadly identified as the $CD34^+/CD38^-$ population. Accordingly, we also found that the $CD34^+/CD38^-$ population showed much higher resistance against AraC+Dnr than the bulk blast population shown by their substantial accumulation in the live fraction post-treatment (median frequency of 1.335% and 54.34% in the control vs highest dose AraC+Dnr treatment, respectively, Figure 2.5C), however we found no correlation between either pre-treatment $CD34^+/CD38^-$ cell frequency or their accumulation in the surviving cell fraction after treatment with relapse (p-value = 0.795, r = 0.0885) (Supplementary figure 2.7E).

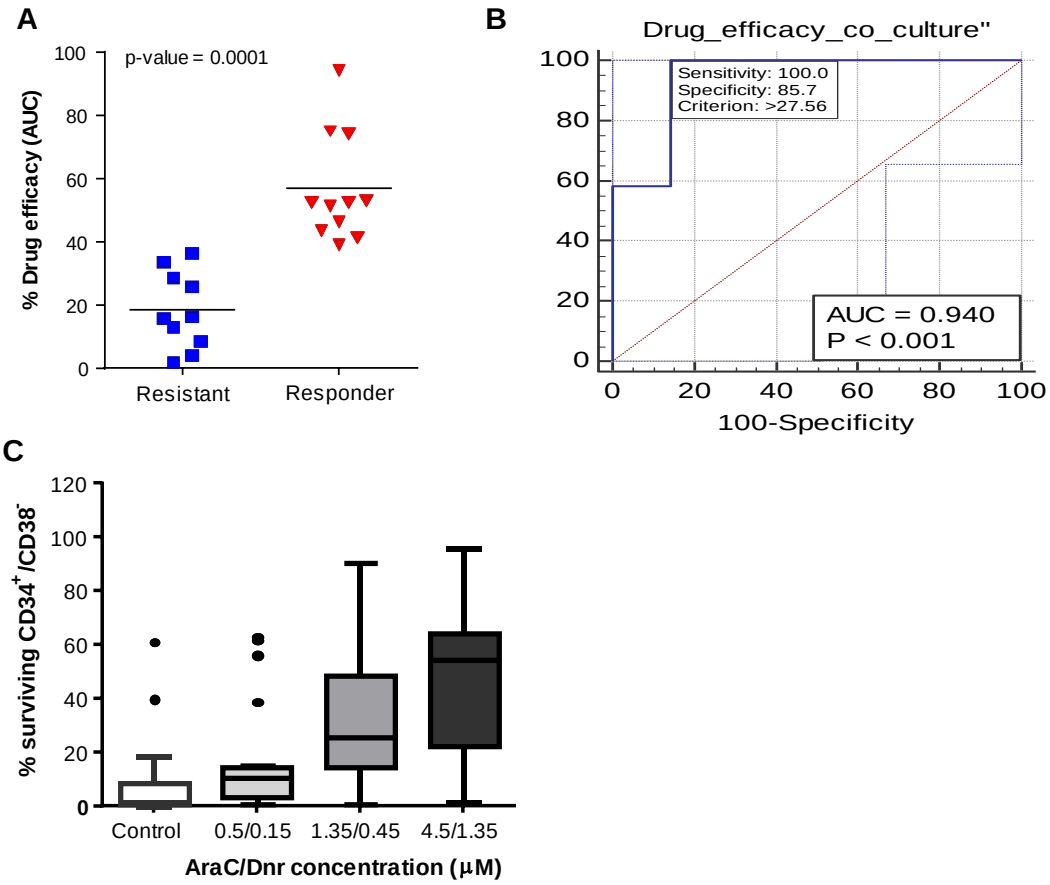

Figure 2.5: Ex vivo layered co-culture assay of the bone marrow stromal cells (BMSC) and bone marrow derived AML cells. Immortalised bone marrow stromal cells (iMSC) were cultured for 48 h followed by the seeding of primary bone marrow derived AML cells on to the layered BMSC. After 24 h of co-culturing the cells were treated with the cytarabine and daunorubicin (AraC+Dnr) to 3:1 molar ratio at three different clinically relevant doses. The cell viability and phenotyping for $CD34^{+}/CD38^{-}$ was conducted after 24 h and 48 h of treatment using flow cytometry. (A) Drug efficiency (%) was calculated using area under curve (AUC) for each time point and doses using trapezoid model showing the statistically significant difference (p-value = 0.0001) among the cohort of resistant and responder to the AraC/Dnr treatment. (B) Area under the ROC curve analysis of the drug efficacy values was calculated for the samples screened in the *ex vivo* co-culture and compared to that of clinical response-resistant or responder. AUC value for prediction model is 0.94 (p-value= <0.001). (C) The percentage of surviving $CD34^{+}/38^{-}$ population in AML patients was monitored before and after 48 h of treatment with AraC/Dnr. There is an enrichment of $CD34^{+}/38^{-}$ population with increase in treatment dosage in the surviving population.

Table 2.2: Clinical characteristics and disease history of primary samples used for drug efficacy testing.

Patient ID	Cytogenetics	% treatment efficacy- 48 h	Clinical drug	*Ex vivo* result	Follow-up	Clinical follow-up
1	t(8;21) - Good risk	53.58	AraC+Dnr	responder	responder	relapsed
3	Monosomy 7 (poor risk)	27.56	AraC+Dnr	resistant	resistant	
4	NK, FLT3$^-$, NPM$^-$	38.51	AraC+Dnr	responder	responder	in remission
5	Intermediate risk cytogenetics	37.89	AraC+Dnr	responder	responder	in remission
7	NK, FLT3$^-$, NPM$^-$	79.62	AraC+Dnr	responder	responder	relapsed
9	FLT3$^-$, NPM$^-$	27.01	AraC+Dnr	resistant	resistant	
10	NK, FLT3$^+$, NPM$^+$	75.75	AraC+Dnr	responder	responder	relapsed
11	Normal Karyotype	13.88	AraC+Dnr	resistant	resistant	
12	NK, FLT3$^-$, NPM$^+$	29.36	AraC+Dnr	resistant	responder	relapsed
13	NK, FLT3$^+$, NPM$^+$	33.44	AraC+Dnr	resistant	partial response	relapsed
14	NK, FLT3$^-$, NPM$^+$	74.33	AraC+Dnr	responder	responder	relapsed
15	NK, FLT3$^+$, NPM$^-$	90.90	AraC+Dnr	responder	responder	in remission
16	Complex cytogenetics (Poor risk)	66.54	AraC+Dnr	responder	responder	in remission
17	Intermediate risk cytogenetics	49.91	AraC+Dnr	responder	responder	in remission
18	NK, FLT3$^-$, NPM$^-$	52.23	AraC+Dnr	responder	resistant	
19	AML-NPM1$^+$, triosomy 8	21.73	AraC+Dnr	resistant	resistant	
20	AML with MDS	37.70	AraC+Dnr	responder	partial response	
21	AML with MPAL t(v;11q23.3); KMT2A rearranged	77.61	AraC+Dnr	responder	responder	in remission
22	AML with Inv(16)p13.1q22	27.14	AraC+Dnr	resistant	resistant	
23	AML with NPM$^+$	4.96	AraC+Dnr	resistant	resistant	

2.5 Discussion

Cytarabine and anthracycline-based treatment is the standard induction therapy for AML patients [406,407]. Once the patients achieve remission, depending on their prognosis, they undergo either chemotherapy-based consolidation therapy or for poor-risk patients, hematopoietic stem cell transplantation [408]. Between 20-55% of patients are however refractory to AraC+anthracycline based induction chemotherapy [409]. The current best practice to predict refractory disease is the prognostic classification by ELN, based on cytogenetics and molecular profiling, however, it is not designed to predict treatment response, but overall prognosis [16,410,411]. The current best model to predict induction treatment failure incorporates aspects of cytogenetics, mutational profile, physical status and gene expression signatures [392,412]. However, the accuracy of these studies could still not reach that of a robust clinic diagnostic tool (AUC above 0.9). Studies conducted by Herold and colleagues [413], Walter and colleagues [100] and Krug and colleagues [414] had AUC values of 0.76, 0.78 and 0.68, respectively. The genetic, epigenetic and biological heterogeneity of AML indicates that a functional drug testing may predict treatment response with higher efficacy than that of gene expression signatures. Our study highlights that a relatively simple, layered co-culture consisting of healthy donor-derived BMSCs and AML blasts isolated from BM aspirates can replicate the *in vivo* drug response and thus can be used as a theranostic test to predict a patient's response to AraC+Dnr induction therapy.

Layered co-cultures to model normal haematopoiesis and to culture AML blasts are broadly used since Dexter and colleagues [415] have first described it in 1977. It is also well established that BMSCs can provide survival signals to AML cells and protect them from cytotoxic drugs[416-419]. However, to our knowledge, this is the first report to show that an *ex vivo* co-culture can predict the patient's clinical response. Supporting our results, the Bonnet laboratory has also shown that a layered co-culture (where the mouse BMSC cell line, MS-5 was used as the feeder layer) could replicate *in vivo* drug sensitivity by comparing the *ex vivo* drug response to that of xenotransplanted AML cells into NSG/SCID IL-2Rγ common chain null mice [359]. Our results show that a similar layered co-culture, although based on human, not mouse immortalised BMSCs, could reliably predict patient response. The model had equally high accuracy in predicting both refractory disease and complete remission. Out of the 20 patient samples tested, we found a mismatch in 2 patients. Patient 12, which appeared to be resistant in the *ex vivo* assay however achieved CR in the clinic, although later relapsed. Patient 18 was a responder in the *ex vivo* assay but was resistant to treatment in the clinic. There are a few possible explanations for why these patients may have a mismatch with the clinical response. Firstly, it is possible that in some cases the *ex vivo* co-culture cannot fully capture the cross-talk between the AML blasts and the BMM and secondly, as it is a short-term assay, it may not capture the knock-on effect of the chemotherapy on the BMM itself. Additionally, further studies to understand the clonal

heterogeneity and evolution of the AML blasts in these patients via single-cell transcriptomics could help to identify the drug-resistant clones and thus better predict treatment outcome.

BMSCs provide an environment to AML blasts, which contains essential factors for their survival. In their absence, the sensitivity of AML blasts to chemotherapeutics and targeted agents is enhanced. BMSCs secreted a large number of trophic factors typical of the bone marrow and deposited an ECM, which formed a proteo-cellular network typical of the bone marrow. Of note, we found that the deposited ECM alone could not provide drug resistance, as a decellularized BMSC-generated ECM could not give any protection against AraC or quizartinib to AML cells (Supplementary Figure 4B&C). We believe that the deposited ECM plays a crucial role in two aspects of the BMM, firstly, in the organisation of the BMSC network required for its optimal functioning and secondly for binding cytokines and chemokines thus creating their concentration gradients and presenting them to the hematopoietic lineage cells [420-422].

While BMSCs are the most abundant cell type in the BMM [310,423,424], the BMM is considerably more complex, containing endothelial cells, sympathetic neurons, osteoblast, adipocytes, all of which have been reported to have an impact on stem cell quiescence, hematopoietic differentiation, clonal expansion, processes interlinked with AML pathogenesis and drug resistance [222,399,417]. Furthermore, there is increasing evidence that the AML cells can reshape the BMM to serve their own advantage. BMSCs isolated from AML patients were found to have impaired functionality and clonogenic potential [284], questioning how faithfully, healthy donor-derived BMSCs can replicate patient-specific BMSC or BMM functions. Importantly, we found that HD-derived BMSCs and the patients' own BMSCs provided a similar level of survival support and drug resistance to AML blasts.

One considerable limitation of layered *ex vivo* co-cultures is their ability to support long-term hematopoietic/leukemic stem cells (LT-HSC). LT-HSCs/LSCs can lay dormant in specialised pockets of the BMM with low metabolic activity making them more resistant to drugs than the more differentiated and proliferating blasts. Selective survival of LSCs is a key driver of relapse [270,425]. Using this model, we found that in all patients, the $CD34^{+}/CD38^{-}$ cell population, encompassing the LSC population was more resistant to AraC+Dnr than the bulk blast population leading to their enrichment in the surviving cell fraction. While we could not find a correlation between the frequency of the $CD34^{+}/CD38^{-}$ population and clinical response or relapse, it is potentially due to the small number of relapsed patients. To be able to assess the contribution of LSCs to relapse, other factors may also need to be taken into consideration, such as the effect of consolidation therapy on LSC survival, and the effects of the treatment on the BMM. AML cells are also known to reshape the bone marrow microenvironment according to their need [222,426,427]. A study by Ding and colleagues [134] has shown that relapse in AML is associated with the acquisitions of specific mutations during the therapy. Thus, predicting relapse may require genetic characterisation of the LSC encompassing $CD34^{+}/CD38^{-}$ sub-populations [403,412].

This study focused on AraC+Dnr treatment as most patients receive this therapy. However, the results warrant further studies whether this assay could be used to predict the efficacy of other drugs and drug combinations, such as FLT3 inhibitors, or BH_3-mimetics.

Ability to predict drug response within days would allow clinicians to consider alternative treatment options for refractory patients. Foreseeing that the patient is resistant to AraC+Dnr can prevent exposure of the patient to a treatment which is not effective and may lead to early death or weakening the patient that they become unfit for alternative chemotherapy. Instead, alternative treatments, such as high dose AraC, myeloablative therapy, or based on molecular profiling, targeted therapeutics, such as IDH1/2 inhibitors, FLT3 inhibitors could be used to achieve CR and prepare the patient for hematopoietic stem cell transplantation.

2.6 Supplementary figures

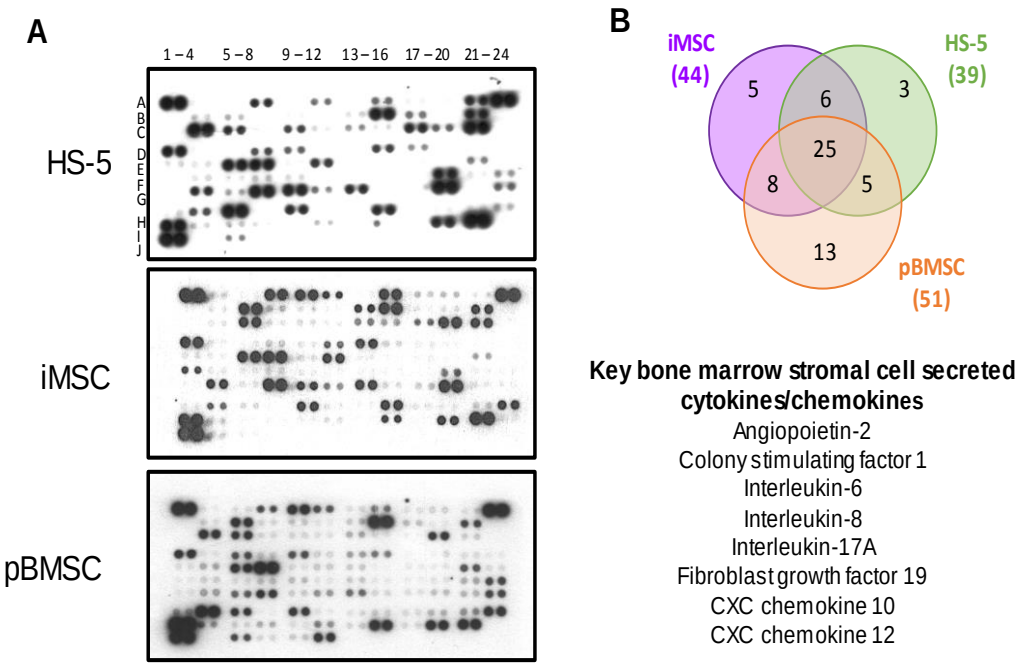

Supplementary Figure 2.1: BMSC secrete a plethora of cytokines and chemokines.
(A) Representative antibody arrays of BMSC culture supernatants.
The identity of the spots on the array can be found here:
https://resources.rndsystems.com/pdfs/datasheets/ary022b.pdf (B) Venn diagram showing the commonality in secreted cytokines/chemokines across BMSCs types.

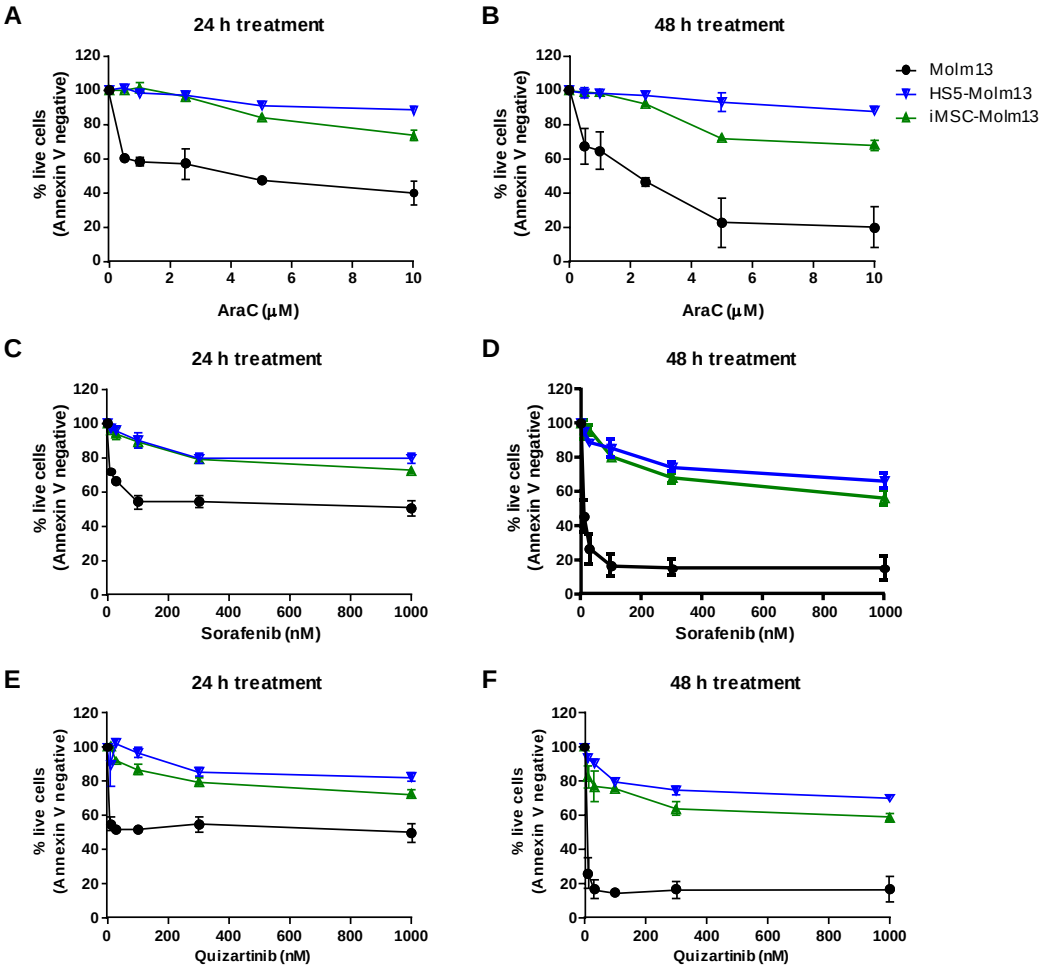

Supplementary Figure 2.2: Bone marrow stromal cell-mediated drug resistance in AML cell lines.

Molm-13 AML cells were seeded on established layers of HS-5 cells and iMSCs. After 24 h of culturing, cells were treated with cytarabine (AraC) (A-B), sorafenib (C-D) and quizartinib (E-F). Molm-13 cell viability was measured after 24 h and 48 h of treatment using Annexin V staining and flow cytometry.

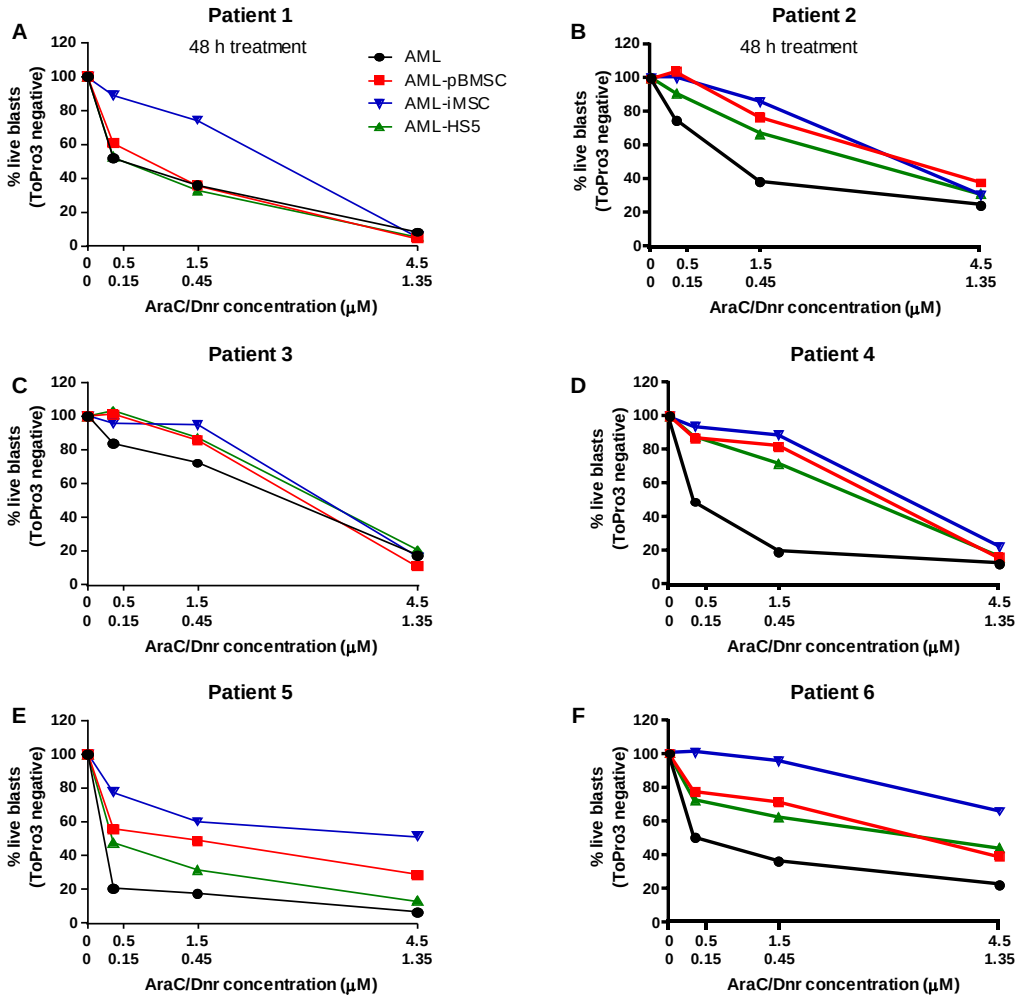

Supplementary Figure 2.3: Comparison of drug resistance against cytarabine and daunorubicin mediated by different BMSCs.
AML blasts from 6 patients were cultured alone or with HS-5, iMSC or matched pBMSC feeder layers for 24 h. Cells were then treated with the combination of AraC+Dnr for 48 h. Induction of cell death in the AML blasts was determined with flow cytometry in the GFP-/CFSE- population using ToPro-3 staining.

A

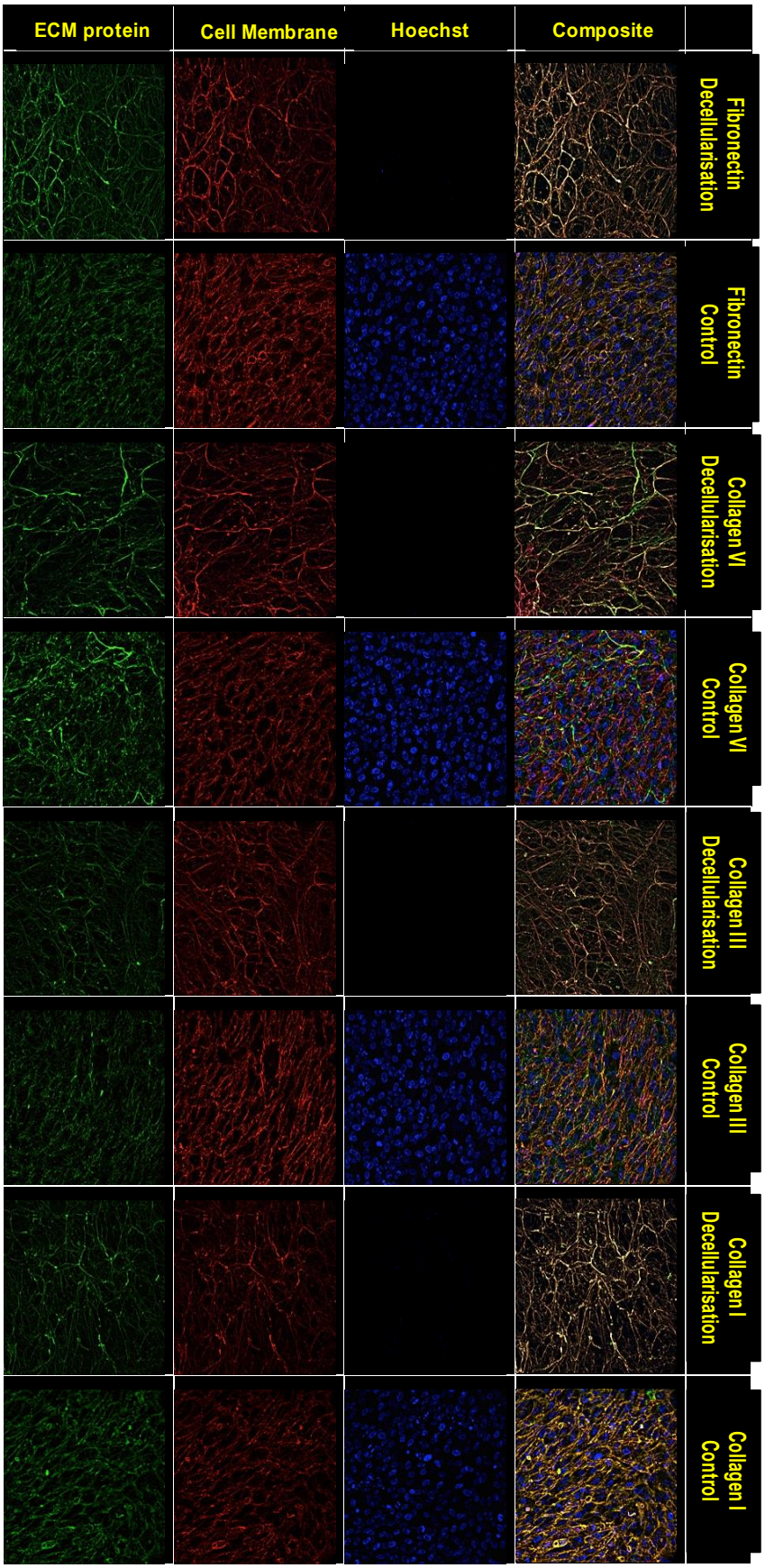
ECM protein
Cell Membrane
Hoechst
Composite
Fibronectin Decellularisation
Fibronectin Control
Collagen VI Decellularisation
Collagen VI Control
Collagen III Decellularisation
Collagen III Control
Collagen I Decellularisation
Collagen I Control

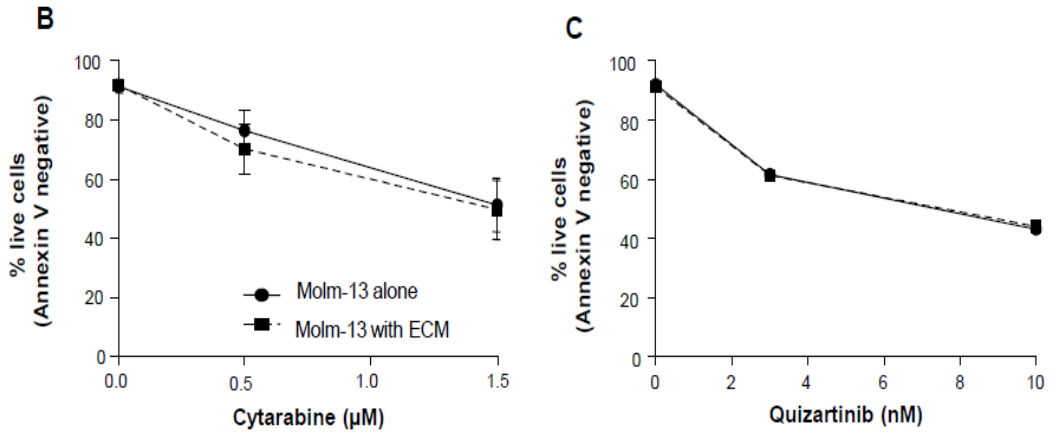

Supplementary Figure 2.4: ECM proteins do not offer drug resistance to AML cells against chemotherapeutics.
For generation of decellularised ECM, iMSCs were cultured in chamber slides for 7 days after which the cells were removed from the ECM as described in Materials and Methods. (A) Immunofluorescence images confirming the removal of cells and retained ECM matrix after decellularization by detecting collagen I, III, VI and fibronectin with immunofluorescence. The top row shows the composite images of the fluorescence channels followed by the images of the individual channels: Hoechst (nuclei, blue), TRITC (red, cell membrane), FITC (ECM protein, green). (B-C) Effect of iMSC-deposited ECM on AML drug resistance. Molm-13 AML cells were cultured alone or on decellularized ECM for 24 h prior to treatment with (B) cytarabine (AraC) and (C) quizartinib. Cell viability was measured with Annexin V staining after 24 h of treatment with flow cytometry.

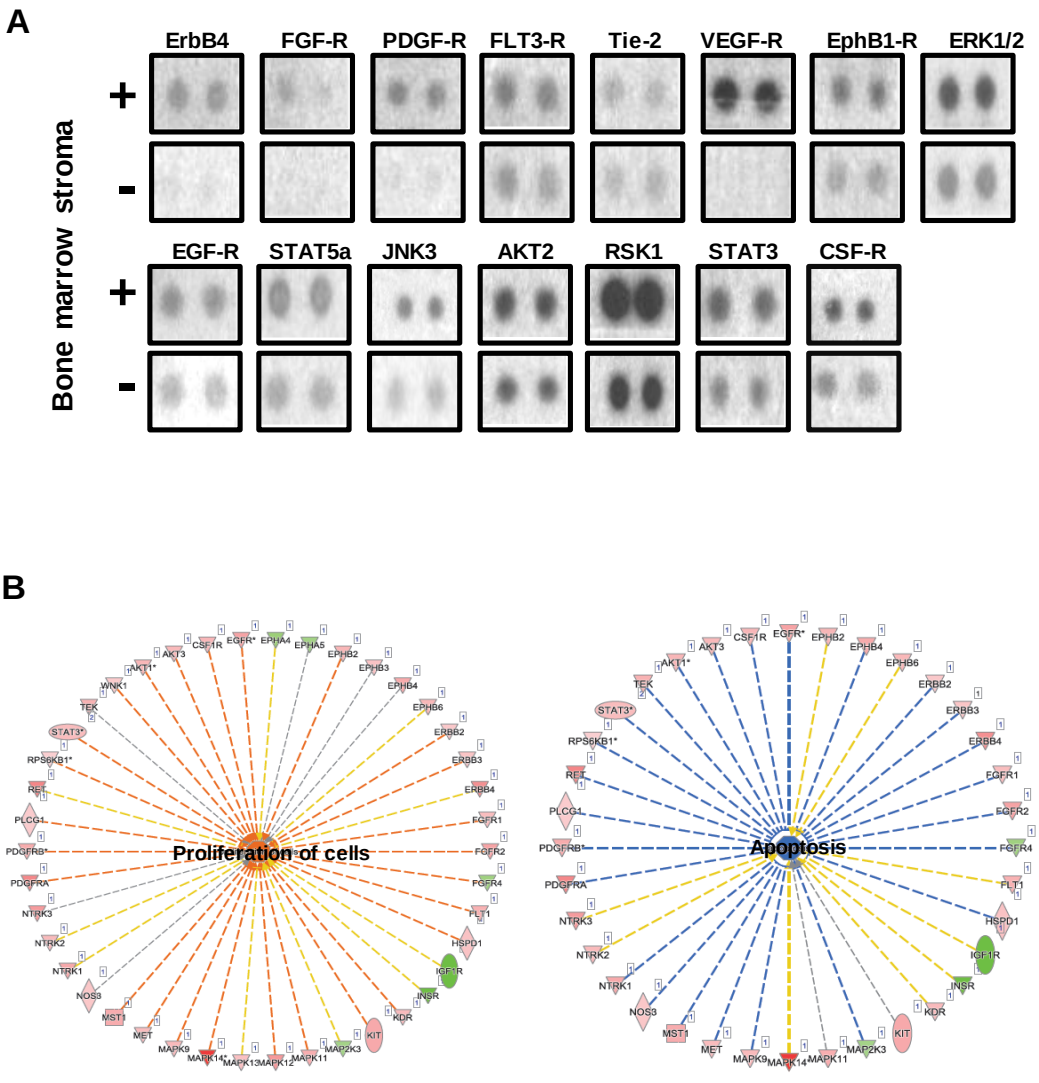

Supplementary Figure 2.5: Phospho-proteomic analysis of FLT3-ITD AML cells in contact with BMSC in the bone marrow microenvironment.
Molm13 cells were cultured with BMSCs for 24 h in a layered co-culture system. Activation of receptor tyrosine kinases (RTK), cytosolic kinases and mitogen activated protein kinases (MAPK) were analysed using antibody array. (A) Examples of the BMM regulated kinases in AML cells as identified in the dot plot. (B) Network analysis was performed to find out the significant and unique interactions. Key targets of the BMM induced kinase signalling in category of cell proliferation and apoptosis.

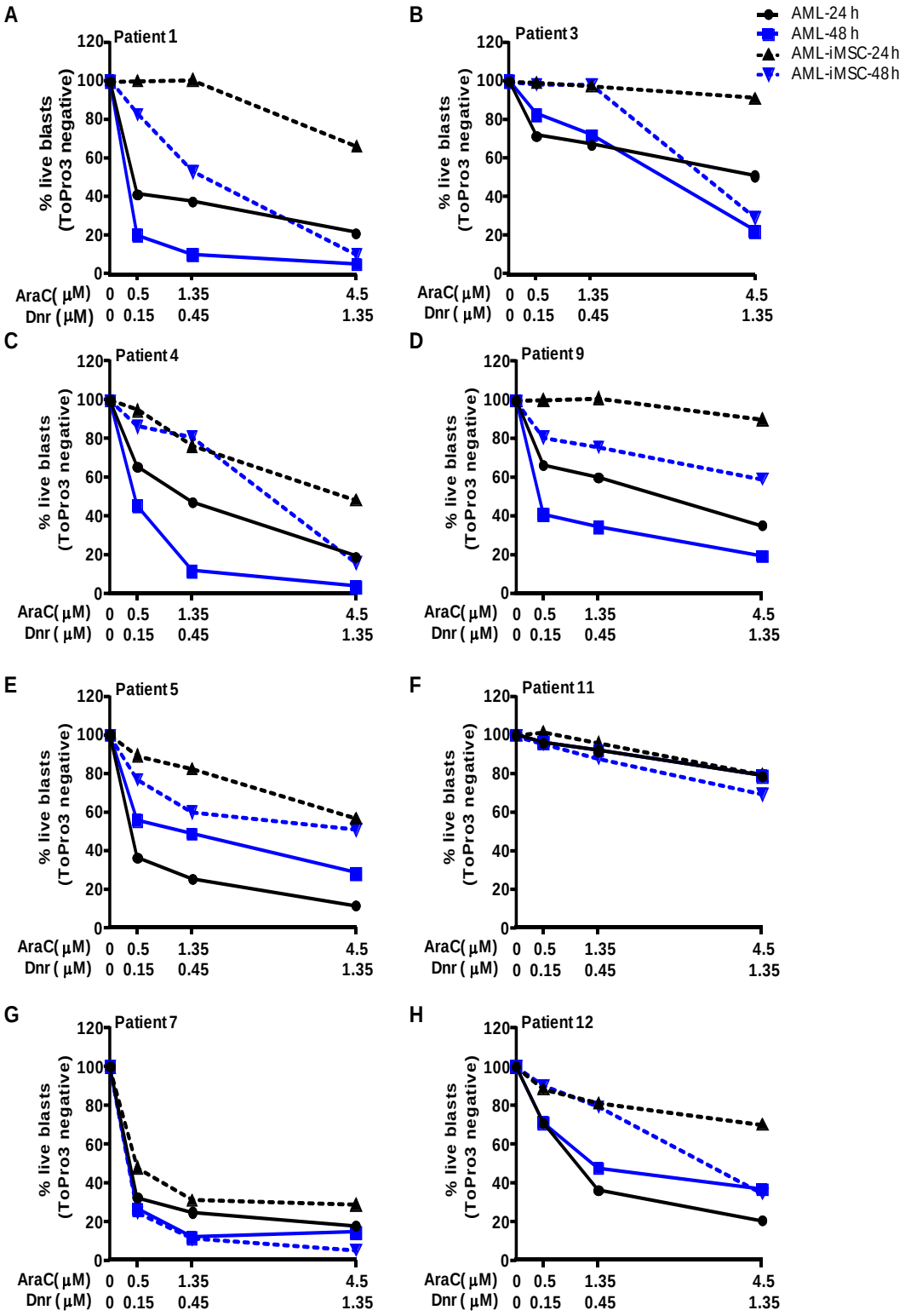
A
Patient 1
B
Patient 3
C
Patient 4
D
Patient 9
E
Patient 5
F
Patient 11
G
Patient 7
H
Patient 12
AML-24 h
AML-48 h
AML-iMSC-24 h
AML-iMSC-48 h
% live blasts (ToPro3 negative)
120
100
80
60
40
20
0
AraC(µM) 0 0.5 1.35 4.5
Dnr (µM) 0 0.15 0.45 1.35

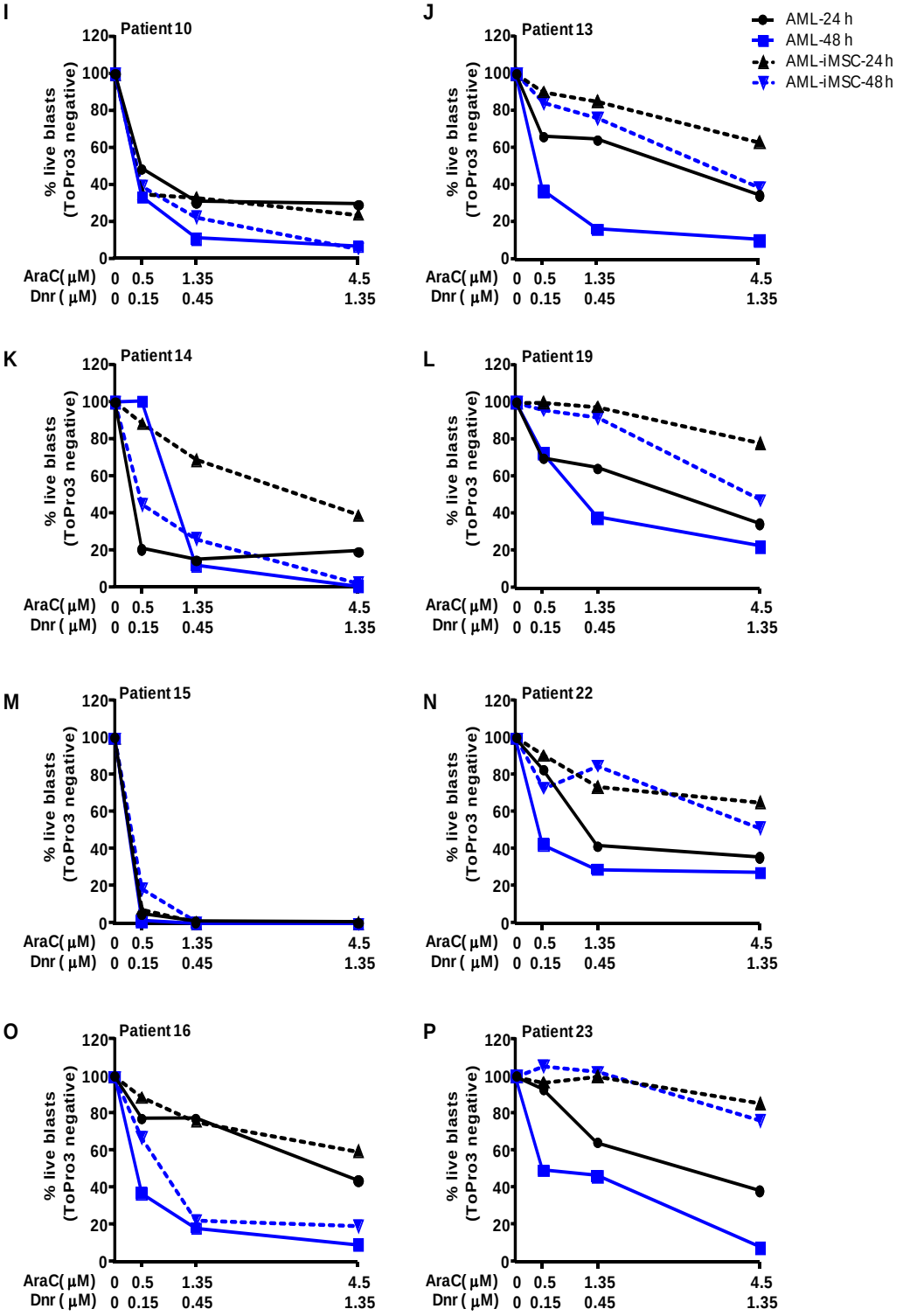
I
Patient 10
J
Patient 13
AML-24 h
AML-48 h
AML-iMSC-24 h
AML-iMSC-48 h
K
Patient 14
L
Patient 19
M
Patient 15
N
Patient 22
O
Patient 16
P
Patient 23
% live blasts (ToPro3 negative)
AraC(µM) 0 0.5 1.35 4.5
Dnr (µM) 0 0.15 0.45 1.35

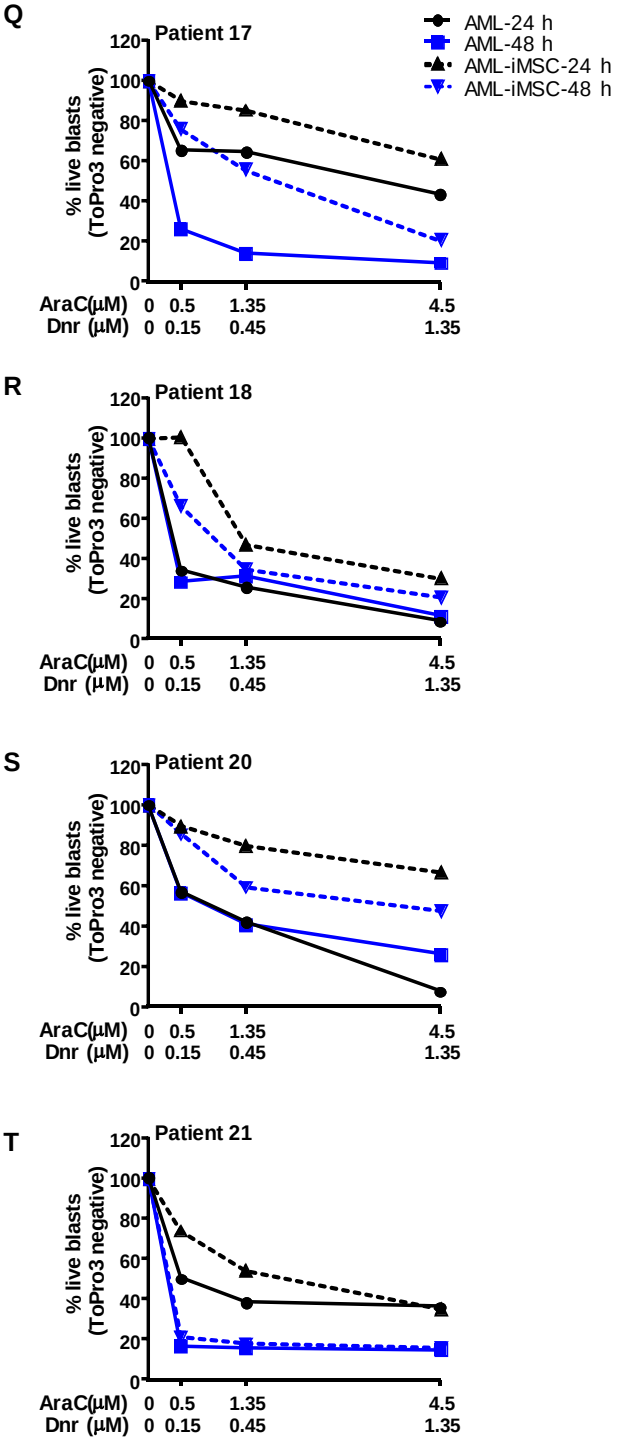

Supplementary Figure 2.6: Ex vivo co-culture of AML blasts with BMSCs can faithfully replicate the patient response in the clinic to AraC+Dnr treatment.
Bone marrow derived AML blasts were cultured with or without the iMSC stromal feeder layer for 24 h followed by treatment with 3:1 molar ratio of cytarabine (AraC) and daunorubicin (Dnr) combination. Cell viability was measured after 24 h and 48 h of treatment using ToPro3 dead cell staining. Graphs on left hand side (A, C, E, G, I, K, M, O, Q, R, S and T) show the percentage of live blasts cells in the bulk population surviving the treatment for the responder patients, while the graphs on the right-hand side (B, D, F, H, J, L, N and P) shows the dose response of the resistant patients.

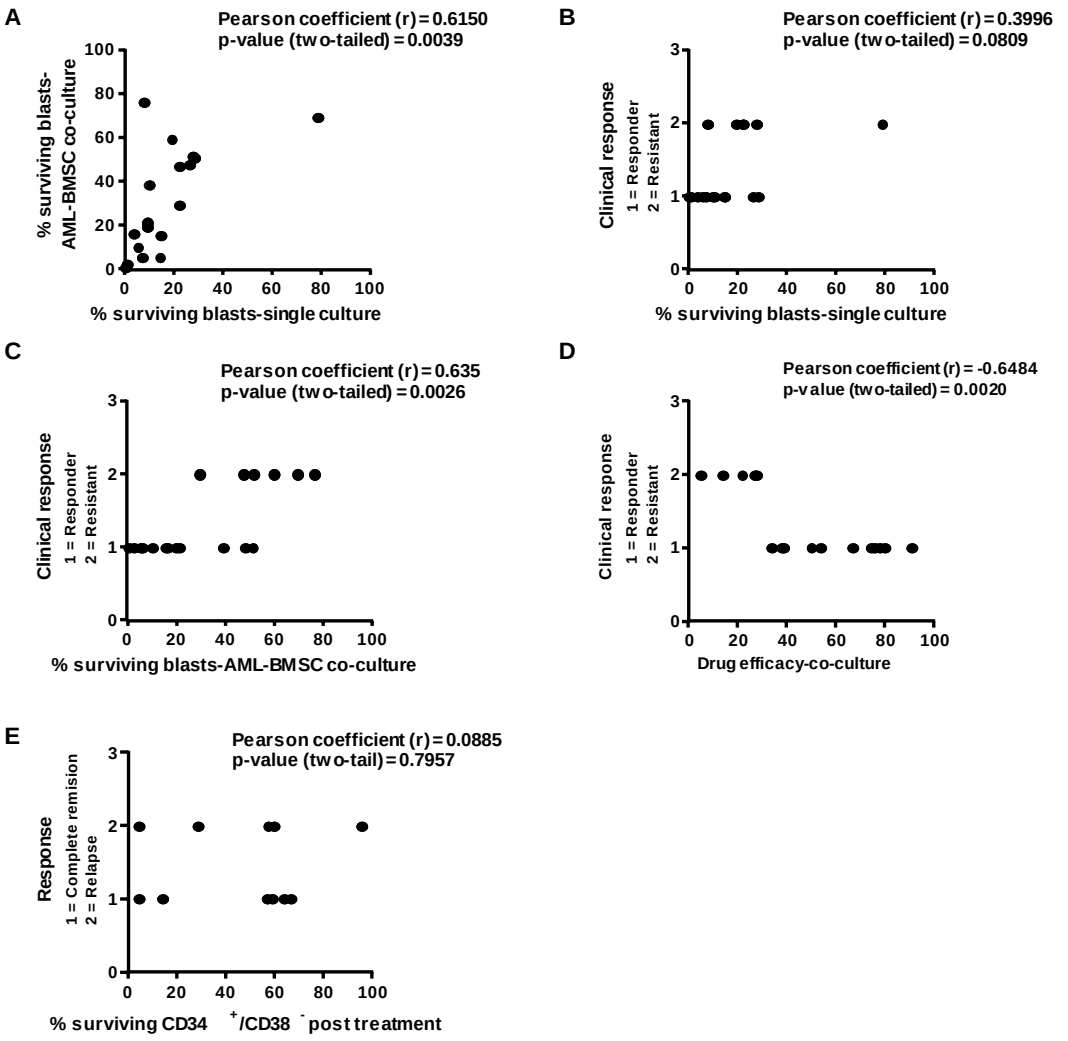

Supplementary Figure 2.7: Pearson correlation plots among different variables showing their association.

(A) Different variables like % surviving population is single culture was compared to that of co-culture, shows a strong association. (B) % surviving population in single culture compared to that of clinical response group (1= responder and 2= resistant to treatment) shows a moderate but non-significant association. (C) % surviving population in co-culture system compared to clinical response shows a moderate and significant association. (D) Pearson correlation of drug efficacy of co-culture system in predicting the clinical response (1= responders and 2= resistant to treatment) shows a strong and significant association. (E) Correlation between % surviving $CD34^{+}/CD38^{-}$ cells in the surviving population in predicting the relapse and complete remission (1= samples which achieved complete remission and 2= samples which had relapse) shows no correlation.

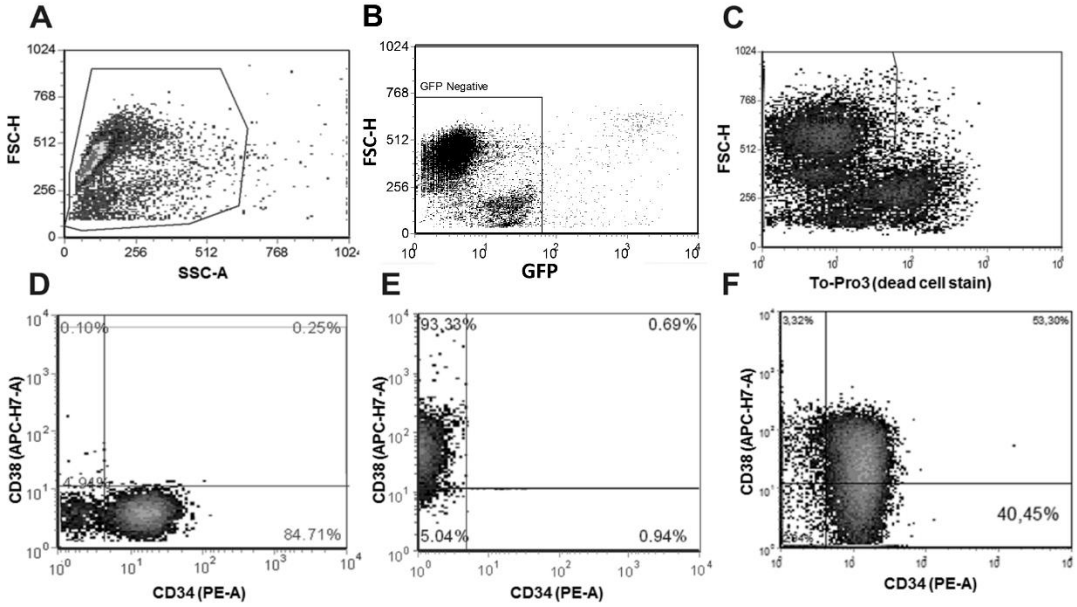

Supplementary Figure 2.8: Flow cytometry gating strategy.
(A) Forward scatter (FSC) Vs side scatter (SSC) plot showing all the events recorded (B) FSC Vs GFP or CFSE dot plot to gate out the detached HS-5 cells (GFP+) or iMSC/pBMSC (CFSE+). (C) Gating the viable cells with To-Pro3 dead cell stain in the bulk AML cell population. (D) CD38 (APC-H7) vs CD34 (PE) dot plot to gate and determine the CD34+ population in single stained sample using anti-CD34 (PE) antibody. (E) CD38 (APC-H7) vs CD34 (PE) dot plot to gate and determine the CD38+ population in single stained sample using anti-CD38 (APC-H7) antibody. (F) CD38 (APC-H7) Vs CD34 (PE) dot plot showing the gating strategy for the CD34+ /CD38- population in the viable AML bulk population.

2.7 Supplementary Tables

Supplementary Table 2.1: List of cytokines/chemokines secreted by HS-5, iMSC and primary BMSC as determined by antibody-based arrays in the conditioned medium.

Table showing the unique cytokines/chemokines for each of the three stromal cell types and common among at least two the stromal cell types.

Gene ID	Gene Symbol	Protein Name
Unique for pBMSC		
176	ACAN	Aggrecan core protein
1401	CRP	C-reactive protein
2638	GC	Vitamin D-binding protein
3082	HGF	Hepatocyte growth factor
3567	IL5	Interleukin-5
3673	ITGA2	Integrin alpha-2
3934	LCN2	Neutrophil gelatinase-associated lipocalin
4353	MPO	Myeloperoxidase
6363	CCL19	C-C motif chemokine; C-C motif chemokine 19
6462	SHBG	Sex hormone-binding globulin
7037	TFRC	Transferrin receptor protein 1
7412	VCAM1	Vascular cell adhesion protein 1
56729	RETN	Resistin
Unique for HS-5		
943	TNFRSF8	Tumor necrosis factor receptor superfamily member 8
2683	B4GALT1	Beta-1,4-galactosyltransferase 1
3553	IL1B	Interleukin-1 beta
Unique for iMSC		
727	C5	Complement C5
2247	FGF2	Fibroblast growth factor 2; Fibroblast growth factor
3383	ICAM1	Intercellular adhesion molecule 1
3485	IGFBP2	Insulin-like growth factor-binding protein 2
6364	CCL20	C-C motif chemokine 20
29949	IL19	Interleukin-19
Common between pBMSC and HS5		
354	KLK3	Prostate-specific antigen
959	CD40LG	CD40 ligand
1803	DPP4	Dipeptidyl peptidase 4
3458	IFNG	Interferon gamma
3552	IL1A	Interleukin-1 alpha
Common between pBMSC and iMSC		
284	ANGPT1	Angiopoietin-1
929	CD14	Monocyte differentiation antigen CD14
1471	CST3	Cystatin-C
2323	FLT3LG	Fms-related tyrosine kinase 3 ligand
3486	IGFBP3	Insulin-like growth factor-binding protein 3

4318	MMP9	Matrix metalloproteinase-9
5154	PDGFA	Platelet-derived growth factor subunit A
6374	CXCL5	C-X-C motif chemokine; C-X-C motif chemokine 5
Common between HS-5 and iMSC		
1437	CSF2	Granulocyte-macrophage colony-stimulating factor
1440	CSF3	Granulocyte colony-stimulating factor
3589	IL11	Interleukin-11
6352	CCL5	C-C motif chemokine; C-C motif chemokine 5
6354	CCL7	C-C motif chemokine 7

Supplementary Table 2.2: List of receptor tyrosine kinases, intracellular phospho kinases and mitogen-activated protein kinases activated in the Molm13 cells upon co-culturing with bone marrow stromal cells (iMSC).

Phosphorylated/activated kinases were identified as a dot plot on antibody array and image analysis was performed using HLImage++ tool. Fold change was calculated by comparing the signal to that of the Molm13 cells cultured alone. Kinases with FDR<0.05 with fold change of 2 were used for analysis and shown below.

Symbol	Gene name	Phosphorylation site	Fold change
	Receptor tyrosine kinase		
5979	RET		8.91
5156	PDGFRA		8.62
2066	ERBB4		7.47
6259	RYK		6.94
4916	NTRK3		6.08
2263	FGFR2		5.22
1956	EGFR		5.18
4914	NTRK1		4.65
3815	c-KIT		4.61
2050	EPHB4		4.59
285220	EPHA6		4.52
5159	PDGFRB		4.51
4485	MST1		4.41
2321	FLT1		3.99
7010	TEK		3.97
2048	EPHB2		3.73
1436	CSF1R		3.66
2051	EPHB6		3.56
2047	EPHB1		3.54
4915	NTRKK2		3.48
2045	EPHA7		3.45
3791	VEGFR2		3.42
4233	MET		3.35
2260	FGFR1		3.24
2049	EPHB3		2.99
2065	ERBB3		2.85

2064	ERBB2		2.65
4593	MUSK		2.23
2261	FGFR3		2.00
Intracellular Phospho kinases			
6774	STAT3	S727	3.302
3329	HSPD1		2.977
6774	STAT3	Y705	2.904
4846	NOS3	S1177	2.746
65125	WNK1	T60	2.541
5335	PLCG1	Y783	2.504
6198	RPS6KB1	T421/S424	2.371
2185	PTK2B	Y402	2.275
Mitogen activated protein kinase			
6300	MAPK12	T183/Y185	6.34
5600	MAPK11	T180/Y183	4.27
1432	MAPK14	T180/Y182	4.25
207	AKT1	S473	3.74
1000	AKT3	S472	3.50
5601	MAPK9	T183/Y185	3.47
5602	MAPK10	T221/Y223	3.30
5603	MAPK13	T180/Y184	3.07
3315	HSP27	S78/S82	2.28

Supplementary table 2.3: Clinical information of the patient cytogenetics, age, treatment and clinical response.

Patient ID	Age	Type	Cytogenetics	Clinical drug	Clinical response
1	46	AML	t(8;21) (good risk)	DA3+10	CR
2	75	secondary AML	Complex cytogenetics (poor risk)	Azacytidine	RD
3	52	AML	Monosomy 7 (poor risk)	DA3+10	RD
4	42	AML-M2	NK, FLT3-, NPM-	3+10 ; 3+8, hdac x 2	CR
5	39	AML	Intermediate risk cytogenetics	DA3+10	CR
6	69	secondary AML	NK, FLT3-, NPM-	1 cycle of clofarabine	RD
7	71	AML-M1	NK, FLT3-, NPM-	DA3+10	CR
8	82	AML	Complex cytogenetics (poor risk)	Azacytidine	RIP before assessment
9	44	AML	FLT3-, NPM-	DA3+10	RD
10	67	AML	NK, FLT3+, NPM+	DA3+10	PR
11	76	AML	Normal karyotype (NK)	DA3+10	RD
12	71	AML	NK, FLT3-, NPM+	DA3+10	CR
13	67	AML	NK, FLT3+, NPM+	Da 3+10	CR
14	71	AML	NK, FLT3-, NPM+	DA3+10	CR
15	60	AML	NK, FLT3+, NPM-	DA3+10	CR
16	53	AML with Fibrosis	Complex cytogenetics (poor risk)	DA3+11	CR
17	41	AML	Intermediate risk cytogenetics	DA3+12	CR
18	67	AML	NK, FLT3-, NPM-	DA3+10	RD

19	69	AML	AML-NPM1+, trisomy 8	DA3+10	RD
20	69	secondary AML	AML with MDS	DA3+10	PR
21	63	AML	AML with MPAL t(v;11q23.3); KMT2A rearranged	DA3+10	CR
22	39	AML	AML with Inv(16)p13,1q22	DA3+10	RD
23	70	AML	AML with NPM+	DA3+10	RD

CHAPTER 3: *Repression of Mcl-1 expression by the CDC7/CDK9 inhibitor PHA-767491 overcomes bone marrow stroma-mediated drug resistance in AML*

Preamble to Chapter 3: Statement of Contribution

This chapter consists of work published in Scientific Reports (O'Reilly et al., 2018). I am the equal contributing author along with Eimear O'Reilly. I performed the experiments corresponding to Figure 3.1 A-D, 3.3 B-C, Figure 3.6 A-B, Figure 3.7, Figure 3.8. Supplementary Figure 3.1, Supplementary Figure 3.2 B-C, Supplementary Figure 3.5, Supplementary Figure 3.6, Supplementary Figure 3.7 and Supplementary Table 3.1. I also contributed to analysing data, performing statistical analysis, writing and editing manuscript.

Repression of Mcl-1 expression by the CDC7/CDK9 inhibitor PHA-767491 overcomes bone marrow stroma-mediated drug resistance in AML

Eimear O' Reilly[1*], Sukhraj Pal S. Dhami[1*], Denis V. Baev[1], Csaba Ortutay[5], Anna Halpin-McCormick[1], Ruth Morrell[1], Corrado Santocanale[2], Afshin Samali[1], John Quinn[3], ME O'Dwyer[1,4], Eva Szegezdi[1,]

[1]Apoptosis Research Centre, School of Natural Sciences, National University of Ireland Galway, Galway, Ireland

[2]Centre for Chromosome Biology, School of Natural Sciences, National University of Ireland Galway, Galway, Ireland

[3]Hematology, Beaumont Hospital, Dublin, Ireland.

[4]Apoptosis Research Centre, School of Medicine, National University of Ireland Galway, Galway, Ireland.

[5]HiDucator Ltd, Kangasala, Finland

* These authors contributed equally.

Scientific Reports 2018 Oct 25;8(1):15752.

3.1 Abstract

Acute myeloid leukaemia (AML) is an aggressive cancer with 50-75% of patients relapsing even after successful chemotherapy. The role of the bone marrow microenvironment (BMM) in protecting AML cells from chemotherapeutics and causing consequent relapse is increasingly recognised. However, the role that the anti-apoptotic Bcl-2 proteins play as effectors of BMM-mediated drug resistance are less understood.

Here we show that bone marrow mesenchymal stromal cells (BMSC) provide resistance to AML cells against BH_3-mimetics, cytarabine and daunorubicin, but this is not mediated by Bcl-2 and/or Bcl-X_L as previously thought. Instead, BMSCs induced Mcl-1 expression over Bcl-2 and/or Bcl-X_L in AML cells and inhibition of Mcl-1 with a small-molecule inhibitor, A1210477, or repressing its expression with the CDC7/CDK9 dual-inhibitor, PHA-767491, restored sensitivity to BH_3-mimetics. Furthermore, combined inhibition of Bcl-2/Bcl-X_L and Mcl-1 could revert BMSC-mediated resistance against cytarabine+daunorubicin. Importantly, the $CD34^+/CD38^-$ leukemic stem cell-encompassing population was equally sensitive to the combination of PHA-767491 and ABT-737.

These results indicate that Bcl-2/Bcl-X_L and Mcl-1 act in a redundant fashion as effectors of BMM-mediated AML drug resistance and highlight the potential of Mcl-1-repression to revert BMM-mediated drug resistance in the leukemic stem cell population, thus, prevent disease relapse and ultimately improve patient survival.

3.2 Introduction

Acute myeloid leukemia (AML) is a complex disease driven by a combination of genetic and epigenetic alterations in the hematopoietic stem or progenitor cells. Despite our increasing understanding of the molecular aberrancies that drive AML, up to 20-30% of young and 40-50% of older AML patients are refractory to treatment. Furthermore, the risk of relapse is high between 50-75%, depending on age [428]. The prognosis following relapse is poor and at this stage, no good treatment strategies available [429]. As our understanding of the molecular aberrations driving AML increases, a number of targeted therapeutics, such as protein kinase inhibitors (FLT3, PI3K, Akt, Erk or Pim inhibitors), inhibitors of DNA methylating- and acetylating enzymes, such as DNMT1, DNMT3, DOT1L and HDACs or BH_3-mimetics against anti-apoptotic Bcl-2 proteins are being developed [430,431]. While the development of these inhibitors is progressing rapidly, understanding the role of the bone marrow microenvironment (BMM) in controlling the epigenetic landscape and driving survival signalling in AML cells is lagging behind. Underlining its importance, bone marrow-mediated protection was found to be the major cause of low FLT3-inhibitor efficacy [417,432].

The most studied mechanism by which bone marrow stromal cells (BMSCs) induce drug resistance is the activation of pro-survival signal transduction, typically culminating in the upregulation of Bcl-2 (BCL2) and/or Bcl-X_L (BCL2L1) [433,434]. Induction of anti-apoptotic Bcl-2 proteins is an inherent feature of normal differentiation of leukocytes as Bcl-2 proteins provide survival advantage to the properly formed mature cells. For example, Mcl-1 (MCL1) is required for the survival of hematopoietic stem cells (HSC) [435], common myeloid progenitors (CMP) and common lymphoid progenitors (CLP), Bcl-2 is induced during the selection of T and B lymphocytes while Bcl-X_L (BCL2L1) is critical for erythrocyte- [436,437], megakaryocyte-[438] and platelet survival [439], and A1 (BCL2A1) supports neutrophil survival [440].

Increased Bcl-2 expression is also a characteristic of several haematological malignancies, including chronic lymphocytic leukemia (CLL) and AML. The notion that leukemic cells become dependent on anti-apoptotic Bcl-2 protein expression for survival is proven by the potent effect of the Bcl-2/Bcl-X_L/Bcl-W inhibitor, ABT-737 and its Bcl-2-selective variant, ABT-199 [441]. The ability of anti-apoptotic Bcl-2 proteins to drive drug resistance is also well established. Accordingly, ABT-737 and/or ABT-199 have been shown to sensitise isolated AML cells to 5-azacytidine [442], FLT3 inhibitors [443] as well as docetaxel [444].

Here we determined the role of anti-apoptotic Bcl-2 proteins as effectors of bone marrow stroma-mediated drug resistance in AML blasts and the $CD34^+/CD38^-$ cells representing a population enriched for leukemic stem cells (LSC) [445]. We show that bone marrow stromal cells (BMSCs) provide resistance against BH_3-mimetics, cytarabine (AraC) and daunorubicin (DnR) and that this protection is also pronounced in the $CD34^+/CD38^-$ cell population. We show that inhibition of Bcl-2 and Bcl-X_L with ABT-737 is not sufficient to revert BMSC-mediated drug resistance against AraC+DnR. On the other hand, BMSC-mediated drug

resistance was associated with increased Mcl-1 expression. Furthermore, Mcl-1 inhibition with A1210477 or repression with PHA-767491 could revert drug resistance mediated by BMSCs. Importantly, repression of Mcl-1 expression with the dual CDC7/CDK9 inhibitor PHA-767491 equally sensitized the $CD34^+/CD38^-$ cell population offering a strategy to eradicate the main cell population responsible for disease relapse.

3.3 Materials and Methods

3.3.1 Reagents

All reagents were purchased from Sigma, unless stated otherwise. ABT-737 and A1210477 from Selleck Chemicals, ABT-199 from Active Biochem and PHA-767491 (provided by Corrado Santocanale, NUI Galway) were dissolved in dimethyl sulfoxide (DMSO). AraC and DnR (Sigma) were dissolved in water. Carboxyfluorescein succinimidyl ester (CFSE) (Biolegend) was dissolved in DMSO.

3.3.2 Cell culture

OCI-AML2, OCI-AML3, HL-60, ML-1 and Molm-13 cell lines were cultured in RPMI-1640 medium (Gibco) containing 10% heat-inactivated HyClone fetal bovine serum (HI-FBS, ThermoFisher), penicillin (100 U/ml), streptomycin (100 μg /ml) and 2 mg/ml L-glutamine. HS-5 cells were cultured in DMEM supplemented with 10% HI-FBS, penicillin (100 U/ml), streptomycin (100 μg/ml). iMSCs (hTERT immortalized primary BMSCs from a healthy donor) and primary BMSCs were cultured in alpha-MEM (Sigma) containing 10% HI-FBS, penicillin (100 U/ml) and streptomycin (100 μg /ml). To enable identification of BMSCs in analyses, HS-5 cells were transfected with GFP, while iMSCs and primary BMSCs were stained with the green fluorescent cell-tracker CFSE by incubating the $1x10^6$ cells/ml with 5 μM CFSE for 30 min prior to seeding.

Primary AML samples were generated from bone marrow aspirates by isolating the mononuclear cell (MNC) fraction with Ficoll gradient-centrifugation as described before [446]. MNCs were stored in liquid nitrogen until use. Upon revival of the cells, viability was determined with trypan blue staining. Only samples with viability above 60% were used. Primary AML blasts were grown in αMEM (Sigma) containing 10% HI-FBS, penicillin (100 U/ml), streptomycin (100 μg /ml), L-glutamine (2 mg/ml) and sodium pyruvate (1 mM).

3.3.3 Ethics Statement

Ethical approval was obtained from the Research Ethics Committee of University College Hospital, Galway and NUI Galway. The ethical approval confirmed that all methods were carried out according to the regulation of NUI Galway and all applied protocols have been

approved by the research ethics committees. Informed consent was obtained from all participants.

3.3.4 Immunophenotyping and viability assay

MNCs were incubated with fluorochrome-conjugated anti-CD34 (phycoerythrin, PE) and anti-CD38 (allophycocyanine (APC)-H7) antibodies (BD Bioscience, San Diego, USA) in PBS/1% BSA (Sigma) for 30 minutes on ice in the dark. After washing off unbound antibodies, cells were stained with ToPro-3 (Molecular Probes) according to the manufacturers' protocol. The samples were analysed using BD FACS Canto II flow cytometer (BD Bioscience, San Diego, USA) by collecting 100,000 events AML blast gate. HS-5 cells were excluded by gating out GFP^{+}/FSC^{high} events. The detailed gating strategy is shown in Supplementary Figure 3.8.

In the AML cell lines cell death was quantified with Annexin V-FITC or propidium iodide (PI) staining. Cells were collected and stained with Annexin V-FITC in Annexin V buffer (10 mM HEPES/NaOH, pH 7.5, 140 mM NaCl, 2.5 mM $CaCl_2$) or propidium iodide (1 µg/ml) for 15 min on ice in the dark. Samples were analyzed on a FACS Canto II flow cytometer. Statistical analysis was performed using FCSExpress (DeNovo Software Inc., USA) and GraphPad Prism (GraphPad Software Inc., La Jolla, USA) software packages.

3.3.5 Western blotting

Cells were lysed in whole cell lysis buffer (1% Igepal-630, 20 mM HEPES pH 7.5, 350 mM NaCl, 1 mM $MgCl_2$, 0.5 mM EDTA, 0.1 mM EGTA, 0.5 mM DTT, and protease inhibitor cocktail). Proteins (30 µg) were electrophoresed and transferred onto nitrocellulose membrane (Protran). After blocking the blots were incubated with rabbit polyclonal antibodies against Mcl-1 (Cell Signaling Technologies (CST), actin (Sigma) and mouse monoclonal antibodies against Bcl-X_L (Santa Cruz) and Bcl-2 (Santa Cruz). For detection, horseradish peroxidase-conjugated goat secondary antibodies were used. Protein bands were visualized with SuperSignal® West Pico Chemiluminescent Substrate (Pierce) or Immobilon western HRP substrate (Millipore) on X-ray film (Agfa). Quantification of the Western blots by densitometry was conducted using Image Studio Lite (Li-Cor). Statistical analysis was performed on normalised band intensities using paired Student's t-test.

3.3.6 Gene expression analysis

Gene expression profiles were investigated in an open-access dataset of 64 samples (Gene Expression Omnibus : GDS3057) [447]. GDS3057 contained 26 AML samples (7 bone marrow (BM) and 19 peripheral blood (PB)) and 38 healthy donors (18 BM and 20 PB). The BM and PB samples were not matched (not from the same patients). Shapiro test was used

to see normality of data groups. Two-tailed t-test was used to estimate significance of difference of mean gene expressions using the R statistical environment.

3.3.7 siRNA transfection

Primary AML mononuclear cells ($1x10^6$) were pelleted and resuspended in 100 µl of Nucleofector solution T (Amaxa, Lonza) containing 50 nM siRNA against Mcl-1 (5'-GUGUUAAGAGAAGCA CUAA-3') or GFP (as a non-specific, control siRNA, 5' -GGCUACGUCCAGGAGCGCAC C-3', Ambion). Cells were transfected by nucleofection using the U-15 program, as per manufacturer's protocol (Amaxa) [448].

3.3.8 Statistical Analysis

Drug combination index (CI) was calculated using the Chou-Talalay median effect equation using the CompuSyn software package. CI values below 1 (CI<1) indicated potent synergy. Statistical analyses applied for specific methods are detailed under each corresponding method subheading.

3.4 Results

3.4.1 Bone marrow mesenchymal stromal cells protect AML cells from therapeutic drugs

In order to determine the effect of anti-apoptotic Bcl-2 proteins in drug resistance mediated by the BMM, a layered stroma-AML co-culture system has been set up. AML cell lines or primary AML blasts were cultured on a monolayer of BMSCs in direct contact. As a model of BMSCs, HS-5 cells, an immortalised healthy donor-derived BMSC cell line, were used. HS-5 cells were chosen over primary BMSCs of AML patients, as the latter were found to be prone to senescence under *ex vivo* culture [284]. As HS-5 cells are only a clone of immortalised BMSCs, they may not represent the full spectrum of function that primary BMSCs have. Thus, we tested how faithfully they could replicate the effect of patients' own BMSCs. To this end, primary AML cells were cultured alone, on the patients' own BMSCs or on two different immortalised BMSC lines; the commercially available HS-5 cells and a non-commercially available hTERT immortalised BMSC cell line that we named iMSC. After 24 h, the cultures were treated with ABT-737 or ABT-199 and induction of cell death was quantified. Both HS-5 cells and iMSCs could both replicate the effect of the patients' own BMSCs in providing a comparable level of resistance to AML cells against both drugs (Figure 3.1 A-D, Supplementary Figure 3.1).

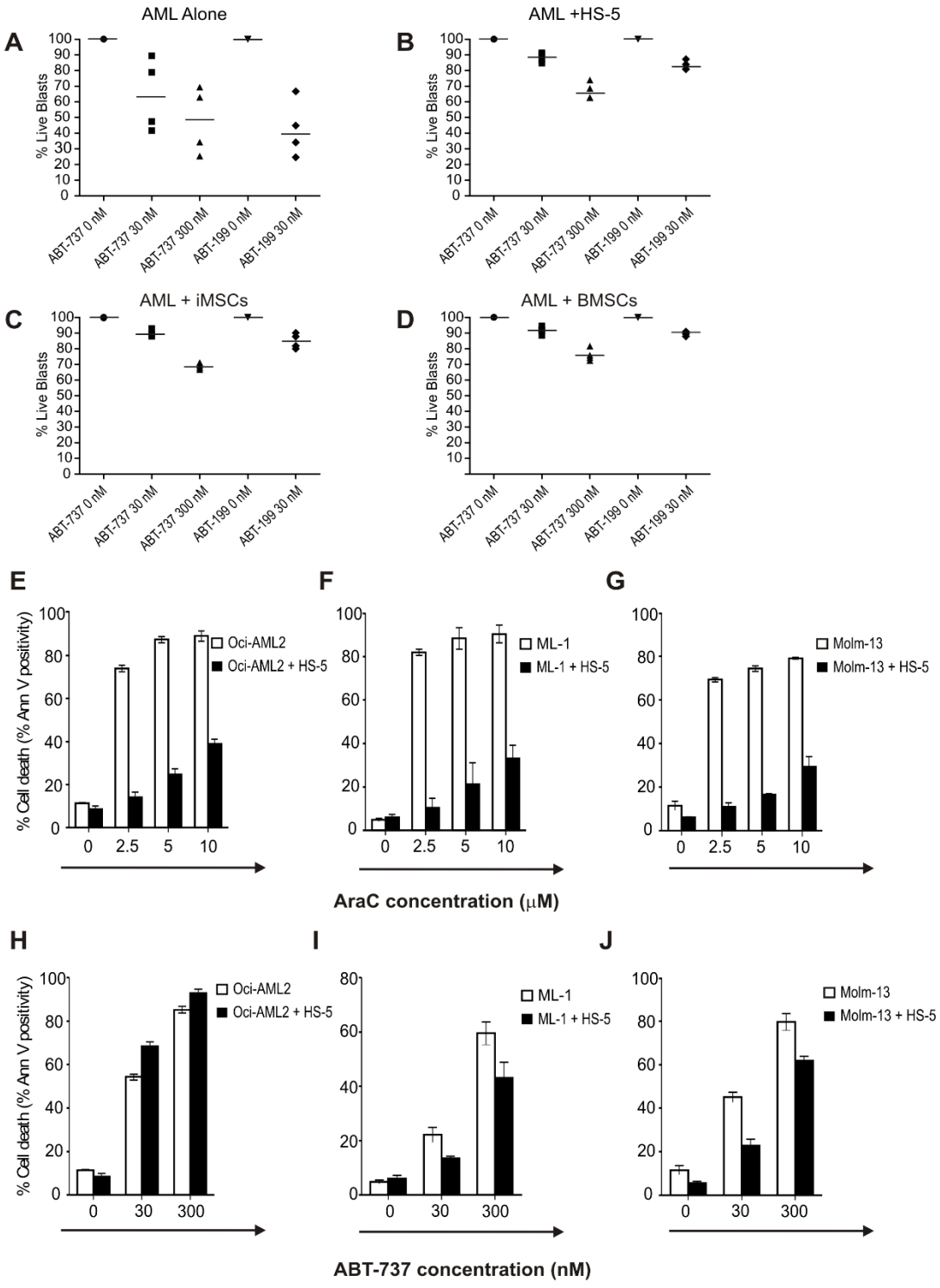

Figure 3.1: Bone marrow mesenchymal cells reduce AML sensitivity to ABT- 737 and cytarabine. (A-D) Immortalised, healthy-donor derived BMSCs can replicate the protective effect of the patients' own BMSCs against BH_3-mimetics. Bone marrow-derived mononuclear cells from AML patients were culture alone (A) or over 3 different bone marrow stromal cell layers; HS-5 cells (B), iMSCs (C) and the patients' own BMSCs (D) for 24 h after which the cells were treated with ABT-737 or ABT-199 for another 24 h. Induction of cell death in the AML population was determined with ToPro-3 staining using flow cytometry. The graphs show % live blasts from 4 different patients normalised to the untreated control. (E-J) HS-5 BMSCs provide protection against cytarabine (AraC) and ABT-737 in AML cell lines. OCI-AML2, ML-1 and Molm-13 cells were cultured in direct contact with HS-5 BMSCs for 24 h followed by treatment with a dosage of AraC (E, F, G) or ABT-737 (H, I, J) for another 24 h and induction of cell death was quantified by flow cytometry using Annexin V. The graphs show the average percentage of dead cells ± stdev from at least three independent repeats.

Cytokine expression as a measure of their ability to model features of the BMM has also been determined using a cytokine proteome array (Bio-Techne, Supplementary. Table 3.1). HS-5 cells secreted the cytokines and chemokines characteristic of the bone marrow [449], including granulocyte-colony stimulating factor (G-CSF), angiopoietin 1 (ANGPT1), angiopoietin 2 (ANGPT2), growth differentiation factor 15 (GDF15), osteopontin, interleukin 1β (IL-1β), fibroblast growth factor 2 (FGF2), C-C motif chemokine ligand 5 (CCL5), CCL7, C-X-C motif chemokine ligand 10 (CXCL10), CXCL12 (SDF1α) (for the complete list of secreted cyto/chemokines, see Supplementary Table 3.1.

The broader effect of BMSCs on AML drug sensitivity was next tested using AraC, DnR and ABT-737 in both AML cell lines and primary AML cells. OCI-AML2, ML-1 and Molm-13 cells were co-cultured with HS-5 cells for 24 h followed by treatment with a dosage of AraC or ABT-737 for 24 h and cell viability was determined with Annexin V staining. With the exception of ABT-737 treatment of OCI-AML2 cells, all co-cultures showed a significantly reduced sensitivity (Figure 3.1E-J).

Similar effects were found using AML blasts. The mononuclear cell fraction isolated from bone marrow aspirates of AML patients (AML blasts) were cultured on HS-5 cells for 24 h followed by exposure to a 3:1 molar ratio of AraC and DnR (corresponding to the molar ratio of the two drugs used in the clinic (7+3 therapy [450]) or a dosage of ABT-737 for 24 h. Induction of cell death in the AML blasts was determined using the viability dye, ToPro-3. Similar to the cell lines, AML blasts gained resistance against both AraC+DnR and ABT-737 when cultured with BMSCs (Figure 3.2A-F). Of note, the resistance against DnR+AraC provided by HS-5 BMSCs was also pronounced in the $CD34^{+}/CD38^{-}$ population shown by their enrichment in the surviving cell fraction (Figure 3.2G and H).

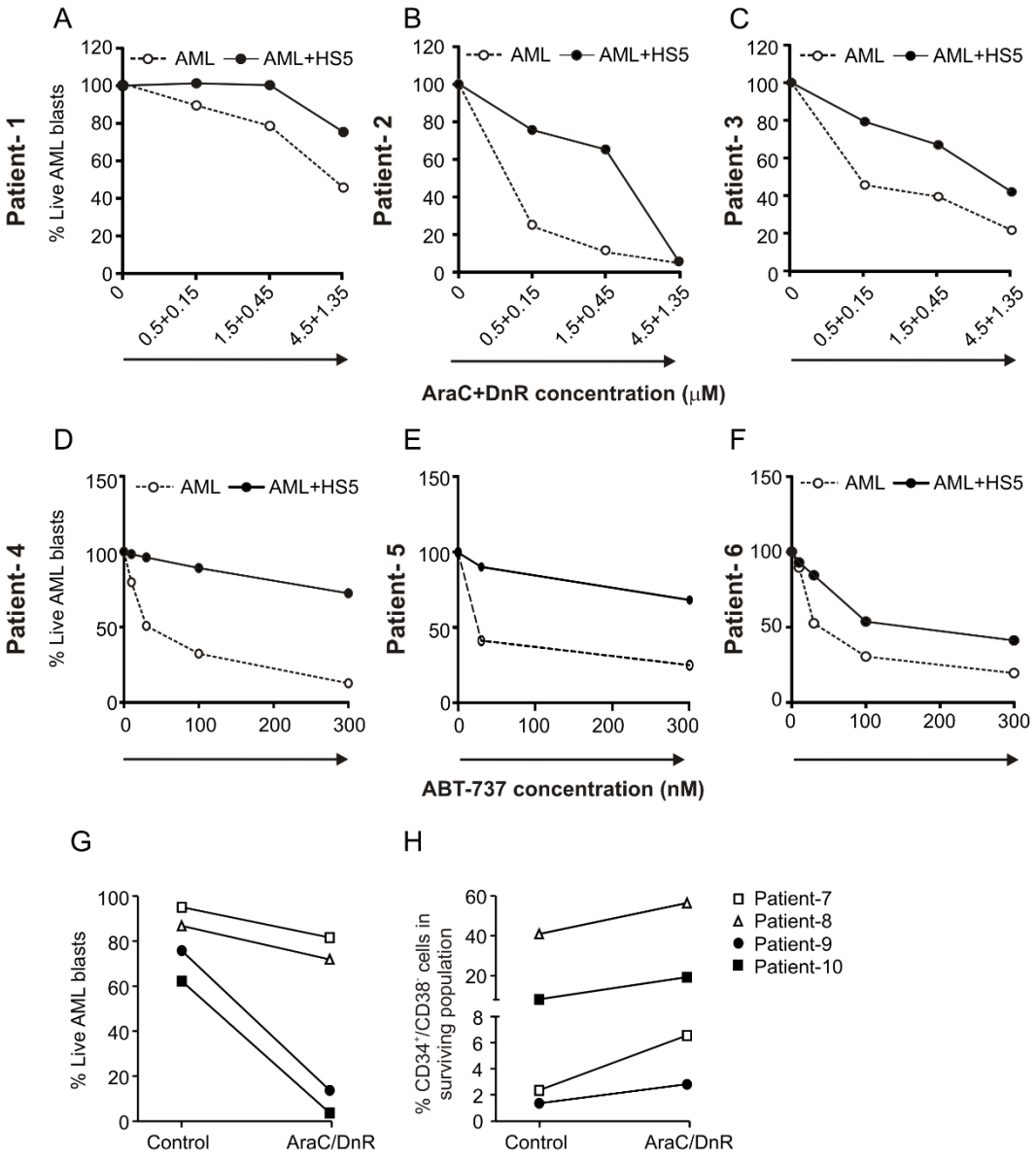

Figure 3.2: Primary AML blasts gain resistance against cytotoxic therapeutics when cultured in contact with BMSCs.
Bone marrow-derived mononuclear cells from AML patients were cultured either alone or with HS-5 BMSCs for 24 h followed by exposure to a 3:1 molar ratio of AraC and DnR (A, B, C) or to a dosage of ABT-737 (D, E, F) for 24 h. Induction of cell death in the AML blasts was determined with ToPro-3 staining using flow cytometry. The graphs show percentage live blasts normalised to the untreated control (G and H). HS-5 BMSCs provide resistance to the LSC-encompassing $CD34^+/CD38^-$ population against AraC+DnR. BM-derived AML blasts from 4 patients were cultured with HS-5 BMSCs and treated with AraC+DnR as in sections A-C. The graph shows the percentage of $CD34^+/CD38^-$ cells within the surviving cell fraction as a measure of their relative enrichment.

3.4.2 AML cells residing in the bone marrow microenvironment have increased Mcl-1 expression

To determine the contribution of anti-apoptotic Bcl-2 proteins to BMM-driven drug resistance, we determined the effect of HS-5 BMSCs on the expression of anti-apoptotic Bcl-2 proteins. A panel of AML cell lines (OCI-AML2, OCI-AML3, HL60, ML-1, Molm-13) was cultured with HS-5 cells for 24 h and changes in the expression of Bcl-2, Bcl-X_L and Mcl-1 were determined

with western blotting. Interestingly, while HS-5 BMSCs did not induce significant change in the expression of Bcl-2 and Bcl-X_L, in 4 out of the 5 cell lines tested, Mcl-1 induction was detected (Figure 3.3A).

To gain insight whether the BMM exerts the same effect *in vivo*, we compared the mRNA expression of Bcl-2, Bcl-X_L and Mcl-1 between bone marrow (BM)-residing and peripheral blood (PB)-circulating AML blasts. To this end, mRNA expression data from the Gene Expression Omnibus dataset, GDS3057 was extracted [451]. The housekeeping genes, GPI (Glucose-6-Phosphate Isomerase), PSMB2 (Proteasome Subunit Beta 2) and EMC (ER Membrane Protein Complex Subunit) were used for normalisation. Bcl-2 and Bcl-X_L expression was comparable between BM and PB. Mcl-1 expression on the other hand showed the opposite trend, it appeared to be lower in PB than in BM (Supplementary Figure 3.2A), however, it did now each a level of significance.

Because there are no gene expression datasets with matched BM and PB samples (i.e. BM and PB sample were not from the same patient) and because mRNA expression may not mirror the actual protein expression, we have tested Mcl-1 protein expression in paired BM and PB samples of 12 AML patient samples. Mcl-1 was expressed in 7 out of the 12 samples, out of which 5 have shown higher expression of Mcl-1 in the BM in comparison to the PB (Figure 3.3B and Supplementary Figure 3.2B). Statistical testing showed no significant difference in Mcl-1 expression between BM and PB with all samples included. After excluding the samples that showed no detectable Mcl-1 expression, a significant difference was apparent between Mcl-1 expression in BM versus PB ($p= 0.033$). This difference in the altered levels of Mcl-1 among patients cannot be explained by their cytogenetics (Supplementary Table 3.3). Though mutation profiling for the Bcl-2 family proteins will shed light into this altered Mcl-1 expression. We then tested whether AML blasts also show Mcl-1 induction upon contact with BMSCs, similar to AML cell lines. For this, BM-derived versus PB-derived AML blasts were cultured in contact with BMSCs (iMSC) for 24 h and Mcl-1 protein expression was determined with Western blotting. Contact with iMSCs induced Mcl-1 expression all 4 samples tested (Figure 3.3C, Supplementary Figure 3.2C and 3.2D). Taken together, these experiments show that in a subset, but not in all patients, the BMM drives MCl-1 expression in the residing AML blasts.

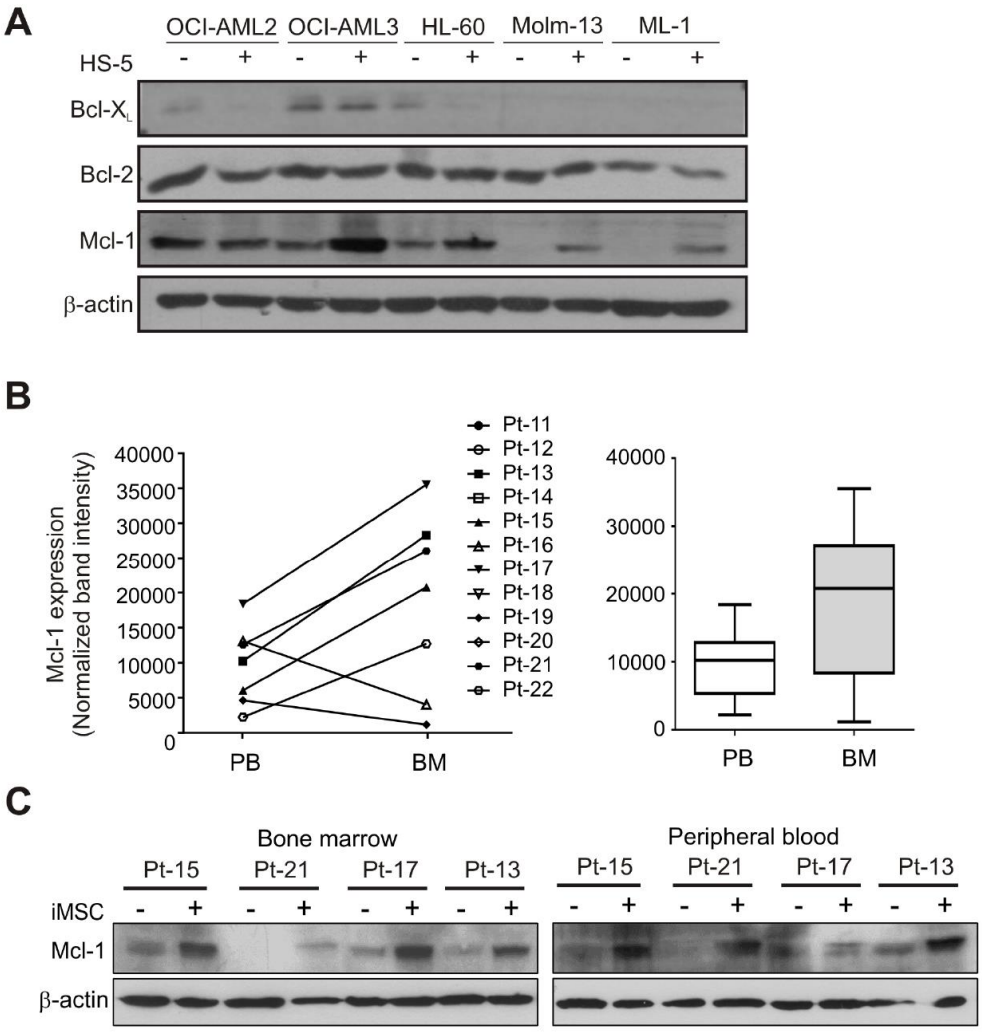

Figure 3.3: Bone marrow stromal cells induce Mcl-1 expression in AML cells.
(A) Expression of anti-apoptotic Bcl-2 family proteins in AML cells cultured on HS-5 BMSCs. OCI-AML2, OCI-AML3, HL60, ML-1, Molm-13 cells were cultured alone or in direct contact with HS-5 cells for 24 h and changes in the expression of Bcl-2, Bcl-X_L and Mcl-1 were determined with Western blotting. Levels of actin were measured as loading control. (B) Expression of Mcl-1 protein in the bone marrow- and peripheral blood-derived AML blasts. Whole cell lysates of mononuclear cells isolated from paired bone marrow aspirates and peripheral blood from 12 AML patients were analysed for the expression of Mcl-1 by Western blotting and quantified with densitometry. The left-hand graph shows the expression values of individual patients and the right-hand graph shows the value distribution as a box-plot. The p-value was determined using a paired t-test. (C) Mcl-1 expression in AML blasts cultured alone or with BMSCs. Mcl-1 protein expression was detected in bone marrow- and peripheral blood-derived MNCs from 4 AML patient cultured alone or on iMSC BMSCs for 24 h. Levels of β-actin were measured as a loading control.

To assess the contribution of anti-apoptotic Bcl-2 proteins to BMM-mediated AML drug resistance, we tested if inhibition of Bcl-2/Bcl-X_L can revert BMSC-mediated resistance to chemotherapeutics. To this end, AML cell lines were cultured with HS-5 BMSCs for 24 h before exposing the cells to AraC for an additional 24 h in the presence or absence of ABT-737. The doses of ABT-737 for each cell line has been selected based on their sensitivity profile (Supplementary Figure 3.3). All cell lines, except OCI-AML3 (Figure 3.4B), showed sensitivity to ABT-737 administered as a single agent, indicating that AML cells depend on

Bcl-2/Bcl-X_L expression for survival even in the BM environment. At the same time, ABT-737 could not revert BMSC-mediated resistance to AraC , indicating that Bcl-2 and Bcl-X_L are not the sole effectors of BMSC-mediated drug resistance (Figure 3.4).

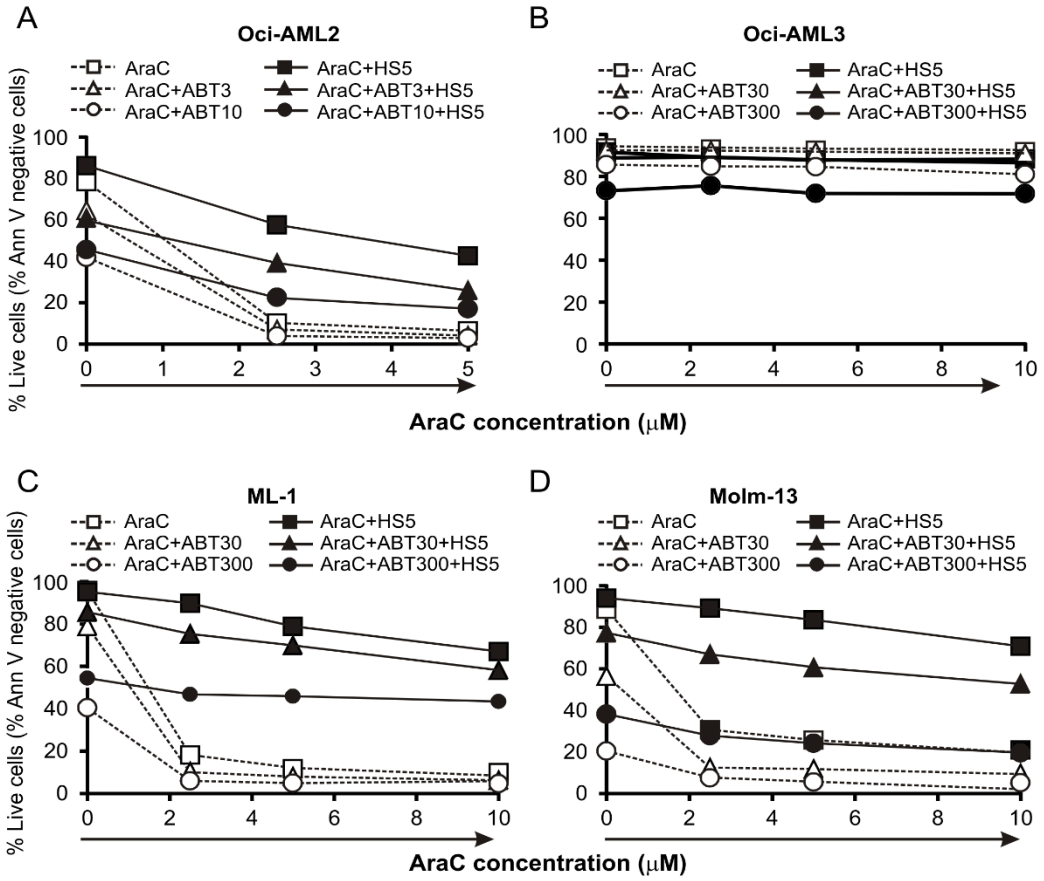

Figure 3.4: Inhibition of Bcl-2 and Bcl-X_L fails to revert BMSC-driven drug resistance.
OCI-AML2 (A), OCI-AML3 (B), ML-1 (C) and Molm-13 (D) cells were cultured on a HS-5 BMSC layer for 24 h before exposing the cells to a combination of AraC and ABT-737 for an additional 24 h. The graphs show the average percentage of live cells ± stdev quantified with Annexin V staining from three independent experiments.

3.4.3 Combined ABT-737 and PHA-767491 treatment targets both the bulk AML blasts and the $CD34^+/CD38^-$ cell population

Given that expression of Mcl-1 consistently increased in AML cells following co-culture with BMSCs as well as reports showing that elevated levels of Mcl-1 are associated with leukemia relapse [452], we tested whether Mcl-1 contributes to reduced ABT-737 sensitivity mediated by HS-5 BMSCs. As the first approach, we have used the CDC7/CDK9 inhibitor PHA-767491 as inhibition of CDK9 represses transcription leading to reduced expression of short half-life time proteins, including Mcl-1 [453,454].

The ABT-737-resistant OCI-AML3 cells (characterised by high Mcl-1 expression) were cultured alone or on a HS-5 BMSC-layer for 24 h. The cultures were pre-treated with PHA-767491 for 4 h followed by a dosage of ABT-737 for an additional 20 h. Repression of Mcl-1 expression was monitored by Western blotting (Figure 3.5A) and induction of cell death was

quantified with Annexin V staining. Treatment with 2 μM of PHA-767491 alone triggered a modest induction of apoptosis but, it potently sensitised the cells to ABT-737 (Figure 3.5B and 3.5C). Importantly, the drug combination retained full efficacy in the presence of HS-5 BMSCs (Figure 3.5C). At this concentration, PHA-767491 downregulated Mcl-1 expression after 3 h of exposure onward (Figure 3.5A). Using the Chou-Talalay median effect equation, the combination index (CI) was calculated (table under the graphs in Figure 3.5B and 3.5C). At each drug concentration, the CI index was well below 1.0, indicating a potent synergy between ABT-737 and PHA-767491.

To confirm that the mechanism of PHA-767491-mediated sensitization involved Mcl-1, a small molecule Mcl-1 inhibitor, A1210477 was employed. A1210477 is a selective, small-molecule inhibitor of Mcl-1 developed by the Soeurs lab [455] shown to have a high selectivity to Mcl-1 over other Bcl-2 family members, multiple kinases and G-protein coupled receptors. Similarly, to treatment with PHA-767491, A1201477 was able to sensitise OCI-AML3 cells to ABT-737 (Figure 3.5D).

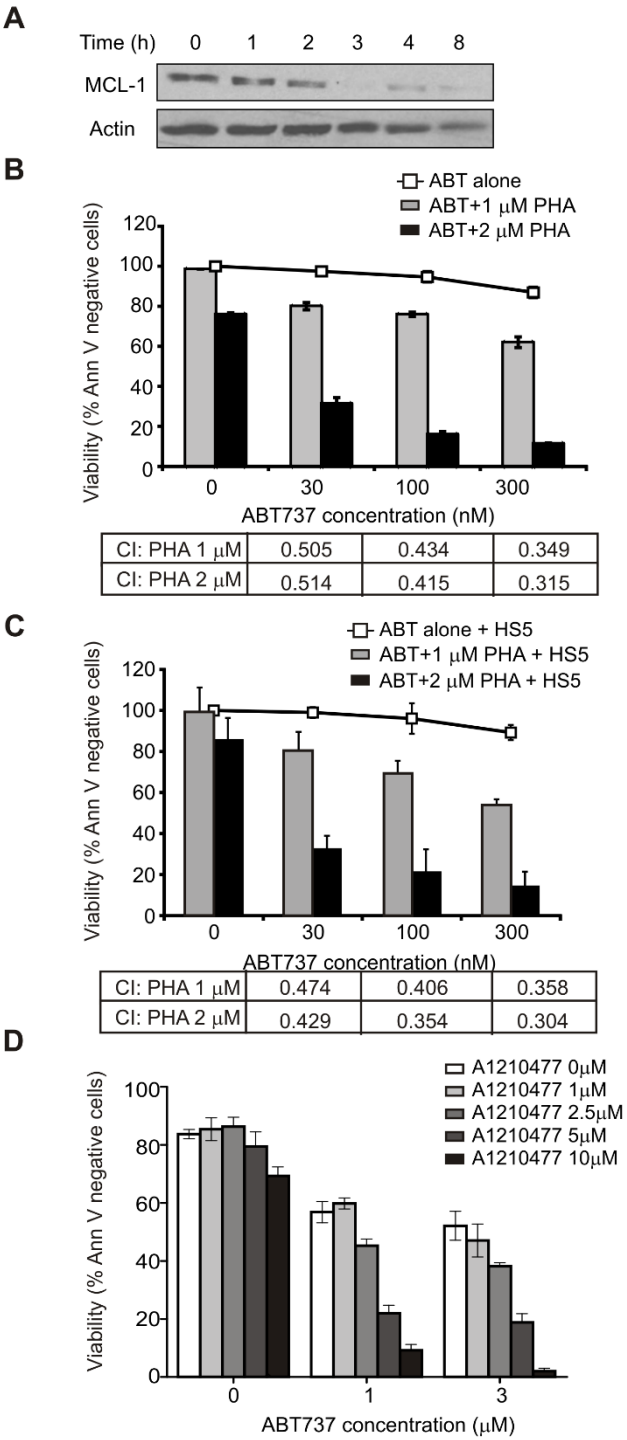

Figure 3.5: AML cells supported by BMSCs display high sensitivity to ABT-737 upon repression of Mcl-1 expression.
(A) Repression of Mcl-1 expression in response to treatment with the dual CDC7/CDK9 inhibitor PHA-767491. OCI-AML3 cells were treated with 2 μM PHA-767491 and whole cell lysates were harvested over an 8 h time course and Mcl-1 expression was monitored by Western blotting. Expression of actin was detected to normalise for protein loading. (B and C) OCI-AML3 cells were cultured alone (B) or over a HS-5 feeder layer (C) and were treated with doses of PHA-767491 for 4 h followed by a dosage of ABT-737 for an additional 20 h. Cell death was quantified using Annexin V staining and flow cytometry. The table under the graphs show the calculated combination index (CI) for the PHA+ABT-treated samples. (D) OCI-AML3 cells were treated with the Mcl-1 inhibitor, A1210477 at the concentrations indicated for 4 h followed by treatment with ABT-737 for a further 20 h. Cell death was quantified using Annexin V and flow cytometry. The graphs show average percentage live cells ± stdev from three independent experiments.

In order to corroborate the above result, the role of Mcl-1 in BMSC-mediated drug resistance was tested in a second AML cell line, with lower Mcl-1 expression. As opposed to OCI-AML3 cells, Molm-13 cells have a low baseline Mcl-1 expression but, they show Mcl-1 induction upon contact with BMSCs (Figure 3.3A) and increased resistance to ABT-737 and AraC (Figure 3.1G and J). Molm-13 cells were cultured alone or in contact with HS-5 BMSCs as before and exposed to ABT-737, with or without a 4 h pre-treatment with A1210477, for 20 h and induction of cell death was determined with Annexin V staining (Figure 3.6A). Co-culture with BMSCs induced a moderate, but consistent protection against both ABT-737 and A1210477. At the same time, A1210477 pre-treatment sensitised Molm-13 cells to ABT-737 both in single culture and in co-culture with HS-5 cells (Figure 3.6A, CI values are under the graph). Notably, the effect of the Mcl-1 inhibitor was more pronounced under the co-culture conditions, reflected also by lower CI indices, indicating that Mcl-1 is an effector of BMSC-mediated ABT-737 resistance (Figure 3.6A).

Similar results were found when the effect of Mcl-1 inhibition on BMSC-mediated AraC-resistance was tested. While ABT-737 could not revert BMSC-mediated AraC resistance, additional inhibition of Mcl-1 fully restored AraC-sensitivity (Figure 3.6B). Of note, inhibition of Mcl-1 in the absence of Bcl-2 inhibition could not revert AraC-sensitivity either, indicating a redundant function between Bcl-2 and Mcl-1 in BMSC-mediated drug resistance.

The finding that AML cells have enhanced sensitivity to the combined inhibition of Bcl-2/Bcl-X_L and Mcl-1 when they are in contact with BMSCs was further explored using AML blasts (Figure 3.7). Samples from 10 patients were cultured on a HS-5 BMSC monolayer for 24 h, followed by treatment with ABT-737 for 24 h (30 nM and 300 nM) with or without a 4 h pre-treatment with PHA-767491 (1-4 μM). Except for one patient (Patient 2), whose cells displayed a high sensitivity for ABT-737, the combination of ABT-737 and PHA-767491 showed a synergistic effect (Figure 3.7A-D, Supplementary Figure 3.4, CI indices in Supplementary Table 3.2). We also carried out these experiments using the patients' own BMSCs and found a similar synergistic effect (Supplementary Figure 3.5A, C, E and G), corroborating the findings. Because the LSC population often has higher drug resistance driving relapse, the sensitivity of the $CD34^+/CD38^-$ LSC-encompassing population was also determined (Supplementary Figure 3.4).

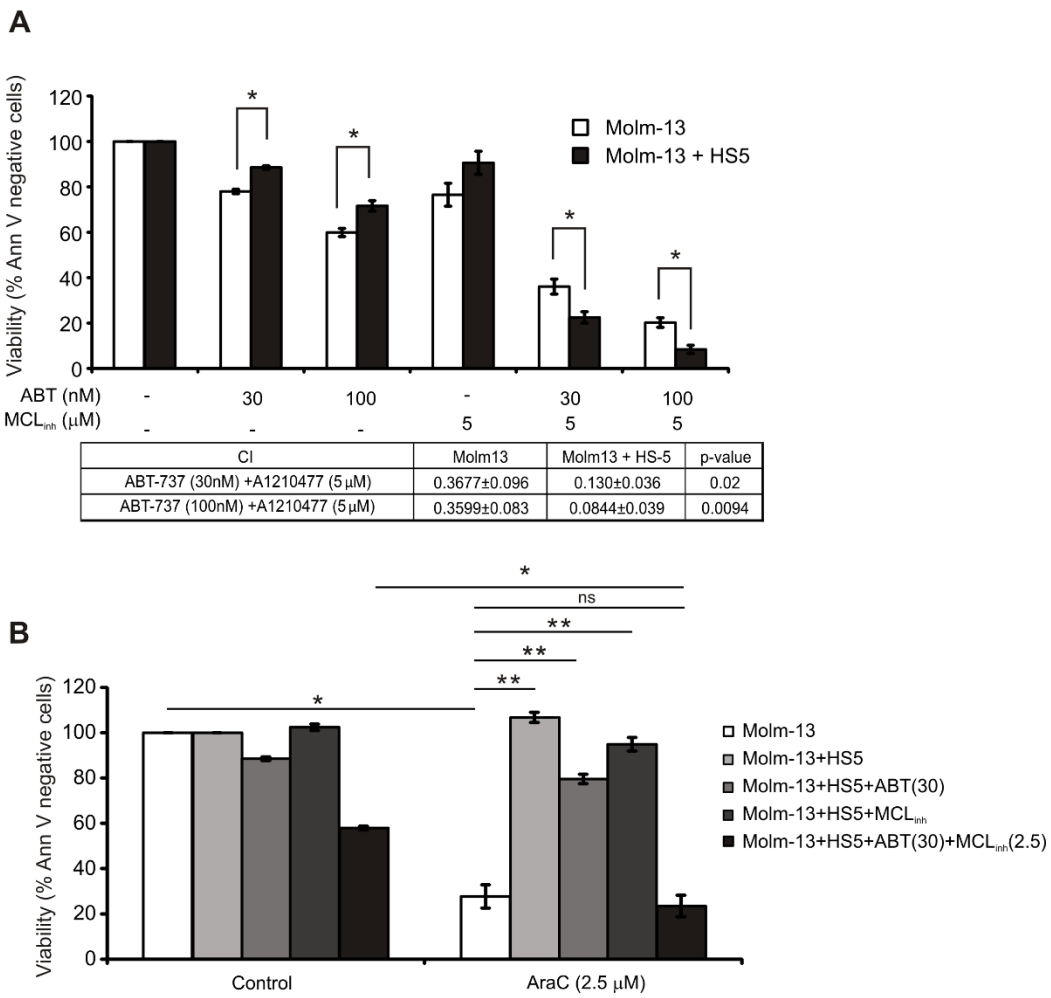

CI	Molm13	Molm13 + HS-5	p-value
ABT-737 (30nM) +A1210477 (5 μM)	0.3677±0.096	0.130±0.036	0.02
ABT-737 (100nM) +A1210477 (5 μM)	0.3599±0.083	0.0844±0.039	0.0094

Figure 3.6: Mcl-1 is an effector of bone marrow stroma-driven drug resistance.
(A) Effect of Mcl-1 inhibition on BMSC-mediated resistance against ABT-737. Molm-13 cells were cultured alone, or in contact with HS-5 BMSCs for 24 h followed by treatment with ABT-737 (ABT) and the small molecule Mcl-1 inhibitor, A1210477 (MCL$_{inh}$) for 24 h. For the combination treatment, Molm-13 cells were pre-treated with MCL$_{inh}$ for 4 h, followed by treatment with ABT for 24 h. Cell viability was determined with Annexin V staining. The table under the graphs shows the CI values of the combination treatment. * indicates significant difference determined with student t-test ($p<0.05$). (B) Bcl-2 and Mcl-1 act in a redundant manner as effectors of BMSC-driven resistance against cytarabine (AraC). Molm-13 cells cultured as described above were treated with AraC (2.5 μM) in the presence of ABT-737 (ABT, 30 nM), A1210477 (MCL$_{inh}$, 2.5 μM) or both for 24 h and Molm-13 cell death was quantified with Annexin V staining. The graphs show the average percentage of live cells ± stdev from three independent experiments (stars indicate significant differences with * meaning $p<0.05$ and ** meaning $p<0.005$, determined with student's t-test).

Looking at the effect of the two drugs individually, the CD34$^+$/CD38$^-$ population showed higher resistance to ABT-737 in 3 out of the 10 samples (Patient 24, 25 and 6) and in 2 samples, they were more resistant to PHA-767491 (Patient 24 and 5). Importantly, the combination treatments showed that PHA-767491 could sensitise the ABT-737 resistant cells and the drug combination had a potent cytotoxic effect. The clinical data (Supplementary Table 3.3) of the tested samples shows that patients with refractory AML are also sensitive to the combination of ABT-737 and PHA-767491, highlighting a potential patient cohort that could benefit from this drug combination.

Because PHA-767491 is likely to repress the expression of a number of genes, not only Mcl-1, Mcl-1 was also inhibited using A1210577 to prove that sensitisation to ABT-737 required Mcl-1 repression. 4 patient samples were treated as before, only replacing PHA-767491 with A1210577 (5 µM, Figure 3.7 E-H). As a single agent, A1210477 had a much lower cytotoxic effect than PHA-767491 in line with its expected, lower non-specific (Mcl-1 independent) effects. A1210477 sensitised 2 out of the 4 samples to ABT-737 (patient 20 and 26), confirming that repression of Mcl-1 is a key mechanism through which PHA-767491 sensitises AML cells under BMSC support to ABT-737. The combination of ABT-737 with A1210477 was also tested using matched BMSCs. Inhibition of Mcl-1 was equally efficient in sensitizing the AML blast cultured with their matched BMSCs, giving an indication for similar potency *in vivo* (Supplementary Figure 3.5 B, D, F and H). To confirm that repression or inhibition of Mcl-1 sensitizes AML blasts under stromal support, a knockdown of Mcl-1 was carried out on primary AML blasts. AML blasts from 2 patients, whose blasts showed resistance to ABT-737 were transfected with siRNA against Mcl-1 using nucleofection (Supplementary Figure 3.6A) and co-cultured with iMSCs for 24 h. Cells were then treated with ABT-737 (30 and 300 nM) for 24 h. While we noticed that the transfection itself stressed the cells and reduced Mcl-1 expression, knockdown of Mcl-1 enhanced sensitivity to ABT-737 (Supplementary Figure 3.6B).

As ABT-737 is only a proof-of-concept drug, we also tested the clinically relevant variant, ABT-199 (Bcl-2 selective inhibitor). In the 4 patient samples tested, pre-treatment with both PHA-767491 or A1210477 enhanced sensitivity to ABT-199. Of note, the sensitisation appears to be lower than to ABT-737, indication that Bcl-X_L may also contribute to drug resistance (Supplementary Figure 3.7).

Since Bcl-2 proteins, including Mcl-1, play fundamental roles in hematopoietic lineage cells, the potential toxic effect of the combined treatment on normal HSCs was measured. For this purpose, we obtained $CD34^+$ HSCs from patients with a disease not associated with aberrant HSCs (the disease profile of these samples is listed in Supplementary Table 3.3, patient 27-30). The samples were analysed in the same co-culture settings as before. Non-malignant HSC-1 and -3 showed a partial sensitivity to high dose PHA767491 (Figure 3.8A, 3.8C) and non-malignant HSC-2 and -4 showed a partial sensitivity to ABT-737 (Figure 3.8B, 3.8D). However, the drug combination failed to induce a synergistic effect, except in non-malignant HSC-1. Of note, both HSC-1 and HSC-3 samples were from multiple myeloma patients, and the disease background might have had an impact on the behaviour of the HSCs. Overall, these results indicate a possible therapeutic window for the targeting of LSCs with the ABT-737 and PHA-767491 drug combination.

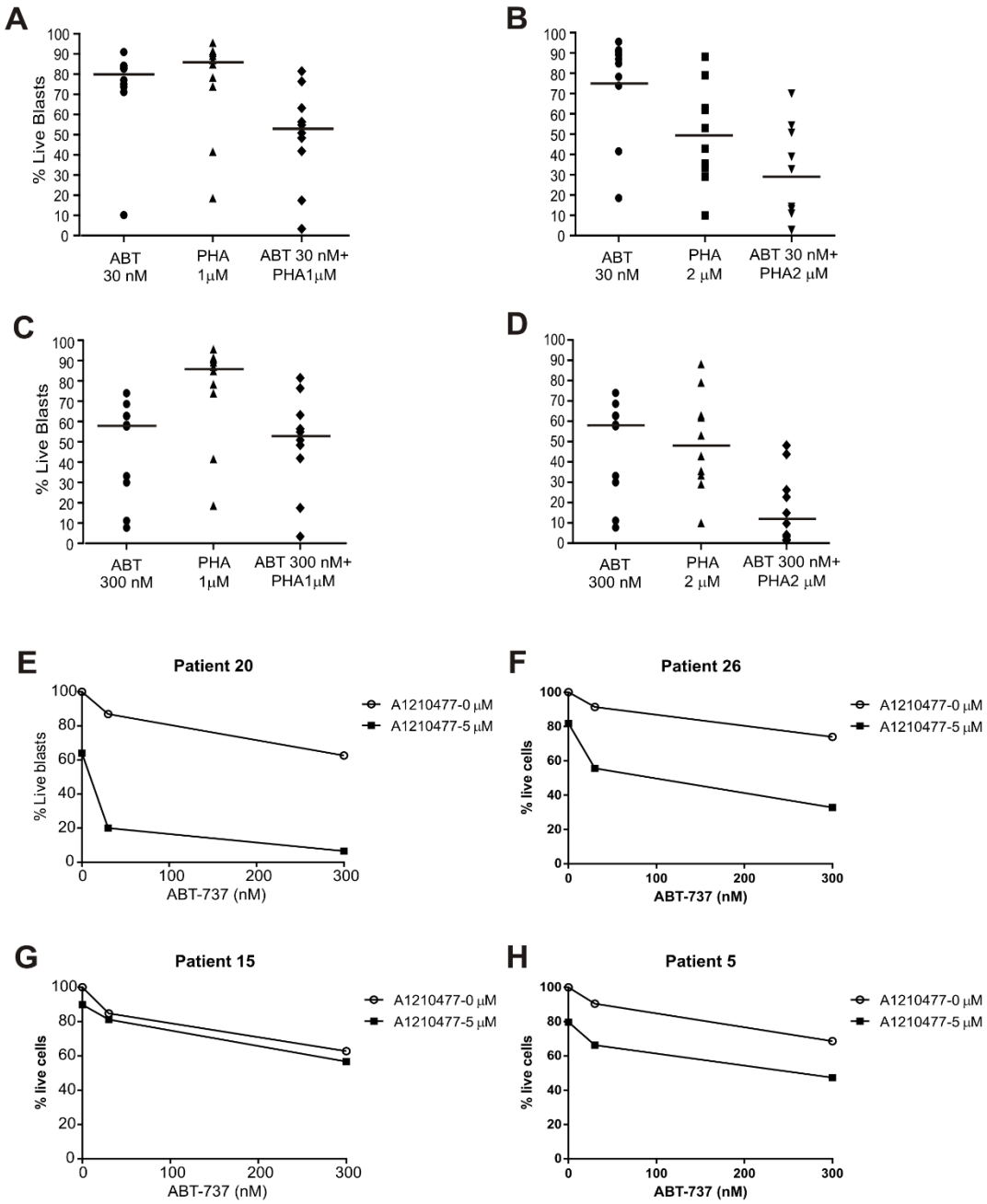

Figure 3.7: Repression of Mcl-1 expression with PHA-767491 or pharmacological inhibition with A1210477 reverts BMSC-driven drug resistance of AML blasts.
(A-D) Repression of Mcl-1 with PHA-767491 enhances sensitivity to ABT-737. AML blasts from 10 patients were cultured on an HS5-BMSC monolayer for 24 h and then treated with ABT-737 with or without a 4 h pre-treatment with the CDC7/CDK9 inhibitor, PHA-767491 (30 nM ABT + 1μM PHA (A); 30 nM ABT + 2 μM PHA (B); 300 nM ABT + 1 μM PHA (C); 300 nM ABT +2 μM PHA (D)) . Induction of cell death was quantified with ToPro-3 viability staining in the bulk AML population. Graphs (A-D) show the percentage of live blasts as a dot plot with the line indicating the median response. (E-H) AML blasts from 4 patients were co-cultured with HS-5 BMSCs for 24 h followed by treatment with ABT-737 (30 and 300 nM) alone or in combination and with the Mcl-1 inhibitor, A1210477 (5 μM) for 24 h. Induction of cell death was measured with ToPro-3 staining for the bulk AML population. The graphs show the percentage of live blasts normalised to the untreated control.

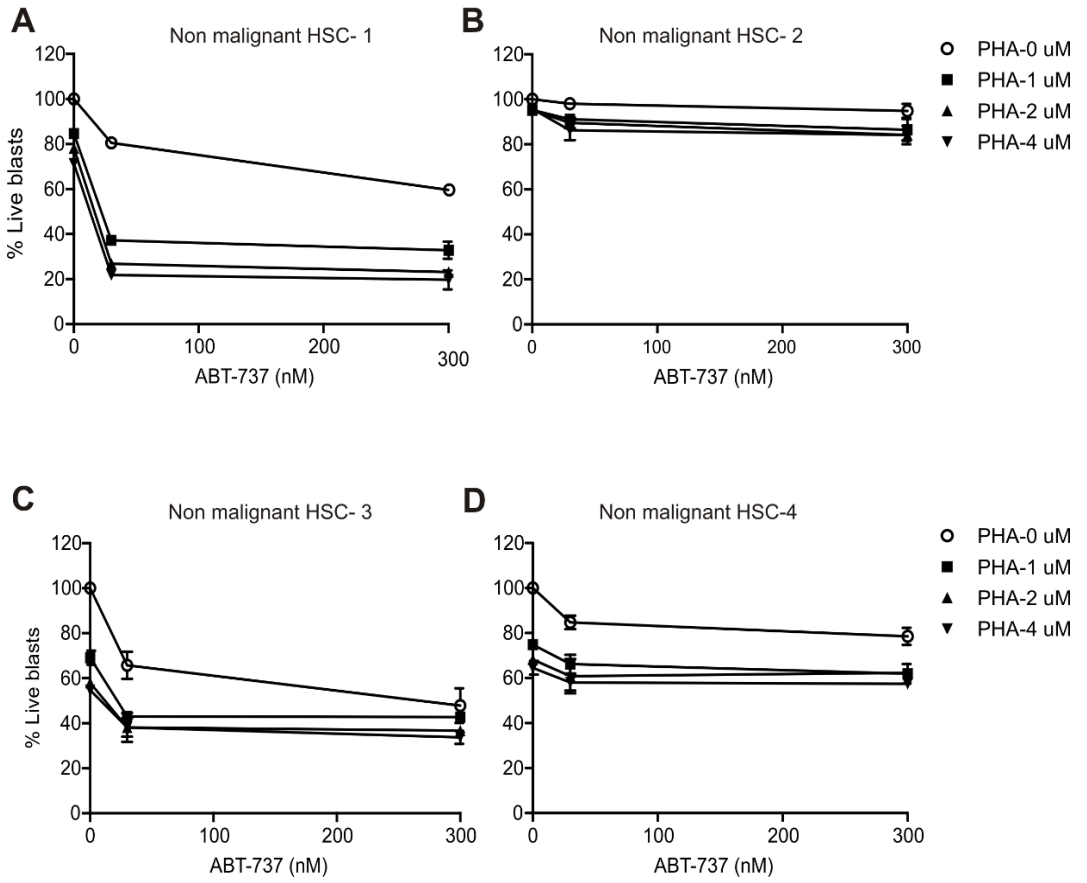

Figure 3.8: PHA-767491 does not sensitise non-AML HSCs to ABT-737.
$CD34^+$ non-malignant HSCs were isolated from four patients with non-AML disorders. These cells were cultured on an HS5-BMSC monolayer for 24 h and then treated with ABT-737 (30 and 300 nM) with or without a 4 h pre-treatment with the CDC7/CDK9 inhibitor, PHA-767491 (1-4 μM). Induction of cell death was quantified with To-Pro-3 staining and flow cytometry. The graphs show the percentage of live blasts. The effect of PHA-767491 alone is shown by the points on the Y axis (zero ABT-737 concentration) and the effect of ABT-737 alone is shown by the PHA 0 μM line (open circles).

3.5 Discussion

Hematopoietic lineage cells are dependent on the expression anti-apoptotic Bcl-2 proteins for survival. Individual Bcl-2 family members are upregulated at different stages of hematopoietic differentiation as well as by cytokine signals, which allows the survival of the properly formed or antigen-reactive cells.

Malignantly transformed leukemic cells appear to have a tighter dependency on anti-apoptotic Bcl-2 proteins than normal leukocytes. The reason for this is that oncogenic and other cellular stresses associated with malignant transformation lead to the induction of pro-apoptotic BH_3-only proteins - such as Bim in lymphoma development - and unless these are neutralised by anti-apoptotic family members the transformed leukemic cells may not survive [456]. In line with this notion, BH_3-mimetic drugs, such as the mainstream Bcl-2/Bcl-X_L/Bcl-W inhibitors ABT-737 and ABT-263 and their Bcl-2-selective derivative, ABT-199 showed remarkable efficacy in clinical trials [457].

High anti-apoptotic Bcl-2 protein expression does not only promote survival of leukemic cells, but it is also associated with treatment-resistance. High percentage of Bcl-2 positive AML cells correlate with low complete remission rates after intensive chemotherapy [458] and high Bcl-2 expression levels in AML cells were found to drive resistance against cytarabine [459]. Bcl-X_L expression has also been associated with chemoresistance, for example against 5-azacytidine in AML or the topoisomerase inhibitor, etoposide in B cell leukemia [442,460].

The effect of the bone marrow microenvironment on drug resistance is well established. However, its effect on the expression of anti-apoptotic Bcl-2 proteins and the impact of BMM-mediated anti-apoptotic Bcl-2 protein expression on resistance against classical chemotherapeutics or BH_3-mimetics is much less understood. Equally, the effect of the BMM on anti-apoptotic Bcl-2 protein expression in the most resistant LSC population and drug resistance conveyed by them is also poorly investigated.

Here we show that BMSCs drive resistance against the mainstream chemotherapeutics AraC+Dnr with the $CD34^+/CD38^-$ cells, representative of an LSC-enriched population, displaying higher resistance than the AML blasts. We found that inhibition of Bcl-2/Bcl-X_L/Bcl-W with ABT-737 could not reverse this resistance. We also found that the BMM induced Mcl-1 expression both *in vitro* in AML cell lines and *in vivo* in a subset of primary samples, while BMM-mediated Bcl-2 and Bcl-X_L induction was less consistent. In line with these findings, Garrido and colleagues have also reported inconsistent or low-level induction of Bcl-2 in primary patient AML cells in *ex vivo* BMSC co-cultures [461].

Normal HSCs are known to depend on Mcl-1 expression for long-term survival. Furthermore, Mcl-1 gene deficiency results in loss of mature B and T lymphocytes over time, demonstrating a central role for Mcl-1 in the long-term maintenance of the mature immune system [462]. Based on these results, Mcl-1 inhibitors were predicted to be toxic. However, while ABT-199 potently kills primary AML blasts, a trend of a negative correlation between Mcl-1 expression and the efficacy of ABT-199 exists [441]. Also, induction of Mcl-1 is frequently observed in relapsed AML [463] and Mcl-1 induction is recognised as the main mechanism of resistance against ABT-263 and ABT-199 [464,465].

Our finding that the bone marrow stroma drives selective upregulation of Mcl-1 identifies a potential mechanism how ABT-263 and ABT-199 resistance may develop *in vivo*. In line with our findings, the study of Glaser and colleagues showed higher dependency of AML cells on Mcl-1 over healthy HSCs, giving grounds for a possible therapeutic window for Mcl-1 targeting [452]. Recent studies also support the potential of Mcl-1-targeting to overcome drug resistance in AML as well as in other leukaemia types [466], with selective Mcl-1 inhibitors showing promise in pre-clinical studies [467].

Mcl-1 has a number of distinguishing features that separates it from Bcl-2 and Bcl-X_L. It lacks a conserved BH4 domain and it has a very short half-life time due to a P-E-S-T motif in its N-terminal portion (resulting a half-life time of only 2-4 h in most cells) [468,469]. This, combined with the multiple pathways that control its (1) transcription (such as the

transcription factors ATF5, E2F1, STAT3, PU.1 and NF-kB), (2) regulate its translation (3) as well as protein stability, create a very dynamic control of Mcl-1 protein levels in response to a wide variety of cellular stresses and signals [469,470].

To date, there was little focus on the role of Mcl-1 in BMM-driven AML drug resistance. Here we found that Bcl-2 and Mcl-1 are both effectors of bone marrow stroma-mediated drug resistance and they act in a redundant manner, i.e. the presence of either Bcl-2 or Mcl-1 was sufficient to provide resistance since simultaneous inhibition of both proteins was required to restore drug-sensitivity.

The CDC7/CDK9 inhibitor, PHA-767491 represses Mcl-1 expression [471]. CDK9 forms the catalytic core of the positive transcription elongation factor b (P-TEFb). P-TEFb phosphorylates RNA polymerase II and thus initiates the elongation phase of transcription [472]. Inhibition of CDK9 thus leads to the depletion of proteins with short half-life times, such as Mcl-1 [453]. Previous studies have shown that combining CDK9 inhibitors with Bcl-2 inhibitors, such as ABT-737 and ABT-199, can overcome drug resistance in a synergistic manner [473-475]. We found that PHA-767491-mediated downregulation of Mcl-1 was very potent in sensitising both AML cell lines and primary AML blasts to ABT-737 and to the recently FDA-approved ABT-199. It has to be noted, that ABT-199 appeared to be inferior in inducing AML cell death compared to ABT-737 in our studies, indicating a possible role of Bcl-X_L as well.

As shown by Jilg and colleagues, the $CD34^+$ population showed sensitivity to ABT-737 [476]. Our studies confirm these findings, but also show that in some patients the $CD34^+/CD38^-$ population is resistant to ABT-737. Importantly, PHA-767491 restored the sensitivity of resistant $CD34^+/CD38^-$ cells to ABT-737. These results highlight the role of Mcl-1 in addition to Bcl-2 as a key effector of BMM-mediated pro-survival signalling and consequent drug resistance. At the same time, non-malignant $CD34^+$ HSCs were not sensitised to ABT-737 by PHA-767491, indicating that Mcl-1 has a differential role in $CD34^+$ cells of AML versus non-malignant HSCs thus offering a therapeutic window to target LSCs. Chemoresistant AML may be a potential patient cohort who could benefit from treatment with ABT-737 and PHA-767491 or other CDK9 inhibitors, as samples from refractory AML patients showed equally high sensitivity to the ABT-737+PHA-767491 treatment. In this regard, a recent report highlighted that feedback activation of STAT3, a key transcriptional regulator of Mcl-1 was induced by the BMM and drove chemotherapy-resistance [477].

Mcl-1 has been shown to play a central role in emergency haematopoiesis, i.e. the regeneration of hematopoietic lineage cells after stress. It is likely that chemotherapy triggers the same effect [478]. This emphasizes the need to consider pharmaceutical inhibition of Mcl-1 to target LSCs and reduce the occurrence of relapse. However, the potential toxic effect of Mcl-1 inhibitors cannot be neglected.

Therapies that target pathways that upregulate Mcl-1 expression in neoplastic cells as opposed to direct inhibition of Mcl-1 may be less toxic. In this regard, CDK9 has been shown

to be aberrantly activated by oncogenic fusion proteins (such as MLL-fusion proteins) driving lymphoid and myeloid leukemia [479-481]. NF-κB (p65) also requires P-TEFb for transcription elongation [482]. As NF-κB signalling is often elevated in AML and it can drive Mcl-1 expression, this represents another mechanism how inhibition of CDK9 can repress abnormal Mcl-1 expression [482]. Finally the Gandhi laboratory reported, although in CLL not AML, that stroma-driven resistance to apoptosis of CLL cells was associated with a cascade of transcriptional events that included increased phosphorylation of RNA Pol II on serine residues at positions 2 and 5 (the phosphorylation site of CDK9), leading to increased rate of global RNA synthesis, and amplification of Mcl-1 transcript levels [483]. These reports provide a strong rationale for targeting Mcl-1 gene expression as opposed to direct inhibition of the Mcl-1 protein (like a BH_3-mimetic)

In conclusion, the results presented here indicate that Bcl-2/Bcl-X_L and Mcl-1 act in a redundant fashion as effectors of BMM-mediated AML drug resistance and indicate that for BH3-mimetic-based treatment of AML the focus must be broadened from sole targeting of Bcl-2 to the additional inhibition or repression of Mcl-1.

3.6 Supplementary Figures

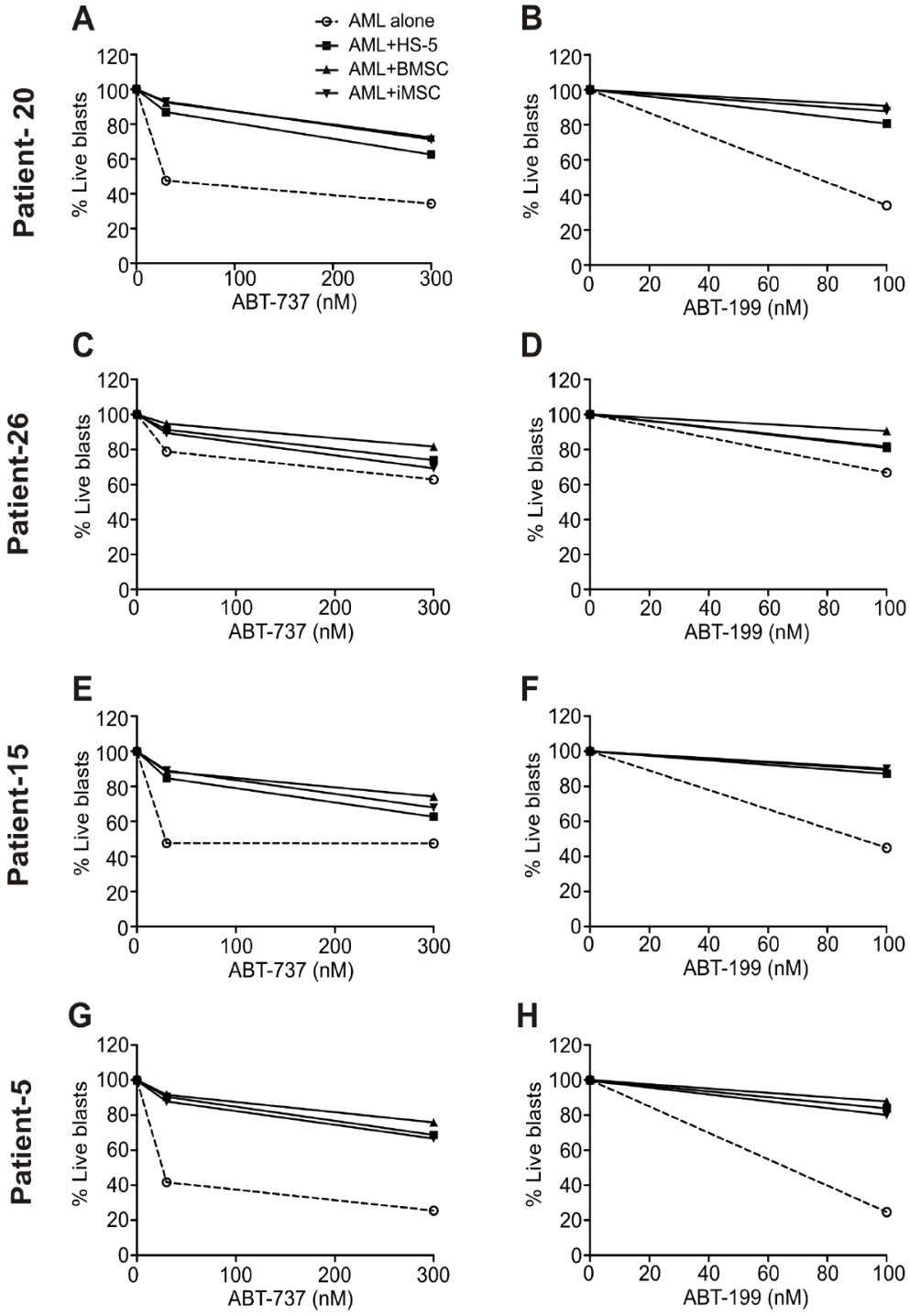

Supplementary Figure 3.1: HS-5 cells can model bone marrow-mediated AML drug resistance. Primary AML cells from 4 patients were cultured for 24 hours alone (A), on matched primary bone marrow mesenchymal stromal cells (BMSC, B), iMSCs (C) or HS-5 cells (D) for 24 h and treated with the indicated doses of ABT-737 (A, C, E, G) or ABT-199 (B, D, F, H). Induction of cell death was measured with ToPro-3 viability staining and flow cytometry.

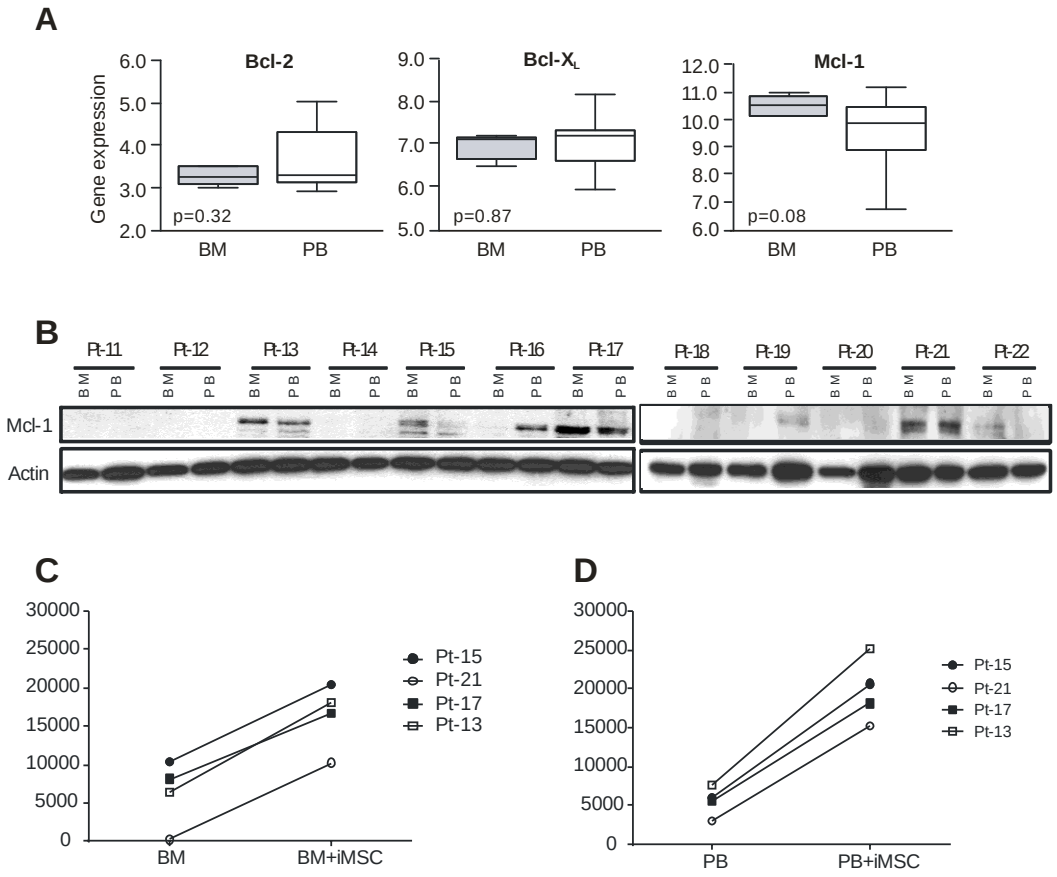

Supplementary Figure 3.2: Mcl-1 protein expression in bone marrow- and peripheral blood-residing AML blasts.
(A) Box plot representation of Bc-2, Bcl-X_L and Mcl-1 mRNA expression in AML blasts isolated from either bone marrow (BM) or peripheral blood (PB). Note: the plotted expression data was extracted from the Gene Expression Omnibus dataset (GDS3057) of non-matched BM and PB samples. (B) Mcl-1 protein expression in matched BM- and PB-derived AML blasts. Whole cell lysates from matched BM- and PB-derived AML blasts were analysed for Mcl-1 expression using Western blotting. β-actin expression is shown as loading control. (C and D) BMSCs drive Mcl-1 expression in co-residing AML blasts. The graphs show densitometric quantitation of Mcl-1 expression in AML blasts isolated from BM (C) or PB (D) cultured alone or on BMSCs (iMSCs) for 24 h. Mcl-1 expression determined from whole cell lysates with Western blotting normalised to β-actin is shown as a dot plot. The original Western blot is shown in Fig. 3D.

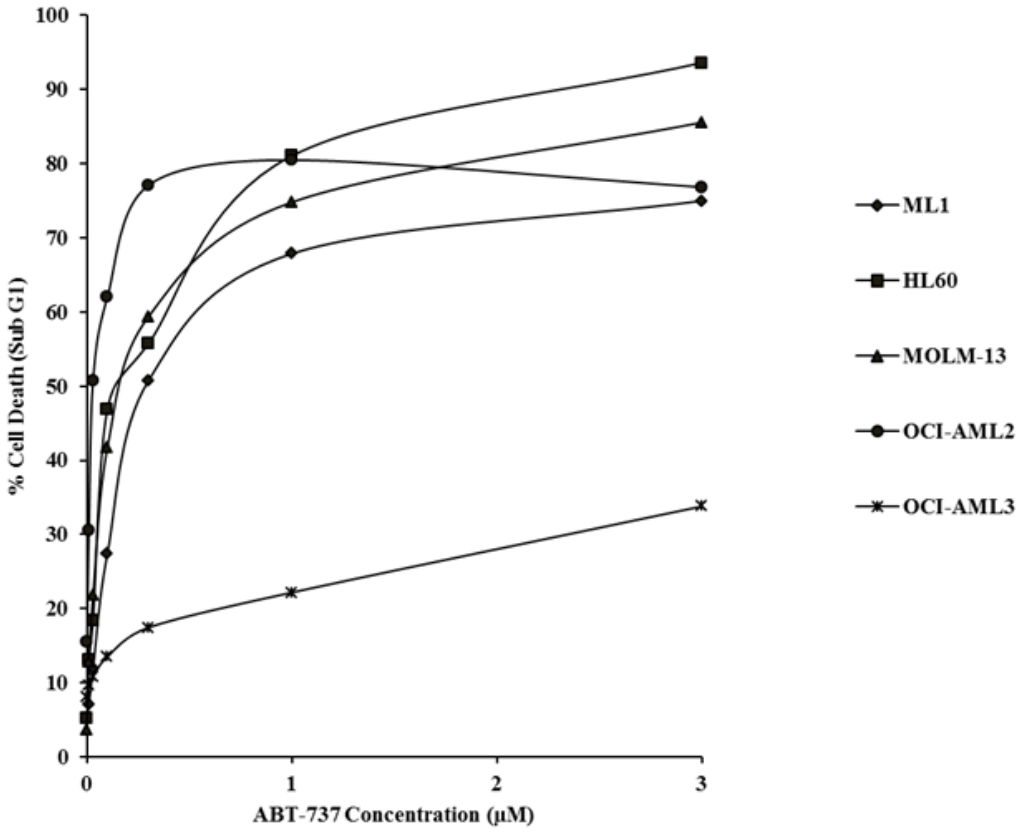

Supplementary Figure 3.3: ABT-737 dose response of AML cell lines.
AML cell lines (ML-1, HL60, Molm-13, OCI-AML2 and OCI-AML-3) were treated with the indicated doses of ABT-737 for 24 h and induction of cell death was quantified by determining the sub-G1 population using propidium iodide staining and flow cytometry.

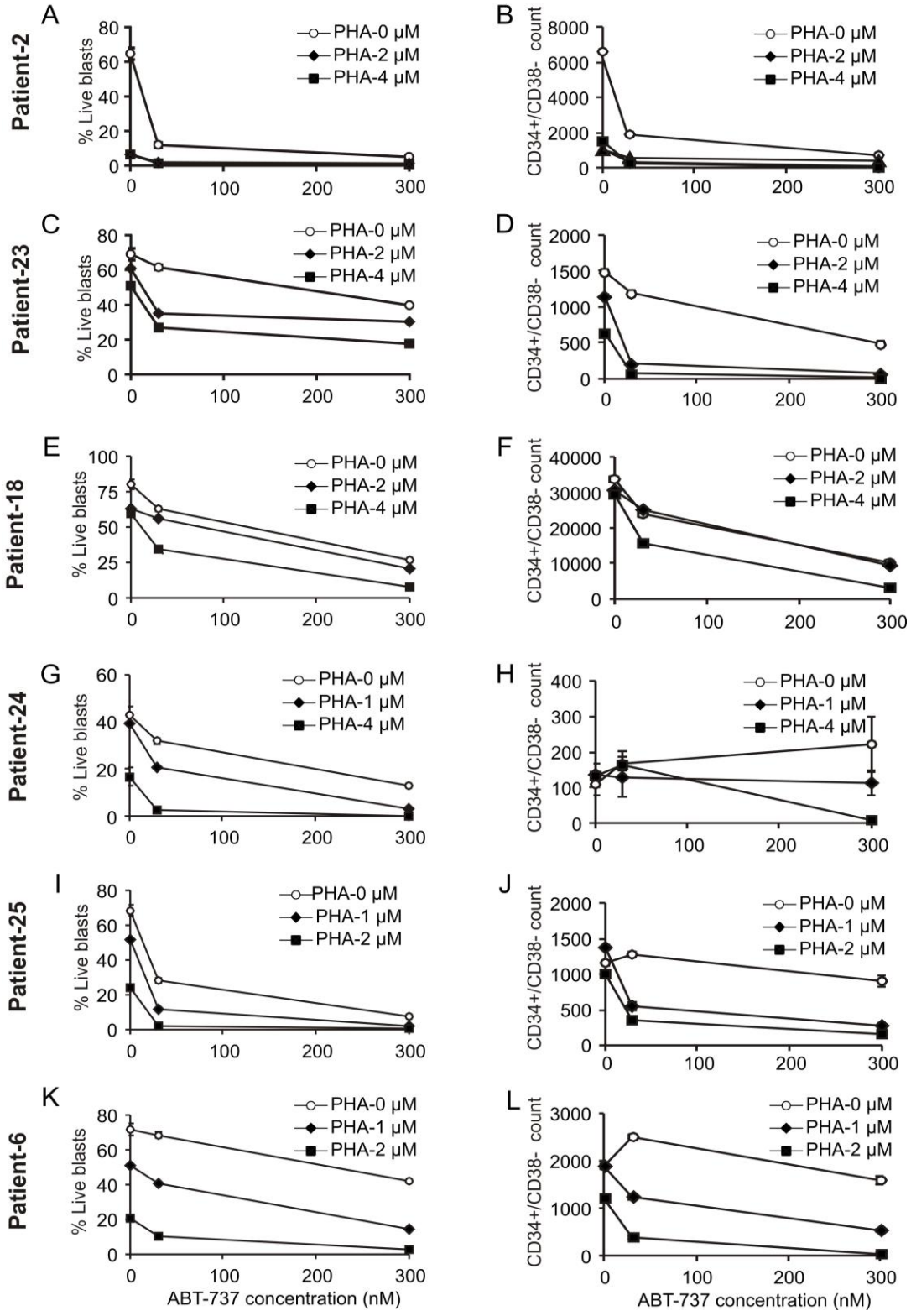
A
Patient-2
% Live blasts
PHA-0 µM
PHA-2 µM
PHA-4 µM
B
CD34+/CD38- count
C
Patient-23
D
E
Patient-18
F
G
Patient-24
PHA-1 µM
H
I
Patient-25
J
K
Patient-6
L
ABT-737 concentration (nM)

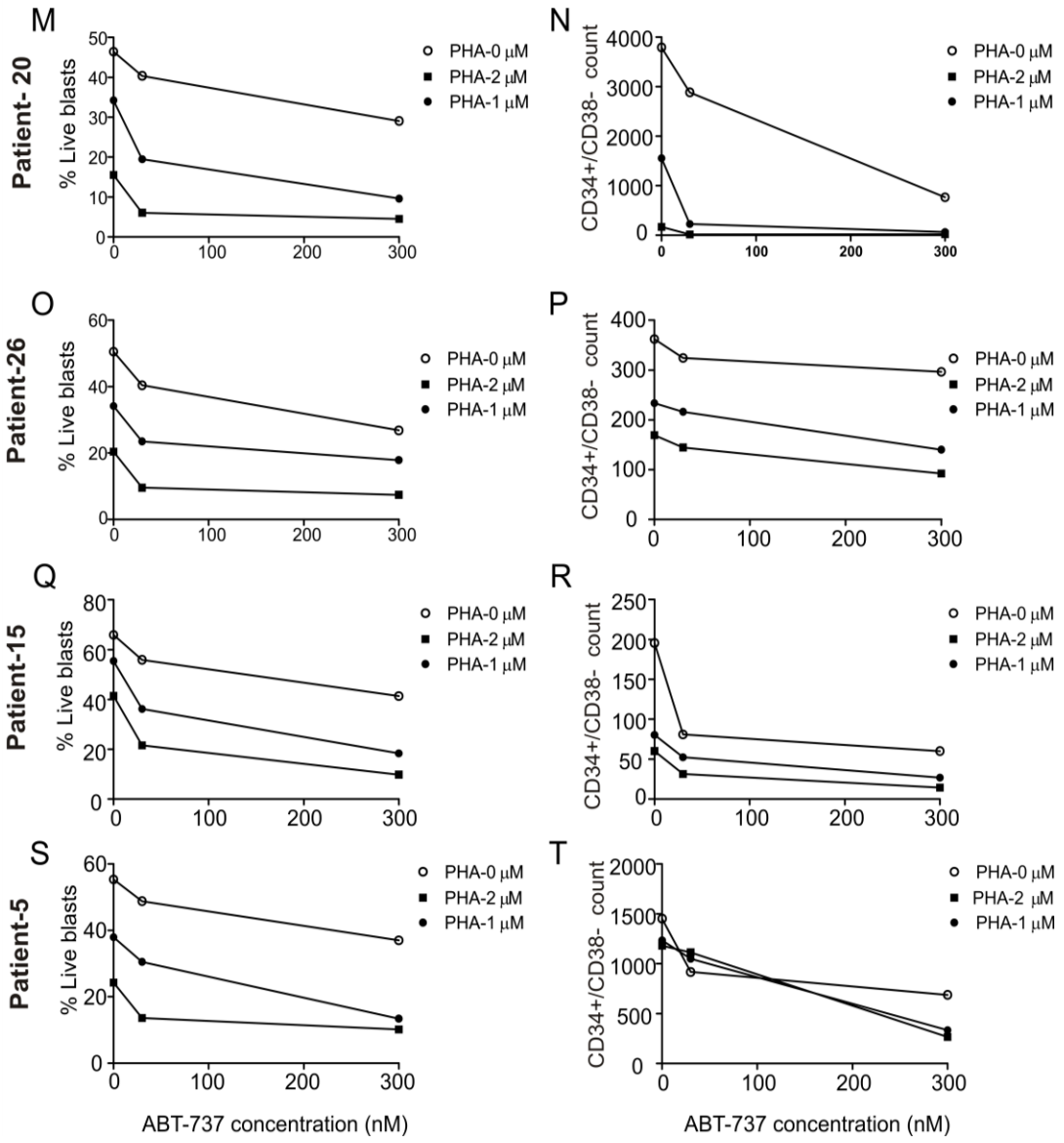

Supplementary Figure 3.4: Inhibition of Mcl-1 expression with PHA-767491 reverts BMSC-driven drug resistance of both AML blasts and CD34$^+$/CD38$^-$ population.
AML blasts from 10 patients were cultured on HS5-BMSC monolayer for 24 hours and then treated with ABT-737 (30 and 300 nM) with or without a 4 h pre-treatment with the CDC7/CDK9 inhibitor, PHA-767491 (1-4 μM). Induction of cell death was quantified with ToPro-3 viability staining both in the bulk AML population and the CD34$^+$/CD38$^-$ LSC-encompassing population. Graphs on the left-hand side (A, C, E, G, I, K, M, O, Q and S) show the percentage of live cells in the bulk blast population, while the graphs on the right-hand side (B, D, F, H, J, L,N, P, R and T) show the number of CD34$^+$/CD38$^–$ cells within the surviving population. The effect of PHA-767491 alone is shown by the points on the Y axis (zero ABT-737 concentration) and the effect of ABT-737 alone is shown by the PHA 0 μM line (open circles).

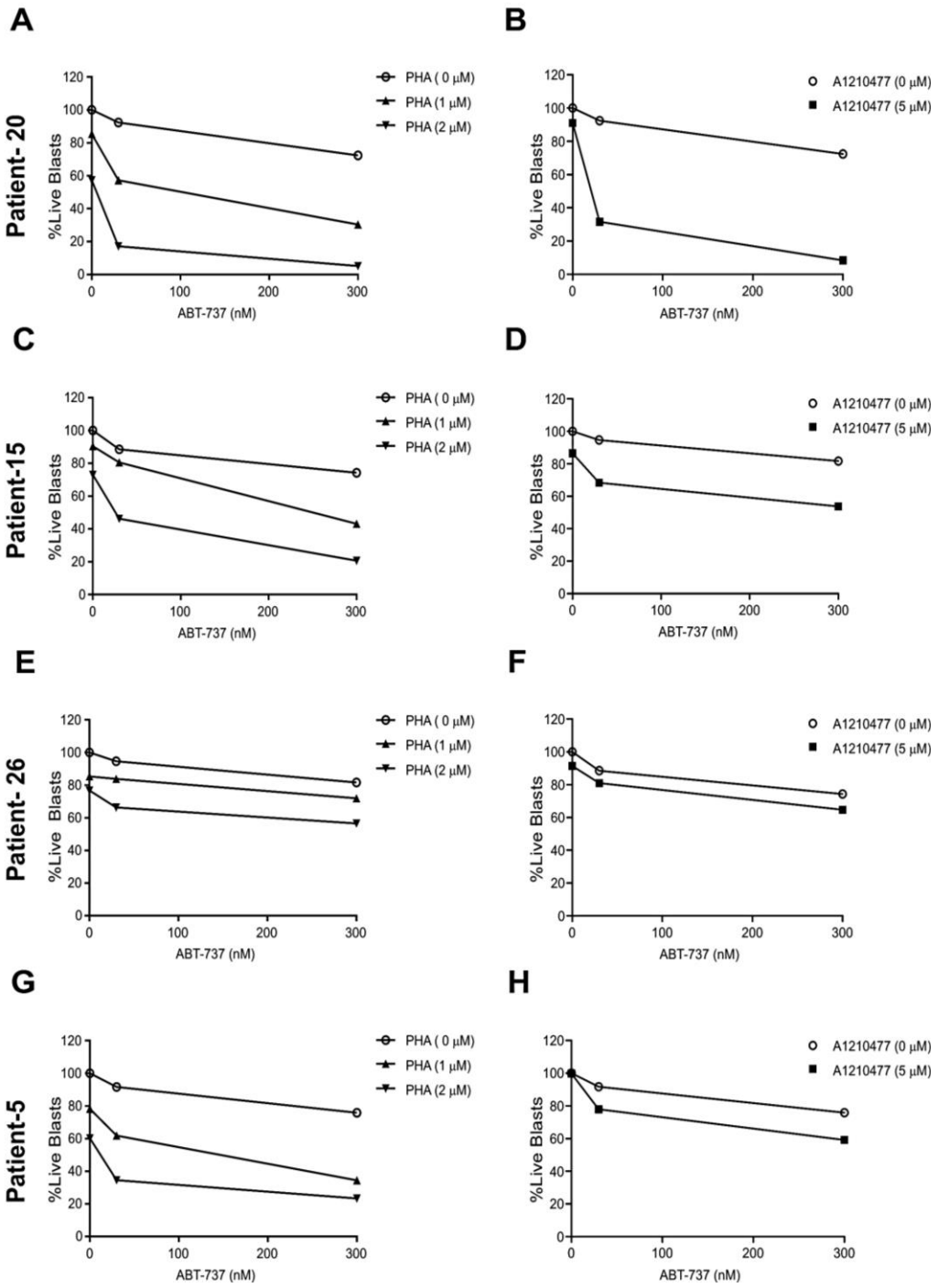

Supplementary Figure 3.5: Repression or inhibition of Mcl-1 sensitises AML blasts cultured on matched BMSCs to ABT-737.

Viability of AML blasts in matched BMSC co-culture treated with ABT-737 plus PHA-767491 or A1210477. BM-derived MNCs from 4 AML patients were cultured with their matched BMSCs for 24 h. Cells were pre-treated with PHA-767491 (1-2 μM) (A, C, E, G) or A1210477 (B, D, F, H) for 4 h followed by ABT-737 (30 and 300 nM) for 24 h. Induction of cell death was measured by ToPro-3 viability staining.

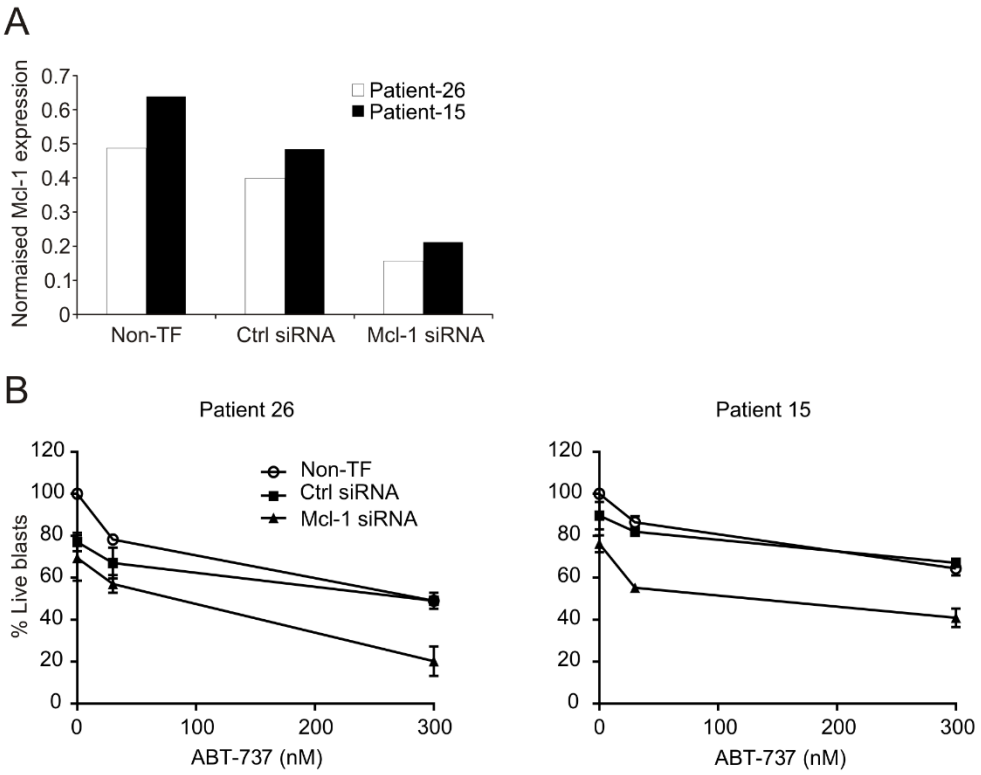

Supplementary Figure 3.6: Knockdown of Mcl-1 sensitises AML blasts to ABT-737.
(A) Efficiency of siRNA-mediated Mcl-1 knockdown in primary AML blasts. Mcl-1 was transfected into primary AML blasts using nucleofection as described in Materials and Methods and Mcl-1 protein expression was quantified 48 h post-transfection using Western blotting. The graphs show densitometric quantification of Mcl-1 expression normalised to β-actin. (B) Effect of Mcl-1 knockdown on ABT-737 sensitivity on AML blasts. Mcl-1 was knocked down in two primary AML samples which showed resistance to ABT-737 and the AML blasts in co-culture with iMSC feeder layer were treated with ABT-737 for an additional 24 h. The graphs show induction of cell death determined with Topro-3 staining and flow cytometry.

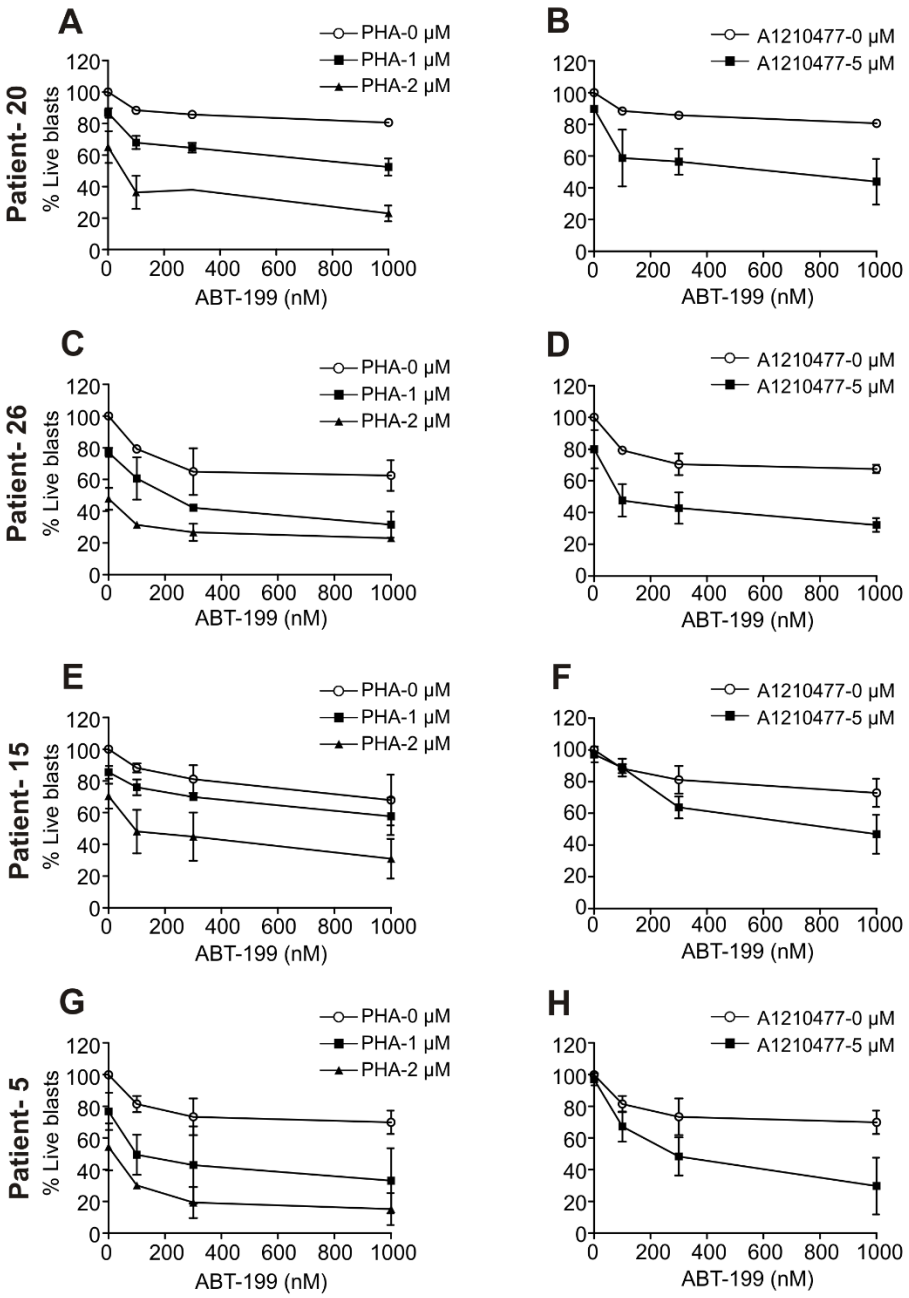

Supplementary Figure 3.7: Repression or inhibition of Mcl-1 sensitises AML blasts cultured in contact with BMSCs (iMSC) to ABT-199.
Viability of AML blasts treated with ABT-199 plus PHA-767491 or A1210477. BM-derived MNCs from 4 AML patients were cultured with iMSC BMSCs for 24 h after which the cultures were pre-treated with the indicated doses of PHA-767491 (A, C, E, G) or A1210477 (B, D, F, H) for 4 h followed by ABT-737 for 24 h. Induction of cell death was measured by ToPro-3 viability staining. The graphs show percentage viability normalised to the untreated control.

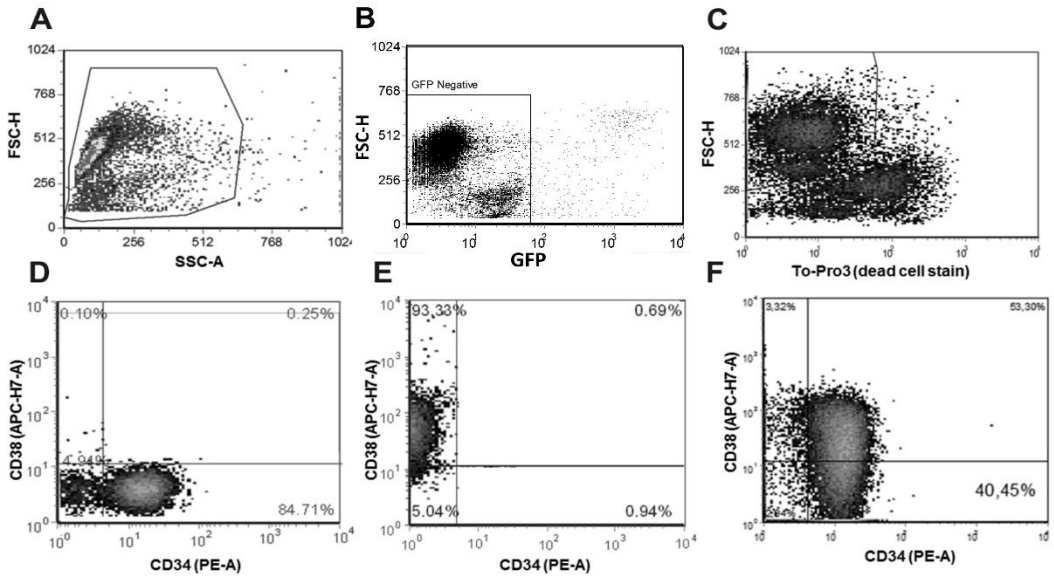

Supplementary Figure 3.8: Flow cytometry gating strategy.
(A) Forward scatter (FSC) vs. side scatter (SSC) plot showing all events and gating of all cells. (B) FSC vs. GFP fluorescence dot plot and the gating to exclude detached GFP-positive HS-5 cells or CFSE-loaded iMSCs and primary BMSCs. (C) FSC vs. ToPro-3 fluorescence intensity dot plot used for determining the percentage of dead AML blasts (in the bulk blasts population). (D) FSC vs. CD34 (PE) dot plot in a sample stained only with anti-CD34 to determine the CD34 gate. (E) FSC vs. CD38 (APC-H7) dot plot in a sample stained only with anti-CD34 to determine the CD34 gate. (F) CD34 vs. CD38 fluorescence intensity dot plot showing the gating strategy for the $CD34^+$ and $CD38^-$ population.

3.7 Supplementary Tables

Supplementary Table 3.1: Cytokines and chemokines secreted by HS-5 BMSCs.

Note: cyto/chemokines with bold typing are factors known to be present in the BMM.

Cytokines	**Gene ID**
Angiogenin	283
Angiopoietin-1	284
Angiopoietin-2	285
BDNF	627
CD30/TNFRSF8	943
CD40L	959
YKL-40/CHITINASE-3 LIKE 1	1116
Dkk1/Dickkopf-1	22943
CD26/Dipeptidyl-peptidase IV	1803
CD147/EMMPRIN	682
Endoglin/CD105	2022
FGFbasic	2247
FGF-19	9965
G-CSF	1440
GDF-15	9518
GM-CSF	1437
ICAM-1	3383
IFNγ	3458
IL-1α	3552
IL-1β	3553
IL-6	3569
IL-11	3589
IL-17A	3605
KLK3/Kallikrein-3	354

Cytokines ctnd	**Gene ID**
LIF	3976
M-CSF	1435
MIF	4282
MMP-9/Gelatinase B	4318
Osteopontin	6696
PDGF-AA	5154
Pentraxin-3	5806
Serpin E1	5054
Thrombospondin-1	7057
PLAUR	5329
VEGF	7422
Vitamin D BP	2683
Chemokines	Gene ID
CXCL5/ENA-78	6374
CXCL1/GRO-α	2919
CXCL10/IP-10	3627
CCL2/MCP-1	6347
MCP-3/CCL7	6354
CCL20/MIP3α	6364
RANTES/CCL5	6352
SDF1α/CXCL12	6387
IL-8/CXCL8	3576

Supplementary Table 3.2: Chow-Talalay's Combination Indexes (CIs) for primary AML samples treated with the combination of PHA-767491 and ABT-737

Patient 2

	PHA-767491, 1.0μM	PHA-767491, 2.0μM	PHA-767491, 4.0μM
ABT-737, 30.0nM	0.01356	0.00819	0.00414
ABT-737, 300.0nM	0.06914	0.02862	0.01146

Patient 23

	PHA-767491, 1.0μM	PHA-767491, 2.0μM	PHA-767491, 4.0μM
ABT-737, 30.0nM	0.52014	0.10794	0.06534
ABT-737, 300.0nM	0.40607	0.51382	0.17972

Patient 18

	PHA-767491, 1.0μM	PHA-767491, 2.0μM	PHA-767491, 4.0μM
ABT-737, 30.0nM	2.04139	0.8538	0.18457
ABT-737, 300.0nM	0.91403	0.67958	0.17622

Patient 24

	PHA-767491, 1.0μM	PHA-767491, 2.0μM	PHA-767491, 4.0μM
ABT-737, 30.0nM	0.63256	0.28856	0.38192
ABT-737, 300.0nM	0.22168	0.21843	0.11431

Patient 25

	PHA-767491, 1.0μM	PHA-767491, 2.0μM	PHA-767491, 4.0μM
ABT-737, 30.0nM	0.53429	0.30939	0.44438
ABT-737, 300.0nM	0.27690	0.27372	0.35501

Patient 6

	PHA-767491, 1.0μM	PHA-767491, 2.0μM	PHA-767491, 4.0μM
ABT-737, 30.0nM	0.86787	0.51221	0.57917
ABT-737, 300.0nM	0.53954	0.24697	0.32821

Patient 20

	PHA-767491, 1.0μM	PHA-767491, 2.0μM	
ABT-737, 30.0nM	0.60271	0.61593	
ABT-737, 300.0nM	0.42895	0.5483	

Patient 26

	PHA-767491, 1.0μM	PHA-767491, 2.0μM	
ABT-737, 30.0nM	0.56897	0.76301	
ABT-737, 300.0nM	0.49271	0.7228	

Patient 15

	PHA-767491, 1.0μM	PHA-767491, 2.0μM	
ABT-737, 30.0nM	0.47218	0.49642	
ABT-737, 300.0nM	0.27142	0.27859	

Patient 5

	PHA-767491, 1.0μM	PHA-767491, 2.0μM	
ABT-737, 30.0nM	0.51069	0.7748	
ABT-737, 300.0nM	0.36243	0.57367	

Supplementary Table 3.3: Clinical data of patient samples

Sample	New diagnosis or relapsed	Age	AML subtype	Cytogenetics (normal vs complex karyotype (NK, CK), etc)	Response to treatment
1	New diagnosis	57	AML w/o maturation	NK, FLT3-ITD$^-$	Refractory
2	New diagnosis	71	RAEB2	NK, FLT3-ITD$^-$	Responder
3	New diagnosis	70	AML w. MDS-related changes	CK	Refractory
4	Relapsed	68	AML	NK, FLT3-ITD$^-$, NPM1$^+$	Refractory
5	New diagnosis	91	N/A	N/A	Supportive care
6	New diagnosis	64	AMML	NK, FLT3-ITD$^+$	Initial responder, then relapse
7	New diagnosis	68	RAEB2	NK, FLT3-ITD$^+$	Refractory
8	New diagnosis	53	AML	CK, FLT3-ITD$^-$	Refractory
9	New diagnosis	62	AML	NK, FLT3-ITD$^+$	Responder
10	New diagnosis	71	AML-M1	NK, FLT3-ITD$^-$	Refractory
11	New diagnosis	45	AML	t(8:21), good risk	Responder
12	New diagnosis	47	MDS	N/A	Responder
13	Relapsed	52	t-AML	NK	Refractory
14	New diagnosis	85	MDS	N/A	Refractory
15	New diagnosis	39	AML	NK, FLT3-ITD$^+$	Responder
16	New diagnosis	66	AML	CK, Poor risk	Refractory
17	New diagnosis	50	AML	NK, Intermediate risk	Responder
18	New diagnosis	73	AML-M1	N/A	Refractory
19	Relapsed	63	sAML	NK	Responder
20	New diagnosis	70	AML-M1	NK, FLT3-ITD$^-$, NPM1$^-$	Responder
21	Relapsed	77	sAML	CK	Refractory
22	Relapsed	76	AML	CK, FLT3-ITD$^+$	Refractory
23	New diagnosis	73	AML	NK	Responder
24	New diagnosis	68	AML	NK, FLT3-ITD$^-$, NPM1$^+$	Refractory
25	New diagnosis	91	AML	N/A	Supportive care
26	New diagnosis	69	sAML	NK	Refractory
27	New diagnosis	N/A	Multiple myeloma	N/A	NA
28	New diagnosis	N/A	Hodgkins lymphoma	N/A	NA
29	New diagnosis	N/A	Multiple myeloma	N/A	NA
30	New diagnosis	N/A	Ewing's Sarcoma	N/A	NA

Abbreviations: AML, acute myeloid leukemia; **RAEB2**, refractory anemia with excess blasts-2; **MDS**, myelodysplastic syndromes; **AMML**, acute myelomonocytic leukemia; **FLT3**, Fms-like tyrosine kinase-3; **ITD**, internal tandem duplication; **NPM1**, nucleophosmin-1, **sAML,** secondary AML and **tAML,** therapy-related AML.

CHAPTER 4: *Inhibition of cullin-ring ligases by Pevonedistat (MLN4924) abrogates the bone marrow microenvironment-leukaemia communication*

Preamble to Chapter 4: Statement of Contribution

For the work presented in this chapter, I performed all the wet lab experiments except for the generating RNA sequencing libraries and running samples on sequencer. This was done in collaboration with Dr Vladimir Benes, EMBL, Heidelberg. I have also generated all the figures, performed statistical analysis, analysed the data and wrote the chapter under guidance of my supervisor.

4.1 Abstract

Acute myeloid leukaemia (AML) is an aggressive form of leukaemia caused by mutations that block hematopoietic differentiation and drive the uncontrolled proliferation of the differentiation-arrested myeloid progenitor cells. Activating mutations in FMS-like tyrosine kinase 3 (FLT3) receptor occur in 30% of AML patients and are associated with poor prognosis and disease relapse. Several tyrosine kinase inhibitors (TKIs) against FLT3 have been developed, but in clinical trials, they showed only limited efficacy. FLT3 inhibitors effectively eliminate the AML blasts circulating in the blood, but they are less effective in eliminating the bone marrow-residing AML cells, indicating a protective effect of the bone marrow microenvironment (BMM). We found that bone marrow stromal cells (BMSC) provide near-complete protection against FLT3-targeting TKIs. This protective effect is largely mediated through paracrine/soluble factors secreted by the BMSCs, which reduce the dependency of AML cells on FLT3-driven survival signalling pathways in the BMM. BMSC also activates several receptor tyrosine kinase, which converge on to STAT3 and PI3K signalling. These survival pathways are also the downstream of FLT3 signalling pathway, indicating how the FLT3-ITD cells do not depend on FLT3 signalling in BMM. To target the BMM interactions with AML cells, mild proteostatic stress by inhibition of neddylation with MLN4924/pevonedistat, is induced in bone marrow stromal cells. This transient stress blocked the ability of the stroma to support AML cell viability and abolishes the stroma-mediated resistance against TKIs and AraC/Dnr. We also observed lipid mediated cytotoxic effect on the co-residing AML cells exerted by the BMSCs conditioned with transient proteostatic stress. These results provide a rationale of using MLN4924 in combination with chemotherapy or FLT3 targeted therapy in targeting the bone marrow residing AML cells.

4.2 Introduction

Acute myeloid leukaemia (AML) is a heterogeneous haematological malignancy characterised by a rapid accumulation of abnormal, partially differentiated myeloid cells in the bone marrow. AML is the 2nd most common type of adult leukaemia with approximately 21,000 new cases in the US annually [8,9]. AML has a poor prognosis with an average 5-year survival rate of below 20% in the elderly population [9]. The most frequent mutation in FLT3 is an internal tandem duplication (ITD) in its juxtamembrane domain [26,484]. The tyrosine kinase domain (TKD) can also be mutated resulting in similar, but not identical activation of FLT3 as the ITD mutation [139,485]. FLT3-ITD/TKD leukemic cells have a survival advantage due to FLT3- mediated activation of the three major survival pathways-PI3k/Akt/mTOR, Jak/STAT and RAS/MEK/ERK [112,486,487]. While FLT3 alone does not drive a robust proliferative signal, it strongly synergises with other trophic factors, such as IL-3 and stem cell factor (SCF)[164]. Small molecule inhibitors to target FLT3-ITD/TKD-dependent AML are currently being developed (Quizartinib, Sorafenib, Midostaurin, Crenolalinib) and tested in clinical trials. Unfortunately, none of these FLT3 targeting drugs have shown promising results in AML patients as a single agent [389,488]. Generally, FLT3-inhibitors effectively kill FLT3-mutant AML cells in the periphery but only cause a transient reduction in the number of AML blasts in the bone marrow [141,489]. Most preclinical studies of FLT3 inhibitors did not take into consideration the effect of the BMM and the synergistic interaction between FLT3-L, IL-3, SCF and other trophic factors within the BMM [139,166,490]. The role of the bone marrow niche is well established in conferring protection to leukemic cells against many different types of therapy, either through paracrine soluble factors (IL-3, IL-6, SCF) or through direct cell-cell contact (CXCR4-CXCL12) [166,491-493].

Malignant cells are protected from the damaging effects of both mutant proteins and altered cellular and organelle function through cellular stress pathways. This can maintain viability and contribute to drug resistance by upregulating pro-survival and/or anti-apoptotic proteins [210,494]. As a trade-off, however, the buffering capacity of these pathways is often exhausted in tumour cells, making them highly sensitive to additional stresses. The proteostatic network is one such example. AML cells have been found to depend on the ubiquitin-proteasome system, offering a potential target for therapy [495,496].

In this study, we investigated the effect of the NEDD8-activating enzyme (NAE) inhibitor pevonedistat (MLN4924, TAK-924) in AML. NEDD8 is an ubiquitin-like protein that can be conjugated to cullin-RING ligases (CRLs), activating them for degradative protein ubiquitination [497]. We found that in AML cells, inhibition of CRL function with pevonedistat induced a circuitry of CEBPα and p53 induction and activation, driving BH3-only Bcl-2 protein induction and culminating Noxa-dependent apoptosis (unpublished data).

In addition, we observed that conditioning of bone marrow stromal cells (BMSC) with mild proteostatic stress reverts its ability to protect AML cells against chemotherapeutics. Importantly, we found that proteostatic stress to the leukaemia BMM itself triggers an anti-

leukemic effect. The BMM nurtures AML cells by providing survival signals. However, exposure of the BMM to proteostatic stress diminished this capacity and reverted the BMM from leukaemia supporting to a leukaemia-rejecting environment. Overall, the stressor causing proteostatic imbalance may have the potential to disrupt the communication between the leukemic cells and the bone marrow niche resulting in anti-leukemic effect and increased drug sensitivity.

4.3 Materials and methods

4.3.1 Reagents

Sorafenib, Quizartinib (Selleckchem, UK), MLN4924 (Active Biochem, USA), ABT-737, ABT-199, Stattic, Idelalisib (Selleckchem, UK), MPA, 5-BPSA, 4-HNE (Cayman Chemicals, UK), PGJ2 and PGE2 (Enzo life sciences, UK) were dissolved in dimethyl sulfoxide (DMSO). Cytarabine (AraC) and daunorubicin (Dnr) (Sigma, USA) were dissolved in water.

4.3.2 Cell culture

Molm13 (ATCC), MV-4-11(DSMZ) and OCI-AML2 (ATCC) were cultured in RPMI-1640 medium (Gibco, Invitrogen) containing 10% foetal bovine serum (FBS) (Hyclone, Corning, USA) penicillin (100 U/ml), streptomycin (100 µg /ml) and 2 mg/ml GlutaMAX (Gibco, Invitrogen, USA). HS-5 (ATCC) cells were cultured in DMEM supplemented with 10% FBS (Hyclone, Corning, USA), penicillin (100 U/ml), streptomycin (100 µg/ml). iMSCs (hTERT immortalized primary BMSCs from healthy donor) were cultured in α-MEM (Sigma) containing 10% FBS, penicillin (100 U/ml) and streptomycin (100 µg /ml).

4.3.3 Patient samples

Mononuclear cells (MNCs) and bone marrow stromal cells (BMSCs) isolated from bone marrow aspirates of newly diagnosed AML patients were provided by Blood Cancer Biobank Ireland (BCBI). Primary AML mononuclear cells were cultured in RPMI1640 medium (Gibco) containing 10% Hyclone FBS, penicillin (100 U/ml), streptomycin (100 µg/ml) and GlutaMAX (2 mM, Gibco) and sodium pyruvate (1 mM, Sigma). Cell viability was assessed at the time of thawing the cells and only samples that showed a minimum of 75% viability were used for experiments.

4.3.4 Ethics Statement

All patients and healthy donors provided written informed consent, in accordance with Research Ethics Board-approved protocols of each BCBI collection sites: University College Hospital, Galway and Beaumont Hospital, Dublin. This study was fully compliant with all

relevant ethical regulations regarding human participants. Informed consent was obtained from all participants.

4.3.5 *Ex vivo* co-culture of AML mononuclear cells with bone marrow stromal cells

BMSCs were fluorescently labelled either by stable expression of green fluorescent protein (GFP, HS-5 cells) or by loading the cells with the long-term cell tracker, CFSE (5-(and 6)-carboxyfluorescein diacetate succinimidyl ester) (Biolegend) (iMSC). BMSCs were then seeded in 24 well plates at the density of 50,000 cells/ml and cultured for 48 h in the αMEM medium after which medium was replaced with primary AML cells seeded at the density of 500,000 cells/ml in RPMI1640 medium. After 24 h of co-culture, the cells were treated with a 3:1 molar ratio of AraC and Dnr (Sigma), TKIs (Sorafenib or Quizartinib) for 24 h and 48 h.

4.3.6 AML cell viability and phenotyping

Mononuclear cells (MNCs) were pipetted off the stromal cell layer and incubated with anti-CD34-PE and anti-CD38-APC-H7 antibodies (BD Bioscience, San Diego, USA) in 1% BSA/PBS (Sigma) for 30 min on ice in the dark. After washing off unbound antibodies, cells were stained with the viability dye, To-Pro3 (Molecular Probes) by adding it in a final concentration of 1 μM for 15 min on ice in the dark. Stained samples were analysed using BD FACS Canto II flow cytometer (BD Bioscience, San Diego, USA). Minimum 50,000 events were collected in the AML blast gate (GFP/CFSE negative cells). Detached BMSCs were excluded from the analysis based on their green fluorescence FSC^{high}/GFP^{+} (GFP expression of HS-5 cells and CFSE-labelling of iMSCs).

Cell death in the AML cell line was quantified with annexin V staining. Cells were collected and stained with annexin V-APC in annexin V buffer (10 mM HEPES/NaOH, pH 7.5, 140 mM NaCl, 2.5 mM $CaCl_2$) for 15 min on ice in the dark. Samples were analysed on a FACS Canto II flow cytometer.

4.3.7 Measurement of mitochondrial transmembrane potential (ΔΨm)

Changes in ΔΨm were detected using the fluorescent dye tetramethylrhodamine ethyl ester perchlorate (TMRE) (Molecular Probes, Life Technologies, USA). Following treatment, cells were collected by gentle trypsinisation and TMRE was added to the cells at a final concentration of 100 nM. Cells were incubated for 30 min at room temperature in the dark. Samples were analysed on a FACS Canto II flow cytometer.

4.3.8 Western blotting

Cells were lysed in whole-cell lysis buffer (1% Triton-X100, 20 mM HEPES pH 7.5, 350 mM NaCl, 1 mM MgCl2, 0.5 mM EDTA, 0.1 mM EGTA, 0.5 mM DTT, and protease inhibitor cocktail). Total proteins (30 µg) were electrophoresed and transferred onto a nitrocellulose membrane (Novax, Invitrogen). After blocking, the blots were incubated with rabbit monoclonal antibodies against XBP1s (Cell signalling technology, CST), Nrf2 (CST), ATF4 (CST), FoXo3a (Santa Cruz Biotechnology, SCBT), p-c-jun (SCBT), c-jun (SCBT), p53 (SCBT), p21 (SCBT), IkBα (CST), p-IkBα (CST) and β-actin (Sigma). For detection, horseradish peroxidase-conjugated secondary antibodies (CST) were used. Protein bands were visualized with SuperSignal® West Pico Chemiluminescent Substrate (Pierce) or Western lightening plus-ECL enhanced HRP substrate (Perkin Elmer) on X-ray film (Agfa-CP-BU).

4.3.9 Cytokine secretome analysis with an antibody array

Soluble factors (chemokines and cytokines) secreted by BMSCs were determined with proteome profiling using the Human XL cytokine array kit (R&D Systems). Conditioned medium from BMSCs was collected after 48 h of culture. Debris from the medium was cleared by centrifugation at 4000 x rpm for 5 min at 4ºC. The medium was then incubated with the antibody array as described in the manufacturer's protocol and developed using X-ray film (Agfa-CP-BU). The X-ray images were analysed using the HLImage^{++} software (Western Vision Software, USA).

4.3.10 Phospho kinome analysis

Intracellular kinases, receptor tyrosine kinases (RTKs) and mitogen-activated phospho kinases (MAPKs) activated in the Molm13 AML cell by bone marrow stromal cells were determined using the Human proteome profiler antibody array from R&D systems (43 intracellular kinases, 49 receptor tyrosine kinases and 26 mitogen-activated phospho kinases). Molm13 cells were co-cultured in the presence and absence of the bone marrow stromal cells (iMSC) for 48 h. After co-culturing, Molm13 cells were harvested, lysed and the arrays were probed with the whole-cell lysates according to the manufacturer's protocol and developed using X-ray film (Agfa-CP-BU). The X-ray images were analysed using the HLImage^{++} software (Western Vision Software, USA). Kinases with FDR<0.05 and expression fold change of 2 are used for analysis.

4.3.11 Gene expression profiling by RNA sequencing

The effect of BMM on the transcriptome of BMSC and Molm13 cells was studied in a layered co-culture model. Single-end RNA sequencing (RNA-seq) was performed on total RNA (1µg)

from HS-5 bone marrow stromal cells, iMSC (hTERT immortalised BMSCs) treated with or without 1μM MLN4924 for 24 h. Molm13 cells are co-cultured with iMSC pre-treated with or without MLN4924 and in a single culture. After co-culturing with AML cells, BMSC (iMSCs) were also collected for sequencing in order to understand the effect of the BMSC-AML cross talk. RNA extraction was done using RNeasy Mini kit (Qiagen, Germany), RNA quality was assessed with Agilent 2100 bioanalyzer using the Agilent RNA Pico kit (Agilent Technologies, USA). Barcoded stranded mRNA sequencing libraries were prepared using Illumina TruSeq RNA sample preparation kit (Illumina, USA). Obtained libraries were pooled in equimolar amounts and loaded onto Illumina sequencer Hiseq 2000 and sequenced unidirectionally, generating ~75 million reads per sample and sequencing reads were aligned against the human GRCh38 (Ensemble) reference genome using STAR aligner. Raw counts were normalised, and transcriptomics analysis was carried out using edgeR package (R-studio). Differential genes were selected based upon FDR cutoff <0.03 and log fold change of 2 were selected for further downstream analysis.

4.3.12 Network and pathway analysis of the activated kinome

The activated kinases (receptor tyrosine kinases, intracellular kinases and mitogen-activated protein kinases) and differential gene expression in Molm13 cells upon co-culturing with bone marrow stromal cells conditioned with or without proteostatic stress were analysed for pathway and network analysis using Ingenuity Pathway Analysis tool (Qiagen, USA). Gene ontology and gene set enrichment analysis was performed using WebGestalt (WEB-based Gene SeT Analysis Toolkit).

4.3.13 Detection of reactive oxygen species (ROS)

To detect the oxidative stress or ROS generation in the co-culture system, Molm13 cells were co-cultured with BMSC cells conditioned with or without proteostatic stress. After 48 h of co-culture, cells were incubated with the CellROX dye (Molecular Probes, Thermo Fisher Scientific, USA) according to the manufacturer's protocol. Oxidation of dye in Molm13 cells was measured by flow cytometry (BD FACS Canto).

4.3.14 Quantitative real-time PCR analysis

Total RNA was extracted from BMSCs (iMSCs and HS-5) conditioned with or without proteostatic stress and Molm13 cells after co-culturing with conditioned BMSC (iMSC) with or without proteostatic stress or from single culture using RNeasy Mini Kit (Qiagen, Germany). Genomic DNA was digested with DNAse I (Qiagen), cDNA was synthesized from 1μg of total RNA using Superscript-IV reverse transcriptase (Invitrogen, USA). Quantitative real-time PCR for Aldo-keto reductase family C1-4 (AKR1C1, AKR1C2, AKR1C3 and

AKR1C4), oxidative stress-induced growth inhibitor 1 (OSGIN1), C-X-C motif chemokine ligand 12 (CXCL12), 17β-Hydroxysteroid dehydrogenase (HSD17), Secretoglobin family 1A member 1 (SCGB1) and Hypoxanthine ribosyl transferase (HPRT) was done using Lighcycler 480 probes master (Roche) on Roche light cycler 480 (Roche, USA) in a 384 well plate with PrimeTime Mini qPCR assay primer and probe set from IDT (Integrated DNA Technologies, USA). All samples were run in triplicate, and experiments were repeated for 3 biological replicates and results were averaged. Differential gene expression was calculated using the $2^{-\Delta\Delta Ct}$ method.

4.3.15 15-deoxy-Prostaglandin J2 ELISA

15-deoxy-$\Delta^{12,14}$-prostaglandin J2 (15-d-PGJ2) ELISA kit (Enzo life sciences, USA) was used to determine the amount of 15-d-PGJ2 present in the conditioned medium from the proteostatic stressed stroma. iMSC were treated with 1μM of MLN4924 and DMSO for 24 h, followed by washout of drug and cells were cultured in a fresh complete growth medium. Conditioned medium was collected after 24 h and 48 h post-washout and debris was removed by spinning the medium at 2000rpm for 5 min at RT. ELISA was performed as per the manufacturer's instructions (Enzo life sciences, ADI-900-023). Data was analysed using 4-parameter logistic (4PL) curve fitting on Graphpad Prism.

4.3.16 Lipid extraction from conditioned medium

To assess the effect of non-protein (lipids) mediator of cell death, we extracted the lipids from iMSC treated with or without the MLN4924 for 24 h. Following washout of the drug, conditioned medium from the stromal cells was collected after 24 h and removed cellular debris by spinning the cells at 2000rpm for 5min at RT. Then the cell-free conditioned medium was subjected to Bligh and Dyer lipid extraction protocol using 1:2 ratio of chloroform:methanol [498]. The tubes were centrifuged at 1000 rpm for 5 min at room temperature to get phase separation. The bottom phase (organic layer) was collected carefully and dried under a stream of nitrogen. The extracted lipids were dissolved in 1:1 ratio of chloroform and ethanol or aqueous solvent 1% BSA in PBS. To test the cytotoxic effect of this lipid extract, Molm13 and MV4-11 cells were treated with various volumes of the extract with or without the presence of BMSC. Cell viability was measured after 48 h of treatment using Annexin V staining.

4.3.17 Statistical analysis

Flow cytometry data analyses were performed on FCS express (DeNovo software Inc. USA) and FlowJo (BD Biosciences, USA). Statistical analysis and data visualization were performed using GraphPad Prism 6 (GraphPad Software Inc., La Jolla, USA) software

packages. Unless otherwise stated, p-values comparing two means were calculated using the two-tailed Student's t-test in Graphpad Prism 6 (GraphPad Software, Inc. La Jolla, CA). A $p < 0.05$ was considered statistically significant, all error bars represents standard deviation.

4.4 Results

4.4.1 Bone marrow stromal cells provide protection to FLT3-ITD AML cells against the cytotoxic effects of chemotherapeutics.

To determine the role of bone marrow stromal cells (BMSC) in providing resistance against tyrosine kinase inhibitors (TKIs), FLT3-ITD AML cell lines (Molm-13 and MV4-11) were cultured either in direct contact with BMSCs (Figure 4.1A, 4.1B), in indirect contact (Figure 4.1C, 4.1D), using transwells (1 μm pore-size) or in BMSC-conditioned medium (Figure 4.1E, 4.1F). After 24 h of culture, the cells were treated with sorafenib and quizartinib and induction of cell death was measured after 48 h of treatment. Stromal cells (both HS-5 and iMSC) provided substantial protection against TKIs in all three-culture conditions, indicating that soluble factors produced by BMSCs are sufficient to mediate TKI resistance (Figure 4.1 A-F). To determine which trophic factors mediate TKI resistance, we measured the expression of 102 cytokines and chemokines released by BMSCs (HS-5 and iMSCs) using proteome profiling array (Biotechne, R&D systems). HS-5 and iMSC BMSCs expressed 39 and 44 different cytokines, respectively, 60% of which were common between them (Supplementary Figure 4.1). The majority of secreted cyto/chemokines are already known BMM-secreted factors, such as C-X-C motif chemokine ligand 12 (CXCL12), C-X-C motif chemokine ligand 10 (CXCL10), fibroblast growth factor 19 (FGF-19), interleukin-6 (IL-6) and angiopoietin 2 (ANGPT2) etc. (Supplementary Table 4.1). A combination of 5 of the BMSC-secreted cyto/chemokines known to drive pro-survival signalling pathways (IL-3, IL-6, IFNγ, CXCL12, FLT3-L) provided the same level of protection as the BMSC conditioned medium (Figure 4.1G). However, we could not find any of the cytokines alone to be able to drive full protection against TKIs (sorafenib and quizartinib) (Supplementary Figure 4.2 A-B) and neither absence of one cytokine from the mixture caused substantial loss of protection (Figure 4.1G); indicating that the pro-survival signal transduction pathways induced by BMM-secreted cytokines are partially redundant/overlapping.

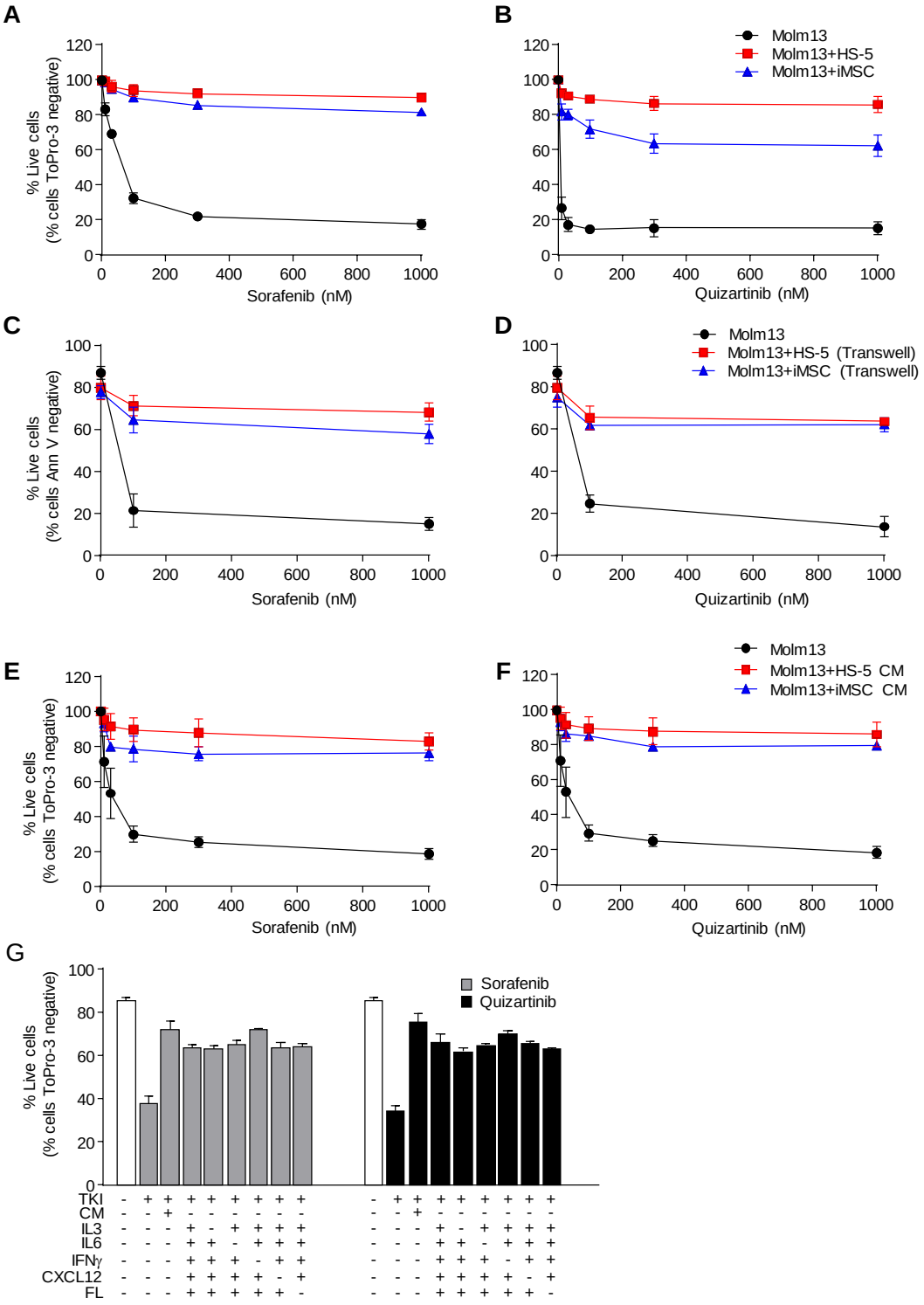

Figure 4.1: Bone marrow stroma blocks the cytotoxic effect of FLT3 inhibitors (sorafenib and quizartinib). FLT3-ITD mutation-carrying Molm13 and MV4-11 AML cells were cultured alone or over bone marrow stromal cells (HS-5 or iMSC) (A, B), non-contact co-culture using transwell inserts (C, D) or in conditioned medium (E, F) for 24 h followed by treatment with indicated doses of the FLT3 inhibitors sorafenib and quizartinib. Induction of cell death was measured after 48 h of treatment using To-Pro-3 staining. To test the effect of individual cytokines Molm13 cells were cultured with 20ng/ml of 5 individual cytokines- IFNγ, IL-3, IL-6, FLT3-L, and CXCL12. Cells were then treated with 1μM of tyrosine kinase inhibitor (sorafenib and quizartinib) (G). Induction of cell death was measured using To-Pro-3 staining after 48 h of treatment. The graphs show the average percentage of live cells and error bars represent the standard deviation. Statistical significance was calculated using Student's t-test. * indicates the p-value <0.05.

4.4.2 Bone marrow stromal cells activate multiple tyrosine kinase receptors driving STAT3 and PI3K signalling in FLT3-ITD AML cells.

To determine the signalling pathways BMM cyto/chemokines drive, and whether there are downstream components they converge on and thus could be targeted to overcome BMSC-mediated TKI resistance, we identified the kinases activated by BMSCs using phospho-kinase proteome assays for receptor tyrosine kinases (RTKs) (49 kinases, R&D Systems), intracellular kinases (43 kinases and kinase substrates, R&D Systems) and mitogen-activated protein kinases (MAPK) (26 kinases and MAPK substrates, R&D Systems). BMSCs activated various kinases, many of which are known to play a role in AML such as vascular endothelial growth factor receptor 2 (VEGFR2), platelet-derived growth factor receptor (PDGFR), stem cell factor receptor (SCFR) and fibroblast growth factor receptor-2 (FGFR2). We also found a unique set of receptor tyrosine kinases which have not been linked to bone marrow stroma-AML interaction (Supplementary Table 4.2), such as epidermal growth factor receptor 4 (ERBB4), neurotrophic receptor tyrosine kinase 3 (NTRK3) and ephrin receptor B4 (EPHB4). Network analysis using Ingenuity Pathway Analysis (Qiagen) identified cell viability and inhibition of apoptosis as the two most significant signal transduction pathways activated by BMSCs (Figure 4.2 A-B). The signalling pathways activated predominantly converged on STAT3 and PI3K signalling (Supplementary Figure 4.3 A-B), the same two mediators as FLT3-signalling, providing an explanation why FLT3-ITD AML cells do not depend on FLT3 in the BMM and are thus resistant to FLT3 inhibitors.

To assess whether inhibition of STAT3 and PI3K can restore AML drug sensitivity, pharmacological inhibitors were used; STAT3 was inhibited with Stattic (binds to SH2 domain and inhibits its activation, dimerisation and nuclear translocation of STAT3), while PI3K was inhibited with idelalisib (blocks the P110δ isoform of PI3K). The inhibitors were added to the co-cultures at the same time when the BMSCs and AML cells (Molm-13 and MV4-11) were combined, incubated for 24 h followed by treatment with quizartinib for 48 h. Inhibition of both STAT3 or PI3K could sensitise AML cells to quizartinib with a synergistic effect (CI ≤ 0.81 for stattic and CI ≤ 0.15 for idelalisib) (Figure 4.2C, 4.2D, Supplementary Table 4.3). To confirm the potential of STAT3 and PI3K-inhibition in AML drug sensitisation, we tested these drugs in bone marrow-derived MNCs from 4 AML patients (Figure 4.2E). Unexpectedly, primary AML blasts did not show the same sensitisation as the AML cell lines, indicating that BMSC-driven survival signalling in primary cells does not require STAT3 or PI3K activity.

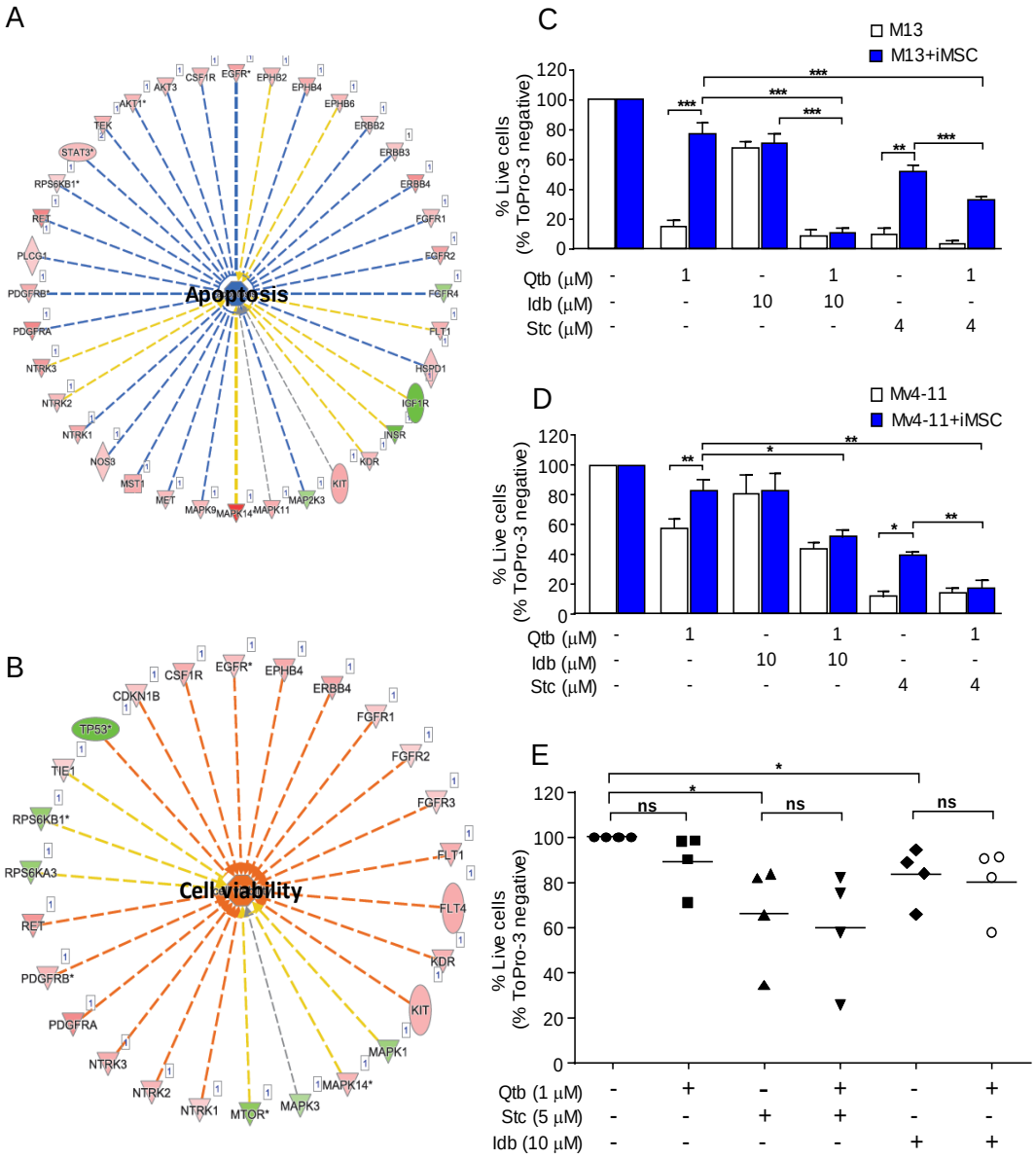

Figure 4.2: The bone marrow stromal cells activate receptor tyrosine kinases that converge on to STAT3 and PI3K signalling pathway. Molm13 cells were cultured with BMSC (iMSC) for 48 h in a layered co-culture system using antibody-based proteome profiling array. BMSC- driven activation of RTKs, MAPKs, and intracellular kinases was analysed using proteome arrays. Network analysis was performed to find out the unique and significant interactions. Key targets of BMM induced kinase signalling in the category of (A) inhibition of apoptosis and (B) cell viability. Red shading node shows activated kinases, green: inhibited kinases, orange node: activation function and blue node: inhibitory function. BMSC-AML cells were treated with STAT3 inhibitor, Stattic (4 μM), PI3K inhibitor, Idelalisib (10 μM), at the time of addition of (C) Molm13 and (D) MV4-11. 24 h post-co-culturing, the cells were treated with quizartinib (1 μM) and cell viability was measured after 48 h of treatment using annexin-V staining. Primary bone marrow-derived AML mononuclear cells from 4 patients were co-cultured with BMSC (iMSC) for 24 h followed by treatment with quizartinib (1 μM), Stattic (4 μM) and Idelalisib (10 μM) in a single drug treatment or in combination with quizartinib. Cell viability was measured after 48 h of treatment using ToPro-3 staining. The graphs show the mean viability of 4 patient samples.

4.4.3 Transient proteostatic stress of bone marrow stromal cells abolish their ability to support leukemic cells

Since many of the BMSC-activated RTKs can drive AML drug resistance, we contemplated whether there is a mechanism that would have an impact on the functionality of multiple tyrosine kinase receptors. RTK-mediated signal transduction is strongly dictated by the dynamics of their turnover. Upon ligand binding, RTKs are rapidly internalised and degraded, which is normally balanced by their synthesis at the endoplasmic reticulum and transportation to the cell surface [499]. The expression of RTKs is also elaborately regulated by ubiquitinating and de-ubiquitinating enzymes [500]. Thus, we non-selectively/indirectly targeted RTKs by interfering with the ubiquitin-proteasomal system using the NEDD8 activating enzyme (NAE)-inhibitor MLN4924/pavonedistat. MLN4924 showed a potent cytotoxic effect on AML cells even in the presence of BMSCs (Figure 4.3A).

Given the fact that proteostatic stress may impact the stromal cells themselves, for example by interfering with secretion of trophic factors, we tested whether exposure of BMSCs to MLN4924 has any effect. Bone marrow stromal cells (HS-5 and iMSC) were treated with MLN4924 for 24 h after which it was washed out and Molm13 cells were layered over the pre-treated stroma. After 24 h, the co-culture was treated with sorafenib and quizartinib and AML cell viability was measured. Pre-treatment of the stromal cells with MLN4924 abolished their ability to support AML cells and sensitised them to TKIs (Figure 4.3C, 4.3D). Interestingly, we observed substantial AML cytotoxicity in the MLN-pre-treated co-cultures not treated with TKIs. We confirmed that this effect was not due to the death of the stromal cells (Figure 4.3B), instead it appeared to be a cytotoxic effect the BMSCs conditioned with transient proteostatic stress exerted on the co-residing AML cells.

Corroborating these results, we found that conditioning of BMSCs with proteostatic stress also exerted a cytotoxic effect on primary AML blasts. We seeded bone marrow-derived AML blasts from 7 patients onto a layer of BMSCs which were pre-exposed to MLN4924 for 24 h. MLN4924 was removed from the BMSC layer by thorough washes. The AML cells were then cultured over the stroma for 24 h, after which they were treated with quizartinib and AML viability was measured after 48 h of treatment. We found that proteostatic stress-conditioned BMSCs were no longer able to support AML viability (Figure 4.3E) and the residing blasts were sensitised to quizartinib (Figure 4.3E). We also tested whether BMSC-conditioning also sensitises AML blasts to cytarabine+daunorubicin (AraC/Dnr) treatment (Figure 4.3F, Supplementary Figure 4.4A-E). As seen before, proteostatic stress-conditioned BMSCs failed to protect AML blasts against AraC/Dnr.

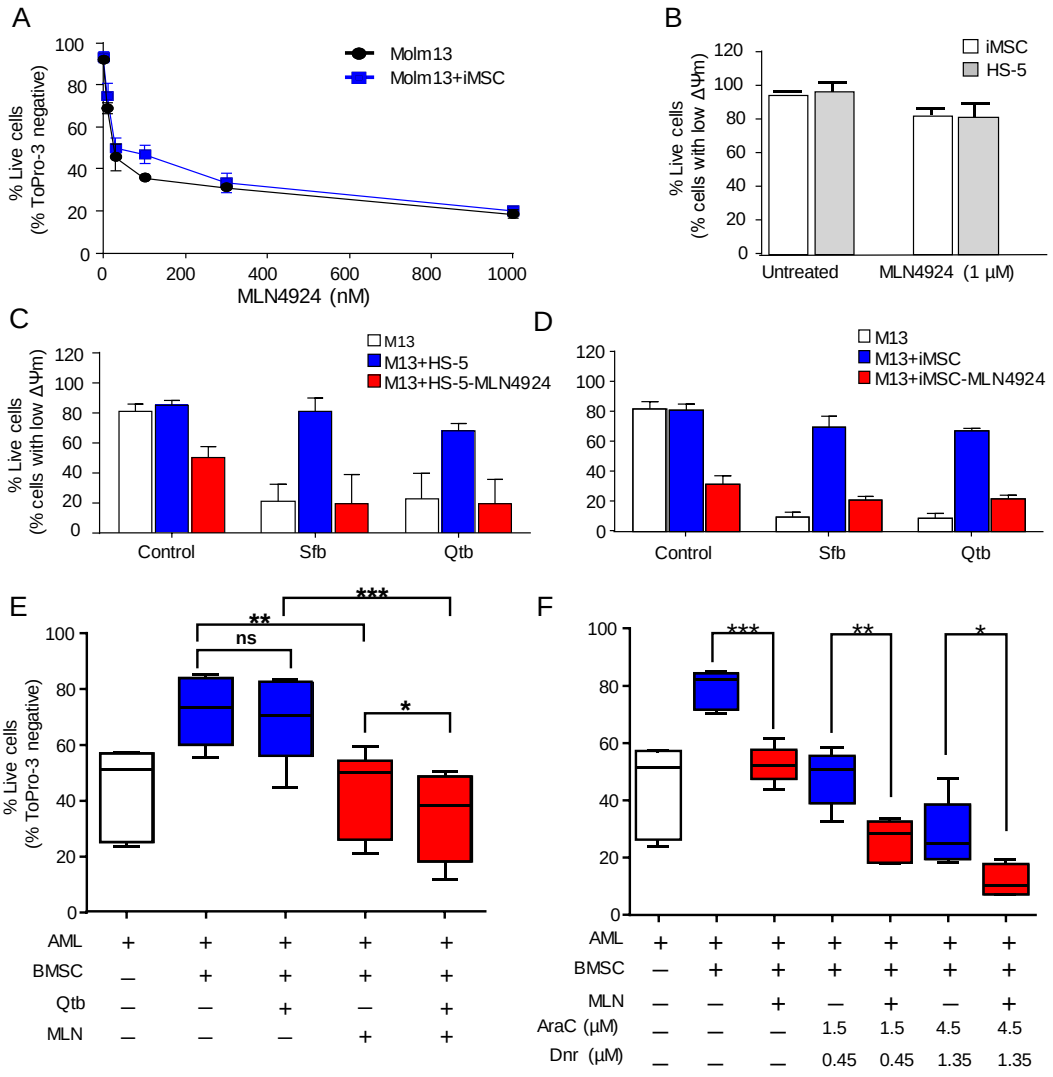

Figure 4.3: Proteostatic stress to BMSCs abolishes their ability to support the AML cell viability and drive drug resistance. Molm13 cells were co-cultured with BMSC (iMSC) for 24 h followed by treatment with 1 μM of MLN4924. (A) Induction of cell death was measured using annexin-V staining after 48 h of treatment. (B) Bone marrow stromal cells (HS-5 and iMSC) were treated with 1 μM MLN4924 for 24 h and induction of cell death was measured using TMRE dye by loss of mitochondrial membrane potential. Bone marrow stromal cells HS-5 (C) or iMSC (D) were treated with 1 μM of MLN4924 to induce proteostatic stress. After 24 h of treatment, the drug was washed off and Molm13 cells were seeded over the proteostatic stress conditioned stroma and untreated stroma for 24 h followed by treatment with tyrosine kinase inhibitors sorafenib and quizartinib. Induction of cell death was measured using TMRE dye after 48 h of treatment. (E) Primary bone marrow-derived AML mononuclear cells (MNC) from 7 patients were co-cultured with BMSC conditioned with or without proteostatic stress for 24 h. (E) After 24 h of co-culturing, cells were treated with 1 μM of quizartinib. Cell viability was measured after 48 h of treatment using ToPro-3 staining. Primary bone marrow-derived AML mononuclear cells (MNC) from 5 patients were co-cultured with untreated stroma and proteostatic stress conditioned stroma for 24 h followed by treatment with 3:1 molar ratio of cytarabine (AraC) and daunorubicin (Dnr). (F) Cell viability was measured after 48 h of treatment using ToPro-3 staining. Student's t-test was applied to determine the significant differences with * indicates $p<0.05$, ** indicates $p<0.005$ and ns meaning non-significant.

4.4.4 Proteostatic stress to the bone marrow stromal cells changes the secretome and stress-responsive transcription factors associated with the secretion of cytokines and chemokines.

To delineate the mechanism through which conditioned BMSCs induce AML cell death, first we determined whether AML cell death requires direct BMSC-AML cell-cell interaction or it is mediated by paracrine factors by using indirect, transwell cultures (BMSCs in bottom chamber and AML cells in the upper chamber, separated by a 1 μm pore-size membrane allowing only secreted soluble factors and extracellular vesicles to pass through). BMSCs were exposed to MLN4924 (1 μM) for 24 h followed by washout of the drug. Molm13 cells were then seeded over the stroma for another 24 h and then treated with quizartinib or sorafenib. Cell death was measured after 48 h of TKI treatment (Figure 4.4 A-D). BMSCs conditioned with proteostatic stress induced cell death in Molm-13 cell and sensitised the AML cells to TKIs, indicating that transient proteostatic stress may alter the BMSC secretome. We thus measured the secretion of 102 cytokines/chemokines in the conditioned medium collected after 24 h of MLN4924 washout using a cytokine array (Human proteome profiler, R&D Systems). Surprisingly, there were only a few cytokines/chemokines whose secretion level reduced by MLN4924 treatment, namely tumour necrosis factor receptor superfamily, member 8 (CD30), chitinase 3 like 1 (CHI3L1), C-X-C motif chemokine ligand 10 (CXCL10), C-C motif chemokine ligand 5 (CCL5), -7, -20 and platelet-derived growth factor subunit A (PDGFα) (Figure 4.5A, Supplementary Table 4.4). On the other hand, there were numerous cytokines/chemokines whose secretion significantly increased after treatment (Figure 4.5B and Supplementary Table 4.4). Many of these are pro-survival, trophic factors, thus making it unlikely that proteostatic stress-induced cyto/chemokine secretome drives AML cell death. We have also found that BMSC proteostatic stress-driven AML killing did not depend on death ligand signalling (Supplementary figure 4.5).

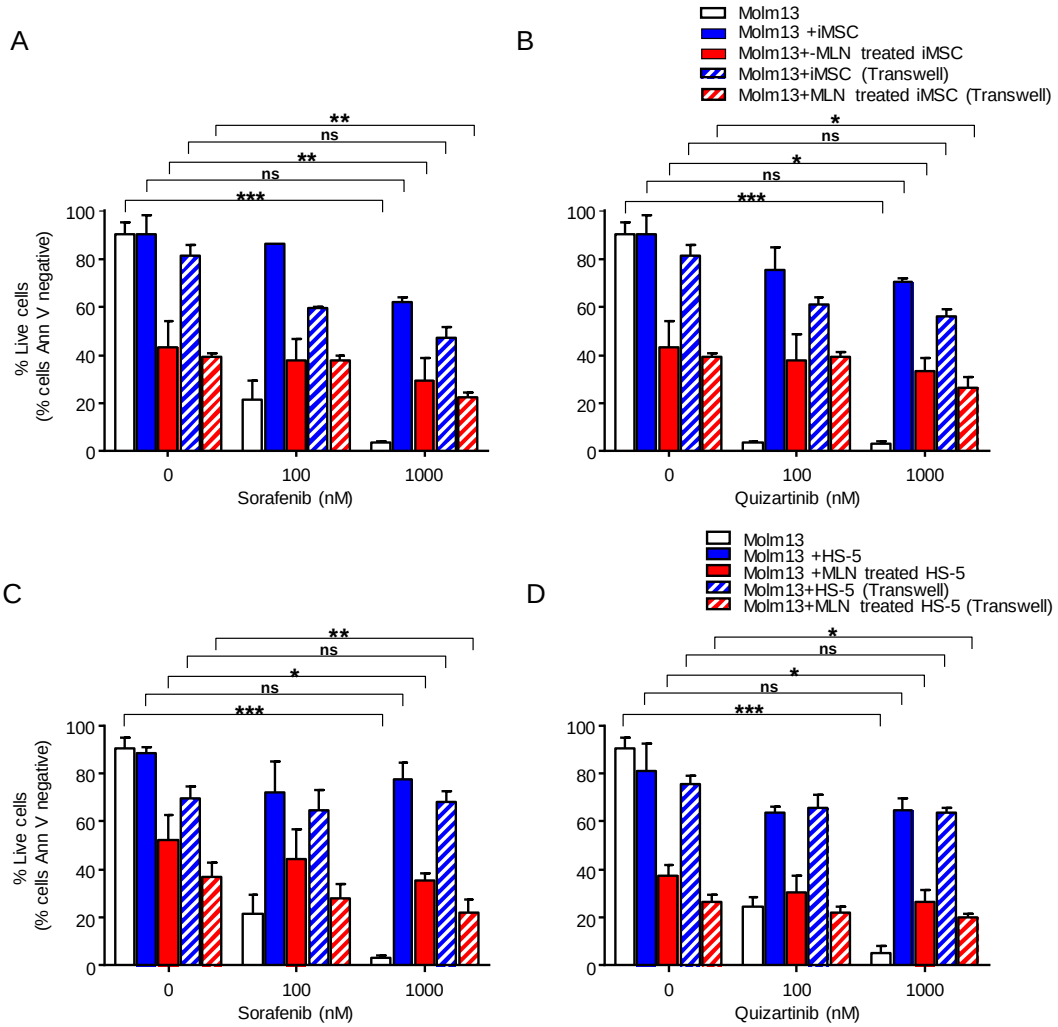

Figure 4.4: Induction of mild proteostatic stress to the bone marrow stroma alters the microenvironment from an AML-supportive to the AML-rejecting. Bone marrow stromal cells iMSC (A-B) and HS-5 (C-D) were treated with 1 μM of MLN4924 for induction of mild proteostatic stress for 24 h and drug was washed out after treatment. Molm13 cells were co-cultured directly over stroma (cell-contact co-culture) or in non-contact co-culture, using transwell inserts with a pore size of 1 μm allowing only secreted soluble factors to pass through it. After 24 h of co-culturing, Molm13 cells were treated with indicated doses of sorafenib (A, C) and quizartinib (B, D). Cell viability was measured after 48 h post-treatment using annexin-V staining. The solid colour bar represents the contact co-culture and dashed bars non-contact transwell co-culture. Student's t-test was applied to determine the significant differences with *p<0.05, **p<0.005 and ns meaning non-significant.

To further understand the changes induced by proteostatic stress in BMSCs, we determined what stress pathways may be activated by determining changes in the expression and/or activity of both the generic stress-induced factors, NF-κB, FoxO3a and JNK as well as transcription factors associated with specific stress conditions, namely ATF4 (integrated stress response), XBP1s (unfolded protein response), Nrf2 (oxidative stress), p53 and its target gene p21 (DNA damage, stress-induced cell cycle arrest) upon treatment with MLN4924 (Figure 4.5C, 4.5D). Proteostatic stress triggered FoxO3a induction and NF-κB activation (seen by phosphorylation and negative feedback induction of IκBα), confirming the induction of cellular stress. Of the stress-specific markers, ATF4, the marker of the integrated stress response and the p53 target, p21 were strongly induced. We observed that the pattern

of stress-induced transcription factor activation is different in AML cells cultured with BMSCs pre-exposed to proteostatic stress, showing that proteostatic stress-conditioned BMSCs exert specific stress on the AML cells (Figure 4.5D).

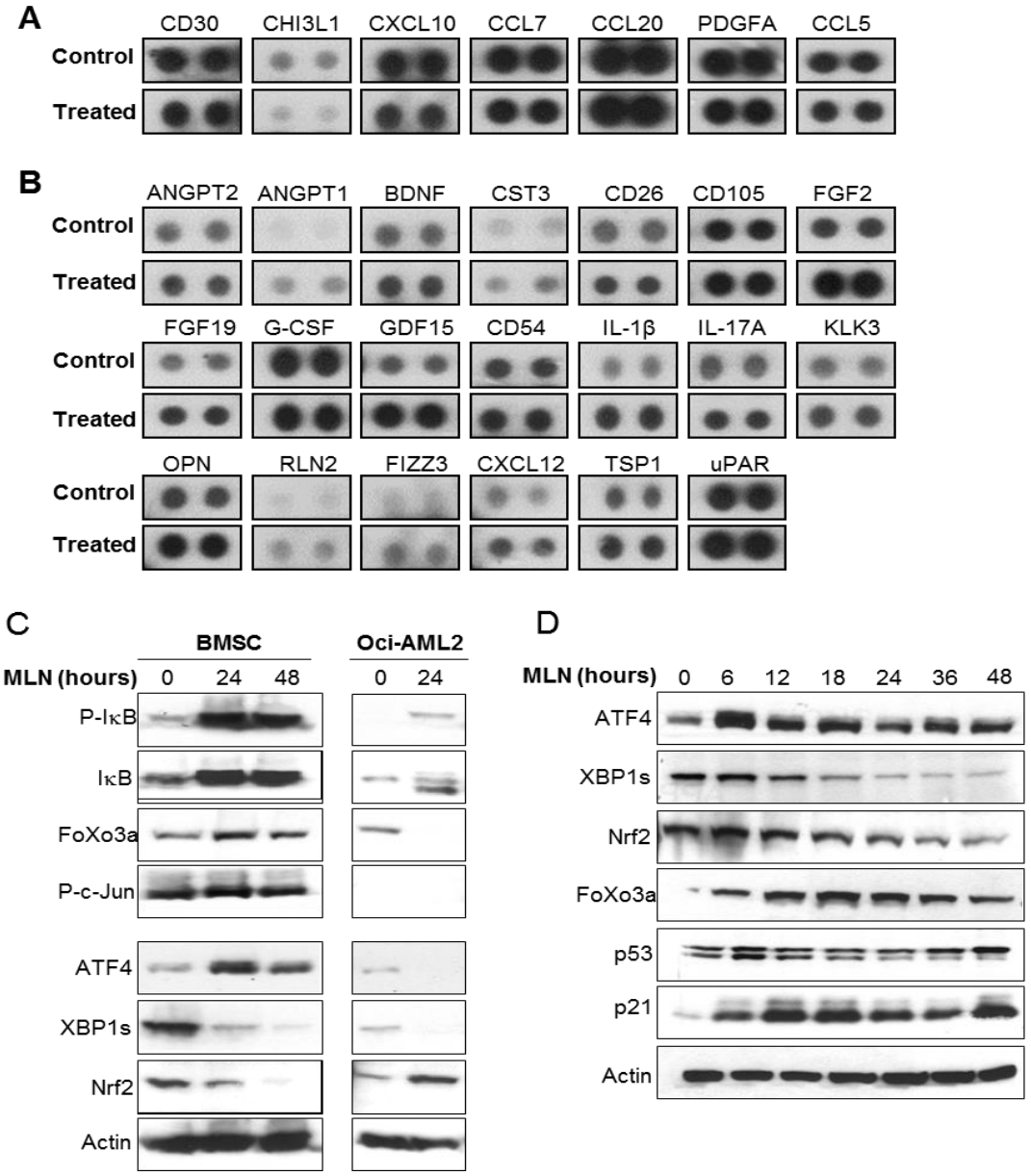

Figure 4.5: Proteostatic stress conditioned bone marrow stroma has altered secretome and induces cellular stress response transcription factors. Changes in the cytokines and chemokines secretion profile of BMSC (HS-5 and iMSC) after induction of proteostatic stress was detected using proteome profiler antibody-based array. Stromal cells were treated with 1 μM of MLN4924 and drug was thoroughly washed out. Conditioned medium was collected after 24 h and used for the detection of the cytokines and chemokines. Representative dot-blot of cyto/chemokines whose expression (A) decreases and (B) increases after induction of proteostatic stress. Image analysis and quantification were done using HLImage ++ software. Proteostatic stress has a different effect on BMSC and Oci-AML2 cells (C) after 24 h and 48 h of treatment. Stress-responsive transcription factors protein expression was detected by western blotting for induction of ATF4, XBP1s, Nrf2, FoxO3a, p53, p21, pIκBα, IκBα, P-c-jun and β-actin as a protein loading control. Samples were collected after 0, 6, 12, 18, 24, 36 and 48 h of treatment with MLN4924.

To further explore the effect of proteostatic stress on stromal cells (HS-5 and iMSC) and its knock-on effect on the AML cells, we performed transcriptome analysis by next-generation sequencing (NGS) on BMSCs treated with MLN4924 (both HS-5 and iMSC cells), as well as Molm13 cells cultured with conditioned BMSCs (iMSCs) for 24 h. $75x10^6$ reads per sample were collected, aligned and normalized and the differentially expressed genes were identified using edgeR (Rstudio)[501]. 860 and 1113 genes were differentially expressed in HS-5 and iMSC respectively after induction of proteostatic stress and 159 genes were common among them cut-off of FDR<0.03 and were ranked according to fold change. While 138, 1209, 615 were differentially expressed in Molm13 cells upon co-culturing with BMSC, with proteostatic stress conditioned stroma and when compared between these two conditions (Supplementary table 4.5). Gene ontology analysis of the differentially expressed genes in Molm13 cells showed that the conditioned stroma led to enrichment for oxidoreductase activity (Figure 4.6A, 4.6B). We also found the enrichment for the functional effect of proteostatic stress conditioned BMSCs in the conversion of lipids involving Aldo-keto reductase family (Figure 4.6C) and generation of reactive oxygen species (ROS) (Figure 4.6D) in Molm13 cells cultured with conditioned stroma. To detect whether proteostatic stress-conditioned BMSCs trigger ROS generation in Molm-13 cells, the oxidation of CellROX dye was measured in Molm13 cells co-cultured with conditioned stroma. A significantly higher level of ROS generation was found in Molm13 cells co-cultured over proteostatic stressed stroma to that of untreated stroma (Figure 4.6E). To rescue the cells from oxidative stress, co-culture was treated with the antioxidants N-acetyl cysteine (NAC) or Vitamin C. Antioxidant treatment partially reduced the ROS generation (Figure 4.6F) but could partially rescue Molm13 from proteostatic stress conditioned BMSC mediated cell death (Supplementary Figure 4.6).

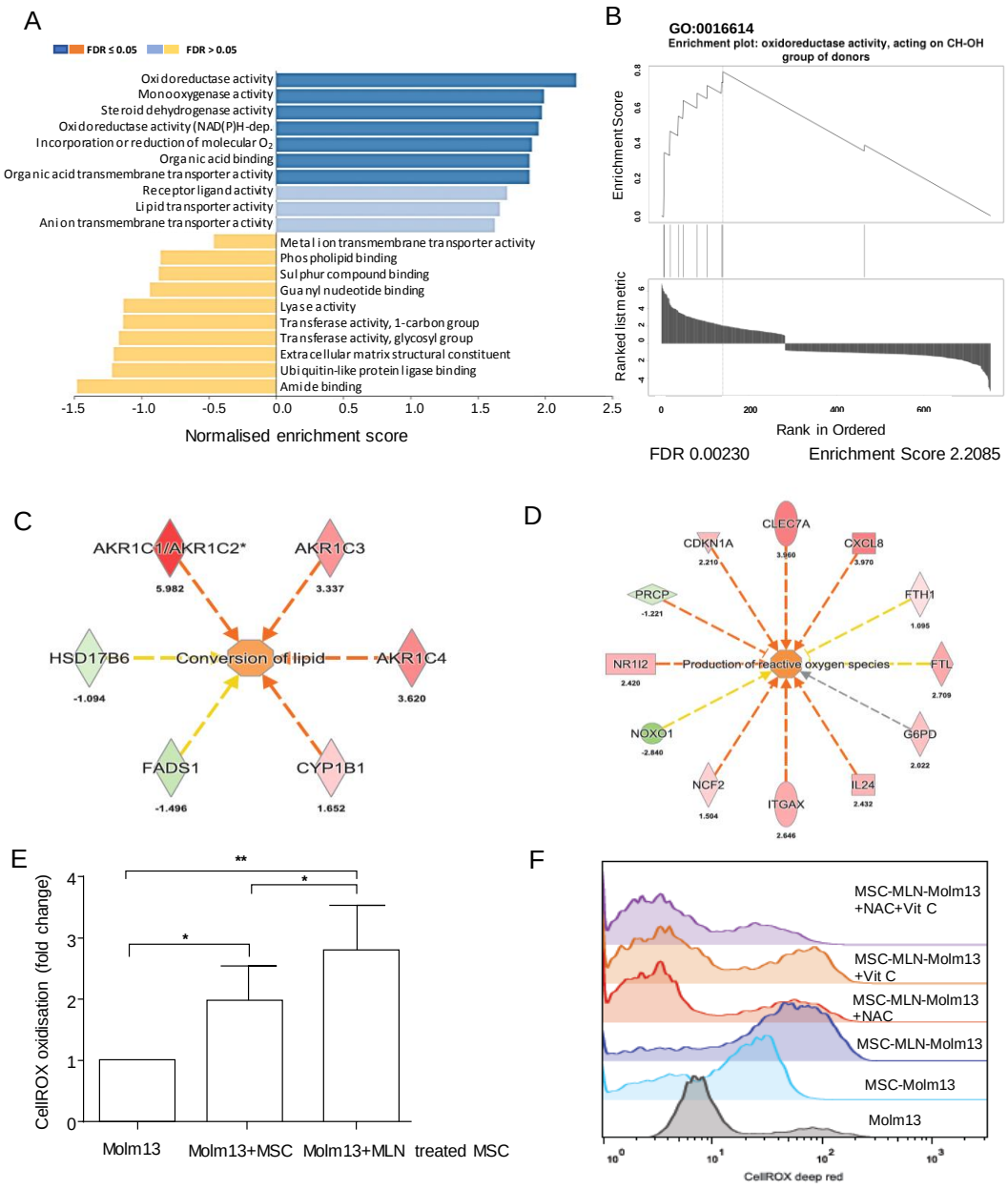

Figure 4.6: Proteostatic stress-conditioned stroma and residing AML cells are enriched for oxidoreductase activity and oxidative stress. Gene ontology analysis of differentially regulated genes in Molm13 cells upon co-culture with proteostatic stress conditioned BMSC reveals the top classifications (A) oxidation-reduction, steroid dehydrogenase activity. Gene set enrichment analysis reveals the enrichment for (B) oxidoreductase activity involving aldo-keto reductase enzymes. Functional analysis by Ingenuity pathway analysis reveals the key significant function like conversion of lipids (C) and production of reactive oxygen species (D). Oxidative stress is measured in AML cells (Molm13) using CellROX dye. Molm13 cells were cultured with BMSC conditioned with or without proteostatic stress and in a single culture. After co-culture with stroma 48 h, Molm13 cells were incubated with CellROX dye and oxidisation of dye was measured in live cells fraction by flow cytometry. (E) The graphs show the fold change of geometric mean intensity of oxidised CellROX dye and error bars represents the standard deviation. Statistical significance was calculated using Student's t-test. * indicates the p-value <0.05, **p-value <0.005. Inhibition of oxidative stress was induced by treatment with antioxidants N-acetyl cysteine (NAC) and Vitamin C (Vit. C). Antioxidants were added to co-culture at the time of seeding Molm13 over-conditioned BMSC either alone or in combination. (F) Oxidative stress was measured after 48 h of co-culture using CellROX dye. Histograms showing representative oxidisation of CellROX dye.

4.4.5 Aldo-keto reductase C family enzymes are involved in driving drug resistance in AML cells

Aldo-keto reductase (AKRs) are a class of enzymes that reduce reactive aldehydes to their corresponding alcohols. Members of the AKR1C family (AKR1C1-4) are hydroxysteroid dehydrogenases or oxidoreductases and are involved in the conversion of lipids or steroid hormones. The RNA sequencing analysis revealed that proteostatic stress-conditioned stroma as well as the co-residing AML cells have higher expression of AKR1C enzyme family genes AKR1C1-3 in BMSC and AKR1C1-4 in Molm13 cells. Oxidative stress-induced growth inhibitor 1 (OSGIN1) was also found to be upregulated in Molm13 cells and in conditioned stromal cells (HS-5 and iMSC). To confirm these findings, we performed determined the expression of these genes by quantitative real-time PCR (Figure 4.7 A-B). These results confirm the strong upregulation of AKR1C enzymes AKR1C1-3 and OSGIN1 in Molm13 cells co-cultured with or without proteostatic stressed conditioned stroma (Figure 4.7A). Conditioned BMSCs (iMSC and HS-5) also showed higher expression level of AKR1C1-C3, and OSGIN1 (Figure 4.7B). Additionally, MLN4924 also led to the induction of secretoglobin family 1A member 1 (SCGB1) and repression of C-X-C motif chemokine ligand 12 (CXCL12) and hydroxysteroid 17-beta dehydrogenase 17 (HSD17) (Figure 4.7B). These results concurred with the RNA sequencing data and highlight a possible role of AKR1C enzymes.

To understand what role these enzymes play in AML cells; i.e. whether they were involved in inducing cell death or have a protective effect on AML cells, we used small molecule inhibitors against AKR1C1 (3-bromo-5-phenylsalicyclic acid, 5-BPSA) or against the AKR1C enzyme family (medroxyprogesterone acetate, MPA). Molm13 cells were treated with these inhibitors in a single culture or in co-culture with conditioned BMSCs. We found that treatment with MPA (Figure 4.7C) and 5-BPSA (Figure 4.7D) did not rescue the AML cells from cell death induced by conditioned BMSCs and had no cytotoxic activity against AML cells in cultured with stroma. This suggests that conditioned stroma does not induce cell death in AML cells through AKR1C enzymes. However, we found that treatment with AKR1C inhibitors (MPA, 5-BPSA) reverted stroma-mediated resistance to quizartinib and potentiated the cytotoxic effect of quizartinib. These findings indicate the role of steroid hormone signalling pathways in providing the resistance to FLT3-ITD cells against tyrosine kinase inhibitors.

Since AKR1C enzymes are involved in lipid conversion and synthesis, we investigated whether lipids or oxidised lipids secreted by the conditioned BMSCs mediate cell death in AML cells. First, we assessed whether the cell death-inducing agent produced by BMSC-conditioning is protein in nature. To this end, we heat-denatured the proteins in the conditioned medium collected from proteostatic stressed BMSC at 100^{o}Cfor 10 min after which the medium was cleared of the denatured protein aggregates by centrifugation. AML cells were then cultured in 1:1 diluted heat-denatured conditioned medium (CM) and fresh growth medium. Heat denatured conditioned medium from proteostatic stressed stroma

retained its cytotoxic ability against Molm13 cells (Figure 4.8A) and MV4-11 cells (Figure 4.8B), indicating that the factor responsible for cell death is a heat stable molecule, most likely a non-protein compound. To further assess what may be the non-protein cytotoxic compound, we extracted the non-polar molecules from the conditioned medium using Bligh-Dyer extraction [498]. The extracted lipids were then dissolved in an organic solvent (1:1 of chloroform:ethanol) (Figure 4.8 C & E) or aqueous solvent (PBS with 1%BSA) (Figure 4.8 D & F). The lipid extract from proteostatic stress-conditioned BMSCs had a cytotoxic effect on AML cells both in single culture and in co-culture with bone marrow stromal cells (Figure 4.8 D, F), suggesting the role of secreted lipid moieties or other small metabolites. Since AKR1C enzymes are involved in conversion of complex lipids or steroid hormones, we tested the effect of prostaglandins or their oxidised product in mimicking the cytotoxic effect of conditioned BMSC. AML cells were treated with prostaglandin E2 (PGE2) or its spontaneously formed oxidation product, prostaglandin J2 (PGJ2) in the presence or absence of conditioned BMSC for 24 h followed by treatment with quizartinib (Figure 4.9 A-B). PGE2 had no anti-leukemic activity, but PGJ2 killed AML cells. BMSCs however protected the AML cells from the cytotoxic effect of PGJ2. While both PGE2 and PGJ2 sensitised AML cells cultured with BMSCs to quizartinib, neither PGE2 nor PGJ2 could replicate the AML-cytotoxic effect of conditioned BMSCs on AML cells (Figure 4.9 A-B).

We also determined whether PGJ2 and its recognised oxidised form, 15-deoxy-$\Delta^{12,14}$-prostaglandin J2 (15-d-PGJ2) is present in the medium of conditioned stroma with ELISA. A statistically significant increase in the concentration of 15-d-PGJ2 was found in the medium of conditioned BMSCs (Figure 4.9 C), but the concentration detected (1.5 ng/ml or 5 nM) was much lower than what was necessary to sensitise AML cells to quizartinib. This indicates that 15-d-PGJ2 is unlikely to be the mediator of AML cell death cultured with conditioned BMSC.

We further studied the role of activation of peroxisome proliferator-activated receptor gamma (PPARγ) by PGJ2, which is its known agonist. Activation of PPARγ induces apoptosis in AML cells by ROS generation and caspase-3 activation [502]. We tested if conditioned stroma mediating cell death is PPARγ activation dependent. We inhibited PPARγ with GW-9662 (PPARγ antagonist) and activate it using rosiglitazone (PPARγ agonist) in BMSC-AML co-cultures at the time of seeding of Molm13. Inhibiting or activating PPARγ activity does not rescue or mimic the effect of conditioned stroma mediated cell death in AML cells (Supplementary figure 4.7A). PGJ2 or 15-d-PGJ2 is also a known inducer of p53 and can mediate DNA damage mediated cell death [503], so we checked if p53 is involved in proteostatic stress-conditioned BMSC-mediated cell death in AML cells. We inhibited p53 with pifithrin-α (inhibitor of p53 transcriptional activity) and pifithrin-μ (by blocking the binding of p53 to Bcl2, Bcl-X_L on the mitochondrial surface, while retaining its transcriptional activity) in BMSC-AML co-cultures at the time of seeding of Molm13 cells. Blocking p53 activity failed to rescue the AML cells from conditioned-BMSC mediated cell death (Supplementary Figure 4.7B).

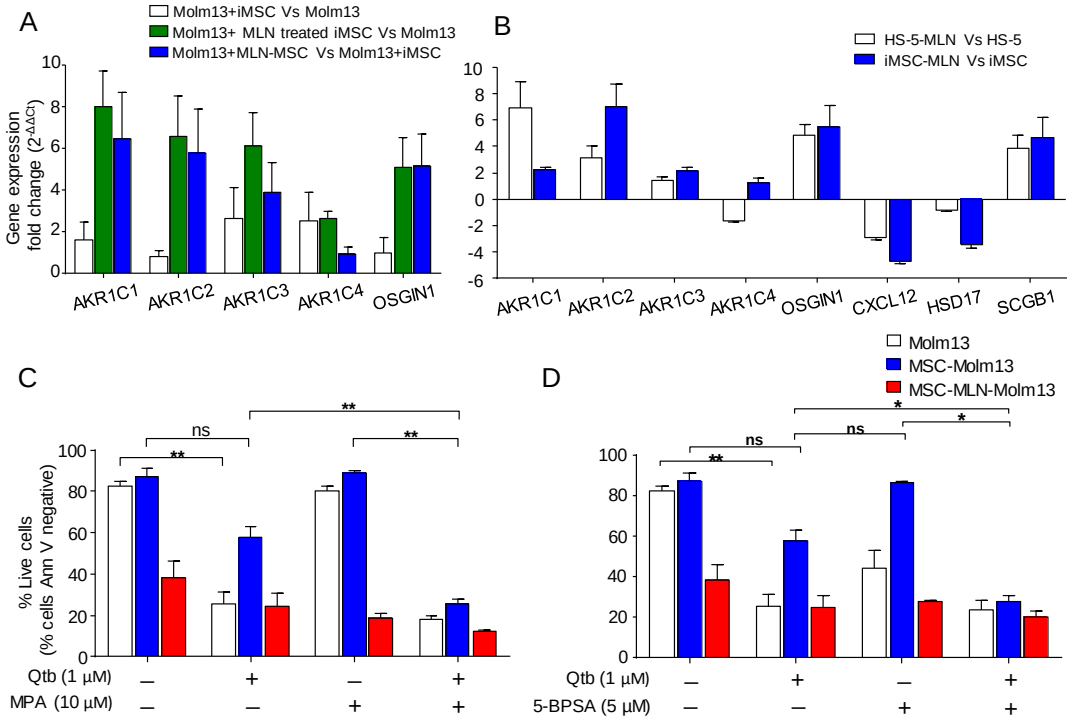

Figure 4.7: Bone marrow stroma induces aldo-keto reductase C enzyme family in AML cells and drives the drug resistance against tyrosine kinase inhibitor. Transcriptome analysis indicates the upregulation of AKR1C1, AKR1C2, AKR1C3, AKR1C4 and OSGIN1 genes in AML cells upon co-culturing with conditioned stroma. (A) Molm13 cells were cultured with BMSC treated with and without MLN4924 for 48 h in a layered co-culture system and gene expression analysis was performed by qRT-PCR. (B) BMSCs (HS-5 and iMSC) were treated with MLN4924 for 24 h followed by washout of drug and cells were harvested after 24 h of culture. qRT-PCR was performed for AKR1C1-C4 enzymes, OSGIN1, CXCL12, HSD17 and SCGB1 genes on Roche Lightcycler 480 using Lightcycler 480 probe master mix. Gene expression analysis was performed using the 2-ΔΔCt method with hypoxanthine phosphoribosyl transferase (HPRT) as a housekeeping gene. The graphs show the mean fold change ± SEM (n=3). Effect of inhibition of AKR1C enzymes with (C) pan-AKR1C inhibitor medroxyprogesterone acetate (MPA) and (D) AKR1C1 inhibition by 5-Bromo-3-phenyl salicylic acid (5-BPSA) was determined. Small molecule inhibitors were added to the co-culture system at the time of seeding of Molm13 over bone marrow stroma (iMSC). After 24 h of co-culture AML cells were treated with 1µM of quizartinib with or without the combination with AKR1C inhibitors. Cell viability was measured after 48 h of treatment with annexin-V staining. Graphs showing the mean viability±std dev. (n=3). Student's t-test was applied to determine the significant differences with * indicates $p<0.05$, ** indicates $p<0.005$ and ns indicates non-significant.

Earlier results with secreted lipids (Figure 4.8 C-F) confirm their role as a mediator of cell death in AML cells, also there is higher ROS generation in conditioned BMSC. Based upon these findings we tested if lipid peroxidation plays a role in it. 4-hydroxynonenal (4-HNE) a lipid peroxidation product was used to treat AML -BMSC co-culture at the time of seeding AML cells for 24 h followed by treatment with quizartinib. We found that 4-HNE treatment has no effect on the AML cell viability, indicating that lipid peroxidation product 4-HNE has no role in conditioned BMSC mediated cell death. However, we also observed that its pre-treatment sensitises the residing Molm13 cells to quizartinib in the presence of BMSC, thus abolishing the stroma mediated drug resistance (Figure 4.9D).

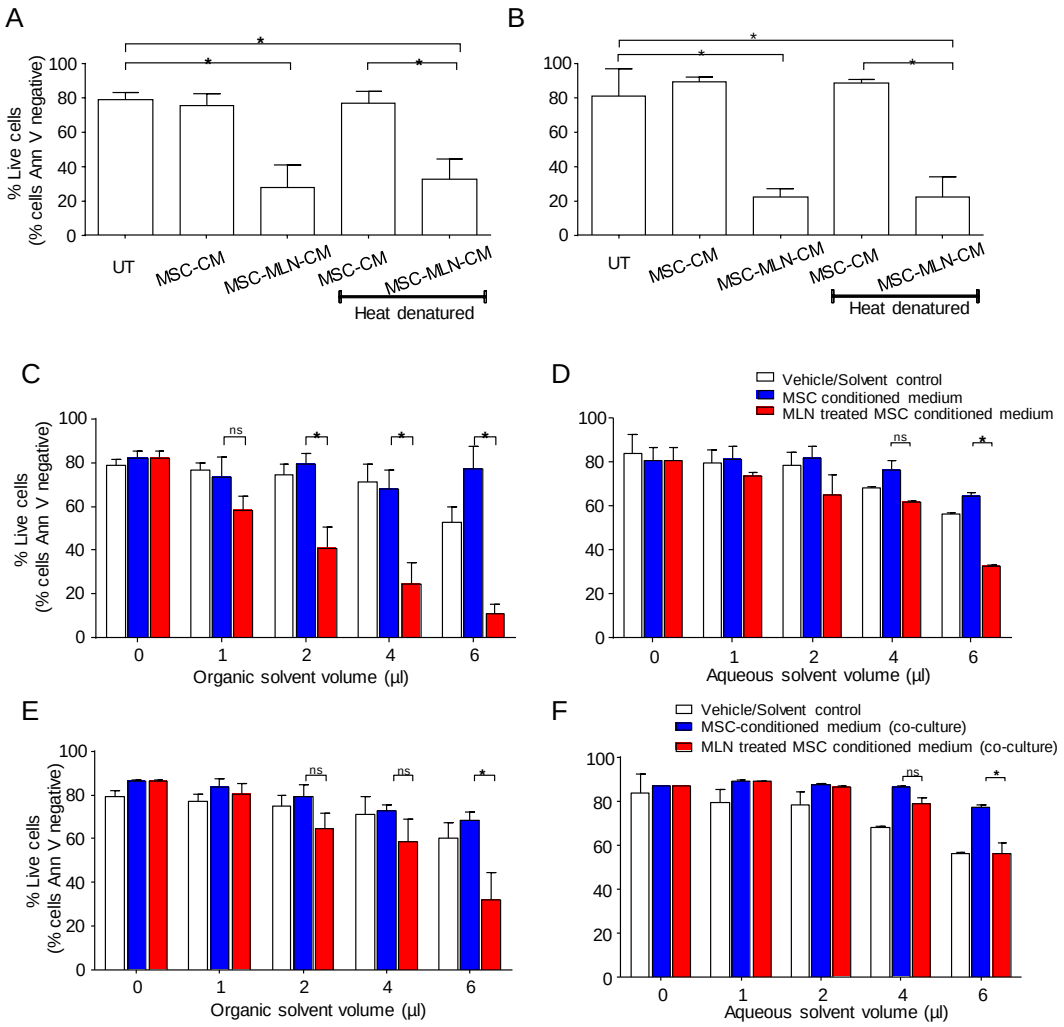

Figure 4.8: Lipids secreted by proteostatic stress conditioned stroma mediates cytotoxic effects on the residing AML cells. Conditioned medium (CM) from the bone marrow stroma (iMSC) treated with or without MLN4924 for 24 h followed by washout of drug and replaced with fresh complete growth medium was collected after 24 h of culture. CM is heat-denatured at 100oC for 10 minutes, immediately cooled on ice and centrifuged to remove protein aggregates. Molm13 cells (A) and MV4-11 (B) were then cultured with 1:1 diluted condition medium with fresh growth medium with or without heat denaturation. Cell viability was measured after 48 h of culturing using annexin V staining. Graphs showing the mean viability±std dev. (n=3). Student's t-test was applied to determine the significant differences with * p-value <0.05. A lipid extract was made by Bligh and Dyer method from the conditioned medium collected from proteostatic stress BMSC and untreated BMSCs. Lipid extracts were then dissolved in the organic solvent (CHCl3: EtOH) (C, E) and aqueous solvent (PBS+1%BSA) (D, F). Molm13 cells were cultured in the absence (C, D) or presence of stroma cells (iMSC) (E, F) and treated with varying volumes of lipid extract. Cell viability was measured after 48 h of treatment using annexin-V staining. Bar graphs showing the mean viability±std dev (n=3). Statistical significance was calculated using Student's t-test. * indicates the p-value <0.05.

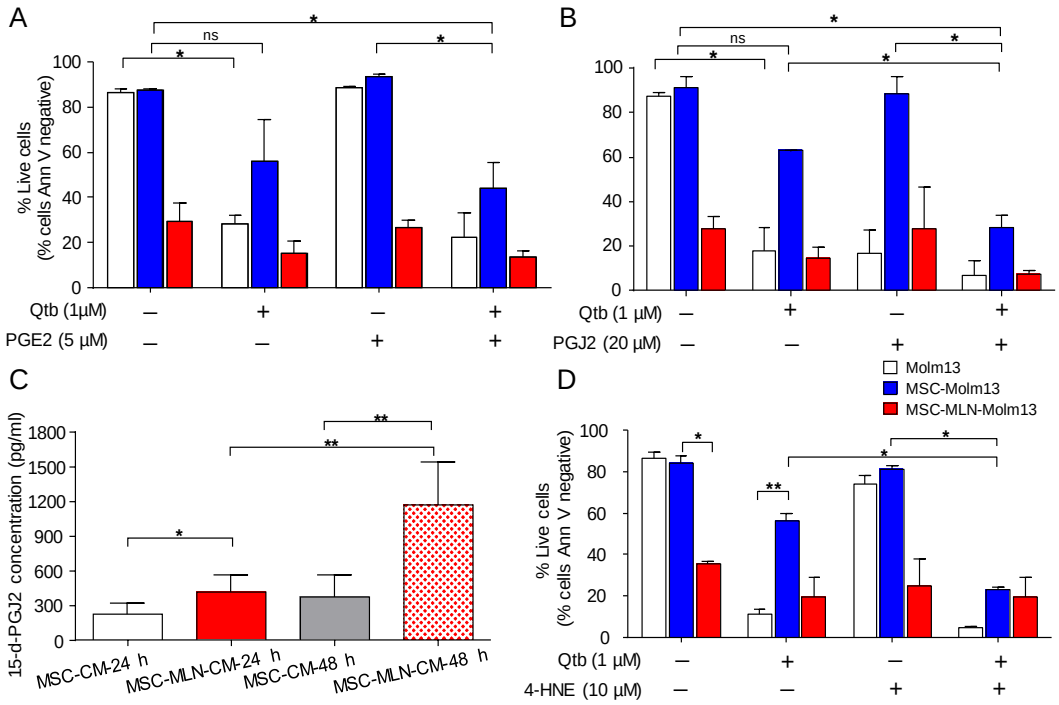

Figure 4.9: Prostaglandins and lipid peroxidation product, 4-HNE pre-treatment abolishes BMSC mediated resistance against tyrosine kinase inhibitor. Molm13-BMSC co-culture was treated with prostaglandin E2 (PGE2) (5 μM) and prostaglandin J2 (PGJ2) (20 μM) at the time of seeding AML cells over stroma. After 24 h of co-culturing cells were treated with quizartinib (1μM) with or without combination with (A) PGE2 and (B) PGJ2. Cell viability was measured after 48 h of treatment by annexin-V staining. Competitive sandwich ELISA assay (Enzo life sciences, USA) was performed to measure the levels of the oxidative product of PGJ2, 15-deoxy-$\Delta^{12,14}$-prostaglandin J2 (15-d-PGJ2). Proteostatic stress conditioned stroma (iMSC), conditioned medium was collected post 24 h and 48 h after washout of the drug. Levels of 15-d-PGJ2 were measured using four parametric logistic (4PL) method and values were plotted on a standard curve. (D) BMSC-AML co-cultures was treated with lipid peroxidation product 4-hydroxy-nonenal (4-HNE) at the time of seeding the Molm13 over stroma. Cells were then co-cultured for 24 h and followed by treatment with quizartinib in combination with or without 4-HNE. Cell viability was measured after 48 h of treatment using annexin-V staining. Graphs showing the mean viability±std dev. (n=3). Statistical significance was calculated using Student's t-test. * indicates the p-value <0.05, ** indicates p<0.005 and ns meaning non-significant.

From these findings, we know that the non-protein moiety or lipids/oxidised lipids are secreted by proteostatic stress conditioned BMSC that has a direct killing effect on the AML cells and synergised with chemotherapeutics to target AML cells. To understand the pathway through which the conditioned stroma induces cell death in AML cells, we blocked three cell death pathways- apoptosis with pan-caspase inhibitor Q-VD-OPH, necroptosis with RIPK1 inhibitor Nec1s and ferroptosis (lipid-mediated cell death pathway) with Ferrostatin-1. These inhibitors were added to the co-cultures at the time the BMSCs and AML cells (Molm-13) were combined. Cell viability was measured after 24 h and 48 h of co-culture (Figure 4.10). Treatment with Q-VD-OPH, Nec-1s and Ferrostatin-1 does not protect the AML cells from cell death induced by conditioned BMSC, but the combination of pan-caspase inhibitor Q-VD-OPH with RIPK1 inhibitor Nec-1s partially rescued the cells (Figure 4.10), suggesting the interplay between apoptotic and necroptosis cell death pathway.

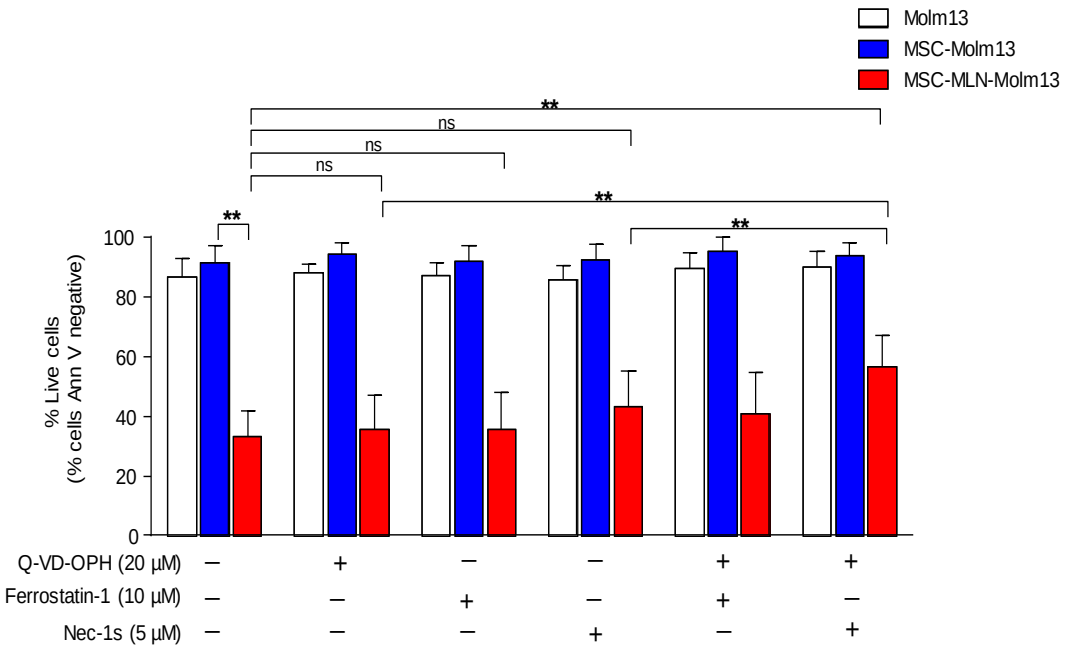

Figure 4.10: Proteostatic stress-conditioned stroma induces cell death through ripoptosome-based interface between apoptosis and necroptosis. Molm13 cells were cultured with bone marrow stroma (iMSC) conditioned with or without proteostatic stress. Pan-caspase inhibitor Q-VD-OPH, necroptosis inhibitor (RIPK1 phosphorylation), Nec1s, and Ferroptosis inhibitor, Ferrostatin-1, were introduced in the co-culture at the time of seeding of Molm13 cells over stroma either individually or in combination. Cell viability was measured using annexin-V staining after 48 h of treatment. Graphs showing the mean viability±std dev (n=3). Statistical significance was calculated using Student's t-test. * indicates the p-value <0.05, ** indicates p<0.005 and ns meaning non-significant.

4.5 Discussion

Despite the improvements made in the treatment of AML, the prognosis remains poor, with a 5-year survival rate of <20% and even higher incidences of relapse [24]. FLT3-ITD mutation is one of the most common type of mutation, occurring in about 30% of AML patients, and is associated with high-risk patient groups or poor survival [484]. FLT3-ITD patients are often associated with refractory disease and need urgent attention or new treatment strategies to target the FLT3-ITD blast population [139,489]. Inhibitors targeting FLT3 are being developed, with Midostaurin (Rydapt) from Novartis recently approved as a targeted therapy for FLT3-ITD AML patients in combination with chemotherapy [151]. Recent studies have shown that drug resistance is the major reason for treatment failure and contributes to poor survival in AML patients. One of the main reasons associated with poor response to FLT3 targeted therapies is the BMM, which provides protection to the residing AML cells against the cytotoxic effect of the drugs, thus, driving drug resistance [166,490]. The primary objective of this study was to target the AML cells in the presence of BMSCs and identify the novel candidates that could target the FLT3-ITD cells in combination with tyrosine kinase inhibitors, like sorafenib or quizartinib. Understanding the AML-BMM cross talk is essential to efficiently target the AML cells. We have shown that BMSCs provide protection to the residing FLT3-ITD AML cells against chemotherapeutics (AraC/Dnr), BH_3 mimetics and FLT3-targeting tyrosine kinase inhibitors (sorafenib and quizartinib) [419].

To design the better and effective therapies against AML, it is important to identify and target the key molecular interactions through which the BMM drives the pathogenesis. Zeng and colleagues [504] have shown that BMSCs activate various pro-survival pathways in AML cells in a contact co-culture system. Our results are also in line with the findings of Garrido and colleagues [461], that BMSCs provide protection to the residing AML cells through direct cell-cell contact and through the secretion of soluble factors. It has also been well established that cytokines or chemokines such as vascular endothelial growth factor (VEGF), fibroblast growth factor (FGF), stem cell factor-1 (SCF-1) and cell-cell signalling like C-X-C motif chemokine ligand 12 (CXCL12)- C-X-C motif receptor 4 (CXCR4), vascular cell adhesion molecule-1 (VCAM-1), E-selectin [504-507] provide protection to AML cells against chemotherapy. It has been reported that FLT3-ITD leukaemia stem/progenitor cells are better protected by bone marrow than FLT3 wild type leukaemia cells [493]. Targeting the leukemic cells or sensitizing the BMM harbouring the leukemic cells with the targeted drugs holds the key to the treatment. The findings of this study suggest that the BMSCs provide resistance to FLT3-ITD AML cells against FLT3 targeting tyrosine kinase inhibitors. This protective effect of the BMSCs is through FLT3 independent signalling pathway. We also found that the FLT3-ITD AML cells, when cultured with conditioned media from BMSC, offer the same level of resistance to tyrosine kinase inhibitors indicating that it is the paracrine factor-mediated activation of survival signalling pathways in FLT3-ITD cells. It has also been found that FLT3-ITD AML cells, when cultured with individual cytokines (IFNγ, IL-3, IL-6), offer some level of resistance to the FLT3 inhibitors. Edwards and colleagues [508] have shown that CSF1R expressing cells secretes the cytokines and chemokines which provide protection to AML cells against chemotherapeutics and targeting CSF1R can eliminate the AML cells. Traer and colleagues [509] have shown that FGF2 from BMM promotes the resistance against FLT3 inhibitor quizartinib. All these results confirm the role of paracrine signalling by BMM in driving the resistance against the FLT3 inhibitors.

We aimed to determine the signalling pathways in FLT3-ITD cells driven by BMM cytokines/chemokines and whether these pathways converge to common downstream components, which could be targeted to overcome BMSC-mediated TKI resistance. We identified the kinases in FLT3-ITD cells activated by BMSCs and found that these predominantly converged on STAT3 and PI3K signalling, the same two mediators for FLT3-signalling, providing an explanation why FLT3-ITD AML cells do not depend on FLT3 in the BMM and thus are resistant to FLT3 inhibitors. It has been shown by Sexauer and colleagues [137], and Yang and colleagues [163] that stroma-AML co-culture drives the ERK-mediated resistance to FLT3 inhibitors, and also STAT3 and STAT5 signalling has been associated in providing the resistance against FLT3 inhibitors [183,510,511]. These findings are similar to those of Wingelhofer and colleagues' study where the combination of the STAT5 inhibitor, AC-4-130, with JAK inhibitor, ruxolitinib, overcame the stroma-mediated drug resistance in the FLT3-ITD AML cells [185].

To break the stroma-AML communication that drives the cell proliferation and survival through receptor tyrosine kinase, we non-selectively targeted the BMSCs by interfering with protein degradation pathway through inhibition of neddylation using MLN4924 (NEDD8 activating enzyme inhibitor). Godbersen and colleagues have shown in CLL B-cells that the stromal cells provide resistance through activation of NF-κB pathway and Bim repression. Pre-treatment of stromal cells with MLN4924 disrupts the NF-κB activation by increasing the phospho-IκBα and induction of Bcl_2 family members towards BH_3 only proteins [512]. Kojima and colleagues have also shown that activation of p53 in BMSC by MDM2 inhibitor (Nutlin 3a) could overcome the stroma mediated drug resistance to FLT3-ITD cells by downregulating the CXCL12/CXCR4 signalling [513]. Based upon these, we tested the effect of MLN4924 in shutting down the protective effect of the stroma mediated drug resistance. We found that induction of mild proteostatic stress to BMSC abolishes their ability to support the AML cell viability and, in turn, sensitises the FLT3-ITD cells to tyrosine kinase inhibitors and AraC/Dnr treatment. This effect is not mediated through altered secretome of the conditioned BMSC nor through expression of death ligands. Proteostatic stress induces the cellular stress in BMSC through induction of FoxO3a, NF-κB, ATF4 and p53 explains the altered secretory profile of conditioned BMSC.

Transcriptome analysis revealed a novel set of enzymes, Aldo-keto reductases (AKRs), AKR1C1-C4 (hydroxysteroid dehydrogenase), which have been strongly associated with lipid/steroid conversion and drug resistance in cancer. Upregulation of AKRs indicates the role of their role in providing a drug resistance to AML cells or as a protective mechanism in AML cells cultured with proteostatic stress conditioned BMSC. AKR1C3 has been associated with blocking myeloid differentiation and promoting proliferation through PPARγ activation. AKR1C3 inhibition by MPA or Indomethacin induces differentiation [514,515]. We found that inhibition of AKR1C with MPA or 5-PBSA acts in a synergistic manner in sensitising the FLT3-ITD cells to quizartinib. These results are in line with findings of Verma and colleagues where they have shown that the inhibition of AKR1C3 by KV37 acts in a synergistic manner with etoposide and daunorubicin [516,517]. These findings indicate that AKR1C enzyme family are involved in providing drug resistance and are strongly induced in the presence of BMSCs. AKR1C enzymes are also involved in conversion of steroid hormones like prostaglandins [518]. AKR1C3 is known to catalyse the conversion of prostaglandin D2 to 15-d-PGJ2 that can induce cell death through PPARγ dependent NF-κB inhibition and ROS generation [519-521]. We found that PGE2 and PGJ2 had no direct cytotoxic effect on AML cells in the presence of BMSC, but their pre-treatment to stroma abolishes their ability to protect the AML from cytotoxic effect of tyrosine kinase inhibitors. Kim and colleagues have shown that 15-d-PGJ2 treatment inhibits the IL-6 induced activation of STAT3 signalling by PPARγ independent mechanism [522]. Blocking or activating PPARγ with small molecule inhibitor does not mimic the effect of proteostatic conditioned BMSC.

We further observed that the secretome of proteostatic stress conditioned stroma is the mediator of cell death and the candidate responsible is a heat-stable or non-protein

molecule. It has been shown that lipids can mediate cell death through lipid peroxidation products [523]. The generation of ROS can alter the lipid membrane and induce lipid peroxidation products like 4-hydroxynonenal (4-HNE) or malonaldehyde (MDA)[524]. This lipid peroxidation product can induce the apoptosis in AML cells [525]. It has been shown in K562 cells, a chronic myeloid leukemia CML) cell line, that low levels of 4-HNE decreases cell proliferation, represses the c-Myc expression and induces the differentiation [526]. Khanim and colleagues have reported that the combination of bezafibrate and MPA has anti-leukemic activity and induces an increase in ROS levels and lipid peroxidation product (4-HNE) [527]. It has been shown by Hassane and colleagues that 4-HNE can eradicate leukemic stem cells, progenitor or bulk population effectively by modulating the redox system of the AML cells [528]. All these reports provide a strong rationale that 4-HNE could be a mediator of proteostatic stress conditioned BMSC. Our results show that targeting the AML cells with 4-HNE in the presence of BMSC has no cytotoxic effect, but it abolishes the stroma mediated resistance against tyrosine kinase inhibitors. Proteostatic stress conditioned BMSC mediates cell death through programmed cell death pathways (apoptosis and necroptosis) in AML cells and potentially these pathways may shuffle through the ripoptosome.

These findings suggest a strong foundation of combining the MLN4924 which is currently being tested in phase II clinical studies as single agent against AML, MDS and ALL (NCT00911066) [529]. Also, in combination with azacitidine for elderly AML patients (Phase Ib) leading to overall response rate of 83% after 6 cycle of dosing [530]. Combining MLN4924 with induction chemotherapy (AraC+Dnr) or FLT3 targeting tyrosine kinase inhibitors (quizartinib, sorafenib or midostaurin) will benefit the AML patients.

In conclusion, the results presented here indicate that FLT3-ITD AML cells rely on alternative signalling pathways when present in BMM and mediate AML drug resistance. This study suggests that proteostatic stress to the bone marrow stroma abrogates its ability to support cell viability and drive drug resistance to AML cells.

4.6 Supplementary Figures

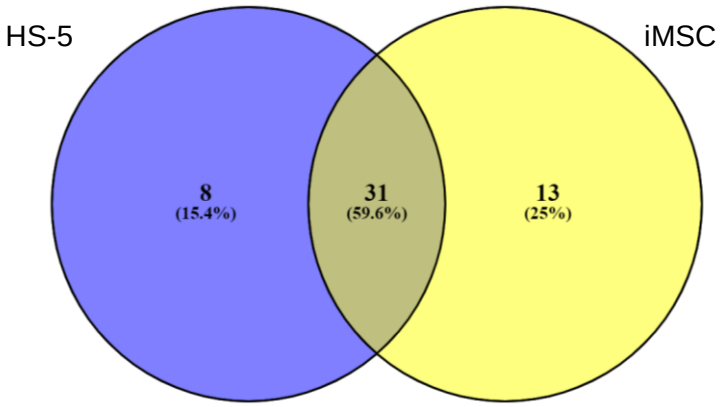

Supplementary Figure 4.1: Bone marrow stromal cells secreted cytokines and chemokines.
Venn diagram showing the commonality in the secreted cytokines/chemokines in the conditioned medium of HS-5 and iMSC as detected using proteome array.

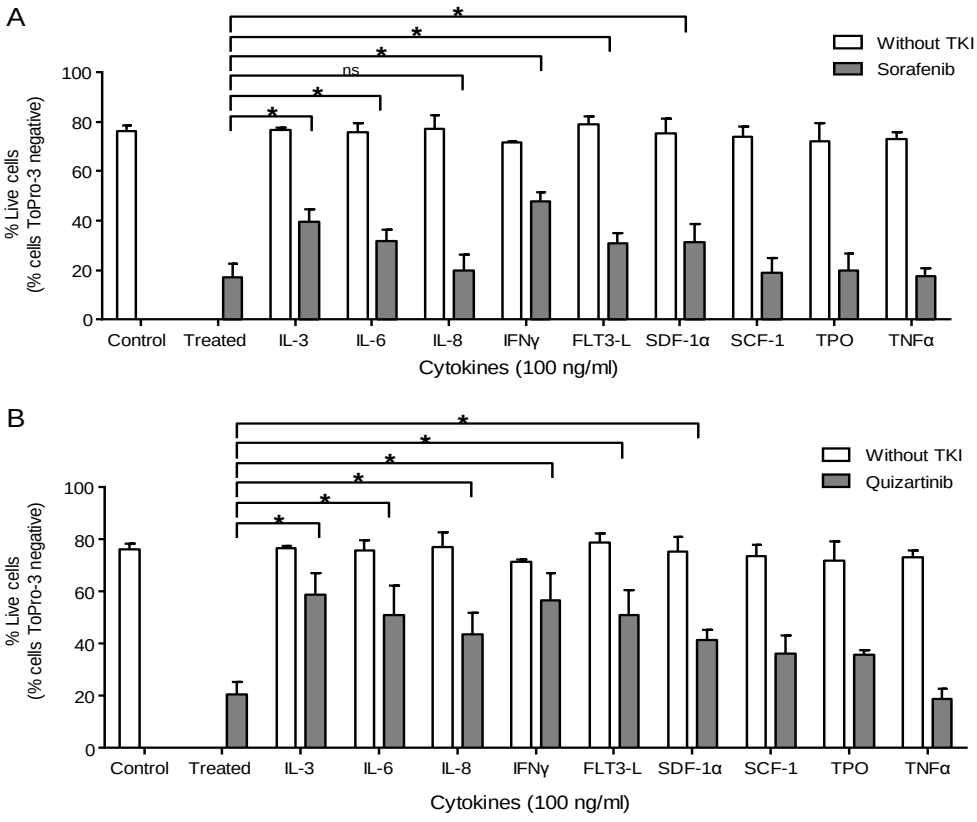

Supplementary Figure 4.2: Individual cytokines/chemokine provide resistance against the tyrosine kinase inhibitor.
Molm13 cells were cultured with 9 individual cytokines (IL-3, IL-6, IL-8, IFN-γ, FLT3-L, SDF-1α, SCF-1, TPO and TNFα, which are known to be secreted by bone marrow stromal cells for 24 h. Cells were then treated with FLT3 targeting tyrosine kinase inhibitor (A) sorafenib and (B) quizartinib. Induction of cell death was measured by ToPro-3 staining. The graph shows the average viability±std dev (n=3). Statistical significance was calculated using Student's t-test. * indicates the p-value <0.05, ** indicates p<0.005 and ns meaning non-significant.

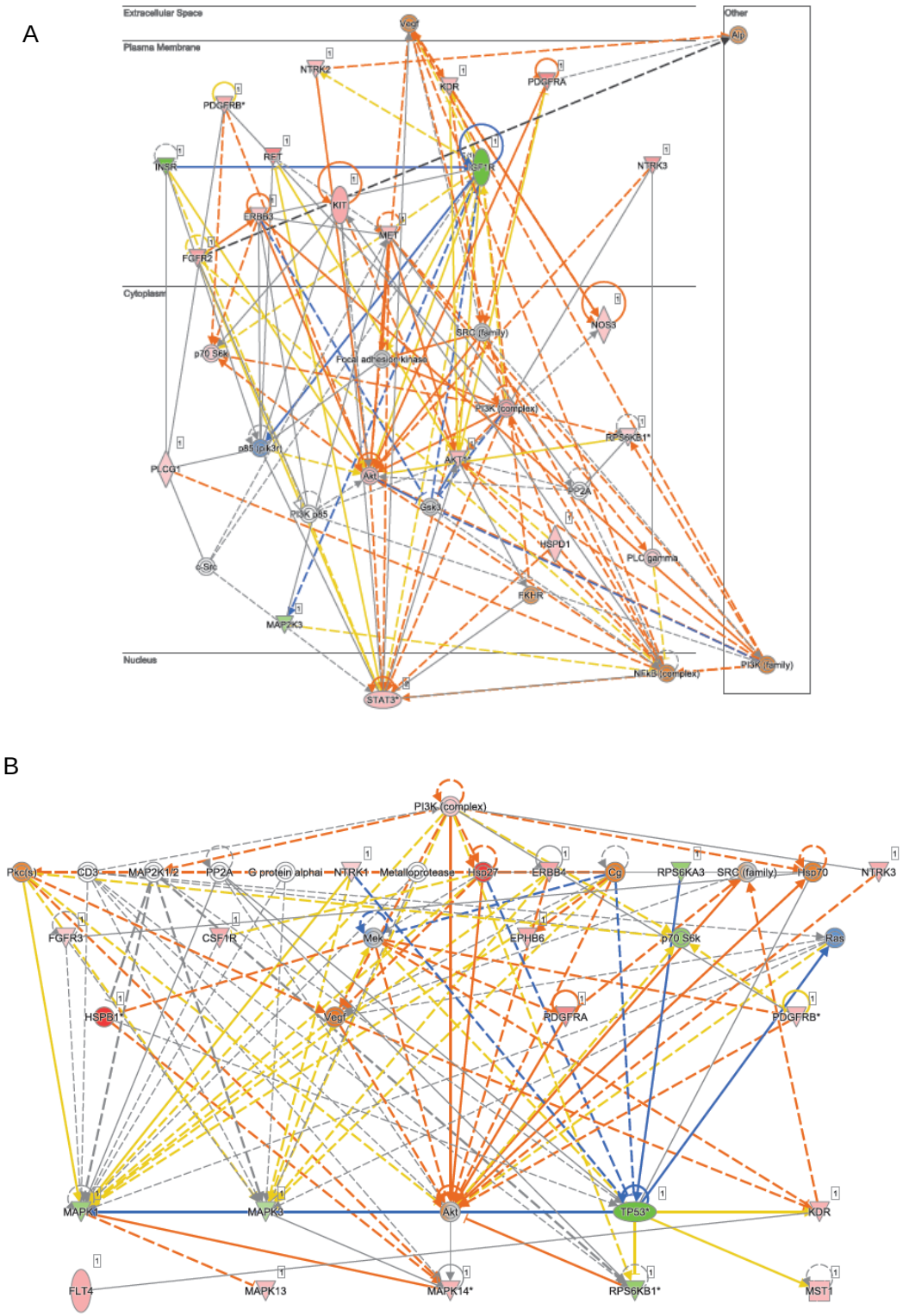

Supplementary Figure 4.3: Network analysis of activated kinases in FLT3-ITD AML cells by bone marrow stromal cells.
Molm13 cells were cultured with BMSC for 48 h in a layered co-culture system. Activation of receptor tyrosine kinases, intracellular kinases and mitogen-activated kinases were analysed using antibody array. (A) Bone marrow microenvironment induced kinase signalling network converge on to drive the STAT3 activation and (B) regulated by PI3K signalling complex.

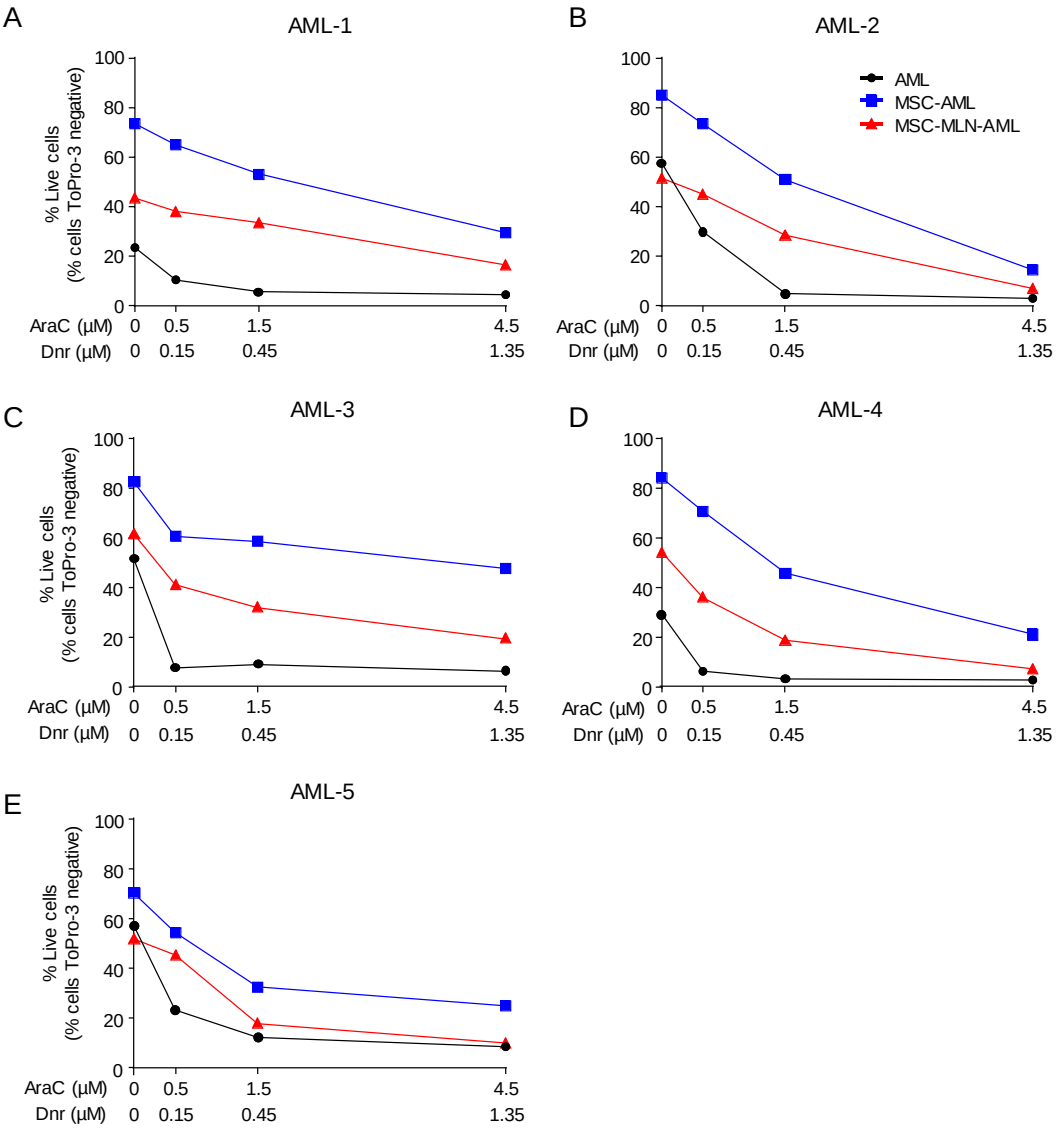

Supplementary Figure 4.4: Proteostatic stress conditioned stroma sensitised the residing AML cell to chemotherapeutics.
Primary bone marrow-derived AML mononuclear cells (MNC) from 5 patients were co-cultured with untreated stroma and proteostatic stress conditioned stroma for 24 h followed by treatment with 3:1 molar ratio of cytarabine (AraC) and daunorubicin (Dnr). Individual graphs for AML patients screened (A-E) showing the cell viability was measured after 48 h of treatment using ToPro-3 staining.

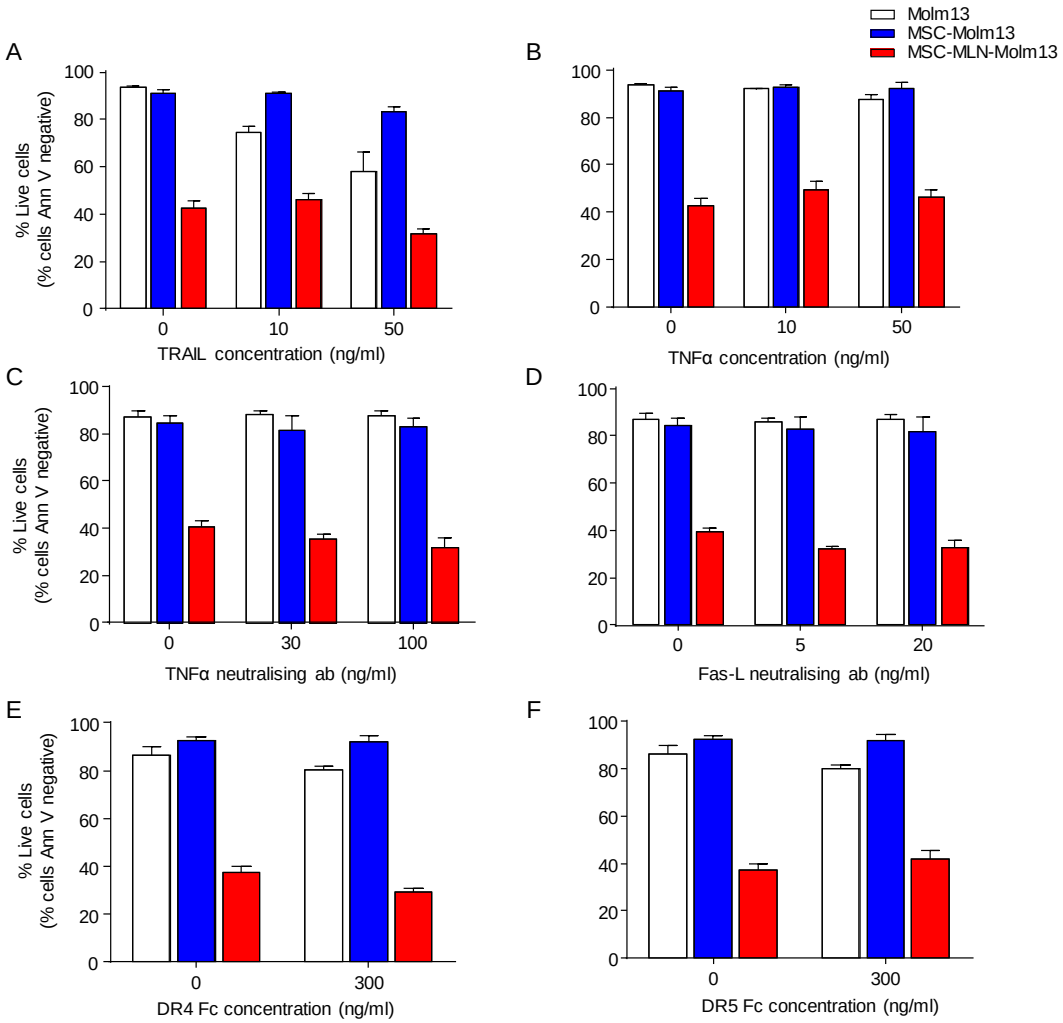

Supplementary Figure 4.5: Proteostatic stress conditioned BMSC does mediate cell death through death ligands.
BMSC-AML co-culture was treated with death ligands such as (A) tumour necrosis factor associated apoptosis-inducing ligand (TRAIL) and (B) tumour necrosis factor-alpha (TNFα) at the time of seeding Molm13 cells over proteostatic stress conditioned stroma and untreated stroma. Cell viability was measured after 48 h of co-culturing using annexin-V staining. BMSC-AML co-culture was also treated with neutralising antibodies against death ligand (C) TNFα and (D) Fas-L as well as soluble Fc protein binding to (E) death receptor- 4 (DR4) and (F) death receptor-5 (DR5). Cell viability was measured after 48 h of co-culturing using annexin-V staining. Graphs showing the average cell viability±std dev (n=3).

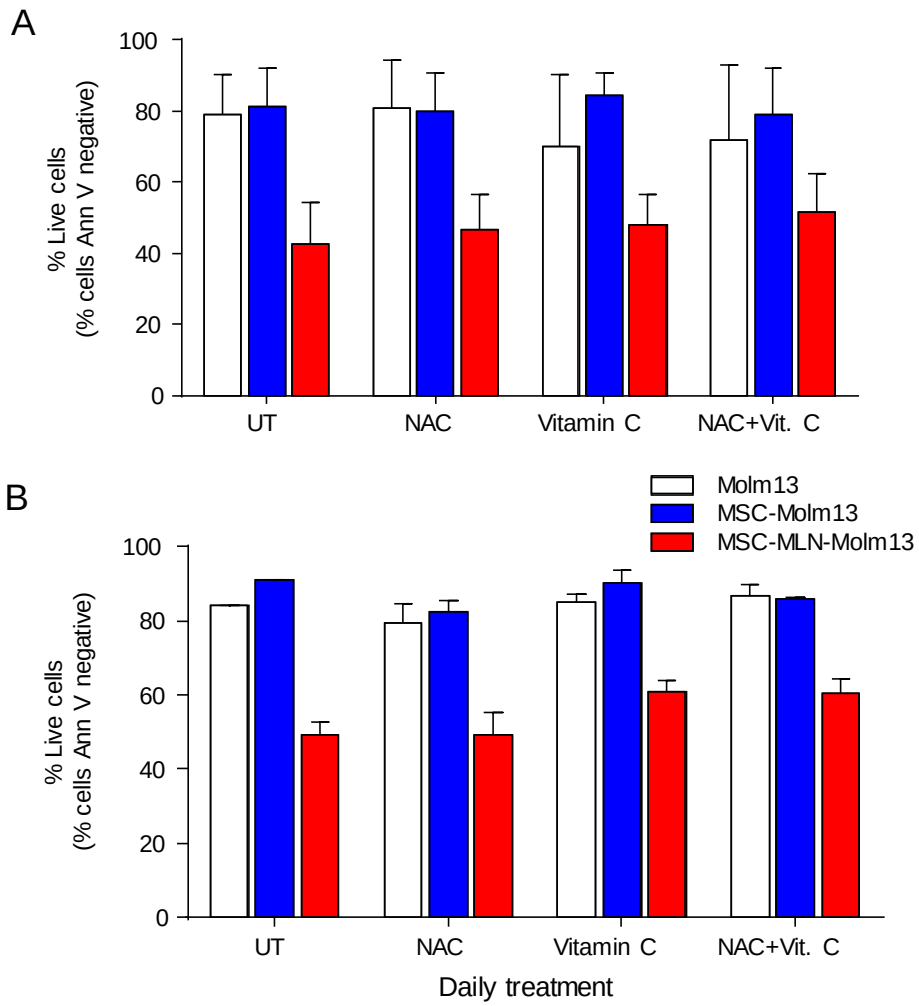

Supplementary Figure 4.6: Treatment with antioxidants does not rescue the AML cells from proteostatic stress conditioned stroma mediated cell death.
BMSC-AML co-cultures was treated with 3mM of N-acetyl cysteine (NAC) and 4 μM of vitamin C at the (A) time of seeding Molm13 over proteostatic stress conditioned stroma. (B) Antioxidants were also added daily to the BMSC-AML co-culture system. Cell viability was measured after 48 h of co-culturing using annexin-V staining. Graphs showing the average cell viability±std dev (n=3).

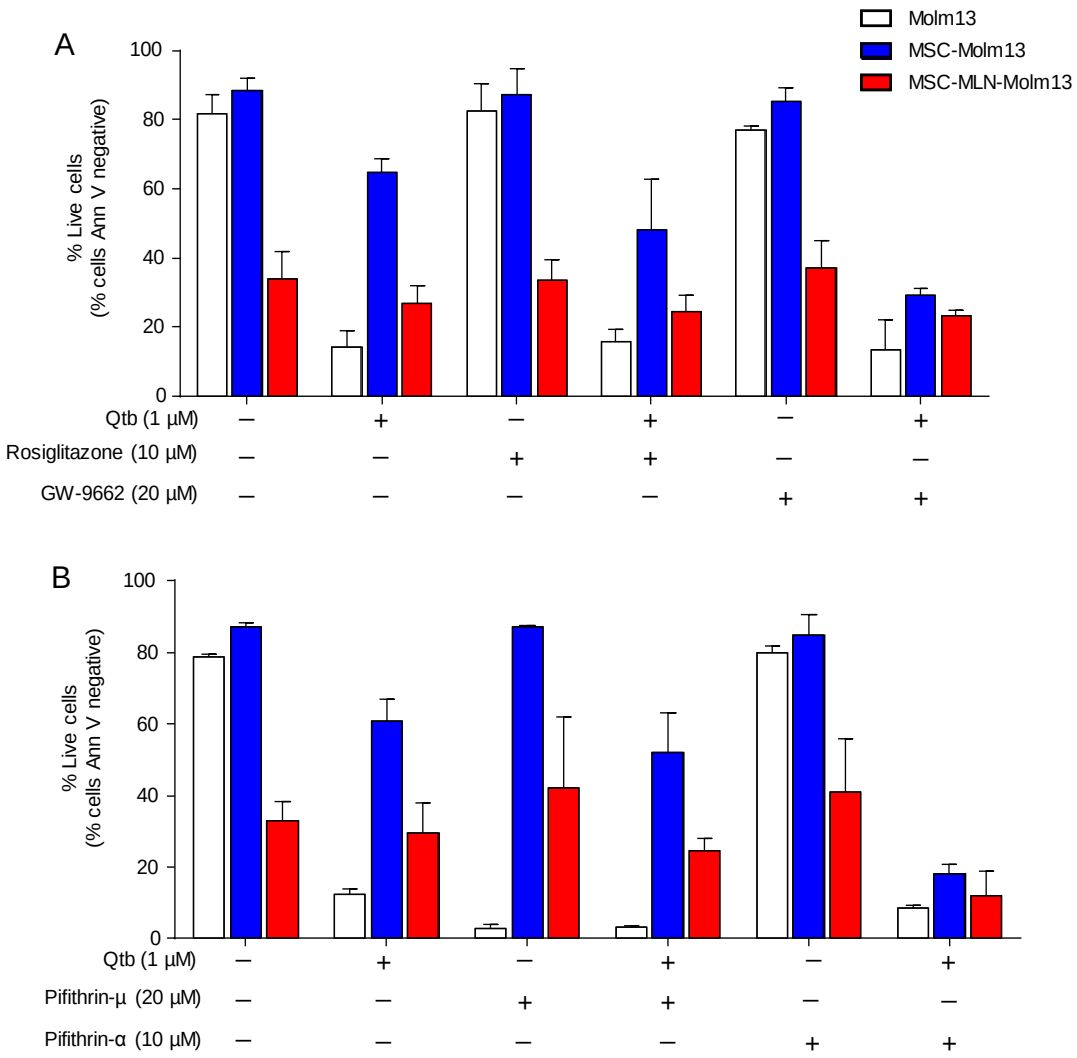

Supplementary Figure 4.7: Proteostatic stress conditioned stroma does not mediate cell death by activation of PPARγ or inhibition of p53.
BMSC-AML co-culture was treated (A) PPARγ agonist, rosiglitazone, and (B) antagonist, GW-9662, at the time of seeding Molm13 over proteostatic stress conditioned stroma for 24 h followed by treatment with quizartinib. Cell viability was measured after 48 h of treatment using annexin v staining. Inhibition of p53 activity was induced by (C) pifithrin-μ and (D) pifithrin-α in BMSC-AML co-culture at the time of seeding Molm13 over proteostatic stress conditioned stroma for 24 h followed by treatment with quizartinib. Cell viability was measured after 48 h of treatment using annexin-V staining.

4.7 Supplementary Tables

Supplementary Table 4.1: List of cytokines and chemokines secreted by HS-5 stromal cells and iMSC whose expression changes after MLN4924 treatment in the conditioned medium.

Cytokines/chemokines common between HS-5 and iMSC		
Gene ID	**Gene Symbol**	**UniProt Protein Name**
4282	MIF	Macrophage migration inhibitory factor
3589	IL11	Interleukin-11
6347	CCL2	C-C motif chemokine 2
682	BSG	Basigin
9518	GDF15	Growth/differentiation factor 15
6352	CCL5	C-C motif chemokine; C-C motif chemokine 5
9965	FGF19	Fibroblast growth factor 19
7057	THBS1	Thrombospondin-1
2022	ENG	Endoglin
6696	SPP1	Osteopontin
1440	CSF3	Granulocyte colony-stimulating factor
283	ANG	Angiogenin
5806	PTX3	Pentraxin-related protein PTX3
6387	CXCL12	Stromal cell-derived factor 1
285	ANGPT2	Angiopoietin-2
6354	CCL7	C-C motif chemokine 7
3976	LIF	Leukemia inhibitory factor
627	BDNF	Brain-derived neurotrophic factor
6364	CCL20	C-C motif chemokine 20
5329	PLAUR	Urokinase plasminogen activator surface receptor
1437	CSF2	Granulocyte-macrophage colony-stimulating factor
7422	VEGFA	Vascular endothelial growth factor A
22943	DKK1	Dickkopf-related protein 1
3627	CXCL10	C-X-C motif chemokine 10; C-X-C motif chemokine
1435	CSF1	Macrophage colony-stimulating factor 1
3569	IL6	Interleukin-6
3576	CXCL8	Interleukin-8; Multifunctional fusion protein
2919	CXCL1	Growth-regulated alpha protein
5054	SERPINE1	Plasminogen activator inhibitor 1
3605	IL17A	Interleukin-17A
1116	CHI3L1	Chitinase-3-like protein 1
Unique for HS-5		
29949	IL19	Interleukin-19
727	C5	Complement C5
1471	CST3	Cystatin; Cystatin-C
3485	IGFBP2	Insulin-like growth factor-binding protein 2
3486	IGFBP3	Insulin-like growth factor-binding protein 3
929	CD14	Monocyte differentiation antigen CD14

2323	FLT3LG	Fms-related tyrosine kinase 3 ligand
284	ANGPT1	Angiopoietin-1
Unique for iMSC		
1803	DPP4	Dipeptidyl peptidase 4
6374	CXCL5	C-X-C motif chemokine; C-X-C motif chemokine 5
354	KLK3	Prostate-specific antigen
4318	MMP9	Matrix metalloproteinase-9
2247	FGF2	Fibroblast growth factor 2
3458	IFNG	Interferon gamma
5154	PDGFA	Platelet-derived growth factor subunit A
3383	ICAM1	Intercellular adhesion molecule 1
3553	IL1B	Interleukin-1 beta
3552	IL1A	Interleukin-1 alpha
2683	B4GALT1	Beta-1,4-galactosyltransferase 1
943	TNFRSF8	Tumor necrosis factor receptor superfamily member 8
959	CD40LG	CD40 ligand

Supplementary Table 4.2: List of receptor tyrosine kinases, mitogen-activated protein kinases and intracellular phospho kinases activated in Molm13 cells upon co-culturing with proteostatic stressed stroma.

Symbol	Gene name	Phosphorylation site	Fold change
	Receptor tyrosine kinase		
5979	RET		8.91
5156	PDGFRA		8.62
2066	ERBB4		7.47
6259	RYK		6.94
4916	NTRK3		6.08
2263	FGFR2		5.22
1956	EGFR		5.18
4914	NTRK1		4.65
3815	c-KIT		4.61
2050	EPHB4		4.59
285220	EPHA6		4.52
5159	PDGFRB		4.51
4485	MST1		4.41
2321	FLT1		3.99
7010	TEK		3.97
2048	EPHB2		3.73
1436	CSF1R		3.66
2051	EPHB6		3.56
2047	EPHB1		3.54
4915	NTRKK2		3.48
2045	EPHA7		3.45
3791	VEGFR2		3.42
4233	MET		3.35
2260	FGFR1		3.24

2049	EPHB3		2.99
2065	ERBB3		2.85
2064	ERBB2		2.65
4593	MUSK		2.23
2261	FGFR3		2.00
Intracellular Phospho kinases			
6774	STAT3	S727	3.302
3329	HSPD1		2.977
6774	STAT3	Y705	2.904
4846	NOS3	S1177	2.746
65125	WNK1	T60	2.541
5335	PLCG1	Y783	2.504
6198	RPS6KB1	T421/S424	2.371
2185	PTK2B	Y402	2.275
Mitogen activated protein kinase			
6300	MAPK12	T183/Y185	6.34
5600	MAPK11	T180/Y183	4.27
1432	MAPK14	T180/Y182	4.25
207	AKT1	S473	3.74
1000	AKT3	S472	3.50
5601	MAPK9	T183/Y185	3.47
5602	MAPK10	T221/Y223	3.30
5603	MAPK13	T180/Y184	3.07
3315	HSP27	S78/S82	2.28

Supplementary Table 4.3: Combination Index calculations using Chou-Talaley method.

CI	Stattic	Idelalisib	MPA	5-BPSA	PGE2	PGJ2	4-HNE
Quizartinib (1μM)	1.25	0.01	0.007	0.019	0.6	0.76	0.2605

Supplementary Table 4.4: List of altered cytokines and chemokines secreted by HS-5 stromal cells, iMSC in the conditioned medium after induction of proteostatic stress.

Cytokines/chemokines with decreased level in HS-5		
Entrez Id	Gene Symbol	Gene Name
943	CD30/TNFRSF8	Tumor Necrosis Factor Receptor Superfamily, Member 8
1116	CHI3L1	Chitinase 3-Like 1 (Cartilage Glycoprotein-39)
3627	IP10/CXCL10	Chemokine (C-X-C Motif) Ligand 10
6354	MCP3/CCL7	Chemokine (C-C Motif) Ligand 7
6364	MIP3α/CCL20	Chemokine (C-C Motif) Ligand 20
5154	PDGFα	Platelet-Derived Growth Factor Alpha Polypeptide
6352	RANTES/CCL5	Chemokine (C-C Motif) Ligand 5
5155	PDGF-BB	Platelet-Derived Growth Factor subunit B
9173	ST2	Interleukin 1 receptor like 1
3603	IL-16	Interleukin 16
4353	MPO	Myeloperoxidase

Cytokines/chemokines with increased level in HS-5		
285	Ang-2/ANGTP2	Angiopoietin 2
627	BDNF	Brain Derived Neurotrophic Factor
1471	CST3/ARMD11	Cystatin C
1803	CD26/DPP4	Dipeptidyl-peptidase IV
2022	ENG/CD105	Endoglin
2247	FGF basic/FGF2	Fibroblast Growth Factor 2 (Basic)
9965	FGF19	Fibroblast Growth Factor 19
1440	G-CSF/CSF3	Colony Stimulating Factor 3 (Granulocyte)
9518	GDF-15/MIC1	Growth Differentiation Factor 15
3383	ICAM1/CD54	Intercellular Adhesion Molecule 1
3605	IL-17A/CTLA8	Interleukin 17A
354	KLK3/ PSA	Kallikrein
6696	OPN	Osteopontin
6019	RLN2/RLXH2	Relaxin 2
56729	RETN/FIZZ3	Resistin
6387	SDF1α/CXCL12	Chemokine (C-X-C Motif) Ligand 12
7057	TSP-1/THBS1	Thrombospondin-1
5329	uPAR/PLAUR	Plasminogen activator urokinase receptor
284	ANGPT1	Angiopoietin-1
3553	IL-1β	Interleukin 1beta
7124	TNF-α	Tumour necrosis factor alpha
9235	IL-32	Interleukin-32
Cytokines/chemokines with decreased level in iMSC		
285	Ang-2	Angiopoietin-2
727	C5/C5α	Complement component 5a
929	CD14	Myeloid Cell-Specific Leucine-Rich Glycoprotein
1116	CHI3L1/YKL-40	Chitinase 3-like 1
1471	CST3	Cystatin-c
3485	IGFBP2	Insulin Like Growth Factor Binding Protein 2
3486	IGFBP-3	Insulin Like Growth Factor Binding Protein 3
29949	IL-19	Interleukin 19
3627	IP-10/CXCL10	C-X-C motif chemokine ligand 10
6354	MCP-3/CCL7	Monocyte Chemoattractant Protein 3
3600	IL-15	Interleukin 15
7039	TGFα	Transforming Growth factor alpha
Cytokines/chemokines with increased level in iMSC		
682	EMMPRIN	CD147/Basigin
2247	FGF basic/FGF-2	Fibroblast Growth Factor 2
3552	IL-1α	Interleukin 1 alpha
3553	IL-1β	Interleukin 1 beta
9518	GDF-15	Growth Differentiation Factor 15
6696	OPN	Osteopontin
3562	IL-3	Interleukin-3

3605	IL-17A	Interleukin 17A
146433	IL-34	Interleukin-34
6348	MIP1alpha	Macrophage Inflammatory Protein 1 alpha
5154	PDGF-AA	Platelet Derived Growth Factor alpha
2252	FGF7	Fibroblast Growth Factor 7
5329	uPAR	Plasminogen Activator Urokinase Receptor
627	BDNF	Brain Derived Neurotrophic Factor
1437	GM-CSF	Granulocyte-macrophage colony stimulating factor
2919	CXCL1	C-X-C Motif Chemokine Ligand 1
1440	G-CSF	Colony Stimulating Factor 3 (Granulocyte)
1471	CST3/ARMD11	Cystatin-c

Supplementary Table 4.5: List of differentially expressed genes as identified by RNA sequencing.

Top 10 upregulated and downregulated genes in proteostatic stress conditioned BMSC and Molm13 cells co-cultured with BMSC. Genes were ranked according to fold change with cutoff of FDR (p-adjusted value) <0.03.

Differentially expressed genes in HS-5 after proteostatic stress			
GENE ID	**Gene Symbol**	**LogFC**	**P-value**
144809	FAM216B	4.653017	9.66E-05
80201	HKDC1	4.269642	5.18E-32
4602	MYB	3.55686	6.62E-05
130497	OSR1	3.548954	1.67E-12
388697	HRNR	3.480511	8.23E-13
84735	CNDP1	3.4513	1.88E-06
1646	AKR1C2	3.45021	7.4E-15
7356	SCGB1A1	3.343094	1.09E-08
6696	SPP1	3.292808	5.02E-12
1645	AKR1C1	3.094433	3.64E-13
7078	TIMP3	-3.68741	1.02E-25
115362	GBP5	-3.86785	1.49E-13
1437	CSF2	-4.14904	2.33E-19
1999	ELF3	-4.45708	2.25E-13
419	ART3	-4.49864	2.92E-45
6354	CCL7	-4.53695	4.19E-16
6347	CCL2	-4.63002	2.53E-24
1440	CSF3	-4.66082	7.09E-54
4884	NPTX1	-5.15111	3.33E-17
3569	IL6	-5.29682	4.11E-45
Differentially expressed genes in iMSC after proteostatic stress			
339416	ANKRD45	8.899202	3.86E-27
80201	HKDC1	7.848848	3.18E-26
477	ATP1A2	7.827255	6.96E-10

151176	ERFE	7.643063	3.11E-24
117156	SCGB3A2	7.153899	3.26E-19
9887	SMG7	6.878091	1.01E-24
128414	NKAIN4	6.131983	3.52E-08
1306	COL15A1	6.118322	2.64E-10
340359	KLHL38	5.821234	0.000861
2788	GNG7	5.742272	1.76E-18
10501	SEMA6B	-6.50361	0.000137
1E+08	ZBTB42	-6.64486	8.94E-05
6492	SIM1	-6.70431	2.16E-05
54873	PALMD	-6.87249	5.42E-06
130497	OSR1	-6.96549	2.07E-05
113675	SDSL	-7.08598	5.63E-05
54328	GPR173	-7.13118	5.47E-07
114794	ELFN2	-7.16379	5.11E-06
7412	VCAM1	-7.17181	4.49E-07
387914	SHISA2	-8.1627	3.12E-08
Differentially expressed genes in Molm13 after co-culture with BMSC			
7045	TGFBI	7.645583	1.16E-06
8322	FZD4	7.262119	1.49E-15
1410	CRYAB	7.255853	2.15E-07
1281	COL3A1	7.04905	5.24E-06
728137	TSPY3	6.876982	1.3E-06
1E+08	TSPY10	6.876982	1.3E-06
7168	TPM1	6.691327	1.08E-05
5361	PLXNA1	5.946596	0.000118
9832	JAKMIP2	5.67266	1.11E-13
1278	COL1A2	5.338478	3.58E-08
1277	COL1A1	5.337566	2.62E-10
10631	POSTN	4.981404	9.64E-06
7015	TERT	4.922928	9.92E-06
6678	SPARC	4.788615	4.5E-06
400999	FLJ42351	4.740649	6.61E-06
727957	MROH1	-1.28161	2.42E-05
79735	TBC1D17	-1.3216	9.18E-05
116236	ABHD15	-1.54651	0.000129
8111	GPR68	-1.71866	6.88E-05
57613	FAM234B	-2.62992	3.7E-14
Differentially expressed genes in Molm13 after co-culture with proteostatic stressed BMSC			
6696	SPP1	8.614907	3.89E-13
2831	NPBWR1	7.527909	7.75E-20
29948	OSGIN1	7.016349	1.7E-07
1410	CRYAB	6.658	6.17E-06
1645	AKR1C1	6.616032	5.34E-81

100505994	LUCAT1	6.584517	7.34E-09
1646	AKR1C2	6.496291	7.94E-71
1807	DPYS	6.346772	7.13E-20
9249	DHRS3	6.341793	3.49E-13
5361	PLXNA1	6.31027	2.3E-05
148741	ANKRD35	-3.48365	0.000808
8323	FZD6	-3.49489	3.09E-07
124056	NOXO1	-3.62751	2.38E-18
7201	TRHR	-3.71858	0.000817
51108	METTL9	-4.05156	3.45E-27
26289	AK5	-4.09717	2.93E-15
419	ART3	-4.4757	4.71E-13
677806	SNORA20	-5.14616	0.000893
100423062	IGLL5	-6.30766	0.000179
90952	ESAM	-6.36891	1.79E-06
Differentially expressed genes in Molm13 co-culture with or without proteostatic stressed BMSC			
6696	SPP1	6.825871	4.17E-12
147645	VSIG10L	6.353284	1.74E-05
1593	CYP27A1	6.251824	6.35E-06
1807	DPYS	6.012468	7.66E-19
1645	AKR1C1	5.982341	6.4E-71
1646	AKR1C2	5.924542	7.06E-63
5996	RGS1	5.645369	0.00013
1089	CEACAM4	5.56002	0.000121
5004	ORM1	5.54318	0.000122
29948	OSGIN1	5.179278	1.31E-06
130916	MTERF4	-3.16907	3.66E-09
79870	BAALC	-3.18509	2.58E-05
286676	ILDR1	-3.23526	0.000312
8323	FZD6	-3.37025	8.09E-07
9832	JAKMIP2	-3.63719	6.64E-08
4311	MME	-3.65708	0.000345
26289	AK5	-3.70836	1.47E-12
1281	COL3A1	-5.03743	0.000164
419	ART3	-5.17984	3.01E-17
90952	ESAM	-5.46016	0.000323

CHAPTER 5: *Conclusion and Future Prospects*

AML is a complex heterogeneous disease with high mortality rate. Standard treatment (7+3, cytarabine + daunorubicin) for the AML has not changed over last two decades. Advances in prognostic risk stratification of patients have helped refining the therapy, but the overall survival remains poor. Relapse has been a major issue in AML. After completion of chemotherapy, some AML cells are resistant to treatment, eventually leading to disease relapse or the onset of refractory disease. Understanding the reason for this relapse or drug resistance has strongly indicated the role of the BMM. Increasing evidence of crosstalk between the leukemic cells and the BMM has highlighted the importance of niche-derived signals which are essential for disease development. Thus, targeting these interactions may lead to new and improved AML therapy.

In this thesis, we have demonstrated that an *ex vivo* layered co-culture model of AML blasts-BMSCs can mimic the BMM and accurately predict the clinical response of patients to induction chemotherapy (AraC/Dnr). This model mimics the key features of the physiological BMM. This assay has capacity to be used as a theranostic tool in predicting the response of the patient to chemotherapy as well as finding out the suitable treatment options for which the patient will respond to. The current best prediction model based upon the genetic, epigenetic, physical status and gene expression signatures could not robustly predict the treatment response. Our assay can predict both the refractory and remission response with higher accuracy than other models. However, we could not predict the disease relapse based upon the surviving $CD34^{+}/CD38^{-}$ population. The only limitation of this co-culture system is to support the long-term hematopoietic/leukemic stem cells (LT-HSCs/LSCs) population, which are responsible for relapse. Further studies to understand the clonal heterogeneity, disease evolution and acquisition of mutations upon chemotherapy in AML blasts of patients via single-cell transcriptomics (scRNA seq) will help to identify the drug-resistant clones. This will aid in efficient treatment therapies and better help in predicting treatment outcome. Also, to test more AML patients' samples for the model validation studies and to test if this *ex vivo* layered co-culture model can predict their clinical response with high accuracy. Further studies using this *ex vivo* co-culture model in predicting the efficacy of targeted drug therapies like FLT3 inhibitors-quizartinib or BH_3 mimetics like navitoclax or venetoclax or drug combinations are recommended.

The role of the BMM in protecting the residing AML blasts against chemotherapeutics is well known. In the second study, we have also revealed that the BMM provides protection to the residing AML blasts against chemotherapeutics and BH_3 mimetics through upregulation of Mcl-1, not Bcl-2 and/or Bcl-X_L. BH_3 mimetics against Bcl-2/Bcl-X_L are known to sensitise the AML cells to chemotherapy. Targeting Mcl-1 with small molecule inhibitor, A1210477, or repression of Mcl-1 with CDC7/CDK9 inhibitor, PHA-767491, abolishes the bone marrow stroma mediated drug resistance. Repression of Mcl-1 expression sensitises the $CD34^{+}/CD38^{-}$ LSC-representative population to chemotherapeutics, thus, offering a strategy to eliminate the population responsible for relapse. We have shown that simultaneous inhibition of Bcl-2 and Mcl-1 is required to restore the drug sensitivity. In summary, the study

indicates that Bcl-2/Bcl-X_L and Mcl-1 act in a redundant fashion as effectors of BMM-mediated AML drug resistance and indicates that for BH_3-mimetic-based treatment of AML, the focus must be broadened from sole targeting of Bcl-2 to the additional inhibition or repression of Mcl-1. Venetoclax (ABT-199) has been approved by FDA in combination with azacytidine, decitabine or low dose cytarabine in newly diagnosed AML patients with age above 75 years. Venetoclax has also been approved for treatment of chronic lymphocytic leukemia (CLL) or small lymphocytic lymphoma (SLL). AML blasts and leukemic stem cells (LSCs) are shown to develop resistance against venetoclax via upregulation of Mcl-1 or alternative antiapoptotic protein like Bcl-XL. Cells can also overexpress Bcl-2 which can lead to insufficient inhibition with venetoclax leading to resistance against it [531]. Failing to inhibit Mcl-1 reduces the treatment efficacy irrespective of whether there is sufficient inhibition of Bcl-2 family antiapoptotic members [532,533]. Alteration in the Bcl-2 phosphorylation causes the conformational changes which alters the affinity of BH3 mimetics like venetoclax against it but does not affect its affinity for endogenous BH3 only family members [534]. Missense mutations in Bcl-2 has been reported to induce venetoclax resistance by altering its BH3-binding domain [535,536]. FLT3-ITD signalling is known to causes Bcl-XL and Mcl-1 upregulation in AML patients providing resistance against the venetoclax. FLT3-ITD activation mediates resistance to the BCL-2 selective antagonist, venetoclax, in FLT3-ITD mutant AML models [133,537]. Clinical response of venetoclax in combination with hypomethylating agents has shown to improve the response rate (CR/CRi) in ELN favourable group and intermediate risk group as compared to adverse group. Also, patients with poor risk cytogenetics who will not be benefited from frontline chemotherapy has shown to benefit from venetoclax and decitabine combination treatment. AML with ASXL1 and TET2 mutations has shown to respond better to the venetoclax and decitabine treatment while AML with U2AF1 mutation were completely non-responsive to treatment [538,539]. These studies provide rational for targeting Mcl-1 with small molecule inhibitor for overcoming the venetoclax or BH3 mimetics resistance. Combination of Mcl-1 and Bcl2 inhibitors can also strategically enhance the duration of response in AML patients. Characterising the BH3 mimetic dependence of AML patients prior to therapy or at the time of relapse could also lead to better designing of treatment strategies for AML.

The third study presented in this thesis shows that the BMM protects the FLT3-ITD AML cells against the cytotoxic effect of tyrosine kinase inhibitors (TKIs) through secreted paracrine factors. Which reduce the dependency of AML cells on FLT3-driven survival signalling pathways in the BMM. BMSC also activates several receptor tyrosine kinases, which converge on to STAT3 and PI3K signalling. These survival pathways are also the downstream of FLT3 signalling pathway, indicating how the FLT3-ITD cells do not depend on FLT3 signalling in BMM. To target these cells, we introduced a mild proteostatic stress to the stroma that alters the stroma-leukaemia communication. Proteostatic stress to the stroma abolishes its ability to support the AML cell viability and has a direct killing effect on the residing AML cells. This effect is mediated through the secreted factors that are non-

protein in nature (lipids or lipid peroxidation products or metabolites). Transcriptomics data has shown the up-regulation of Aldo-keto reductase C family (AKR1C) in AML cells by BMM and by inhibiting these enzymes with small molecule inhibitors, (Medroxyprogesterone or 3-Bromo-5-phenylsalicyclic acid), we can sensitise the FLT3-ITD AML cells to TKIs in the presence of BMSCs. A similar effect was also seen with lipid peroxidation product 4-hydroxynonenal (4-HNE). These combination treatment with quizartinib can definitely be beneficial for further preclinical testing in *in vivo* mouse models for FLT3-ITD driven leukemia. Quizartinib as a single drug treatment was not approved recently by FDA, but combining it with MLN4924, Prostaglandin J2, 5-BPSA/MPA and 4-HNE can greatly enhance its effect in targeting the AML cells residing in the bone marrow microenvironment. These results suggest the alternative ways through which the BMM protects the FLT3-ITD AML cells against quizartinib monotherapy. Quizartinib in combination with ADE (AraC/Daunorubicin/Etoposide) chemotherapy is being tested in phase 3 AML18 clinical trial [540]. Quizartinib in combination with azacytidine is also being tested in clinical trial [541] for newly diagnosed and relapse/refractory FLT3-ITD AML patients. Suggesting that combination of quizartinib with targeted therapy can also provide the survival benefit to AML patients. Development of prostaglandin J2, aldo-keto reductase inhibitor, 4-HNE for further pre-clinical studies in mouse models can shed a light on their further development into a clinical drug.

These results offer a novel way to target the FLT3-ITD cells in a combination therapy in the presence of BMSC. This study shows that proteostatic stress conditioned stroma alters its leukaemia-supporting function to leukaemia-rejecting function. Finding out the mediator of this effect will help in finding a novel molecule that can disrupt the stroma-leukaemia crosstalk.

Together, results from these studies highlight the role of microenvironment in disease development and driving the drug resistance against chemotherapeutics. Significantly, the work presented in this thesis indicates various strategies that can be adapted to target these interactions between leukemic cells and microenvironment. Pharmacological inhibition of these interactions by small molecules has sensitised the residing leukemic cells to chemotherapeutics, thus restoring drug sensitivity. Finally, the findings reported here can help develop novel therapeutics to efficiently target the malignantly transformed cells residing in microenvironment.

References

1. Sell S: **Leukemia: stem cells, maturation arrest, and differentiation therapy**. *Stem Cell Rev* 2005, **1**:197-205.

2. Adams GB, Scadden DT: **The hematopoietic stem cell in its place**. *Nat Immunol* 2006, **7**:333-337.

3. Akashi K, Traver D, Miyamoto T, Weissman IL: **A clonogenic common myeloid progenitor that gives rise to all myeloid lineages**. *Nature* 2000, **404**:193-197.

4. Wilson A, Laurenti E, Oser G, van der Wath RC, Blanco-Bose W, Jaworski M, Offner S, Dunant CF, Eshkind L, Bockamp E, et al.: **Hematopoietic stem cells reversibly switch from dormancy to self-renewal during homeostasis and repair**. *Cell* 2008, **135**:1118-1129.

5. Lowenberg B, Downing JR, Burnett A: **Acute myeloid leukemia**. *N Engl J Med* 1999, **341**:1051-1062.

6. Bonnet D, Dick JE: **Human acute myeloid leukemia is organized as a hierarchy that originates from a primitive hematopoietic cell**. *Nat Med* 1997, **3**:730-737.

7. Dohner H, Estey EH, Amadori S, Appelbaum FR, Buchner T, Burnett AK, Dombret H, Fenaux P, Grimwade D, Larson RA, et al.: **Diagnosis and management of acute myeloid leukemia in adults: recommendations from an international expert panel, on behalf of the European LeukemiaNet**. *Blood* 2010, **115**:453-474.

8. Institute NC: **Cancer Stat facts: Leukemia-Acute Myeloid Leukemia (AML)**. Edited by; 2019. vol 2019.]

9. Society AC: **Cancer Facts & Figures 2019**. Edited by; 2019. vol 2019.]

10. Appelbaum FR, Gundacker H, Head DR, Slovak ML, Willman CL, Godwin JE, Anderson JE, Petersdorf SH: **Age and acute myeloid leukemia**. *Blood* 2006, **107**:3481-3485.

11. Dohner H, Weisdorf DJ, Bloomfield CD: **Acute Myeloid Leukemia**. *N Engl J Med* 2015, **373**:1136-1152.

12. Krug U, Buchner T, Berdel WE, Muller-Tidow C: **The treatment of elderly patients with acute myeloid leukemia**. *Dtsch Arztebl Int* 2011, **108**:863-870.

13. Estey E, Dohner H: **Acute myeloid leukaemia**. *Lancet* 2006, **368**:1894-1907.

14. Bennett JM, Catovsky D, Daniel MT, Flandrin G, Galton DA, Gralnick HR, Sultan C: **Proposed revised criteria for the classification of acute myeloid leukemia. A report of the French-American-British Cooperative Group**. *Ann Intern Med* 1985, **103**:620-625.

15. Arber DA, Orazi A, Hasserjian R, Thiele J, Borowitz MJ, Le Beau MM, Bloomfield CD, Cazzola M, Vardiman JW: **The 2016 revision to the World Health Organization classification of myeloid neoplasms and acute leukemia**. *Blood* 2016, **127**:2391-2405.

16. DiNardo CD, Cortes JE: **Mutations in AML: prognostic and therapeutic implications**. *Hematology Am Soc Hematol Educ Program* 2016, **2016**:348-355.

17. Grove CS, Vassiliou GS: **Acute myeloid leukaemia: a paradigm for the clonal evolution of cancer?** *Dis Model Mech* 2014, **7**:941-951.

18. Parkin B, Ouillette P, Li Y, Keller J, Lam C, Roulston D, Li C, Shedden K, Malek SN: **Clonal evolution and devolution after chemotherapy in adult acute myelogenous leukemia**. *Blood* 2013, **121**:369-377.

19. Welch JS, Ley TJ, Link DC, Miller CA, Larson DE, Koboldt DC, Wartman LD, Lamprecht TL, Liu F, Xia J, et al.: **The origin and evolution of mutations in acute myeloid leukemia**. *Cell* 2012, **150**:264-278.

20. Nik-Zainal S, Van Loo P, Wedge DC, Alexandrov LB, Greenman CD, Lau KW, Raine K, Jones D, Marshall J, Ramakrishna M, et al.: **The life history of 21 breast cancers**. *Cell* 2012, **149**:994-1007.

21. Kronke J, Bullinger L, Teleanu V, Tschurtz F, Gaidzik VI, Kuhn MW, Rucker FG, Holzmann K, Paschka P, Kapp-Schworer S, et al.: **Clonal evolution in relapsed NPM1-mutated acute myeloid leukemia**. *Blood* 2013, **122**:100-108.

22. Welch JS: **Mutation position within evolutionary subclonal architecture in AML**. *Semin Hematol* 2014, **51**:273-281.

23. Gilliland DG, Griffin JD: **The roles of FLT3 in hematopoiesis and leukemia**. *Blood* 2002, **100**:1532-1542.

24. De Kouchkovsky I, Abdul-Hay M: **'Acute myeloid leukemia: a comprehensive review and 2016 update'**. *Blood Cancer J* 2016, **6**:e441.

25. Kihara R, Nagata Y, Kiyoi H, Kato T, Yamamoto E, Suzuki K, Chen F, Asou N, Ohtake S, Miyawaki S, et al.: **Comprehensive analysis of genetic alterations and their prognostic impacts in adult acute myeloid leukemia patients**. *Leukemia* 2014, **28**:1586-1595.

26. Cancer Genome Atlas Research N, Ley TJ, Miller C, Ding L, Raphael BJ, Mungall AJ, Robertson A, Hoadley K, Triche TJ, Jr., Laird PW, et al.: **Genomic and epigenomic landscapes of adult de novo acute myeloid leukemia**. *N Engl J Med* 2013, **368**:2059-2074.

27. Dombret H: **Gene mutation and AML pathogenesis**. *Blood* 2011, **118**:5366-5367.

28. Shlush LI, Zandi S, Mitchell A, Chen WC, Brandwein JM, Gupta V, Kennedy JA, Schimmer AD, Schuh AC, Yee KW, et al.: **Identification of pre-leukaemic haematopoietic stem cells in acute leukaemia**. *Nature* 2014, **506**:328-333.

29. Corces-Zimmerman MR, Hong WJ, Weissman IL, Medeiros BC, Majeti R: **Preleukemic mutations in human acute myeloid leukemia affect epigenetic regulators and persist in remission**. *Proc Natl Acad Sci U S A* 2014, **111**:2548-2553.

30. Paschka P: **Core binding factor acute myeloid leukemia**. *Semin Oncol* 2008, **35**:410-417.

31. Bullinger L, Dohner K, Bair E, Frohling S, Schlenk RF, Tibshirani R, Dohner H, Pollack JR: **Use of gene-expression profiling to identify prognostic subclasses in adult acute myeloid leukemia**. *N Engl J Med* 2004, **350**:1605-1616.

32. Valk PJ, Verhaak RG, Beijen MA, Erpelinck CA, Barjesteh van Waalwijk van Doorn-Khosrovani S, Boer JM, Beverloo HB, Moorhouse MJ, van der Spek PJ, Lowenberg B, et al.: **Prognostically useful gene-expression profiles in acute myeloid leukemia**. *N Engl J Med* 2004, **350**:1617-1628.

33. Pollard JA, Alonzo TA, Gerbing RB, Ho PA, Zeng R, Ravindranath Y, Dahl G, Lacayo NJ, Becton D, Chang M, et al.: **Prevalence and prognostic significance of KIT mutations in pediatric patients with core binding factor AML enrolled on serial pediatric cooperative trials for de novo AML**. *Blood* 2010, **115**:2372-2379.

34. Shen Y, Zhu YM, Fan X, Shi JY, Wang QR, Yan XJ, Gu ZH, Wang YY, Chen B, Jiang CL, et al.: **Gene mutation patterns and their prognostic impact in a cohort of 1185 patients with acute myeloid leukemia**. *Blood* 2011, **118**:5593-5603.

35. Ravandi F, Kantarjian H, Faderl S, Garcia-Manero G, O'Brien S, Koller C, Pierce S, Brandt M, Kennedy D, Cortes J, et al.: **Outcome of patients with FLT3-mutated acute myeloid leukemia in first relapse**. *Leuk Res* 2010, **34**:752-756.

36. Pratcorona M, Brunet S, Nomdedeu J, Ribera JM, Tormo M, Duarte R, Escoda L, Guardia R, Queipo de Llano MP, Salamero O, et al.: **Favorable outcome of patients with acute myeloid leukemia harboring a low-allelic burden FLT3-ITD mutation and concomitant NPM1 mutation: relevance to post-remission therapy**. *Blood* 2013, **121**:2734-2738.

37. Schlenk RF, Dohner K, Krauter J, Frohling S, Corbacioglu A, Bullinger L, Habdank M, Spath D, Morgan M, Benner A, et al.: **Mutations and treatment outcome in cytogenetically normal acute myeloid leukemia**. *N Engl J Med* 2008, **358**:1909-1918.

38. Kayser S, Schlenk RF, Londono MC, Breitenbuecher F, Wittke K, Du J, Groner S, Spath D, Krauter J, Ganser A, et al.: **Insertion of FLT3 internal tandem duplication in the tyrosine kinase domain-1 is associated with resistance to chemotherapy and inferior outcome**. *Blood* 2009, **114**:2386-2392.

39. Bacher U, Haferlach C, Kern W, Haferlach T, Schnittger S: **Prognostic relevance of FLT3-TKD mutations in AML: the combination matters--an analysis of 3082 patients**. *Blood* 2008, **111**:2527-2537.

40. Papaemmanuil E, Gerstung M, Bullinger L, Gaidzik VI, Paschka P, Roberts ND, Potter NE, Heuser M, Thol F, Bolli N, et al.: **Genomic Classification and Prognosis in Acute Myeloid Leukemia**. *N Engl J Med* 2016, **374**:2209-2221.

41. Meyer SC, Levine RL: **Translational implications of somatic genomics in acute myeloid leukaemia**. *Lancet Oncol* 2014, **15**:e382-394.

42. Bacher U, Haferlach T, Schoch C, Kern W, Schnittger S: **Implications of NRAS mutations in AML: a study of 2502 patients**. *Blood* 2006, **107**:3847-3853.

43. Berman JN, Gerbing RB, Alonzo TA, Ho PA, Miller K, Hurwitz C, Heerema NA, Hirsch B, Raimondi SC, Lange B, et al.: **Prevalence and clinical implications of NRAS mutations in childhood AML: a report from the Children's Oncology Group**. *Leukemia* 2011, **25**:1039-1042.

44. Liu TC, Lin PM, Chang JG, Lee JP, Chen TP, Lin SF: **Mutation analysis of PTEN/MMAC1 in acute myeloid leukemia**. *Am J Hematol* 2000, **63**:170-175.

45. Aggerholm A, Gronbaek K, Guldberg P, Hokland P: **Mutational analysis of the tumour suppressor gene MMAC1/PTEN in malignant myeloid disorders**. *Eur J Haematol* 2000, **65**:109-113.

46. Wouters BJ, Lowenberg B, Erpelinck-Verschueren CA, van Putten WL, Valk PJ, Delwel R: **Double CEBPA mutations, but not single CEBPA mutations, define a subgroup of acute myeloid leukemia with a distinctive gene expression profile that is uniquely associated with a favorable outcome**. *Blood* 2009, **113**:3088-3091.

47. Taskesen E, Bullinger L, Corbacioglu A, Sanders MA, Erpelinck CA, Wouters BJ, van der Poel-van de Luytgaarde SC, Damm F, Krauter J, Ganser A, et al.: **Prognostic impact, concurrent genetic mutations, and gene expression features of AML with CEBPA mutations in a cohort of 1182 cytogenetically normal AML patients: further evidence for CEBPA double mutant AML as a distinctive disease entity**. *Blood* 2011, **117**:2469-2475.

48. Falini B, Mecucci C, Tiacci E, Alcalay M, Rosati R, Pasqualucci L, La Starza R, Diverio D, Colombo E, Santucci A, et al.: **Cytoplasmic nucleophosmin in acute myelogenous leukemia with a normal karyotype**. *N Engl J Med* 2005, **352**:254-266.

49. Haferlach C, Mecucci C, Schnittger S, Kohlmann A, Mancini M, Cuneo A, Testoni N, Rege-Cambrin G, Santucci A, Vignetti M, et al.: **AML with mutated NPM1 carrying a normal or aberrant karyotype show overlapping biologic, pathologic, immunophenotypic, and prognostic features**. *Blood* 2009, **114**:3024-3032.

50. Chen W, Rassidakis GZ, Li J, Routbort M, Jones D, Kantarjian H, Medeiros LJ, Bueso-Ramos CE: **High frequency of NPM1 gene mutations in acute myeloid leukemia with prominent nuclear invaginations ("cuplike" nuclei)**. *Blood* 2006, **108**:1783-1784.

51. Falini B, Mecucci C, Saglio G, Lo Coco F, Diverio D, Brown P, Pane F, Mancini M, Martelli MP, Pileri S, et al.: **NPM1 mutations and cytoplasmic nucleophosmin are mutually exclusive of recurrent genetic abnormalities: a comparative analysis of 2562 patients with acute myeloid leukemia**. *Haematologica* 2008, **93**:439-442.

52. Verhaak RG, Goudswaard CS, van Putten W, Bijl MA, Sanders MA, Hugens W, Uitterlinden AG, Erpelinck CA, Delwel R, Lowenberg B, et al.: **Mutations in nucleophosmin (NPM1) in acute myeloid leukemia (AML): association with other gene abnormalities and previously established gene expression signatures and their favorable prognostic significance**. *Blood* 2005, **106**:3747-3754.

53. Grossmann V, Schnittger S, Kohlmann A, Eder C, Roller A, Dicker F, Schmid C, Wendtner CM, Staib P, Serve H, et al.: **A novel hierarchical prognostic model of AML solely based on molecular mutations**. *Blood* 2012, **120**:2963-2972.

54. Patel JP, Gonen M, Figueroa ME, Fernandez H, Sun Z, Racevskis J, Van Vlierberghe P, Dolgalev I, Thomas S, Aminova O, et al.: **Prognostic relevance of integrated genetic profiling in acute myeloid leukemia**. *N Engl J Med* 2012, **366**:1079-1089.

55. Tang JL, Hou HA, Chen CY, Liu CY, Chou WC, Tseng MH, Huang CF, Lee FY, Liu MC, Yao M, et al.: **AML1/RUNX1 mutations in 470 adult patients with de novo acute myeloid leukemia: prognostic implication and interaction with other gene alterations**. *Blood* 2009, **114**:5352-5361.

56. You E, Cho YU, Jang S, Seo EJ, Lee JH, Lee JH, Lee KH, Koh KN, Im HJ, Seo JJ, et al.: **Frequency and Clinicopathologic Features of RUNX1 Mutations in Patients With Acute Myeloid Leukemia Not Otherwise Specified**. *Am J Clin Pathol* 2017, **148**:64-72.

57. Khan M, Cortes J, Kadia T, Naqvi K, Brandt M, Pierce S, Patel KP, Borthakur G, Ravandi F, Konopleva M, et al.: **Clinical Outcomes and Co-Occurring Mutations in Patients with RUNX1-Mutated Acute Myeloid Leukemia**. *Int J Mol Sci* 2017, **18**.

58. Paschka P, Marcucci G, Ruppert AS, Whitman SP, Mrozek K, Maharry K, Langer C, Baldus CD, Zhao W, Powell BL, et al.: **Wilms' tumor 1 gene mutations independently predict poor outcome in adults with cytogenetically normal acute myeloid leukemia: a cancer and leukemia group B study**. *J Clin Oncol* 2008, **26**:4595-4602.

59. Virappane P, Gale R, Hills R, Kakkas I, Summers K, Stevens J, Allen C, Green C, Quentmeier H, Drexler H, et al.: **Mutation of the Wilms' tumor 1 gene is a poor prognostic factor associated with chemotherapy resistance in normal karyotype acute myeloid leukemia: the United Kingdom Medical Research Council Adult Leukaemia Working Party**. *J Clin Oncol* 2008, **26**:5429-5435.

60. Gaidzik VI, Schlenk RF, Moschny S, Becker A, Bullinger L, Corbacioglu A, Krauter J, Schlegelberger B, Ganser A, Dohner H, et al.: **Prognostic impact of WT1 mutations in cytogenetically normal acute myeloid leukemia: a study of the German-Austrian AML Study Group**. *Blood* 2009, **113**:4505-4511.

61. Zeichner SB, Alghamdi S, Elhammady G, Poppiti RJ: **Prognostic significance of TP53 mutations and single nucleotide polymorphisms in acute myeloid leukemia: a case series and literature review**. *Asian Pac J Cancer Prev* 2014, **15**:1603-1609.

62. Haferlach C, Dicker F, Herholz H, Schnittger S, Kern W, Haferlach T: **Mutations of the TP53 gene in acute myeloid leukemia are strongly associated with a complex aberrant karyotype**. *Leukemia* 2008, **22**:1539-1541.

63. Bowen D, Groves MJ, Burnett AK, Patel Y, Allen C, Green C, Gale RE, Hills R, Linch DC: **TP53 gene mutation is frequent in patients with acute myeloid leukemia and complex karyotype, and is associated with very poor prognosis**. *Leukemia* 2009, **23**:203-206.

64. Paschka P, Schlenk RF, Gaidzik VI, Habdank M, Kronke J, Bullinger L, Spath D, Kayser S, Zucknick M, Gotze K, et al.: **IDH1 and IDH2 mutations are frequent genetic alterations in acute myeloid leukemia and confer adverse prognosis in cytogenetically normal acute myeloid leukemia with NPM1 mutation without FLT3 internal tandem duplication**. *J Clin Oncol* 2010, **28**:3636-3643.

65. Marcucci G, Maharry K, Wu YZ, Radmacher MD, Mrozek K, Margeson D, Holland KB, Whitman SP, Becker H, Schwind S, et al.: **IDH1 and IDH2 gene mutations identify novel molecular subsets within de novo cytogenetically normal acute myeloid leukemia: a Cancer and Leukemia Group B study**. *J Clin Oncol* 2010, **28**:2348-2355.

66. Abbas S, Lugthart S, Kavelaars FG, Schelen A, Koenders JE, Zeilemaker A, van Putten WJ, Rijneveld AW, Lowenberg B, Valk PJ: **Acquired mutations in the genes encoding IDH1 and IDH2 both are recurrent aberrations in acute myeloid leukemia: prevalence and prognostic value**. *Blood* 2010, **116**:2122-2126.

67. Gaidzik VI, Paschka P, Spath D, Habdank M, Kohne CH, Germing U, von Lilienfeld-Toal M, Held G, Horst HA, Haase D, et al.: **TET2 mutations in acute myeloid leukemia (AML): results from a comprehensive genetic and clinical analysis of the AML study group**. *J Clin Oncol* 2012, **30**:1350-1357.

68. Metzeler KH, Becker H, Maharry K, Radmacher MD, Kohlschmidt J, Mrozek K, Nicolet D, Whitman SP, Wu YZ, Schwind S, et al.: **ASXL1 mutations identify a high-risk subgroup of older patients with primary cytogenetically normal AML within the ELN Favorable genetic category**. *Blood* 2011, **118**:6920-6929.

69. Tanaka S, Miyagi S, Sashida G, Chiba T, Yuan J, Mochizuki-Kashio M, Suzuki Y, Sugano S, Nakaseko C, Yokote K, et al.: **Ezh2 augments leukemogenicity by reinforcing differentiation blockage in acute myeloid leukemia**. *Blood* 2012, **120**:1107-1117.

70. Ernst T, Chase AJ, Score J, Hidalgo-Curtis CE, Bryant C, Jones AV, Waghorn K, Zoi K, Ross FM, Reiter A, et al.: **Inactivating mutations of the histone methyltransferase gene EZH2 in myeloid disorders**. *Nat Genet* 2010, **42**:722-726.

71. Winters AC, Bernt KM: **MLL-Rearranged Leukemias-An Update on Science and Clinical Approaches**. *Front Pediatr* 2017, **5**:4.

72. Lugthart S, van Drunen E, van Norden Y, van Hoven A, Erpelinck CA, Valk PJ, Beverloo HB, Lowenberg B, Delwel R: **High EVI1 levels predict adverse outcome in acute myeloid leukemia: prevalence of EVI1 overexpression and chromosome 3q26 abnormalities underestimated**. *Blood* 2008, **111**:4329-4337.

73. Groschel S, Lugthart S, Schlenk RF, Valk PJ, Eiwen K, Goudswaard C, van Putten WJ, Kayser S, Verdonck LF, Lubbert M, et al.: **High EVI1 expression predicts outcome in younger adult patients with acute myeloid leukemia and is associated with distinct cytogenetic abnormalities**. *J Clin Oncol* 2010, **28**:2101-2107.

74. Heuser M, Argiropoulos B, Kuchenbauer F, Yung E, Piper J, Fung S, Schlenk RF, Dohner K, Hinrichsen T, Rudolph C, et al.: **MN1 overexpression induces acute myeloid leukemia in mice and predicts ATRA resistance in patients with AML**. *Blood* 2007, **110**:1639-1647.

75. Langer C, Marcucci G, Holland KB, Radmacher MD, Maharry K, Paschka P, Whitman SP, Mrozek K, Baldus CD, Vij R, et al.: **Prognostic importance of MN1 transcript levels, and biologic insights from MN1-associated gene and microRNA expression signatures in cytogenetically normal acute myeloid leukemia: a cancer and leukemia group B study**. *J Clin Oncol* 2009, **27**:3198-3204.

76. Mrozek K, Marcucci G, Paschka P, Whitman SP, Bloomfield CD: **Clinical relevance of mutations and gene-expression changes in adult acute myeloid leukemia with normal cytogenetics: are we ready for a prognostically prioritized molecular classification?** *Blood* 2007, **109**:431-448.

77. Baldus CD, Tanner SM, Ruppert AS, Whitman SP, Archer KJ, Marcucci G, Caligiuri MA, Carroll AJ, Vardiman JW, Powell BL, et al.: **BAALC expression predicts clinical outcome of de novo acute myeloid leukemia patients with normal cytogenetics: a Cancer and Leukemia Group B Study**. *Blood* 2003, **102**:1613-1618.

78. Marcucci G, Maharry K, Whitman SP, Vukosavljevic T, Paschka P, Langer C, Mrozek K, Baldus CD, Carroll AJ, Powell BL, et al.: **High expression levels of the ETS-related gene, ERG, predict adverse outcome and improve molecular risk-based classification of cytogenetically normal acute myeloid leukemia: a Cancer and Leukemia Group B Study**. *J Clin Oncol* 2007, **25**:3337-3343.

79. Marcucci G, Maharry K, Radmacher MD, Mrozek K, Vukosavljevic T, Paschka P, Whitman SP, Langer C, Baldus CD, Liu CG, et al.: **Prognostic significance of, and gene and microRNA expression signatures associated with, CEBPA mutations in cytogenetically normal acute myeloid leukemia with high-risk molecular features: a Cancer and Leukemia Group B Study**. *J Clin Oncol* 2008, **26**:5078-5087.

80. Debernardi S, Skoulakis S, Molloy G, Chaplin T, Dixon-McIver A, Young BD: **MicroRNA miR-181a correlates with morphological sub-class of acute myeloid leukaemia and the expression of its target genes in global genome-wide analysis**. *Leukemia* 2007, **21**:912-916.

81. Corces MR, Chang HY, Majeti R: **Preleukemic Hematopoietic Stem Cells in Human Acute Myeloid Leukemia**. *Front Oncol* 2017, **7**:263.

82. Jan M, Chao MP, Cha AC, Alizadeh AA, Gentles AJ, Weissman IL, Majeti R: **Prospective separation of normal and leukemic stem cells based on differential expression of TIM3, a human acute myeloid leukemia stem cell marker**. *Proc Natl Acad Sci U S A* 2011, **108**:5009-5014.

83. Kikushige Y, Shima T, Takayanagi S, Urata S, Miyamoto T, Iwasaki H, Takenaka K, Teshima T, Tanaka T, Inagaki Y, et al.: **TIM-3 is a promising target to selectively kill acute myeloid leukemia stem cells**. *Cell Stem Cell* 2010, **7**:708-717.

84. Chung SS, Eng WS, Hu W, Khalaj M, Garrett-Bakelman FE, Tavakkoli M, Levine RL, Carroll M, Klimek VM, Melnick AM, et al.: **CD99 is a therapeutic target on disease stem cells in myeloid malignancies**. *Sci Transl Med* 2017, **9**.

85. Jan M, Snyder TM, Corces-Zimmerman MR, Vyas P, Weissman IL, Quake SR, Majeti R: **Clonal evolution of preleukemic hematopoietic stem cells precedes human acute myeloid leukemia**. *Sci Transl Med* 2012, **4**:149ra118.

86. Eriksson A, Lennartsson A, Lehmann S: **Epigenetic aberrations in acute myeloid leukemia: Early key events during leukemogenesis**. *Exp Hematol* 2015, **43**:609-624.

87. Sato H, Wheat JC, Steidl U, Ito K: **DNMT3A and TET2 in the Pre-Leukemic Phase of Hematopoietic Disorders**. *Front Oncol* 2016, **6**:187.

88. Chotirat S, Thongnoppakhun W, Wanachiwanawin W, Auewarakul CU: **Acquired somatic mutations of isocitrate dehydrogenases 1 and 2 (IDH1 and IDH2) in preleukemic disorders**. *Blood Cells Mol Dis* 2015, **54**:286-291.

89. Thomson HJ, Brydon WG, Obekpa PO, Smith AN: **Screening for acute pancreatitis**. *J R Coll Surg Edinb* 1987, **32**:348-351.

90. Genovese G, Kahler AK, Handsaker RE, Lindberg J, Rose SA, Bakhoum SF, Chambert K, Mick E, Neale BM, Fromer M, et al.: **Clonal hematopoiesis and blood-cancer risk inferred from blood DNA sequence**. *N Engl J Med* 2014, **371**:2477-2487.

91. Jaiswal S, Fontanillas P, Flannick J, Manning A, Grauman PV, Mar BG, Lindsley RC, Mermel CH, Burtt N, Chavez A, et al.: **Age-related clonal hematopoiesis associated with adverse outcomes**. *N Engl J Med* 2014, **371**:2488-2498.

92. Steensma DP: **Clinical consequences of clonal hematopoiesis of indeterminate potential**. *Blood Adv* 2018, **2**:3404-3410.

93. Watson CJ, Papula A, Poon YPG, Wong WH, Young AL, Druley TE, Fisher DS, Blundell JR: **The evolutionary dynamics and fitness landscape of clonal haematopoiesis**. *bioRxiv* 2019.

94. Jawhar M, Schwaab J, Schnittger S, Sotlar K, Horny HP, Metzgeroth G, Muller N, Schneider S, Naumann N, Walz C, et al.: **Molecular profiling of myeloid progenitor cells in multi-mutated advanced systemic mastocytosis identifies KIT D816V as a distinct and late event**. *Leukemia* 2015, **29**:1115-1122.

95. Itzykson R, Kosmider O, Fenaux P: **Somatic mutations and epigenetic abnormalities in myelodysplastic syndromes**. *Best Pract Res Clin Haematol* 2013, **26**:355-364.

96. Haferlach T, Nagata Y, Grossmann V, Okuno Y, Bacher U, Nagae G, Schnittger S, Sanada M, Kon A, Alpermann T, et al.: **Landscape of genetic lesions in 944 patients with myelodysplastic syndromes**. *Leukemia* 2014, **28**:241-247.

97. Makishima H, Yoshizato T, Yoshida K, Sekeres MA, Radivoyevitch T, Suzuki H, Przychodzen B, Nagata Y, Meggendorfer M, Sanada M, et al.: **Dynamics of clonal evolution in myelodysplastic syndromes**. *Nat Genet* 2017, **49**:204-212.

98. Dohner H, Estey E, Grimwade D, Amadori S, Appelbaum FR, Buchner T, Dombret H, Ebert BL, Fenaux P, Larson RA, et al.: **Diagnosis and management of AML in adults: 2017 ELN recommendations from an international expert panel**. *Blood* 2017, **129**:424-447.

99. Mrozek K, Heerema NA, Bloomfield CD: **Cytogenetics in acute leukemia**. *Blood Rev* 2004, **18**:115-136.

100. Walter RB, Othus M, Paietta EM, Racevskis J, Fernandez HF, Lee JW, Sun Z, Tallman MS, Patel J, Gonen M, et al.: **Effect of genetic profiling on prediction of therapeutic resistance and survival in adult acute myeloid leukemia**. *Leukemia* 2015, **29**:2104-2107.

101. Grimwade D, Freeman SD: **Defining minimal residual disease in acute myeloid leukemia: which platforms are ready for "prime time"?** *Blood* 2014, **124**:3345-3355.

102. Estey EH: **Acute myeloid leukemia: 2014 update on risk-stratification and management**. *Am J Hematol* 2014, **89**:1063-1081.

103. Burnett AK, Russell NH, Hills RK, Hunter AE, Kjeldsen L, Yin J, Gibson BE, Wheatley K, Milligan D: **Optimization of chemotherapy for younger patients with acute myeloid leukemia: results of the medical research council AML15 trial**. *J Clin Oncol* 2013, **31**:3360-3368.

104. Lowenberg B, Zittoun R, Kerkhofs H, Jehn U, Abels J, Debusscher L, Cauchie C, Peetermans M, Solbu G, Suciu S, et al.: **On the value of intensive remission-induction chemotherapy in elderly patients of 65+ years with acute myeloid leukemia: a randomized phase III study of the European Organization for Research and Treatment of Cancer Leukemia Group**. *J Clin Oncol* 1989, **7**:1268-1274.

105. Yanada M, Matsuo K, Emi N, Naoe T: **Efficacy of allogeneic hematopoietic stem cell transplantation depends on cytogenetic risk for acute myeloid leukemia in first disease remission: a metaanalysis**. *Cancer* 2005, **103**:1652-1658.

106. Lowenberg B: **Sense and nonsense of high-dose cytarabine for acute myeloid leukemia**. *Blood* 2013, **121**:26-28.

107. Li D, Wang L, Zhu H, Dou L, Liu D, Fu L, Ma C, Ma X, Yao Y, Zhou L, et al.: **Efficacy of Allogeneic Hematopoietic Stem Cell Transplantation in Intermediate-Risk Acute Myeloid Leukemia Adult Patients in First Complete Remission: A Meta-Analysis of Prospective Studies**. *PLoS One* 2015, **10**:e0132620.

108. Schetelig J, Schaich M, Schafer-Eckart K, Hanel M, Aulitzky WE, Einsele H, Schmitz N, Rosler W, Stelljes M, Baldus CD, et al.: **Hematopoietic cell transplantation in patients with intermediate and high-risk AML: results from the randomized Study Alliance Leukemia (SAL) AML 2003 trial**. *Leukemia* 2015, **29**:1060-1068.

109. Walter RB, Buckley SA, Pagel JM, Wood BL, Storer BE, Sandmaier BM, Fang M, Gyurkocza B, Delaney C, Radich JP, et al.: **Significance of minimal residual disease before myeloablative allogeneic hematopoietic cell transplantation for AML in first and second complete remission**. *Blood* 2013, **122**:1813-1821.

110. DiNardo CD, Cortes JE: **New treatment for acute myelogenous leukemia**. *Expert Opin Pharmacother* 2015, **16**:95-106.

111. Lin M, Chen B: **Advances in the drug therapies of acute myeloid leukemia (except acute wpromyelocytic leukemia)**. *Drug Des Devel Ther* 2018, **12**:1009-1017.

112. Grafone T, Palmisano M, Nicci C, Storti S: **An overview on the role of FLT3-tyrosine kinase receptor in acute myeloid leukemia: biology and treatment**. *Oncol Rev* 2012, **6**:e8.

113. Rosnet O, Schiff C, Pebusque MJ, Marchetto S, Tonnelle C, Toiron Y, Birg F, Birnbaum D: **Human FLT3/FLK2 gene: cDNA cloning and expression in hematopoietic cells**. *Blood* 1993, **82**:1110-1119.

114. Meshinchi S, Appelbaum FR: **Structural and functional alterations of FLT3 in acute myeloid leukemia**. *Clin Cancer Res* 2009, **15**:4263-4269.

115. Ozeki K, Kiyoi H, Hirose Y, Iwai M, Ninomiya M, Kodera Y, Miyawaki S, Kuriyama K, Shimazaki C, Akiyama H, et al.: **Biologic and clinical significance of the FLT3 transcript level in acute myeloid leukemia**. *Blood* 2004, **103**:1901-1908.

116. Stirewalt DL, Kopecky KJ, Meshinchi S, Engel JH, Pogosova-Agadjanyan EL, Linsley J, Slovak ML, Willman CL, Radich JP: **Size of FLT3 internal tandem duplication has prognostic significance in patients with acute myeloid leukemia**. *Blood* 2006, **107**:3724-3726.

117. Meshinchi S, Stirewalt DL, Alonzo TA, Zhang Q, Sweetser DA, Woods WG, Bernstein ID, Arceci RJ, Radich JP: **Activating mutations of RTK/ras signal transduction pathway in pediatric acute myeloid leukemia**. *Blood* 2003, **102**:1474-1479.

118. Kiyoi H, Towatari M, Yokota S, Hamaguchi M, Ohno R, Saito H, Naoe T: **Internal tandem duplication of the FLT3 gene is a novel modality of elongation mutation which causes constitutive activation of the product**. *Leukemia* 1998, **12**:1333-1337.

119. Kiyoi H, Ohno R, Ueda R, Saito H, Naoe T: **Mechanism of constitutive activation of FLT3 with internal tandem duplication in the juxtamembrane domain**. *Oncogene* 2002, **21**:2555-2563.

120. Hayakawa F, Towatari M, Kiyoi H, Tanimoto M, Kitamura T, Saito H, Naoe T: **Tandem-duplicated Flt3 constitutively activates STAT5 and MAP kinase and introduces autonomous cell growth in IL-3-dependent cell lines**. *Oncogene* 2000, **19**:624-631.

121. Yamamoto Y, Kiyoi H, Nakano Y, Suzuki R, Kodera Y, Miyawaki S, Asou N, Kuriyama K, Yagasaki F, Shimazaki C, et al.: **Activating mutation of D835 within the activation loop of FLT3 in human hematologic malignancies**. *Blood* 2001, **97**:2434-2439.

122. Abu-Duhier FM, Goodeve AC, Wilson GA, Care RS, Peake IR, Reilly JT: **Identification of novel FLT-3 Asp835 mutations in adult acute myeloid leukaemia**. *Br J Haematol* 2001, **113**:983-988.

123. Spiekermann K, Bagrintseva K, Schoch C, Haferlach T, Hiddemann W, Schnittger S: **A new and recurrent activating length mutation in exon 20 of the FLT3 gene in acute myeloid leukemia**. *Blood* 2002, **100**:3423-3425.

124. Griffith J, Black J, Faerman C, Swenson L, Wynn M, Lu F, Lippke J, Saxena K: **The structural basis for autoinhibition of FLT3 by the juxtamembrane domain**. *Mol Cell* 2004, **13**:169-178.

125. Schmidt-Arras D, Bohmer SA, Koch S, Muller JP, Blei L, Cornils H, Bauer R, Korasikha S, Thiede C, Bohmer FD: **Anchoring of FLT3 in the endoplasmic reticulum alters signaling quality**. *Blood* 2009, **113**:3568-3576.

126. Choudhary C, Olsen JV, Brandts C, Cox J, Reddy PN, Bohmer FD, Gerke V, Schmidt-Arras DE, Berdel WE, Muller-Tidow C, et al.: **Mislocalized activation of oncogenic RTKs switches downstream signaling outcomes**. *Mol Cell* 2009, **36**:326-339.

127. Mizuki M, Fenski R, Halfter H, Matsumura I, Schmidt R, Muller C, Gruning W, Kratz-Albers K, Serve S, Steur C, et al.: **Flt3 mutations from patients with acute myeloid leukemia induce transformation of 32D cells mediated by the Ras and STAT5 pathways**. *Blood* 2000, **96**:3907-3914.

128. Irish JM, Anensen N, Hovland R, Skavland J, Borresen-Dale AL, Bruserud O, Nolan GP, Gjertsen BT: **Flt3 Y591 duplication and Bcl-2 overexpression are detected in acute myeloid leukemia cells with high levels of phosphorylated wild-type p53**. *Blood* 2007, **109**:2589-2596.

129. Brandts CH, Sargin B, Rode M, Biermann C, Lindtner B, Schwable J, Buerger H, Muller-Tidow C, Choudhary C, McMahon M, et al.: **Constitutive activation of Akt by Flt3 internal tandem duplications is necessary for increased survival, proliferation, and myeloid transformation**. *Cancer Res* 2005, **65**:9643-9650.

130. Choudhary C, Muller-Tidow C, Berdel WE, Serve H: **Signal transduction of oncogenic Flt3**. *Int J Hematol* 2005, **82**:93-99.

131. Kim KT, Baird K, Davis S, Piloto O, Levis M, Li L, Chen P, Meltzer P, Small D: **Constitutive Fms-like tyrosine kinase 3 activation results in specific changes in gene expression in myeloid leukaemic cells**. *Br J Haematol* 2007, **138**:603-615.

132. van Lohuizen M, Verbeek S, Krimpenfort P, Domen J, Saris C, Radaszkiewicz T, Berns A: **Predisposition to lymphomagenesis in pim-1 transgenic mice: cooperation with c-myc and N-myc in murine leukemia virus-induced tumors**. *Cell* 1989, **56**:673-682.

133. Yoshimoto G, Miyamoto T, Jabbarzadeh-Tabrizi S, Iino T, Rocnik JL, Kikushige Y, Mori Y, Shima T, Iwasaki H, Takenaka K, et al.: **FLT3-ITD up-regulates MCL-1 to promote survival of stem cells in acute myeloid leukemia via FLT3-ITD-specific STAT5 activation**. *Blood* 2009, **114**:5034-5043.

134. Ding L, Ley TJ, Larson DE, Miller CA, Koboldt DC, Welch JS, Ritchey JK, Young MA, Lamprecht T, McLellan MD, et al.: **Clonal evolution in relapsed acute myeloid leukaemia revealed by whole-genome sequencing**. *Nature* 2012, **481**:506-510.

135. Grimwade D, Mrozek K: **Diagnostic and prognostic value of cytogenetics in acute myeloid leukemia**. *Hematol Oncol Clin North Am* 2011, **25**:1135-1161, vii.

136. Khaled S, Al Malki M, Marcucci G: **Acute Myeloid Leukemia: Biologic, Prognostic, and Therapeutic Insights**. *Oncology (Williston Park)* 2016, **30**:318-329.

137. Sexauer A, Perl A, Yang X, Borowitz M, Gocke C, Rajkhowa T, Thiede C, Frattini M, Nybakken GE, Pratz K, et al.: **Terminal myeloid differentiation in vivo is induced by FLT3 inhibition in FLT3/ITD AML**. *Blood* 2012, **120**:4205-4214.

138. Daver N, Cortes J, Ravandi F, Patel KP, Burger JA, Konopleva M, Kantarjian H: **Secondary mutations as mediators of resistance to targeted therapy in leukemia**. *Blood* 2015, **125**:3236-3245.

139. Daver N, Schlenk RF, Russell NH, Levis MJ: **Targeting FLT3 mutations in AML: review of current knowledge and evidence**. *Leukemia* 2019, **33**:299-312.

140. Stone RM, DeAngelo DJ, Klimek V, Galinsky I, Estey E, Nimer SD, Grandin W, Lebwohl D, Wang Y, Cohen P, et al.: **Patients with acute myeloid leukemia and an activating mutation in FLT3 respond to a small-molecule FLT3 tyrosine kinase inhibitor, PKC412**. *Blood* 2005, **105**:54-60.

141. Wander SA, Levis MJ, Fathi AT: **The evolving role of FLT3 inhibitors in acute myeloid leukemia: quizartinib and beyond**. *Ther Adv Hematol* 2014, **5**:65-77.

142. Smith BD, Levis M, Beran M, Giles F, Kantarjian H, Berg K, Murphy KM, Dauses T, Allebach J, Small D: **Single-agent CEP-701, a novel FLT3 inhibitor, shows biologic and clinical activity in patients with relapsed or refractory acute myeloid leukemia**. *Blood* 2004, **103**:3669-3676.

143. Pratz KW, Cortes J, Roboz GJ, Rao N, Arowojolu O, Stine A, Shiotsu Y, Shudo A, Akinaga S, Small D, et al.: **A pharmacodynamic study of the FLT3 inhibitor KW-2449 yields insight into the basis for clinical response**. *Blood* 2009, **113**:3938-3946.

144. Fiedler W, Kayser S, Kebenko M, Janning M, Krauter J, Schittenhelm M, Gotze K, Weber D, Gohring G, Teleanu V, et al.: **A phase I/II study of sunitinib and intensive chemotherapy in patients over 60 years of age with acute myeloid leukaemia and activating FLT3 mutations**. *Br J Haematol* 2015, **169**:694-700.

145. Rollig C, Serve H, Huttmann A, Noppeney R, Muller-Tidow C, Krug U, Baldus CD, Brandts CH, Kunzmann V, Einsele H, et al.: **Addition of sorafenib versus placebo to standard therapy in patients aged 60 years or younger with newly diagnosed acute myeloid leukaemia (SORAML): a multicentre, phase 2, randomised controlled trial**. *Lancet Oncol* 2015, **16**:1691-1699.

146. Levis M, Ravandi F, Wang ES, Baer MR, Perl A, Coutre S, Erba H, Stuart RK, Baccarani M, Cripe LD, et al.: **Results from a randomized trial of salvage chemotherapy followed by lestaurtinib for patients with FLT3 mutant AML in first relapse**. *Blood* 2011, **117**:3294-3301.

147. Fiedler W, Serve H, Dohner H, Schwittay M, Ottmann OG, O'Farrell AM, Bello CL, Allred R, Manning WC, Cherrington JM, et al.: **A phase 1 study of SU11248 in the treatment of patients with refractory or resistant acute myeloid leukemia (AML) or not amenable to conventional therapy for the disease**. *Blood* 2005, **105**:986-993.

148. Borthakur G, Kantarjian H, Ravandi F, Zhang W, Konopleva M, Wright JJ, Faderl S, Verstovsek S, Mathews S, Andreeff M, et al.: **Phase I study of sorafenib in patients with refractory or relapsed acute leukemias**. *Haematologica* 2011, **96**:62-68.

149. Serve H, Krug U, Wagner R, Sauerland MC, Heinecke A, Brunnberg U, Schaich M, Ottmann O, Duyster J, Wandt H, et al.: **Sorafenib in combination with intensive chemotherapy in elderly patients with acute myeloid leukemia: results from a randomized, placebo-controlled trial**. *J Clin Oncol* 2013, **31**:3110-3118.

150. Ravandi F, Arana Yi C, Cortes JE, Levis M, Faderl S, Garcia-Manero G, Jabbour E, Konopleva M, O'Brien S, Estrov Z, et al.: **Final report of phase II study of sorafenib, cytarabine and idarubicin for initial therapy in younger patients with acute myeloid leukemia**. *Leukemia* 2014, **28**:1543-1545.

151. Levis M: **Midostaurin approved for FLT3-mutated AML**. *Blood* 2017, **129**:3403-3406.

152. Fischer T, Stone RM, Deangelo DJ, Galinsky I, Estey E, Lanza C, Fox E, Ehninger G, Feldman EJ, Schiller GJ, et al.: **Phase IIB trial of oral Midostaurin (PKC412), the FMS-like tyrosine kinase 3 receptor (FLT3) and multi-targeted kinase inhibitor, in patients with acute myeloid leukemia and high-risk myelodysplastic syndrome with either wild-type or mutated FLT3**. *J Clin Oncol* 2010, **28**:4339-4345.

153. Perl AE, Altman JK, Cortes J, Smith C, Litzow M, Baer MR, Claxton D, Erba HP, Gill S, Goldberg S, et al.: **Selective inhibition of FLT3 by gilteritinib in relapsed or refractory acute myeloid leukaemia: a multicentre, first-in-human, open-label, phase 1-2 study**. *Lancet Oncol* 2017, **18**:1061-1075.

154. Cortes JE, Kantarjian HM, Kadia TM, Borthakur G, Konopleva M, Garcia-Manero G, Daver NG, Pemmaraju N, Jabbour E, Estrov Z, et al.: **Crenolanib besylate, a type I pan-FLT3 inhibitor, to demonstrate clinical activity in multiply relapsed FLT3-ITD and D835 AML**. *Journal of Clinical Oncology* 2016, **34**:7008-7008.

155. Gunawardane RN, Nepomuceno RR, Rooks AM, Hunt JP, Ricono JM, Belli B, Armstrong RC: **Transient exposure to quizartinib mediates sustained inhibition of FLT3 signaling while specifically inducing apoptosis in FLT3-activated leukemia cells**. *Mol Cancer Ther* 2013, **12**:438-447.

156. Cortes J, Perl AE, Dohner H, Kantarjian H, Martinelli G, Kovacsovics T, Rousselot P, Steffen B, Dombret H, Estey E, et al.: **Quizartinib, an FLT3 inhibitor, as monotherapy in patients with relapsed or refractory acute myeloid leukaemia: an open-label, multicentre, single-arm, phase 2 trial**. *Lancet Oncol* 2018, **19**:889-903.

157. Swaminathan M, Kantarjian HM, Daver N, Borthakur G, Ohanian M, Kadia T, DiNardo CD, Jain N, Estrov Z, Ferrajoli A, et al.: **The Combination of Quizartinib with Azacitidine or Low Dose Cytarabine Is Highly Active in Patients (Pts) with FLT3-ITD Mutated Myeloid Leukemias: Interim Report of a Phase I/II Trial**. *Blood* 2017, **130**:723-723.

158. Sandmaier BM, Khaled S, Oran B, Gammon G, Trone D, Frankfurt O: **Results of a phase 1 study of quizartinib as maintenance therapy in subjects with acute myeloid leukemia in remission following allogeneic hematopoietic stem cell transplant**. *Am J Hematol* 2018, **93**:222-231.

159. Inc. AP: **XOSPATA® (gilteritinib) Approved by U.S. FDA for Adult Patients with Relapsed/Refractory Acute Myeloid Leukemia (AML) with a FLT3 Mutation**. Edited by. TOKYO; 2018. vol 2019.]

160. NDA 212166 Quizartinib Applicant: Daiichi-Sankyo I: **FDA Briefing Document Oncologic Drugs Advisory Committee (ODAC) Meeting**. Edited by; 2019. vol 2019.]

161. Piloto O, Wright M, Brown P, Kim KT, Levis M, Small D: **Prolonged exposure to FLT3 inhibitors leads to resistance via activation of parallel signaling pathways**. *Blood* 2007, **109**:1643-1652.

162. Sato T, Yang X, Knapper S, White P, Smith BD, Galkin S, Small D, Burnett A, Levis M: **FLT3 ligand impedes the efficacy of FLT3 inhibitors in vitro and in vivo**. *Blood* 2011, **117**:3286-3293.

163. Yang X, Sexauer A, Levis M: **Bone marrow stroma-mediated resistance to FLT3 inhibitors in FLT3-ITD AML is mediated by persistent activation of extracellular regulated kinase**. *Br J Haematol* 2014, **164**:61-72.

164. Tsapogas P, Mooney CJ, Brown G, Rolink A: **The Cytokine Flt3-Ligand in Normal and Malignant Hematopoiesis**. *Int J Mol Sci* 2017, **18**.

165. Staudt D, Murray HC, McLachlan T, Alvaro F, Enjeti AK, Verrills NM, Dun MD: **Targeting Oncogenic Signaling in Mutant FLT3 Acute Myeloid Leukemia: The Path to Least Resistance**. *Int J Mol Sci* 2018, **19**.

166. Ghiaur G, Levis M: **Mechanisms of Resistance to FLT3 Inhibitors and the Role of the Bone Marrow Microenvironment**. *Hematol Oncol Clin North Am* 2017, **31**:681-692.

167. Dutreix C, Munarini F, Lorenzo S, Roesel J, Wang Y: **Investigation into CYP3A4-mediated drug-drug interactions on midostaurin in healthy volunteers**. *Cancer Chemother Pharmacol* 2013, **72**:1223-1234.

168. Chang YT, Hernandez D, Alonso S, Gao M, Su M, Ghiaur G, Levis MJ, Jones RJ: **Role of CYP3A4 in bone marrow microenvironment-mediated protection of FLT3/ITD AML from tyrosine kinase inhibitors**. *Blood Adv* 2019, **3**:908-916.

169. Sung PJ, Sugita M, Koblish H, Perl AE, Carroll M: **Hematopoietic cytokines mediate resistance to targeted therapy in FLT3-ITD acute myeloid leukemia**. *Blood Adv* 2019, **3**:1061-1072.

170. Heidel F, Solem FK, Breitenbuecher F, Lipka DB, Kasper S, Thiede MH, Brandts C, Serve H, Roesel J, Giles F, et al.: **Clinical resistance to the kinase inhibitor PKC412 in acute myeloid leukemia by mutation of Asn-676 in the FLT3 tyrosine kinase domain**. *Blood* 2006, **107**:293-300.

171. Smith CC, Wang Q, Chin CS, Salerno S, Damon LE, Levis MJ, Perl AE, Travers KJ, Wang S, Hunt JP, et al.: **Validation of ITD mutations in FLT3 as a therapeutic target in human acute myeloid leukaemia**. *Nature* 2012, **485**:260-263.

172. von Bubnoff N, Engh RA, Aberg E, Sanger J, Peschel C, Duyster J: **FMS-like tyrosine kinase 3-internal tandem duplication tyrosine kinase inhibitors display a nonoverlapping profile of resistance mutations in vitro**. *Cancer Res* 2009, **69**:3032-3041.

173. Lu C, Ward PS, Kapoor GS, Rohle D, Turcan S, Abdel-Wahab O, Edwards CR, Khanin R, Figueroa ME, Melnick A, et al.: **IDH mutation impairs histone demethylation and results in a block to cell differentiation**. *Nature* 2012, **483**:474-478.

174. Dang L, Jin S, Su SM: **IDH mutations in glioma and acute myeloid leukemia**. *Trends Mol Med* 2010, **16**:387-397.

175. Dang L, White DW, Gross S, Bennett BD, Bittinger MA, Driggers EM, Fantin VR, Jang HG, Jin S, Keenan MC, et al.: **Cancer-associated IDH1 mutations produce 2-hydroxyglutarate**. *Nature* 2009, **462**:739-744.

176. Ward PS, Cross JR, Lu C, Weigert O, Abel-Wahab O, Levine RL, Weinstock DM, Sharp KA, Thompson CB: **Identification of additional IDH mutations associated with oncometabolite R(-)-2-hydroxyglutarate production**. *Oncogene* 2012, **31**:2491-2498.

177. Wang F, Travins J, DeLaBarre B, Penard-Lacronique V, Schalm S, Hansen E, Straley K, Kernytsky A, Liu W, Gliser C, et al.: **Targeted inhibition of mutant IDH2 in leukemia cells induces cellular differentiation**. *Science* 2013, **340**:622-626.

178. Wang F, Travins J, Chen Y, Yang H, Straley K, Choe S, Dorsch M, Schenkein DP, Agresta S, Biller S, et al.: **AG-221 Offers a Survival Advantage In a Primary Human IDH2 Mutant AML Xenograft Model**. *Blood* 2013, **122**:240-240.

179. DiNardo CD, De Botton S, Stein EM, Roboz GJ, Mims AS, Pollyea DA, Swords RT, Altman JK, Collins RH, Mannis GN, et al.: **Ivosidenib (AG-120) in Mutant IDH1 AML and Advanced Hematologic Malignancies: Results of a Phase 1 Dose Escalation and Expansion Study**. *Blood* 2017, **130**:725-725.

180. Chan SM, Thomas D, Corces-Zimmerman MR, Xavy S, Rastogi S, Hong WJ, Zhao F, Medeiros BC, Tyvoll DA, Majeti R: **Isocitrate dehydrogenase 1 and 2 mutations induce BCL-2 dependence in acute myeloid leukemia**. *Nat Med* 2015, **21**:178-184.

181. Ragon BK, DiNardo CD: **Targeting IDH1 and IDH2 Mutations in Acute Myeloid Leukemia**. *Curr Hematol Malig Rep* 2017, **12**:537-546.

182. Rezvani K, Barrett J: **STAT3: the "Achilles" heel for AML?** *Blood* 2014, **123**:1-2.

183. Zhou J, Bi C, Janakakumara JV, Liu SC, Chng WJ, Tay KG, Poon LF, Xie Z, Palaniyandi S, Yu H, et al.: **Enhanced activation of STAT pathways and overexpression of survivin confer resistance to FLT3 inhibitors and could be therapeutic targets in AML**. *Blood* 2009, **113**:4052-4062.

184. Bar-Natan M, Nelson EA, Xiang M, Frank DA: **STAT signaling in the pathogenesis and treatment of myeloid malignancies**. *JAKSTAT* 2012, **1**:55-64.

185. Wingelhofer B, Maurer B, Heyes EC, Cumaraswamy AA, Berger-Becvar A, de Araujo ED, Orlova A, Freund P, Ruge F, Park J, et al.: **Pharmacologic inhibition of STAT5 in acute myeloid leukemia**. *Leukemia* 2018, **32**:1135-1146.

186. Kantarjian HM, Erba HP, Claxton D, Arellano M, Lyons RM, Kovascovics T, Gabrilove J, Craig M, Douer D, Maris M, et al.: **Phase II study of clofarabine monotherapy in previously untreated older adults with acute myeloid leukemia and unfavorable prognostic factors**. *J Clin Oncol* 2010, **28**:549-555.

187. Ravandi F, Ritchie EK, Sayar H, Lancet JE, Craig MD, Vey N, Strickland SA, Schiller GJ, Jabbour E, Erba HP, et al.: **Vosaroxin plus cytarabine versus placebo plus cytarabine in patients with first relapsed or refractory acute myeloid leukaemia (VALOR): a randomised, controlled, double-blind, multinational, phase 3 study**. *Lancet Oncol* 2015, **16**:1025-1036.

188. Lancet JE, Cortes JE, Hogge DE, Tallman MS, Kovacsovics TJ, Damon LE, Komrokji R, Solomon SR, Kolitz JE, Cooper M, et al.: **Phase 2 trial of CPX-351, a fixed 5:1 molar ratio of cytarabine/daunorubicin, vs cytarabine/daunorubicin in older adults with untreated AML**. *Blood* 2014, **123**:3239-3246.

189. Herman JG, Baylin SB: **Gene silencing in cancer in association with promoter hypermethylation**. *N Engl J Med* 2003, **349**:2042-2054.

190. Blagitko-Dorfs N, Schlosser P, Greve G, Pfeifer D, Meier R, Baude A, Brocks D, Plass C, Lubbert M: **Combination treatment of acute myeloid leukemia cells with DNMT and HDAC inhibitors: predominant synergistic gene downregulation associated with gene body demethylation**. *Leukemia* 2019, **33**:945-956.

191. Cooper SL, Brown PA: **Treatment of pediatric acute lymphoblastic leukemia**. *Pediatr Clin North Am* 2015, **62**:61-73.

192. Crucitti L, Crocchiolo R, Toffalori C, Mazzi B, Greco R, Signori A, Sizzano F, Chiesa L, Zino E, Lupo Stanghellini MT, et al.: **Incidence, risk factors and clinical outcome of leukemia relapses with loss of the mismatched HLA after partially incompatible hematopoietic stem cell transplantation**. *Leukemia* 2015, **29**:1143-1152.

193. Zhou H, Li Y, Liu B, Shan Y, Li Y, Zhao L, Su Z, Jia L: **Downregulation of miR-224 and let-7i contribute to cell survival and chemoresistance in chronic myeloid leukemia cells by regulating ST3GAL IV expression**. *Gene* 2017, **626**:106-118.

194. Acheampong DO, Adokoh CK, Asante DB, Asiamah EA, Barnie PA, Bonsu DOM, Kyei F: **Immunotherapy for acute myeloid leukemia (AML): a potent alternative therapy**. *Biomed Pharmacother* 2018, **97**:225-232.

195. Gangadhar TC, Vonderheide RH: **Mitigating the toxic effects of anticancer immunotherapy**. *Nat Rev Clin Oncol* 2014, **11**:91-99.

196. Saito Y, Kitamura H, Hijikata A, Tomizawa-Murasawa M, Tanaka S, Takagi S, Uchida N, Suzuki N, Sone A, Najima Y, et al.: **Identification of therapeutic targets for quiescent, chemotherapy-resistant human leukemia stem cells**. *Sci Transl Med* 2010, **2**:17ra19.

197. Maus MV, Fraietta JA, Levine BL, Kalos M, Zhao Y, June CH: **Adoptive immunotherapy for cancer or viruses**. *Annu Rev Immunol* 2014, **32**:189-225.

198. Gasiorowski RE, Clark GJ, Bradstock K, Hart DN: **Antibody therapy for acute myeloid leukaemia**. *Br J Haematol* 2014, **164**:481-495.

199. Sievers EL, Larson RA, Stadtmauer EA, Estey E, Lowenberg B, Dombret H, Karanes C, Theobald M, Bennett JM, Sherman ML, et al.: **Efficacy and safety of gemtuzumab ozogamicin in patients with CD33-positive acute myeloid leukemia in first relapse**. *J Clin Oncol* 2001, **19**:3244-3254.

200. Borthakur G, Cortes JE, Estey EE, Jabbour E, Faderl S, O'Brien S, Garcia-Manero G, Kadia TM, Wang X, Patel K, et al.: **Gemtuzumab ozogamicin with fludarabine, cytarabine, and granulocyte colony stimulating factor (FLAG-GO) as front-line regimen in patients with core binding factor acute myelogenous leukemia**. *Am J Hematol* 2014, **89**:964-968.

201. Liu Y, Bewersdorf JP, Stahl M, Zeidan AM: **Immunotherapy in acute myeloid leukemia and myelodysplastic syndromes: The dawn of a new era?** *Blood Rev* 2019, **34**:67-83.

202. Bagley CJ, Woodcock JM, Stomski FC, Lopez AF: **The structural and functional basis of cytokine receptor activation: lessons from the common beta subunit of the granulocyte-macrophage colony-stimulating factor, interleukin-3 (IL-3), and IL-5 receptors**. *Blood* 1997, **89**:1471-1482.

203. Testa U, Riccioni R, Militi S, Coccia E, Stellacci E, Samoggia P, Latagliata R, Mariani G, Rossini A, Battistini A, et al.: **Elevated expression of IL-3Ralpha in acute myelogenous leukemia is associated with enhanced blast proliferation, increased cellularity, and poor prognosis**. *Blood* 2002, **100**:2980-2988.

204. Li F, Sutherland MK, Yu C, Walter RB, Westendorf L, Valliere-Douglass J, Pan L, Cronkite A, Sussman D, Klussman K, et al.: **Characterization of SGN-CD123A, A Potent CD123-Directed Antibody-Drug Conjugate for Acute Myeloid Leukemia**. *Mol Cancer Ther* 2018, **17**:554-564.

205. Kovtun Y, Jones GE, Adams S, Harvey L, Audette CA, Wilhelm A, Bai C, Rui L, Laleau R, Liu F, et al.: **A CD123-targeting antibody-drug conjugate, IMGN632, designed to eradicate AML while sparing normal bone marrow cells**. *Blood Adv* 2018, **2**:848-858.

206. Luo Y, Chang L-J, Hu Y, Dong L, Wei G, Huang H: **First-in-Man CD123-Specific Chimeric Antigen Receptor-Modified T Cells for the Treatment of Refractory Acute Myeloid Leukemia**. *Blood* 2015, **126**:3778-3778.

207. Jetani H, Garcia-Cadenas I, Nerreter T, Thomas S, Rydzek J, Meijide JB, Bonig H, Herr W, Sierra J, Einsele H, et al.: **CAR T-cells targeting FLT3 have potent activity against FLT3(-)ITD(+) AML and act synergistically with the FLT3-inhibitor crenolanib**. *Leukemia* 2018, **32**:1168-1179.

208. Stahl M, Goldberg AD: **Immune Checkpoint Inhibitors in Acute Myeloid Leukemia: Novel Combinations and Therapeutic Targets**. *Curr Oncol Rep* 2019, **21**:37.

209. Bryan JC, Jabbour EJ: **Management of Relapsed/Refractory Acute Myeloid Leukemia in the Elderly: Current Strategies and Developments**. *Drugs Aging* 2015, **32**:623-637.

210. Zhang J, Gu Y, Chen B: **Mechanisms of drug resistance in acute myeloid leukemia**. *Onco Targets Ther* 2019, **12**:1937-1945.

211. Thomas D, Majeti R: **Biology and relevance of human acute myeloid leukemia stem cells**. *Blood* 2017, **129**:1577-1585.

212. Jordan CT, Guzman ML, Noble M: **Cancer stem cells**. *N Engl J Med* 2006, **355**:1253-1261.

213. Eppert K, Takenaka K, Lechman ER, Waldron L, Nilsson B, van Galen P, Metzeler KH, Poeppl A, Ling V, Beyene J, et al.: **Stem cell gene expression programs influence clinical outcome in human leukemia**. *Nat Med* 2011, **17**:1086-1093.

214. Levine JH, Simonds EF, Bendall SC, Davis KL, Amir el AD, Tadmor MD, Litvin O, Fienberg HG, Jager A, Zunder ER, et al.: **Data-Driven Phenotypic Dissection of AML Reveals Progenitor-like Cells that Correlate with Prognosis**. *Cell* 2015, **162**:184-197.

215. Tabe Y, Konopleva M: **Role of Microenvironment in Resistance to Therapy in AML**. *Curr Hematol Malig Rep* 2015, **10**:96-103.

216. Boyd AL, Aslostovar L, Reid J, Ye W, Tanasijevic B, Porras DP, Shapovalova Z, Almakadi M, Foley R, Leber B, et al.: **Identification of Chemotherapy-Induced Leukemic-Regenerating Cells Reveals a Transient Vulnerability of Human AML Recurrence**. *Cancer Cell* 2018, **34**:483-498 e485.

217. Ebinger S, Ozdemir EZ, Ziegenhain C, Tiedt S, Castro Alves C, Grunert M, Dworzak M, Lutz C, Turati VA, Enver T, et al.: **Characterization of Rare, Dormant, and Therapy-Resistant Cells in Acute Lymphoblastic Leukemia**. *Cancer Cell* 2016, **30**:849-862.

218. Passaro D, Di Tullio A, Abarrategi A, Rouault-Pierre K, Foster K, Ariza-McNaughton L, Montaner B, Chakravarty P, Bhaw L, Diana G, et al.: **Increased Vascular Permeability in the Bone Marrow Microenvironment Contributes to Disease Progression and Drug Response in Acute Myeloid Leukemia**. *Cancer Cell* 2017, **32**:324-341 e326.

219. Burke PJ, Karp JE, Braine HG, Vaughan WP: **Timed sequential therapy of human leukemia based upon the response of leukemic cells to humoral growth factors**. *Cancer Res* 1977, **37**:2138-2146.

220. Lane SW, Scadden DT, Gilliland DG: **The leukemic stem cell niche: current concepts and therapeutic opportunities**. *Blood* 2009, **114**:1150-1157.

221. Korn C, Mendez-Ferrer S: **Myeloid malignancies and the microenvironment**. *Blood* 2017, **129**:811-822.

222. Krause DS, Scadden DT: **A hostel for the hostile: the bone marrow niche in hematologic neoplasms**. *Haematologica* 2015, **100**:1376-1387.

223. Arai F, Suda T: **Maintenance of quiescent hematopoietic stem cells in the osteoblastic niche**. *Ann N Y Acad Sci* 2007, **1106**:41-53.

224. Arai F, Hirao A, Ohmura M, Sato H, Matsuoka S, Takubo K, Ito K, Koh GY, Suda T: **Tie2/angiopoietin-1 signaling regulates hematopoietic stem cell quiescence in the bone marrow niche**. *Cell* 2004, **118**:149-161.

225. Schepers K, Campbell TB, Passegue E: **Normal and leukemic stem cell niches: insights and therapeutic opportunities**. *Cell Stem Cell* 2015, **16**:254-267.

226. Han L, Konopleva M: **Chapter Six - Alterations of HSC Niche in Myeloid Malignancies**. In *Advances in Stem Cells and their Niches*. Edited by Bonnet D: Elsevier; 2017:123-153. vol 1.]

227. Kunisaki Y, Bruns I, Scheiermann C, Ahmed J, Pinho S, Zhang D, Mizoguchi T, Wei Q, Lucas D, Ito K, et al.: **Arteriolar niches maintain haematopoietic stem cell quiescence**. *Nature* 2013, **502**:637-643.

228. Kfoury Y, Mercier F, Scadden DT: **SnapShot: The hematopoietic stem cell niche**. *Cell* 2014, **158**:228-228 e221.

229. Semenza GL: **Oxygen-dependent regulation of mitochondrial respiration by hypoxia-inducible factor 1**. *Biochem J* 2007, **405**:1-9.

230. Lord BI, Testa NG, Hendry JH: **The relative spatial distributions of CFUs and CFUc in the normal mouse femur**. *Blood* 1975, **46**:65-72.

231. Calvi LM, Link DC: **The hematopoietic stem cell niche in homeostasis and disease**. *Blood* 2015, **126**:2443-2451.

232. Shahnazari M, Chu V, Wronski TJ, Nissenson RA, Halloran BP: **CXCL12/CXCR4 signaling in the osteoblast regulates the mesenchymal stem cell and osteoclast lineage populations**. *FASEB J* 2013, **27**:3505-3513.

233. Christopher MJ, Liu F, Hilton MJ, Long F, Link DC: **Suppression of CXCL12 production by bone marrow osteoblasts is a common and critical pathway for cytokine-induced mobilization**. *Blood* 2009, **114**:1331-1339.

234. Azizidoost S, Vijay V, Cogle CR, Khodadi E, Saki N: **The role and clinical implications of the endosteal niche and osteoblasts in regulating leukemia**. *Clin Transl Oncol* 2017, **19**:1059-1066.

235. Zhang J, Niu C, Ye L, Huang H, He X, Tong WG, Ross J, Haug J, Johnson T, Feng JQ, et al.: **Identification of the haematopoietic stem cell niche and control of the niche size**. *Nature* 2003, **425**:836-841.

236. Varnum-Finney B, Xu L, Brashem-Stein C, Nourigat C, Flowers D, Bakkour S, Pear WS, Bernstein ID: **Pluripotent, cytokine-dependent, hematopoietic stem cells are immortalized by constitutive Notch1 signaling**. *Nat Med* 2000, **6**:1278-1281.

237. Stier S, Cheng T, Dombkowski D, Carlesso N, Scadden DT: **Notch1 activation increases hematopoietic stem cell self-renewal in vivo and favors lymphoid over myeloid lineage outcome**. *Blood* 2002, **99**:2369-2378.

238. Wang W, Yu S, Zimmerman G, Wang Y, Myers J, Yu VW, Huang D, Huang X, Shim J, Huang Y, et al.: **Notch Receptor-Ligand Engagement Maintains Hematopoietic Stem Cell Quiescence and Niche Retention**. *Stem Cells* 2015, **33**:2280-2293.

239. Bowers M, Zhang B, Ho Y, Agarwal P, Chen CC, Bhatia R: **Osteoblast ablation reduces normal long-term hematopoietic stem cell self-renewal but accelerates leukemia development**. *Blood* 2015, **125**:2678-2688.

240. Nakamura Y, Arai F, Iwasaki H, Hosokawa K, Kobayashi I, Gomei Y, Matsumoto Y, Yoshihara H, Suda T: **Isolation and characterization of endosteal niche cell populations that regulate hematopoietic stem cells**. *Blood* 2010, **116**:1422-1432.

241. Stier S, Ko Y, Forkert R, Lutz C, Neuhaus T, Grunewald E, Cheng T, Dombkowski D, Calvi LM, Rittling SR, et al.: **Osteopontin is a hematopoietic stem cell niche component that negatively regulates stem cell pool size**. *J Exp Med* 2005, **201**:1781-1791.

242. Pelus LM, Horowitz D, Cooper SC, King AG: **Peripheral blood stem cell mobilization. A role for CXC chemokines**. *Crit Rev Oncol Hematol* 2002, **43**:257-275.

243. Nervi B, Link DC, DiPersio JF: **Cytokines and hematopoietic stem cell mobilization**. *J Cell Biochem* 2006, **99**:690-705.

244. Tamma R, Ribatti D: **Bone Niches, Hematopoietic Stem Cells, and Vessel Formation**. *Int J Mol Sci* 2017, **18**.

245. Semerad CL, Christopher MJ, Liu F, Short B, Simmons PJ, Winkler I, Levesque JP, Chappel J, Ross FP, Link DC: **G-CSF potently inhibits osteoblast activity and CXCL12 mRNA expression in the bone marrow**. *Blood* 2005, **106**:3020-3027.

246. Ikuta K, Weissman IL: **Evidence that hematopoietic stem cells express mouse c-kit but do not depend on steel factor for their generation**. *Proc Natl Acad Sci U S A* 1992, **89**:1502-1506.

247. Bryder D, Rossi DJ, Weissman IL: **Hematopoietic stem cells: the paradigmatic tissue-specific stem cell**. *Am J Pathol* 2006, **169**:338-346.

248. Nagasawa T: **Microenvironmental niches in the bone marrow required for B-cell development**. *Nat Rev Immunol* 2006, **6**:107-116.

249. Kusumbe AP, Ramasamy SK, Itkin T, Mae MA, Langen UH, Betsholtz C, Lapidot T, Adams RH: **Age-dependent modulation of vascular niches for haematopoietic stem cells**. *Nature* 2016, **532**:380-384.

250. Benayahu D, Akavia UD, Shur I: **Differentiation of bone marrow stroma-derived mesenchymal cells**. *Curr Med Chem* 2007, **14**:173-179.

251. Hu X, Garcia M, Weng L, Jung X, Murakami JL, Kumar B, Warden CD, Todorov I, Chen CC: **Identification of a common mesenchymal stromal progenitor for the adult haematopoietic niche**. *Nat Commun* 2016, **7**:13095.

252. Takizawa H, Regoes RR, Boddupalli CS, Bonhoeffer S, Manz MG: **Dynamic variation in cycling of hematopoietic stem cells in steady state and inflammation**. *J Exp Med* 2011, **208**:273-284.

253. Omatsu Y, Sugiyama T, Kohara H, Kondoh G, Fujii N, Kohno K, Nagasawa T: **The essential functions of adipo-osteogenic progenitors as the hematopoietic stem and progenitor cell niche**. *Immunity* 2010, **33**:387-399.

254. Itkin T, Gur-Cohen S, Spencer JA, Schajnovitz A, Ramasamy SK, Kusumbe AP, Ledergor G, Jung Y, Milo I, Poulos MG, et al.: **Distinct bone marrow blood vessels differentially regulate haematopoiesis**. *Nature* 2016, **532**:323-328.

255. Asada N, Takeishi S, Frenette PS: **Complexity of bone marrow hematopoietic stem cell niche**. *Int J Hematol* 2017, **106**:45-54.

256. Mendez-Ferrer S, Lucas D, Battista M, Frenette PS: **Haematopoietic stem cell release is regulated by circadian oscillations**. *Nature* 2008, **452**:442-447.

257. Fleming HE, Janzen V, Lo Celso C, Guo J, Leahy KM, Kronenberg HM, Scadden DT: **Wnt signaling in the niche enforces hematopoietic stem cell quiescence and is necessary to preserve self-renewal in vivo**. *Cell Stem Cell* 2008, **2**:274-283.

258. Poulos MG, Guo P, Kofler NM, Pinho S, Gutkin MC, Tikhonova A, Aifantis I, Frenette PS, Kitajewski J, Rafii S, et al.: **Endothelial Jagged-1 is necessary for homeostatic and regenerative hematopoiesis**. *Cell Rep* 2013, **4**:1022-1034.

259. Batard P, Monier MN, Fortunel N, Ducos K, Sansilvestri-Morel P, Phan T, Hatzfeld A, Hatzfeld JA: **TGF-(beta)1 maintains hematopoietic immaturity by a reversible negative control of cell cycle and induces CD34 antigen up-modulation**. *J Cell Sci* 2000, **113 (Pt 3)**:383-390.

260. Bhatia M, Bonnet D, Wu D, Murdoch B, Wrana J, Gallacher L, Dick JE: **Bone morphogenetic proteins regulate the developmental program of human hematopoietic stem cells**. *J Exp Med* 1999, **189**:1139-1148.

261. Katayama Y, Hidalgo A, Furie BC, Vestweber D, Furie B, Frenette PS: **PSGL-1 participates in E-selectin-mediated progenitor homing to bone marrow: evidence for cooperation between E-selectin ligands and alpha4 integrin**. *Blood* 2003, **102**:2060-2067.

262. Nilsson SK, Haylock DN, Johnston HM, Occhiodoro T, Brown TJ, Simmons PJ: **Hyaluronan is synthesized by primitive hemopoietic cells, participates in their lodgment at the endosteum following transplantation, and is involved in the regulation of their proliferation and differentiation in vitro**. *Blood* 2003, **101**:856-862.

263. Ye H, Adane B, Khan N, Sullivan T, Minhajuddin M, Gasparetto M, Stevens B, Pei S, Balys M, Ashton JM, et al.: **Leukemic Stem Cells Evade Chemotherapy by Metabolic Adaptation to an Adipose Tissue Niche**. *Cell Stem Cell* 2016, **19**:23-37.

264. Zhang W, Trachootham D, Liu J, Chen G, Pelicano H, Garcia-Prieto C, Lu W, Burger JA, Croce CM, Plunkett W, et al.: **Stromal control of cystine metabolism promotes cancer cell survival in chronic lymphocytic leukaemia**. *Nat Cell Biol* 2012, **14**:276-286.

265. Sison EA, McIntyre E, Magoon D, Brown P: **Dynamic chemotherapy-induced upregulation of CXCR4 expression: a mechanism of therapeutic resistance in pediatric AML**. *Mol Cancer Res* 2013, **11**:1004-1016.

266. Ishikawa F, Yoshida S, Saito Y, Hijikata A, Kitamura H, Tanaka S, Nakamura R, Tanaka T, Tomiyama H, Saito N, et al.: **Chemotherapy-resistant human AML stem cells home to and engraft within the bone-marrow endosteal region**. *Nat Biotechnol* 2007, **25**:1315-1321.

267. Costello RT, Mallet F, Gaugler B, Sainty D, Arnoulet C, Gastaut JA, Olive D: **Human acute myeloid leukemia CD34+/CD38- progenitor cells have decreased sensitivity to chemotherapy and Fas-induced apoptosis, reduced immunogenicity, and impaired dendritic cell transformation capacities**. *Cancer Res* 2000, **60**:4403-4411.

268. Sarry JE, Murphy K, Perry R, Sanchez PV, Secreto A, Keefer C, Swider CR, Strzelecki AC, Cavelier C, Recher C, et al.: **Human acute myelogenous leukemia stem cells are rare and heterogeneous when assayed in NOD/SCID/IL2Rgammac-deficient mice**. *J Clin Invest* 2011, **121**:384-395.

269. Saito Y, Uchida N, Tanaka S, Suzuki N, Tomizawa-Murasawa M, Sone A, Najima Y, Takagi S, Aoki Y, Wake A, et al.: **Induction of cell cycle entry eliminates human leukemia stem cells in a mouse model of AML**. *Nat Biotechnol* 2010, **28**:275-280.

270. Pollyea DA, Jordan CT: **Therapeutic targeting of acute myeloid leukemia stem cells**. *Blood* 2017, **129**:1627-1635.

271. Behrmann L, Wellbrock J, Fiedler W: **Acute Myeloid Leukemia and the Bone Marrow Niche-Take a Closer Look**. *Front Oncol* 2018, **8**:444.

272. Wei J, Wunderlich M, Fox C, Alvarez S, Cigudosa JC, Wilhelm JS, Zheng Y, Cancelas JA, Gu Y, Jansen M, et al.: **Microenvironment determines lineage fate in a human model of MLL-AF9 leukemia**. *Cancer Cell* 2008, **13**:483-495.

273. Blau O, Hofmann WK, Baldus CD, Thiel G, Serbent V, Schumann E, Thiel E, Blau IW: **Chromosomal aberrations in bone marrow mesenchymal stroma cells from patients with myelodysplastic syndrome and acute myeloblastic leukemia**. *Exp Hematol* 2007, **35**:221-229.

274. Huang JC, Basu SK, Zhao X, Chien S, Fang M, Oehler VG, Appelbaum FR, Becker PS: **Mesenchymal stromal cells derived from acute myeloid leukemia bone marrow exhibit aberrant cytogenetics and cytokine elaboration**. *Blood Cancer J* 2015, **5**:e302.

275. von der Heide EK, Neumann M, Vosberg S, James AR, Schroeder MP, Ortiz-Tanchez J, Isaakidis K, Schlee C, Luther M, Johrens K, et al.: **Molecular alterations in bone marrow mesenchymal stromal cells derived from acute myeloid leukemia patients**. *Leukemia* 2017, **31**:1069-1078.

276. Raaijmakers MH, Mukherjee S, Guo S, Zhang S, Kobayashi T, Schoonmaker JA, Ebert BL, Al-Shahrour F, Hasserjian RP, Scadden EO, et al.: **Bone progenitor dysfunction induces myelodysplasia and secondary leukaemia**. *Nature* 2010, **464**:852-857.

277. Kode A, Manavalan JS, Mosialou I, Bhagat G, Rathinam CV, Luo N, Khiabanian H, Lee A, Murty VV, Friedman R, et al.: **Leukaemogenesis induced by an activating beta-catenin mutation in osteoblasts**. *Nature* 2014, **506**:240-244.

278. Dong L, Yu WM, Zheng H, Loh ML, Bunting ST, Pauly M, Huang G, Zhou M, Broxmeyer HE, Scadden DT, et al.: **Leukaemogenic effects of Ptpn11 activating mutations in the stem cell microenvironment**. *Nature* 2016, **539**:304-308.

279. Le PM, Andreeff M, Battula VL: **Osteogenic niche in the regulation of normal hematopoiesis and leukemogenesis**. *Haematologica* 2018, **103**:1945-1955.

280. Barrera-Ramirez J, Lavoie JR, Maganti HB, Stanford WL, Ito C, Sabloff M, Brand M, Rosu-Myles M, Le Y, Allan DS: **Micro-RNA Profiling of Exosomes from Marrow-Derived Mesenchymal Stromal Cells in Patients with Acute Myeloid Leukemia: Implications in Leukemogenesis**. *Stem Cell Rev Rep* 2017, **13**:817-825.

281. Marlein CR, Zaitseva L, Piddock RE, Robinson SD, Edwards DR, Shafat MS, Zhou Z, Lawes M, Bowles KM, Rushworth SA: **NADPH oxidase-2 derived superoxide drives mitochondrial transfer from bone marrow stromal cells to leukemic blasts**. *Blood* 2017, **130**:1649-1660.

282. Moschoi R, Imbert V, Nebout M, Chiche J, Mary D, Prebet T, Saland E, Castellano R, Pouyet L, Collette Y, et al.: **Protective mitochondrial transfer from bone marrow stromal cells to acute myeloid leukemic cells during chemotherapy**. *Blood* 2016, **128**:253-264.

283. Flores-Figueroa E, Varma S, Montgomery K, Greenberg PL, Gratzinger D: **Distinctive contact between CD34+ hematopoietic progenitors and CXCL12+ CD271+ mesenchymal stromal cells in benign and myelodysplastic bone marrow**. *Lab Invest* 2012, **92**:1330-1341.

284. Kim JA, Shim JS, Lee GY, Yim HW, Kim TM, Kim M, Leem SH, Lee JW, Min CK, Oh IH: **Microenvironmental remodeling as a parameter and prognostic factor of heterogeneous leukemogenesis in acute myelogenous leukemia**. *Cancer Res* 2015, **75**:2222-2231.

285. Schuch G, Machluf M, Bartsch G, Jr., Nomi M, Richard H, Atala A, Soker S: **In vivo administration of vascular endothelial growth factor (VEGF) and its antagonist, soluble neuropilin-1, predicts a role of VEGF in the progression of acute myeloid leukemia in vivo**. *Blood* 2002, **100**:4622-4628.

286. Battula VL, Le PM, Sun JC, Nguyen K, Yuan B, Zhou X, Sonnylal S, McQueen T, Ruvolo V, Michel KA, et al.: **AML-induced osteogenic differentiation in mesenchymal stromal cells supports leukemia growth**. *JCI Insight* 2017, **2**.

287. Chen JY, Lai YS, Tsai HJ, Kuo CC, Yen BL, Yeh SP, Sun HS, Hung WC: **The oncometabolite R-2-hydroxyglutarate activates NF-kappaB-dependent tumor-promoting stromal niche for acute myeloid leukemia cells**. *Sci Rep* 2016, **6**:32428.

288. Chandran P, Le Y, Li Y, Sabloff M, Mehic J, Rosu-Myles M, Allan DS: **Mesenchymal stromal cells from patients with acute myeloid leukemia have altered capacity to expand differentiated hematopoietic progenitors**. *Leuk Res* 2015, **39**:486-493.

289. Geyh S, Rodriguez-Paredes M, Jager P, Khandanpour C, Cadeddu RP, Gutekunst J, Wilk CM, Fenk R, Zilkens C, Hermsen D, et al.: **Functional inhibition of mesenchymal stromal cells in acute myeloid leukemia**. *Leukemia* 2016, **30**:683-691.

290. Le Y, Fraineau S, Chandran P, Sabloff M, Brand M, Lavoie JR, Gagne R, Rosu-Myles M, Yauk CL, Richardson RB, et al.: **Adipogenic Mesenchymal Stromal Cells from Bone Marrow and Their Hematopoietic Supportive Role: Towards Understanding the Permissive Marrow Microenvironment in Acute Myeloid Leukemia**. *Stem Cell Rev Rep* 2016, **12**:235-244.

291. Binato R, de Almeida Oliveira NC, Du Rocher B, Abdelhay E: **The molecular signature of AML mesenchymal stromal cells reveals candidate genes related to the leukemogenic process**. *Cancer Lett* 2015, **369**:134-143.

292. Huan J, Hornick NI, Goloviznina NA, Kamimae-Lanning AN, David LL, Wilmarth PA, Mori T, Chevillet JR, Narla A, Roberts CT, Jr., et al.: **Coordinate regulation of residual bone marrow function by paracrine trafficking of AML exosomes**. *Leukemia* 2015, **29**:2285-2295.

293. Paggetti J, Haderk F, Seiffert M, Janji B, Distler U, Ammerlaan W, Kim YJ, Adam J, Lichter P, Solary E, et al.: **Exosomes released by chronic lymphocytic leukemia cells induce the transition of stromal cells into cancer-associated fibroblasts**. *Blood* 2015, **126**:1106-1117.

294. Lagadinou ED, Sach A, Callahan K, Rossi RM, Neering SJ, Minhajuddin M, Ashton JM, Pei S, Grose V, O'Dwyer KM, et al.: **BCL-2 inhibition targets oxidative phosphorylation and selectively eradicates quiescent human leukemia stem cells**. *Cell Stem Cell* 2013, **12**:329-341.

295. Ito K, Bernardi R, Morotti A, Matsuoka S, Saglio G, Ikeda Y, Rosenblatt J, Avigan DE, Teruya-Feldstein J, Pandolfi PP: **PML targeting eradicates quiescent leukaemia-initiating cells**. *Nature* 2008, **453**:1072-1078.

296. Zeng Z, Shi YX, Samudio IJ, Wang RY, Ling X, Frolova O, Levis M, Rubin JB, Negrin RR, Estey EH, et al.: **Targeting the leukemia microenvironment by CXCR4 inhibition overcomes resistance to kinase inhibitors and chemotherapy in AML**. *Blood* 2009, **113**:6215-6224.

297. Cho BS, Zeng Z, Mu H, Wang Z, Konoplev S, McQueen T, Protopopova M, Cortes J, Marszalek JR, Peng SB, et al.: **Antileukemia activity of the novel peptidic CXCR4 antagonist LY2510924 as monotherapy and in combination with chemotherapy**. *Blood* 2015, **126**:222-232.

298. Uy GL, Rettig MP, Motabi IH, McFarland K, Trinkaus KM, Hladnik LM, Kulkarni S, Abboud CN, Cashen AF, Stockerl-Goldstein KE, et al.: **A phase 1/2 study of chemosensitization with the CXCR4 antagonist plerixafor in relapsed or refractory acute myeloid leukemia**. *Blood* 2012, **119**:3917-3924.

299. Jin L, Hope KJ, Zhai Q, Smadja-Joffe F, Dick JE: **Targeting of CD44 eradicates human acute myeloid leukemic stem cells**. *Nat Med* 2006, **12**:1167-1174.

300. Krause DS, Lazarides K, von Andrian UH, Van Etten RA: **Requirement for CD44 in homing and engraftment of BCR-ABL-expressing leukemic stem cells**. *Nat Med* 2006, **12**:1175-1180.

301. Jacamo R, Chen Y, Wang Z, Ma W, Zhang M, Spaeth EL, Wang Y, Battula VL, Mak PY, Schallmoser K, et al.: **Reciprocal leukemia-stroma VCAM-1/VLA-4-dependent activation of NF-kappaB mediates chemoresistance**. *Blood* 2014, **123**:2691-2702.

302. Guzman ML, Rossi RM, Neelakantan S, Li X, Corbett CA, Hassane DC, Becker MW, Bennett JM, Sullivan E, Lachowicz JL, et al.: **An orally bioavailable parthenolide**

analog selectively eradicates acute myelogenous leukemia stem and progenitor cells. *Blood* 2007, **110**:4427-4435.

303. Hsieh YT, Gang EJ, Shishido SN, Kim HN, Pham J, Khazal S, Osborne A, Esguerra ZA, Kwok E, Jang J, et al.: **Effects of the small-molecule inhibitor of integrin alpha4, TBC3486, on pre-B-ALL cells**. *Leukemia* 2014, **28**:2101-2104.

304. Liesveld JL, Rosell KE, Lu C, Bechelli J, Phillips G, Lancet JE, Abboud CN: **Acute myelogenous leukemia--microenvironment interactions: role of endothelial cells and proteasome inhibition**. *Hematology* 2005, **10**:483-494.

305. Romanski A, Schwarz K, Keller M, Wietbrauk S, Vogel A, Roos J, Oancea C, Brill B, Kramer OH, Serve H, et al.: **Deacetylase inhibitors modulate proliferation and self-renewal properties of leukemic stem and progenitor cells**. *Cell Cycle* 2012, **11**:3219-3226.

306. Hartwell KA, Miller PG, Mukherjee S, Kahn AR, Stewart AL, Logan DJ, Negri JM, Duvet M, Jaras M, Puram R, et al.: **Niche-based screening identifies small-molecule inhibitors of leukemia stem cells**. *Nat Chem Biol* 2013, **9**:840-848.

307. Konopleva MY, Jordan CT: **Leukemia stem cells and microenvironment: biology and therapeutic targeting**. *J Clin Oncol* 2011, **29**:591-599.

308. Ding L, Saunders TL, Enikolopov G, Morrison SJ: **Endothelial and perivascular cells maintain hematopoietic stem cells**. *Nature* 2012, **481**:457-462.

309. Morrison SJ, Scadden DT: **The bone marrow niche for hematopoietic stem cells**. *Nature* 2014, **505**:327-334.

310. Mendelson A, Frenette PS: **Hematopoietic stem cell niche maintenance during homeostasis and regeneration**. *Nat Med* 2014, **20**:833-846.

311. Davidson AJ, Zon LI: **The 'definitive' (and 'primitive') guide to zebrafish hematopoiesis**. *Oncogene* 2004, **23**:7233-7246.

312. Stern HM, Zon LI: **Cancer genetics and drug discovery in the zebrafish**. *Nat Rev Cancer* 2003, **3**:533-539.

313. Bolli N, Payne EM, Grabher C, Lee JS, Johnston AB, Falini B, Kanki JP, Look AT: **Expression of the cytoplasmic NPM1 mutant (NPMc+) causes the expansion of hematopoietic cells in zebrafish**. *Blood* 2010, **115**:3329-3340.

314. Forrester AM, Grabher C, McBride ER, Boyd ER, Vigerstad MH, Edgar A, Kai FB, Da'as SI, Payne E, Look AT, et al.: **NUP98-HOXA9-transgenic zebrafish develop a myeloproliferative neoplasm and provide new insight into mechanisms of myeloid leukemogenesis**. *Br J Haematol* 2011, **155**:167-181.

315. Shen LJ, Chen FY, Zhang Y, Cao LF, Kuang Y, Zhong M, Wang T, Zhong H: **MYCN transgenic zebrafish model with the characterization of acute myeloid leukemia and altered hematopoiesis**. *PLoS One* 2013, **8**:e59070.

316. He BL, Shi X, Man CH, Ma AC, Ekker SC, Chow HC, So CW, Choi WW, Zhang W, Zhang Y, et al.: **Functions of flt3 in zebrafish hematopoiesis and its relevance to human acute myeloid leukemia**. *Blood* 2014, **123**:2518-2529.

317. Deveau AP, Forrester AM, Coombs AJ, Wagner GS, Grabher C, Chute IC, Leger D, Mingay M, Alexe G, Rajan V, et al.: **Epigenetic therapy restores normal hematopoiesis in a zebrafish model of NUP98-HOXA9-induced myeloid disease**. *Leukemia* 2015, **29**:2086-2097.

318. Moloney WC, Boschetti AE, King VP: **Spontaneous leukemia in Fischer rats**. *Cancer Res* 1970, **30**:41-43.

319. Greenberger JS, Bocaccino CA, Szot SJ, Moloney WC: **Chemotherapeutic remissions in Wistar Furth rat acute myelogenous leukemia: a model for human AML**. *Acta Haematol* 1977, **57**:233-241.

320. Richter MN, Macdowell EC: **Studies on Leukemia in Mice : I. The Experimental Transmission of Leukemia**. *J Exp Med* 1930, **51**:659-673.

321. Rask-Nielsen HC, Rask-Nielsen R: **FURTHER STUDIES ON A TRANSMISSIBLE MYELOID LEUKOSIS IN WHITE MICE. II**. *Acta Pathologica Microbiologica Scandinavica* 1938, **15**:169-175.

322. Law LW, Miller JH: **The influence of thymectomy on the incidence of carcinogen-induced leukemia in strain DBA mice**. *J Natl Cancer Inst* 1950, **11**:425-437.

323. Skipper HE, Schabel FM, Jr.: **Spontaneous AK leukemia (lymphoma) as a model for human leukemias and lymphomas**. *Cancer Chemother Rep 3* 1972, **3**:3-5.

324. Schabel FM, Jr., Skipper HE, Trader MW, Laster WR, Jr., Simpson-Herren L: **Spontaneous AK leukemia (lymphoma) as a model system**. *Cancer Chemother Rep* 1969, **53**:329-344.

325. Largaespada DA: **Genetic heterogeneity in acute myeloid leukemia: maximizing information flow from MuLV mutagenesis studies**. *Leukemia* 2000, **14**:1174-1184.

326. Ichikawa Y, Maeda M, Horuichi M: **In vitro differentiation of Rauscher-virus-induced myeloid leukemia cells**. *Int J Cancer* 1976, **17**:789-787.

327. Capecchi MR: **Altering the genome by homologous recombination**. *Science* 1989, **244**:1288-1292.

328. Lobato MN, Metzler M, Drynan L, Forster A, Pannell R, Rabbitts TH: **Modeling chromosomal translocations using conditional alleles to recapitulate initiating events in human leukemias**. *J Natl Cancer Inst Monogr* 2008:58-63.

329. Zuber J, Radtke I, Pardee TS, Zhao Z, Rappaport AR, Luo W, McCurrach ME, Yang MM, Dolan ME, Kogan SC, et al.: **Mouse models of human AML accurately predict chemotherapy response**. *Genes Dev* 2009, **23**:877-889.

330. Heckl D, Kowalczyk MS, Yudovich D, Belizaire R, Puram RV, McConkey ME, Thielke A, Aster JC, Regev A, Ebert BL: **Generation of mouse models of myeloid malignancy with combinatorial genetic lesions using CRISPR-Cas9 genome editing**. *Nat Biotechnol* 2014, **32**:941-946.

331. Pruvot B, Jacquel A, Droin N, Auberger P, Bouscary D, Tamburini J, Muller M, Fontenay M, Chluba J, Solary E: **Leukemic cell xenograft in zebrafish embryo for investigating drug efficacy**. *Haematologica* 2011, **96**:612-616.

332. Corkery DP, Dellaire G, Berman JN: **Leukemia xenotransplantation in zebrafish--chemotherapy response assay in vivo**. *Br J Haematol* 2011, **153**:786-789.

333. Pearce DJ, Taussig D, Zibara K, Smith LL, Ridler CM, Preudhomme C, Young BD, Rohatiner AZ, Lister TA, Bonnet D: **AML engraftment in the NOD/SCID assay reflects the outcome of AML: implications for our understanding of the heterogeneity of AML**. *Blood* 2006, **107**:1166-1173.

334. Sanchez PV, Perry RL, Sarry JE, Perl AE, Murphy K, Swider CR, Bagg A, Choi JK, Biegel JA, Danet-Desnoyers G, et al.: **A robust xenotransplantation model for acute myeloid leukemia**. *Leukemia* 2009, **23**:2109-2117.

335. De Lord C, Clutterbuck R, Titley J, Ormerod M, Gordon-Smith T, Millar J, Powles R: **Growth of primary human acute leukemia in severe combined immunodeficient mice**. *Exp Hematol* 1991, **19**:991-993.

336. Grisolano JL, Wesselschmidt RL, Pelicci PG, Ley TJ: **Altered myeloid development and acute leukemia in transgenic mice expressing PML-RAR alpha under control of cathepsin G regulatory sequences**. *Blood* 1997, **89**:376-387.

337. Cheng GX, Zhu XH, Men XQ, Wang L, Huang QH, Jin XL, Xiong SM, Zhu J, Guo WM, Chen JQ, et al.: **Distinct leukemia phenotypes in transgenic mice and different corepressor interactions generated by promyelocytic leukemia variant fusion genes PLZF-RARalpha and NPM-RARalpha**. *Proc Natl Acad Sci U S A* 1999, **96**:6318-6323.

338. Prins HJ, Rozemuller H, Vonk-Griffioen S, Verweij VG, Dhert WJ, Slaper-Cortenbach IC, Martens AC: **Bone-forming capacity of mesenchymal stromal cells when cultured in the presence of human platelet lysate as substitute for fetal bovine serum**. *Tissue Eng Part A* 2009, **15**:3741-3751.

339. Chen Y, Jacamo R, Shi YX, Wang RY, Battula VL, Konoplev S, Strunk D, Hofmann NA, Reinisch A, Konopleva M, et al.: **Human extramedullary bone marrow in mice: a novel in vivo model of genetically controlled hematopoietic microenvironment**. *Blood* 2012, **119**:4971-4980.

340. Groen RW, Noort WA, Raymakers RA, Prins HJ, Aalders L, Hofhuis FM, Moerer P, van Velzen JF, Bloem AC, van Kessel B, et al.: **Reconstructing the human hematopoietic niche in immunodeficient mice: opportunities for studying primary multiple myeloma**. *Blood* 2012, **120**:e9-e16.

341. Walsh NC, Kenney LL, Jangalwe S, Aryee KE, Greiner DL, Brehm MA, Shultz LD: **Humanized Mouse Models of Clinical Disease**. *Annu Rev Pathol* 2017, **12**:187-215.

342. Wunderlich M, Chou FS, Link KA, Mizukawa B, Perry RL, Carroll M, Mulloy JC: **AML xenograft efficiency is significantly improved in NOD/SCID-IL2RG mice constitutively expressing human SCF, GM-CSF and IL-3**. *Leukemia* 2010, **24**:1785-1788.

343. Kamel-Reid S, Dick JE: **Engraftment of immune-deficient mice with human hematopoietic stem cells**. *Science* 1988, **242**:1706-1709.

344. Rongvaux A, Willinger T, Takizawa H, Rathinam C, Auerbach W, Murphy AJ, Valenzuela DM, Yancopoulos GD, Eynon EE, Stevens S, et al.: **Human thrombopoietin knockin mice efficiently support human hematopoiesis in vivo**. *Proc Natl Acad Sci U S A* 2011, **108**:2378-2383.

345. Rongvaux A, Willinger T, Martinek J, Strowig T, Gearty SV, Teichmann LL, Saito Y, Marches F, Halene S, Palucka AK, et al.: **Development and function of human innate immune cells in a humanized mouse model**. *Nat Biotechnol* 2014, **32**:364-372.

346. McIntosh BE, Brown ME, Duffin BM, Maufort JP, Vereide DT, Slukvin, II, Thomson JA: **Nonirradiated NOD,B6.SCID Il2rgamma-/- Kit(W41/W41) (NBSGW) mice support multilineage engraftment of human hematopoietic cells**. *Stem Cell Reports* 2015, **4**:171-180.

347. Billerbeck E, Barry WT, Mu K, Dorner M, Rice CM, Ploss A: **Development of human CD4+FoxP3+ regulatory T cells in human stem cell factor-, granulocyte-macrophage colony-stimulating factor-, and interleukin-3-expressing NOD-SCID IL2Rgamma(null) humanized mice**. *Blood* 2011, **117**:3076-3086.

348. Klco JM, Spencer DH, Miller CA, Griffith M, Lamprecht TL, O'Laughlin M, Fronick C, Magrini V, Demeter RT, Fulton RS, et al.: **Functional heterogeneity of genetically defined subclones in acute myeloid leukemia**. *Cancer Cell* 2014, **25**:379-392.

349. Krevvata M, Shan X, Zhou C, Dos Santos C, Habineza Ndikuyeze G, Secreto A, Glover J, Trotman W, Brake-Silla G, Nunez-Cruz S, et al.: **Cytokines increase engraftment of human acute myeloid leukemia cells in immunocompromised**

mice but not engraftment of human myelodysplastic syndrome cells. *Haematologica* 2018, **103**:959-971.

350. Herndler-Brandstetter D, Shan L, Yao Y, Stecher C, Plajer V, Lietzenmayer M, Strowig T, de Zoete MR, Palm NW, Chen J, et al.: **Humanized mouse model supports development, function, and tissue residency of human natural killer cells**. *Proc Natl Acad Sci U S A* 2017, **114**:E9626-E9634.

351. Abarrategi A, Mian SA, Passaro D, Rouault-Pierre K, Grey W, Bonnet D: **Modeling the human bone marrow niche in mice: From host bone marrow engraftment to bioengineering approaches**. *J Exp Med* 2018, **215**:729-743.

352. Antonelli A, Noort WA, Jaques J, de Boer B, de Jong-Korlaar R, Brouwers-Vos AZ, Lubbers-Aalders L, van Velzen JF, Bloem AC, Yuan H, et al.: **Establishing human leukemia xenograft mouse models by implanting human bone marrow-like scaffold-based niches**. *Blood* 2016, **128**:2949-2959.

353. Chao MP, Gentles AJ, Chatterjee S, Lan F, Reinisch A, Corces MR, Xavy S, Shen J, Haag D, Chanda S, et al.: **Human AML-iPSCs Reacquire Leukemic Properties after Differentiation and Model Clonal Variation of Disease**. *Cell Stem Cell* 2017, **20**:329-344 e327.

354. Gutierrez A, Pan L, Groen RW, Baleydier F, Kentsis A, Marineau J, Grebliunaite R, Kozakewich E, Reed C, Pflumio F, et al.: **Phenothiazines induce PP2A-mediated apoptosis in T cell acute lymphoblastic leukemia**. *J Clin Invest* 2014, **124**:644-655.

355. Reinisch A, Gratzinger D, Hong W-J, Majeti R: **A Novel Humanized Bone Marrow Niche Xenotransplantation Model Allows Superior Engraftment of Human Normal and Malignant Hematopoietic Cells and Reveals Myelofibrosis-Initiating Cells in the HSC Compartment**. *Blood* 2014, **124**:349-349.

356. Piacibello W, Sanavio F, Garetto L, Severino A, Bergandi D, Ferrario J, Fagioli F, Berger M, Aglietta M: **Extensive amplification and self-renewal of human primitive hematopoietic stem cells from cord blood**. *Blood* 1997, **89**:2644-2653.

357. van Gosliga D, Schepers H, Rizo A, van der Kolk D, Vellenga E, Schuringa JJ: **Establishing long-term cultures with self-renewing acute myeloid leukemia stem/progenitor cells**. *Exp Hematol* 2007, **35**:1538-1549.

358. Ito S, Barrett AJ, Dutra A, Pak E, Miner S, Keyvanfar K, Hensel NF, Rezvani K, Muranski P, Liu P, et al.: **Long term maintenance of myeloid leukemic stem cells cultured with unrelated human mesenchymal stromal cells**. *Stem Cell Res* 2015, **14**:95-104.

359. Griessinger E, Anjos-Afonso F, Pizzitola I, Rouault-Pierre K, Vargaftig J, Taussig D, Gribben J, Lassailly F, Bonnet D: **A niche-like culture system allowing the maintenance of primary human acute myeloid leukemia-initiating cells: a new tool to decipher their chemoresistance and self-renewal mechanisms**. *Stem Cells Transl Med* 2014, **3**:520-529.

360. Leisten I, Kramann R, Ventura Ferreira MS, Bovi M, Neuss S, Ziegler P, Wagner W, Knuchel R, Schneider RK: **3D co-culture of hematopoietic stem and progenitor cells and mesenchymal stem cells in collagen scaffolds as a model of the hematopoietic niche**. *Biomaterials* 2012, **33**:1736-1747.

361. Broxmeyer HE, Hangoc G, Cooper S, Ribeiro RC, Graves V, Yoder M, Wagner J, Vadhan-Raj S, Benninger L, Rubinstein P, et al.: **Growth characteristics and expansion of human umbilical cord blood and estimation of its potential for transplantation in adults**. *Proc Natl Acad Sci U S A* 1992, **89**:4109-4113.

362. Mohamed AA, Ibrahim AM, El-Masry MW, Mansour IM, Khroshied MA, Gouda HM, Riad RM: **Ex vivo expansion of stem cells: defining optimum conditions using various cytokines**. *Lab Hematol* 2006, **12**:86-93.

363. Yao CL, Chu IM, Hsieh TB, Hwang SM: **A systematic strategy to optimize ex vivo expansion medium for human hematopoietic stem cells derived from umbilical cord blood mononuclear cells**. *Exp Hematol* 2004, **32**:720-727.

364. Ferreira MS, Jahnen-Dechent W, Labude N, Bovi M, Hieronymus T, Zenke M, Schneider RK, Neuss S: **Cord blood-hematopoietic stem cell expansion in 3D fibrin scaffolds with stromal support**. *Biomaterials* 2012, **33**:6987-6997.

365. Flores-Guzman P, Flores-Figueroa E, Montesinos JJ, Martinez-Jaramillo G, Fernandez-Sanchez V, Valencia-Plata I, Alarcon-Santos G, Mayani H: **Individual and combined effects of mesenchymal stromal cells and recombinant stimulatory cytokines on the in vitro growth of primitive hematopoietic cells from human umbilical cord blood**. *Cytotherapy* 2009, **11**:886-896.

366. Levac K, Karanu F, Bhatia M: **Identification of growth factor conditions that reduce ex vivo cord blood progenitor expansion but do not alter human repopulating cell function in vivo**. *Haematologica* 2005, **90**:166-172.

367. Choi YS, Noh SE, Lim SM, Kim DI: **Optimization of ex vivo hematopoietic stem cell expansion in intermittent dynamic cultures**. *Biotechnol Lett* 2010, **32**:1969-1975.

368. Wang TY, Brennan JK, Wu JH: **Multilineal hematopoiesis in a three-dimensional murine long-term bone marrow culture**. *Exp Hematol* 1995, **23**:26-32.

369. Dexter TM, Moore MA, Sheridan AP: **Maintenance of hemopoietic stem cells and production of differentiated progeny in allogeneic and semiallogeneic bone marrow chimeras in vitro**. *J Exp Med* 1977, **145**:1612-1616.

370. Eaves C, Fraser C, Udomsakdi C, Sutherland H, Barnett M, Szilvassy S, Hogge D, Lansdorp P, Eaves A: **Manipulation of the hematopoietic stem cell in vitro**. *Leukemia* 1992, **6 Suppl 1**:27-30.

371. Tsuji T, Nishimura-Morita Y, Watanabe Y, Hirano D, Nakanishi S, Mori KJ, Yatsunami K: **A murine stromal cell line promotes the expansion of CD34high+-primitive progenitor cells isolated from human umbilical cord blood in combination with human cytokines**. *Growth Factors* 1999, **16**:225-240.

372. Heike T, Nakahata T: **Ex vivo expansion of hematopoietic stem cells by cytokines**. *Biochim Biophys Acta* 2002, **1592**:313-321.

373. Ueda T, Tsuji K, Yoshino H, Ebihara Y, Yagasaki H, Hisakawa H, Mitsui T, Manabe A, Tanaka R, Kobayashi K, et al.: **Expansion of human NOD/SCID-repopulating cells by stem cell factor, Flk2/Flt3 ligand, thrombopoietin, IL-6, and soluble IL-6 receptor**. *J Clin Invest* 2000, **105**:1013-1021.

374. Hogge DE, Lansdorp PM, Reid D, Gerhard B, Eaves CJ: **Enhanced detection, maintenance, and differentiation of primitive human hematopoietic cells in cultures containing murine fibroblasts engineered to produce human steel factor, interleukin-3, and granulocyte colony-stimulating factor**. *Blood* 1996, **88**:3765-3773.

375. Sontakke P, Carretta M, Capala M, Schepers H, Schuringa JJ: **Ex vivo assays to study self-renewal, long-term expansion, and leukemic transformation of genetically modified human hematopoietic and patient-derived leukemic stem cells**. *Methods Mol Biol* 2014, **1185**:195-210.

376. Hartwell KA, Miller PG, Mukherjee S, Kahn AR, Stewart AL, Logan DJ, Negri JM, Duvet M, Jaras M, Puram R, et al.: **Niche-based screening identifies small-molecule inhibitors of leukemia stem cells**. *Nat Chem Biol* 2013, **9**:840-848.

377. Panoskaltsis N, Mantalaris A, Wu JH: **Engineering a mimicry of bone marrow tissue ex vivo**. *J Biosci Bioeng* 2005, **100**:28-35.

378. Owen SC, Shoichet MS: **Design of three-dimensional biomimetic scaffolds**. *J Biomed Mater Res A* 2010, **94**:1321-1331.

379. Sharma MB, Limaye LS, Kale VP: **Mimicking the functional hematopoietic stem cell niche in vitro: recapitulation of marrow physiology by hydrogel-based three-dimensional cultures of mesenchymal stromal cells**. *Haematologica* 2012, **97**:651-660.

380. Tiwari A, Tursky ML, Mushahary D, Wasnik S, Collier FM, Suma K, Kirkland MA, Pande G: **Ex vivo expansion of hematopoietic stem/progenitor cells from human umbilical cord blood on acellular scaffolds prepared from MS-5 stromal cell line**. *J Tissue Eng Regen Med* 2013, **7**:871-883.

381. Aljitawi OS, Li D, Xiao Y, Zhang D, Ramachandran K, Stehno-Bittel L, Van Veldhuizen P, Lin TL, Kambhampati S, Garimella R: **A novel three-dimensional stromal-based model for in vitro chemotherapy sensitivity testing of leukemia cells**. *Leuk Lymphoma* 2014, **55**:378-391.

382. Blanco TM, Mantalaris A, Bismarck A, Panoskaltsis N: **The development of a three-dimensional scaffold for ex vivo biomimicry of human acute myeloid leukemia**. *Biomaterials* 2010, **31**:2243-2251.

383. Lai W, Li Y, Mak S, Ho F, Chow S, Chooi W, Chow C, Leung A, Chan B: **Reconstitution of bone-like matrix in osteogenically differentiated mesenchymal stem cell-collagen constructs: A three-dimensional in vitro model to study hematopoietic stem cell niche**. *J Tissue Eng* 2013, **4**:2041731413508668.

384. Rosa RG, Bianco JER, dos Santos GP, Waldman SD, Weber J, Joazeiro PP, Saad STO: **Natural Scaffold, from Bovine Bone Marrow, Reproduces Native Microenvironment and Supports CD34+ and Stromal Cells**. *Blood* 2015, **126**:2400-2400.

385. Tiwari A, Tursky ML, Kirkland MA, Pande G: **Expansion of human hematopoietic stem/progenitor cells on decellularized matrix scaffolds**. *Curr Protoc Stem Cell Biol* 2014, **28**:Unit 1C 15.

386. Raic A, Rodling L, Kalbacher H, Lee-Thedieck C: **Biomimetic macroporous PEG hydrogels as 3D scaffolds for the multiplication of human hematopoietic stem and progenitor cells**. *Biomaterials* 2014, **35**:929-940.

387. Di Maggio N, Piccinini E, Jaworski M, Trumpp A, Wendt DJ, Martin I: **Toward modeling the bone marrow niche using scaffold-based 3D culture systems**. *Biomaterials* 2011, **32**:321-329.

388. Torisawa YS, Spina CS, Mammoto T, Mammoto A, Weaver JC, Tat T, Collins JJ, Ingber DE: **Bone marrow-on-a-chip replicates hematopoietic niche physiology in vitro**. *Nat Methods* 2014, **11**:663-669.

389. Dombret H, Gardin C: **An update of current treatments for adult acute myeloid leukemia**. *Blood* 2016, **127**:53-61.

390. Thol F, Schlenk RF, Heuser M, Ganser A: **How I treat refractory and early relapsed acute myeloid leukemia**. *Blood* 2015, **126**:319-327.

391. Burnett AK, Russell NH, Hills RK, Kell J, Cavenagh J, Kjeldsen L, McMullin MF, Cahalin P, Dennis M, Friis L, et al.: **A randomized comparison of daunorubicin 90 mg/m2 vs 60 mg/m2 in AML induction: results from the UK NCRI AML17 trial in 1206 patients**. *Blood* 2015, **125**:3878-3885.

392. Thol F: **Can we forecast induction failure in acute myeloid leukemia?** *Haematologica* 2018, **103**:375-377.

393. Rao AV: **Fitness in the elderly: how to make decisions regarding acute myeloid leukemia induction**. *Hematology Am Soc Hematol Educ Program* 2016, **2016**:339-347.

394. Almeida AM, Ramos F: **Acute myeloid leukemia in the older adults**. *Leuk Res Rep* 2016, **6**:1-7.

395. Stein EM, Tallman MS: **Emerging therapeutic drugs for AML**. *Blood* 2016, **127**:71-78.

396. Dhami SPS, Kappala SS, Thompson A, Szegezdi E: **Three-dimensional ex vivo co-culture models of the leukaemic bone marrow niche for functional drug testing**. *Drug Discov Today* 2016, **21**:1464-1471.

397. Houshmand M, Soleimani M, Atashi A, Saglio G, Abdollahi M, Nikougoftar Zarif M: **Mimicking the Acute Myeloid Leukemia Niche for Molecular Study and Drug Screening**. *Tissue Eng Part C Methods* 2017, **23**:72-85.

398. Blanco TM, Mantalaris A, Bismarck A, Panoskaltsis N: **The development of a three-dimensional scaffold for ex vivo biomimicry of human acute myeloid leukaemia**. *Biomaterials* 2010, **31**:2243-2251.

399. Goulard M, Dosquet C, Bonnet D: **Role of the microenvironment in myeloid malignancies**. *Cell Mol Life Sci* 2018, **75**:1377-1391.

400. Dominici M, Le Blanc K, Mueller I, Slaper-Cortenbach I, Marini F, Krause D, Deans R, Keating A, Prockop D, Horwitz E: **Minimal criteria for defining multipotent mesenchymal stromal cells. The International Society for Cellular Therapy position statement**. *Cytotherapy* 2006, **8**:315-317.

401. Abdallah BM, Haack-Sorensen M, Burns JS, Elsnab B, Jakob F, Hokland P, Kassem M: **Maintenance of differentiation potential of human bone marrow mesenchymal stem cells immortalized by human telomerase reverse transcriptase gene despite [corrected] extensive proliferation**. *Biochem Biophys Res Commun* 2005, **326**:527-538.

402. Gomariz A, Helbling PM, Isringhausen S, Suessbier U, Becker A, Boss A, Nagasawa T, Paul G, Goksel O, Szekely G, et al.: **Quantitative spatial analysis of haematopoiesis-regulating stromal cells in the bone marrow microenvironment by 3D microscopy**. *Nat Commun* 2018, **9**:2532.

403. Shlush LI, Mitchell A, Heisler L, Abelson S, Ng SWK, Trotman-Grant A, Medeiros JJF, Rao-Bhatia A, Jaciw-Zurakowsky I, Marke R, et al.: **Tracing the origins of relapse in acute myeloid leukaemia to stem cells**. *Nature* 2017, **547**:104-108.

404. Terpstra W, Ploemacher RE, Prins A, van Lom K, Pouwels K, Wognum AW, Wagemaker G, Lowenberg B, Wielenga JJ: **Fluorouracil selectively spares acute myeloid leukemia cells with long-term growth abilities in immunodeficient mice and in culture**. *Blood* 1996, **88**:1944-1950.

405. Menge H, Robinson JW, Riecken EO: **[Adaptive changes in intestinal mucosa of the small intestine as a result of intraluminal stress]**. *Z Gastroenterol* 1976, **14**:420-433.

406. Preisler H, Davis RB, Kirshner J, Dupre E, Richards F, 3rd, Hoagland HC, Kopel S, Levy RN, Carey R, Schulman P, et al.: **Comparison of three remission induction regimens and two postinduction strategies for the treatment of acute nonlymphocytic leukemia: a cancer and leukemia group B study**. *Blood* 1987, **69**:1441-1449.

407. Wiernik PH, Banks PL, Case DC, Jr., Arlin ZA, Periman PO, Todd MB, Ritch PS, Enck RE, Weitberg AB: **Cytarabine plus idarubicin or daunorubicin as induction and consolidation therapy for previously untreated adult patients with acute myeloid leukemia**. *Blood* 1992, **79**:313-319.

408. Schlenk RF: **Post-remission therapy for acute myeloid leukemia**. *Haematologica* 2014, **99**:1663-1670.

409. Ossenkoppele G, Lowenberg B: **How I treat the older patient with acute myeloid leukemia**. *Blood* 2015, **125**:767-774.

410. Roloff GW, Griffiths EA: **When to obtain genomic data in acute myeloid leukemia (AML) and which mutations matter**. *Blood Adv* 2018, **2**:3070-3080.

411. Grimwade D, Walker H, Oliver F, Wheatley K, Harrison C, Harrison G, Rees J, Hann I, Stevens R, Burnett A, et al.: **The importance of diagnostic cytogenetics on outcome in AML: analysis of 1,612 patients entered into the MRC AML 10 trial. The Medical Research Council Adult and Children's Leukaemia Working Parties**. *Blood* 1998, **92**:2322-2333.

412. Ng SW, Mitchell A, Kennedy JA, Chen WC, McLeod J, Ibrahimova N, Arruda A, Popescu A, Gupta V, Schimmer AD, et al.: **A 17-gene stemness score for rapid determination of risk in acute leukaemia**. *Nature* 2016, **540**:433-437.

413. Herold T, Jurinovic V, Batcha AMN, Bamopoulos SA, Rothenberg-Thurley M, Ksienzyk B, Hartmann L, Greif PA, Phillippou-Massier J, Krebs S, et al.: **A 29-gene and cytogenetic score for the prediction of resistance to induction treatment in acute myeloid leukemia**. *Haematologica* 2018, **103**:456-465.

414. Krug U, Rollig C, Koschmieder A, Heinecke A, Sauerland MC, Schaich M, Thiede C, Kramer M, Braess J, Spiekermann K, et al.: **Complete remission and early death after intensive chemotherapy in patients aged 60 years or older with acute myeloid leukaemia: a web-based application for prediction of outcomes**. *Lancet* 2010, **376**:2000-2008.

415. Dexter TM, Wright EG, Krizsa F, Lajtha LG: **Regulation of haemopoietic stem cell proliferation in long term bone marrow cultures**. *Biomedicine* 1977, **27**:344-349.

416. Macanas-Pirard P, Broekhuizen R, Gonzalez A, Oyanadel C, Ernst D, Garcia P, Montecinos VP, Court F, Ocqueteau M, Ramirez P, et al.: **Resistance of leukemia cells to cytarabine chemotherapy is mediated by bone marrow stroma, involves cell-surface equilibrative nucleoside transporter-1 removal and correlates with patient outcome**. *Oncotarget* 2017, **8**:23073-23086.

417. Zeng Z, Samudio IJ, Munsell M, An J, Huang Z, Estey E, Andreeff M, Konopleva M: **Inhibition of CXCR4 with the novel RCP168 peptide overcomes stroma-mediated chemoresistance in chronic and acute leukemias**. *Mol Cancer Ther* 2006, **5**:3113-3121.

418. Baev DV, Krawczyk J, M OD, Szegezdi E: **The BH3-mimetic ABT-737 effectively kills acute myeloid leukemia initiating cells**. *Leuk Res Rep* 2014, **3**:79-82.

419. E OR, Dhami SPS, Baev DV, Ortutay C, Halpin-McCormick A, Morrell R, Santocanale C, Samali A, Quinn J, O'Dwyer ME, et al.: **Repression of Mcl-1 expression by the CDC7/CDK9 inhibitor PHA-767491 overcomes bone marrow stroma-mediated drug resistance in AML**. *Sci Rep* 2018, **8**:15752.

420. Domingues MJ, Cao H, Heazlewood SY, Cao B, Nilsson SK: **Niche Extracellular Matrix Components and Their Influence on HSC**. *J Cell Biochem* 2017, **118**:1984-1993.

421. Gattazzo F, Urciuolo A, Bonaldo P: **Extracellular matrix: a dynamic microenvironment for stem cell niche**. *Biochim Biophys Acta* 2014, **1840**:2506-2519.

422. Schonherr E, Hausser HJ: **Extracellular matrix and cytokines: a functional unit**. *Dev Immunol* 2000, **7**:89-101.

423. Morrison SJ, Scadden DT: **The bone marrow niche for haematopoietic stem cells**. *Nature* 2014, **505**:327-334.

424. Wei Q, Frenette PS: **Niches for Hematopoietic Stem Cells and Their Progeny**. *Immunity* 2018, **48**:632-648.

425. Ho TC, LaMere M, Stevens BM, Ashton JM, Myers JR, O'Dwyer KM, Liesveld JL, Mendler JH, Guzman M, Morrissette JD, et al.: **Evolution of acute myelogenous**

leukemia stem cell properties after treatment and progression. *Blood* 2016, **128**:1671-1678.

426. Duarte D, Hawkins ED, Lo Celso C: **The interplay of leukemia cells and the bone marrow microenvironment**. *Blood* 2018, **131**:1507-1511.

427. Medyouf H: **The microenvironment in human myeloid malignancies: emerging concepts and therapeutic implications**. *Blood* 2017, **129**:1617-1626.

428. Sarkozy C, Gardin C, Gachard N, Merabet F, Turlure P, Malfuson JV, Pautas C, Micol JB, Thomas X, Quesnel B, et al.: **Outcome of older patients with acute myeloid leukemia in first relapse**. *Am J Hematol* 2013, **88**:758-764.

429. Burnett A, Wetzler M, Lowenberg B: **Therapeutic advances in acute myeloid leukemia**. *J Clin Oncol* 2011, **29**:487-494.

430. Ruter B, Wijermans PW, Lubbert M: **DNA methylation as a therapeutic target in hematologic disorders: recent results in older patients with myelodysplasia and acute myeloid leukemia**. *Int J Hematol* 2004, **80**:128-135.

431. Schoofs T, Muller-Tidow C: **DNA methylation as a pathogenic event and as a therapeutic target in AML**. *Cancer Treat Rev* 2011, **37 Suppl 1**:S13-18.

432. Rombouts EJ, Pavic B, Lowenberg B, Ploemacher RE: **Relation between CXCR-4 expression, Flt3 mutations, and unfavorable prognosis of adult acute myeloid leukemia**. *Blood* 2004, **104**:550-557.

433. Veiga JP, Costa LF, Sallan SE, Nadler LM, Cardoso AA: **Leukemia-stimulated bone marrow endothelium promotes leukemia cell survival**. *Exp Hematol* 2006, **34**:610-621.

434. Konopleva M, Konoplev S, Hu W, Zaritskey AY, Afanasiev BV, Andreeff M: **Stromal cells prevent apoptosis of AML cells by up-regulation of anti-apoptotic proteins**. *Leukemia* 2002, **16**:1713-1724.

435. Opferman JT: **Life and death during hematopoietic differentiation**. *Curr Opin Immunol* 2007, **19**:497-502.

436. Rhodes MM, Kopsombut P, Bondurant MC, Price JO, Koury MJ: **Bcl-x(L) prevents apoptosis of late-stage erythroblasts but does not mediate the antiapoptotic effect of erythropoietin**. *Blood* 2005, **106**:1857-1863.

437. Aerbajinai W, Giattina M, Lee YT, Raffeld M, Miller JL: **The proapoptotic factor Nix is coexpressed with Bcl-xL during terminal erythroid differentiation**. *Blood* 2003, **102**:712-717.

438. Kodama T, Hikita H, Kawaguchi T, Shigekawa M, Shimizu S, Hayashi Y, Li W, Miyagi T, Hosui A, Tatsumi T, et al.: **Mcl-1 and Bcl-xL regulate Bak/Bax-dependent apoptosis of the megakaryocytic lineage at multistages**. *Cell Death and Differentiation* 2012, **19**:1856-1869.

439. Zhang H, Nimmer PM, Tahir SK, Chen J, Fryer RM, Hahn KR, Iciek LA, Morgan SJ, Nasarre MC, Nelson R, et al.: **Bcl-2 family proteins are essential for platelet survival**. *Cell Death Differ* 2007, **14**:943-951.

440. Moulding DA, Akgul C, Derouet M, White MR, Edwards SW: **BCL-2 family expression in human neutrophils during delayed and accelerated apoptosis**. *J Leukoc Biol* 2001, **70**:783-792.

441. Pan R, Hogdal LJ, Benito JM, Bucci D, Han L, Borthakur G, Cortes J, DeAngelo DJ, Debose L, Mu H, et al.: **Selective BCL-2 inhibition by ABT-199 causes on-target cell death in acute myeloid leukemia**. *Cancer Discov* 2014, **4**:362-375.

442. Bogenberger JM, Kornblau SM, Pierceall WE, Lena R, Chow D, Shi CX, Mantei J, Ahmann G, Gonzales IM, Choudhary A, et al.: **BCL-2 family proteins as 5-**

Azacytidine-sensitizing targets and determinants of response in myeloid malignancies. *Leukemia* 2014, **28**:1657-1665.

443. Kohl TM, Hellinger C, Ahmed F, Buske C, Hiddemann W, Bohlander SK, Spiekermann K: **BH3 mimetic ABT-737 neutralizes resistance to FLT3 inhibitor treatment mediated by FLT3-independent expression of BCL2 in primary AML blasts**. *Leukemia* 2007, **21**:1763-1772.

444. Oakes SR, Vaillant F, Lim E, Lee L, Breslin K, Feleppa F, Deb S, Ritchie ME, Takano E, Ward T, et al.: **Sensitization of BCL-2-expressing breast tumors to chemotherapy by the BH3 mimetic ABT-737**. *Proc Natl Acad Sci U S A* 2012, **109**:2766-2771.

445. Gerber JM, Smith BD, Ngwang B, Zhang H, Vala MS, Morsberger L, Galkin S, Collector MI, Perkins B, Levis MJ, et al.: **A clinically relevant population of leukemic CD34(+)CD38(-) cells in acute myeloid leukemia**. *Blood* 2012, **119**:3571-3577.

446. Baev DV, Krawczyk J, O′Dwyer M, Szegezdi E: **The BH3-mimetic ABT-737 effectively kills acute myeloid leukemia initiating cells**. *Leukemia Research Reports* 2014, **3**:79-82.

447. Stirewalt DL, Meshinchi S, Kopecky KJ, Fan W, Pogosova-Agadjanyan EL, Engel JH, Cronk MR, Dorcy KS, McQuary AR, Hockenbery D, et al.: **Identification of genes with abnormal expression changes in acute myeloid leukemia**. *Genes, Chromosomes and Cancer* 2008, **47**:8-20.

448. van Dijk M, Halpin-McCormick A, Sessler T, Samali A, Szegezdi E: **Resistance to TRAIL in non-transformed cells is due to multiple redundant pathways**. *Cell Death &Amp; Disease* 2013, **4**:e702.

449. Torok-Storb B, Iwata M, Graf L, Gianotti J, Horton H, Byrne MC: **Dissecting the marrow microenvironment**. *Ann N Y Acad Sci* 1999, **872**:164-170.

450. Rai KR, Holland JF, Glidewell OJ, Weinberg V, Brunner K, Obrecht JP, Preisler HD, Nawabi IW, Prager D, Carey RW, et al.: **Treatment of acute myelocytic leukemia: a study by cancer and leukemia group B**. *Blood* 1981, **58**:1203-1212.

451. Su AI, Wiltshire T, Batalov S, Lapp H, Ching KA, Block D, Zhang J, Soden R, Hayakawa M, Kreiman G, et al.: **A gene atlas of the mouse and human protein-encoding transcriptomes**. *Proc Natl Acad Sci U S A* 2004, **101**:6062-6067.

452. Glaser SP, Lee EF, Trounson E, Bouillet P, Wei A, Fairlie WD, Izon DJ, Zuber J, Rappaport AR, Herold MJ, et al.: **Anti-apoptotic Mcl-1 is essential for the development and sustained growth of acute myeloid leukemia**. *Genes Dev* 2012, **26**:120-125.

453. Natoni A, Murillo LS, Kliszczak AE, Catherwood MA, Montagnoli A, Samali A, O'Dwyer M, Santocanale C: **Mechanisms of action of a dual Cdc7/Cdk9 kinase inhibitor against quiescent and proliferating CLL cells**. *Mol Cancer Ther* 2011, **10**:1624-1634.

454. Yecies D, Carlson NE, Deng J, Letai A: **Acquired resistance to ABT-737 in lymphoma cells that up-regulate MCL-1 and BFL-1**. *Blood* 2010, **115**:3304-3313.

455. Bruncko M, Wang L, Sheppard GS, Phillips DC, Tahir SK, Xue J, Erickson S, Fidanze S, Fry E, Hasvold L, et al.: **Structure-guided design of a series of MCL-1 inhibitors with high affinity and selectivity**. *J Med Chem* 2015, **58**:2180-2194.

456. Grabow S, Delbridge AR, Aubrey BJ, Vandenberg CJ, Strasser A: **Loss of a Single Mcl-1 Allele Inhibits MYC-Driven Lymphomagenesis by Sensitizing Pro-B Cells to Apoptosis**. *Cell Rep* 2016, **14**:2337-2347.

457. Konopleva M, Pollyea DA, Potluri J, Chyla BJ, Busman T, McKeegan E, Salem A, Zhu M, Ricker JL, Blum W, et al.: **A Phase 2 Study of ABT-199 (GDC-0199) in Patients with Acute Myelogenous Leukemia (AML)**. *Blood* 2014, **124**:118-118.

458. Campos L, Sabido O, Rouault JP, Guyotat D: **Effects of BCL-2 antisense oligodeoxynucleotides on in vitro proliferation and survival of normal marrow progenitors and leukemic cells**. *Blood* 1994, **84**:595-600.

459. Ishizawa J, Kojima K, McQueen T, Ruvolo V, Chachad D, Nogueras-Gonzalez GM, Huang X, Pierceall WE, Dettman EJ, Cardone MH, et al.: **Mitochondrial Profiling of Acute Myeloid Leukemia in the Assessment of Response to Apoptosis Modulating Drugs**. *PLoS One* 2015, **10**:e0138377.

460. Fennell DA, Corbo MV, Dean NM, Monia BP, Cotter FE: **In vivo suppression of Bcl-XL expression facilitates chemotherapy-induced leukaemia cell death in a SCID/NOD-Hu model**. *Br J Haematol* 2001, **112**:706-713.

461. Garrido SM, Appelbaum FR, Willman CL, Banker DE: **Acute myeloid leukemia cells are protected from spontaneous and drug-induced apoptosis by direct contact with a human bone marrow stromal cell line (HS-5)**. *Exp Hematol* 2001, **29**:448-457.

462. Opferman JT, Iwasaki H, Ong CC, Suh H, Mizuno S, Akashi K, Korsmeyer SJ: **Obligate role of anti-apoptotic MCL-1 in the survival of hematopoietic stem cells**. *Science* 2005, **307**:1101-1104.

463. Kaufmann SH, Karp JE, Svingen PA, Krajewski S, Burke PJ, Gore SD, Reed JC: **Elevated expression of the apoptotic regulator Mcl-1 at the time of leukemic relapse**. *Blood* 1998, **91**:991-1000.

464. Choudhary GS, Al-Harbi S, Mazumder S, Hill BT, Smith MR, Bodo J, Hsi ED, Almasan A: **MCL-1 and BCL-xL-dependent resistance to the BCL-2 inhibitor ABT-199 can be overcome by preventing PI3K/AKT/mTOR activation in lymphoid malignancies**. *Cell Death Dis* 2015, **6**:e1593.

465. Al-Harbi S, Hill BT, Mazumder S, Singh K, Devecchio J, Choudhary G, Rybicki LA, Kalaycio M, Maciejewski JP, Houghton JA, et al.: **An antiapoptotic BCL-2 family expression index predicts the response of chronic lymphocytic leukemia to ABT-737**. *Blood* 2011, **118**:3579-3590.

466. Kasper S, Breitenbuecher F, Heidel F, Hoffarth S, Markova B, Schuler M, Fischer T: **Targeting MCL-1 sensitizes FLT3-ITD-positive leukemias to cytotoxic therapies**. *Blood Cancer J* 2012, **2**:e60.

467. Doi K, Liu Q, Gowda K, Barth BM, Claxton D, Amin S, Loughran TP, Jr., Wang HG: **Maritoclax induces apoptosis in acute myeloid leukemia cells with elevated Mcl-1 expression**. *Cancer Biol Ther* 2014, **15**.

468. Akgul C, Moulding DA, White MR, Edwards SW: **In vivo localisation and stability of human Mcl-1 using green fluorescent protein (GFP) fusion proteins**. *FEBS Lett* 2000, **478**:72-76.

469. Quinn BA, Dash R, Azab B, Sarkar S, Das SK, Kumar S, Oyesanya RA, Dasgupta S, Dent P, Grant S, et al.: **Targeting Mcl-1 for the therapy of cancer**. *Expert Opin Investig Drugs* 2011, **20**:1397-1411.

470. Warr MR, Shore GC: **Unique biology of Mcl-1: therapeutic opportunities in cancer**. *Curr Mol Med* 2008, **8**:138-147.

471. Montagnoli A, Valsasina B, Croci V, Menichincheri M, Rainoldi S, Marchesi V, Tibolla M, Tenca P, Brotherton D, Albanese C, et al.: **A Cdc7 kinase inhibitor restricts initiation of DNA replication and has antitumor activity**. *Nat Chem Biol* 2008, **4**:357-365.

472. Price DH: **P-TEFb, a cyclin-dependent kinase controlling elongation by RNA polymerase II**. *Mol Cell Biol* 2000, **20**:2629-2634.

473. Xie S, Jiang H, Zhai X-w, Wei F, Wang S-d, Ding J, Chen Y: **Antitumor action of CDK inhibitor LS-007 as a single agent and in combination with ABT-199 against human acute leukemia cells**. *Acta Pharmacologica Sinica* 2016, **37**:1481.

474. Bogenberger J, Whatcott C, Hansen N, Delman D, Shi CX, Kim W, Haws H, Soh K, Lee YS, Peterson P, et al.: **Combined venetoclax and alvocidib in acute myeloid leukemia**. *Oncotarget* 2017, **8**:107206-107222.

475. Polier G, Giaisi M, Köhler R, Müller WW, Lutz C, Buss EC, Krammer PH, Li-Weber M: **Targeting CDK9 by wogonin and related natural flavones potentiates the anti-cancer efficacy of the Bcl-2 family inhibitor ABT-263**. *International Journal of Cancer* 2014, **136**:688-698.

476. Jilg S, Reidel V, Muller-Thomas C, Konig J, Schauwecker J, Hockendorf U, Huberle C, Gorka O, Schmidt B, Burgkart R, et al.: **Blockade of BCL-2 proteins efficiently induces apoptosis in progenitor cells of high-risk myelodysplastic syndromes patients**. *Leukemia* 2016, **30**:112-123.

477. Lee H-J, Zhuang G, Cao Y, Du P, Kim H-J, Settleman J: **Drug Resistance via Feedback Activation of Stat3 in Oncogene-Addicted Cancer Cells**. *Cancer Cell* 2014, **26**:207-221.

478. Delbridge AR, Opferman JT, Grabow S, Strasser A: **Antagonism between MCL-1 and PUMA governs stem/progenitor cell survival during hematopoietic recovery from stress**. *Blood* 2015, **125**:3273-3280.

479. Sobhian B, Laguette N, Yatim A, Nakamura M, Levy Y, Kiernan R, Benkirane M: **HIV-1 Tat assembles a multifunctional transcription elongation complex and stably associates with the 7SK snRNP**. *Mol Cell* 2010, **38**:439-451.

480. Lin C, Smith ER, Takahashi H, Lai KC, Martin-Brown S, Florens L, Washburn MP, Conaway JW, Conaway RC, Shilatifard A: **AFF4, a component of the ELL/P-TEFb elongation complex and a shared subunit of MLL chimeras, can link transcription elongation to leukemia**. *Mol Cell* 2010, **37**:429-437.

481. Mueller D, Bach C, Zeisig D, Garcia-Cuellar MP, Monroe S, Sreekumar A, Zhou R, Nesvizhskii A, Chinnaiyan A, Hess JL, et al.: **A role for the MLL fusion partner ENL in transcriptional elongation and chromatin modification**. *Blood* 2007, **110**:4445-4454.

482. Barboric M, Nissen RM, Kanazawa S, Jabrane-Ferrat N, Peterlin BM: **NF-kappaB binds P-TEFb to stimulate transcriptional elongation by RNA polymerase II**. *Mol Cell* 2001, **8**:327-337.

483. Balakrishnan K, Burger JA, Fu M, Doifode T, Wierda WG, Gandhi V: **Regulation of Mcl-1 expression in context to bone marrow stromal microenvironment in chronic lymphocytic leukemia**. *Neoplasia* 2014, **16**:1036-1046.

484. Kindler T, Lipka DB, Fischer T: **FLT3 as a therapeutic target in AML: still challenging after all these years**. *Blood* 2010, **116**:5089-5102.

485. Zheng R, Bailey E, Nguyen B, Yang X, Piloto O, Levis M, Small D: **Further activation of FLT3 mutants by FLT3 ligand**. *Oncogene* 2011, **30**:4004-4014.

486. Breitenbuecher F, Markova B, Kasper S, Carius B, Stauder T, Bohmer FD, Masson K, Ronnstrand L, Huber C, Kindler T, et al.: **A novel molecular mechanism of primary resistance to FLT3-kinase inhibitors in AML**. *Blood* 2009, **113**:4063-4073.

487. Takahashi S: **Downstream molecular pathways of FLT3 in the pathogenesis of acute myeloid leukemia: biology and therapeutic implications**. *J Hematol Oncol* 2011, **4**:13.

488. Estey E, Levine RL, Lowenberg B: **Current challenges in clinical development of "targeted therapies": the case of acute myeloid leukemia**. *Blood* 2015, **125**:2461-2466.

489. Grunwald MR, Levis MJ: **FLT3 inhibitors for acute myeloid leukemia: a review of their efficacy and mechanisms of resistance**. *Int J Hematol* 2013, **97**:683-694.

490. Weisberg E, Sattler M, Ray A, Griffin JD: **Drug resistance in mutant FLT3-positive AML**. *Oncogene* 2010, **29**:5120-5134.

491. Ayala F, Dewar R, Kieran M, Kalluri R: **Contribution of bone microenvironment to leukemogenesis and leukemia progression**. *Leukemia* 2009, **23**:2233-2241.

492. Meads MB, Hazlehurst LA, Dalton WS: **The bone marrow microenvironment as a tumor sanctuary and contributor to drug resistance**. *Clin Cancer Res* 2008, **14**:2519-2526.

493. Parmar A, Marz S, Rushton S, Holzwarth C, Lind K, Kayser S, Dohner K, Peschel C, Oostendorp RA, Gotze KS: **Stromal niche cells protect early leukemic FLT3-ITD+ progenitor cells against first-generation FLT3 tyrosine kinase inhibitors**. *Cancer Res* 2011, **71**:4696-4706.

494. Mohammad RM, Muqbil I, Lowe L, Yedjou C, Hsu HY, Lin LT, Siegelin MD, Fimognari C, Kumar NB, Dou QP, et al.: **Broad targeting of resistance to apoptosis in cancer**. *Semin Cancer Biol* 2015, **35 Suppl**:S78-S103.

495. Crawford LJ, Irvine AE: **Targeting the ubiquitin proteasome system in haematological malignancies**. *Blood Rev* 2013, **27**:297-304.

496. Ma W, Kantarjian H, Zhang X, Wang X, Estrov Z, O'Brien S, Albitar M: **Ubiquitin-proteasome system profiling in acute leukemias and its clinical relevance**. *Leuk Res* 2011, **35**:526-533.

497. Petroski MD, Deshaies RJ: **Function and regulation of cullin-RING ubiquitin ligases**. *Nat Rev Mol Cell Biol* 2005, **6**:9-20.

498. Bligh EG, Dyer WJ: **A rapid method of total lipid extraction and purification**. *Can J Biochem Physiol* 1959, **37**:911-917.

499. Goh LK, Sorkin A: **Endocytosis of receptor tyrosine kinases**. *Cold Spring Harb Perspect Biol* 2013, **5**:a017459.

500. Critchley WR, Pellet-Many C, Ringham-Terry B, Harrison MA, Zachary IC, Ponnambalam S: **Receptor Tyrosine Kinase Ubiquitination and De-Ubiquitination in Signal Transduction and Receptor Trafficking**. *Cells* 2018, **7**.

501. Robinson MD, McCarthy DJ, Smyth GK: **edgeR: a Bioconductor package for differential expression analysis of digital gene expression data**. *Bioinformatics* 2010, **26**:139-140.

502. Chen YC, Shen SC, Tsai SH: **Prostaglandin D(2) and J(2) induce apoptosis in human leukemia cells via activation of the caspase 3 cascade and production of reactive oxygen species**. *Biochim Biophys Acta* 2005, **1743**:291-304.

503. Kim DH, Song NY, Kim EH, Na HK, Joe Y, Chung HT, Surh YJ: **15-deoxy-Delta12,14-prostaglandin J(2) induces p53 expression through Nrf2-mediated upregulation of heme oxygenase-1 in human breast cancer cells**. *Free Radic Res* 2014, **48**:1018-1027.

504. Zeng Z, Shi YX, Tsao T, Qiu Y, Kornblau SM, Baggerly KA, Liu W, Jessen K, Liu Y, Kantarjian H, et al.: **Targeting of mTORC1/2 by the mTOR kinase inhibitor PP242 induces apoptosis in AML cells under conditions mimicking the bone marrow microenvironment**. *Blood* 2012, **120**:2679-2689.

505. Sison EA, Brown P: **The bone marrow microenvironment and leukemia: biology and therapeutic targeting**. *Expert Rev Hematol* 2011, **4**:271-283.

506. Manabe A, Murti KG, Coustan-Smith E, Kumagai M, Behm FG, Raimondi SC, Campana D: **Adhesion-dependent survival of normal and leukemic human B lymphoblasts on bone marrow stromal cells**. *Blood* 1994, **83**:758-766.

507. Weisberg E, Wright RD, McMillin DW, Mitsiades C, Ray A, Barrett R, Adamia S, Stone R, Galinsky I, Kung AL, et al.: **Stromal-mediated protection of tyrosine kinase inhibitor-treated BCR-ABL-expressing leukemia cells**. *Mol Cancer Ther* 2008, **7**:1121-1129.

508. Edwards DKt, Watanabe-Smith K, Rofelty A, Damnernsawad A, Laderas T, Lamble A, Lind EF, Kaempf A, Mori M, Rosenberg M, et al.: **CSF1R inhibitors exhibit antitumor activity in acute myeloid leukemia by blocking paracrine signals from support cells**. *Blood* 2019, **133**:588-599.

509. Traer E, Martinez J, Javidi-Sharifi N, Agarwal A, Dunlap J, English I, Kovacsovics T, Tyner JW, Wong M, Druker BJ: **FGF2 from Marrow Microenvironment Promotes Resistance to FLT3 Inhibitors in Acute Myeloid Leukemia**. *Cancer Res* 2016, **76**:6471-6482.

510. Spiekermann K, Bagrintseva K, Schwab R, Schmieja K, Hiddemann W: **Overexpression and constitutive activation of FLT3 induces STAT5 activation in primary acute myeloid leukemia blast cells**. *Clin Cancer Res* 2003, **9**:2140-2150.

511. Patel A, Pomicter AD, Eiring AM, Hein T, Heaton WL, O'Hare T, Deininger MW: **Stroma-Based Activation of pSTAT3^{Y705} Confers Resistance to FLT3 Inhibitors in FLT3 ITD-Positive AML**. *Blood* 2016, **128**:34-34.

512. Godbersen JC, Humphries LA, Danilova OV, Kebbekus PE, Brown JR, Eastman A, Danilov AV: **The Nedd8-activating enzyme inhibitor MLN4924 thwarts microenvironment-driven NF-kappaB activation and induces apoptosis in chronic lymphocytic leukemia B cells**. *Clin Cancer Res* 2014, **20**:1576-1589.

513. Kojima K, McQueen T, Chen Y, Jacamo R, Konopleva M, Shinojima N, Shpall E, Huang X, Andreeff M: **p53 activation of mesenchymal stromal cells partially abrogates microenvironment-mediated resistance to FLT3 inhibition in AML through HIF-1alpha-mediated down-regulation of CXCL12**. *Blood* 2011, **118**:4431-4439.

514. Khanim F, Davies N, Velica P, Hayden R, Ride J, Pararasa C, Chong MG, Gunther U, Veerapen N, Winn P, et al.: **Selective AKR1C3 inhibitors do not recapitulate the anti-leukaemic activities of the pan-AKR1C inhibitor medroxyprogesterone acetate**. *Br J Cancer* 2014, **110**:1506-1516.

515. Desmond JC, Mountford JC, Drayson MT, Walker EA, Hewison M, Ride JP, Luong QT, Hayden RE, Vanin EF, Bunce CM: **The aldo-keto reductase AKR1C3 is a novel suppressor of cell differentiation that provides a plausible target for the non-cyclooxygenase-dependent antineoplastic actions of nonsteroidal anti-inflammatory drugs**. *Cancer Res* 2003, **63**:505-512.

516. Verma K, Zang T, Gupta N, Penning TM, Trippier PC: **Selective AKR1C3 Inhibitors Potentiate Chemotherapeutic Activity in Multiple Acute Myeloid Leukemia (AML) Cell Lines**. *ACS Med Chem Lett* 2016, **7**:774-779.

517. Trippier PC: **Small molecule inhibitors for acute myeloid leukemia: where is the field heading?** *Future Med Chem* 2017, **9**:1453-1456.

518. Rizner TL, Penning TM: **Role of aldo-keto reductase family 1 (AKR1) enzymes in human steroid metabolism**. *Steroids* 2014, **79**:49-63.

519. Straus DS, Glass CK: **Cyclopentenone prostaglandins: new insights on biological activities and cellular targets**. *Med Res Rev* 2001, **21**:185-210.

520. Wu JS, Tsai HD, Huang CY, Chen JJ, Lin TN: **15-Deoxy-12,14-PGJ 2, by activating peroxisome proliferator-activated receptor-gamma, suppresses p22phox**

transcription to protect brain endothelial cells against hypoxia-induced apoptosis. *Mol Neurobiol* 2014, **50**:221-238.

521. Shin SW, Seo CY, Han H, Han JY, Jeong JS, Kwak JY, Park JI: **15d-PGJ2 induces apoptosis by reactive oxygen species-mediated inactivation of Akt in leukemia and colorectal cancer cells and shows in vivo antitumor activity**. *Clin Cancer Res* 2009, **15**:5414-5425.

522. Kim HJ, Rho YH, Choi SJ, Lee YH, Cheon H, Um JW, Sohn J, Song GG, Ji JD: **15-Deoxy-delta12,14-PGJ2 inhibits IL-6-induced Stat3 phosphorylation in lymphocytes**. *Exp Mol Med* 2005, **37**:179-185.

523. Gaschler MM, Stockwell BR: **Lipid peroxidation in cell death**. *Biochem Biophys Res Commun* 2017, **482**:419-425.

524. Barrera G: **Oxidative stress and lipid peroxidation products in cancer progression and therapy**. *ISRN Oncol* 2012, **2012**:137289.

525. Zhang J, Lei W, Chen X, Wang S, Qian W: **Oxidative stress response induced by chemotherapy in leukemia treatment**. *Mol Clin Oncol* 2018, **8**:391-399.

526. Fazio VM, Barrera G, Martinotti S, Farace MG, Giglioni B, Frati L, Manzari V, Dianzani MU: **4-Hydroxynonenal, a product of cellular lipid peroxidation, which modulates c-myc and globin gene expression in K562 erythroleukemic cells**. *Cancer Res* 1992, **52**:4866-4871.

527. Khanim FL, Hayden RE, Birtwistle J, Lodi A, Tiziani S, Davies NJ, Ride JP, Viant MR, Gunther UL, Mountford JC, et al.: **Combined bezafibrate and medroxyprogesterone acetate: potential novel therapy for acute myeloid leukaemia**. *PLoS One* 2009, **4**:e8147.

528. Hassane DC, Guzman ML, Corbett C, Li X, Abboud R, Young F, Liesveld JL, Carroll M, Jordan CT: **Discovery of agents that eradicate leukemia stem cells using an in silico screen of public gene expression data**. *Blood* 2008, **111**:5654-5662.

529. Swords RT, Erba HP, DeAngelo DJ, Bixby DL, Altman JK, Maris M, Hua Z, Blakemore SJ, Faessel H, Sedarati F, et al.: **Pevonedistat (MLN4924), a First-in-Class NEDD8-activating enzyme inhibitor, in patients with acute myeloid leukaemia and myelodysplastic syndromes: a phase 1 study**. *Br J Haematol* 2015, **169**:534-543.

530. Swords RT, Coutre S, Maris MB, Zeidner JF, Foran JM, Cruz J, Erba HP, Berdeja JG, Tam W, Vardhanabhuti S, et al.: **Pevonedistat, a first-in-class NEDD8-activating enzyme inhibitor, combined with azacitidine in patients with AML**. *Blood* 2018, **131**:1415-1424.

531. Guerra VA, DiNardo C, Konopleva M: **Venetoclax-based therapies for acute myeloid leukemia**. *Best Pract Res Clin Haematol* 2019, **32**:145-153.

532. Akgul C: **Mcl-1 is a potential therapeutic target in multiple types of cancer**. *Cell Mol Life Sci* 2009, **66**:1326-1336.

533. Luedtke DA, Niu X, Pan Y, Zhao J, Liu S, Edwards H, Chen K, Lin H, Taub JW, Ge Y: **Inhibition of Mcl-1 enhances cell death induced by the Bcl-2-selective inhibitor ABT-199 in acute myeloid leukemia cells**. *Signal Transduct Target Ther* 2017, **2**:17012.

534. Song T, Chai G, Liu Y, Yu X, Wang Z, Zhang Z: **Bcl-2 phosphorylation confers resistance on chronic lymphocytic leukaemia cells to the BH3 mimetics ABT-737, ABT-263 and ABT-199 by impeding direct binding**. *Br J Pharmacol* 2016, **173**:471-483.

535. Fresquet V, Rieger M, Carolis C, Garcia-Barchino MJ, Martinez-Climent JA: **Acquired mutations in BCL2 family proteins conferring resistance to the BH3 mimetic ABT-199 in lymphoma**. *Blood* 2014, **123**:4111-4119.

536. Tahir SK, Smith ML, Hessler P, Rapp LR, Idler KB, Park CH, Leverson JD, Lam LT: **Potential mechanisms of resistance to venetoclax and strategies to circumvent it**. *BMC Cancer* 2017, **17**:399.

537. Mali R, Lasater EA, Doyle K, Malla R, Boghaert E, Souers A, Leverson J, Sampath D: **Abstract B052: FLT3-ITD activation mediates resistance to the BCL-2 selective antagonist, venetoclax, in FLT3-ITD mutant AML models**. *Molecular Cancer Therapeutics* 2018, **17**:B052-B052.

538. Aldoss I, Yang D, Pillai R, Sanchez JF, Mei M, Aribi A, Ali H, Sandhu K, Al Malki MM, Salhotra A, et al.: **Association of leukemia genetics with response to venetoclax and hypomethylating agents in relapsed/refractory acute myeloid leukemia**. *Am J Hematol* 2019, **94**:E253-E255.

539. Mei M, Aldoss I, Marcucci G, Pullarkat V: **Hypomethylating agents in combination with venetoclax for acute myeloid leukemia: Update on clinical trial data and practical considerations for use**. *Am J Hematol* 2019, **94**:358-362.

540. Burnett AK, Bowen D, Russell N, Knapper S, Milligan D, Hunter AE, Khwaja A, Clark RE, Culligan D, Clark H, et al.: **AC220 (Quizartinib) Can Be Safely Combined With Conventional Chemotherapy In Older Patients With Newly Diagnosed Acute Myeloid Leukaemia: Experience From The AML18 Pilot Trial**. *Blood* 2013, **122**:622-622.

541. Daver NG, Zhang W, Graydon R, Dawra V, Xie J, Kumar P, Andreeff M: **A phase I study of milademetan in combination with quizartinib in patients (pts) with newly diagnosed (ND) or relapsed/refractory (R/R) FLT3-ITD acute myeloid leukemia (AML)**. *Journal of Clinical Oncology* 2019, **37**:TPS7067-TPS7067.

Appendices

Appendix A: Publications arising from this thesis

1. **Dhami SPS**, Tirincsi A, Baev DV, Krawczyk J,Quinn J, Szegezdi E. (2018). Ex Vivo Co-Culture of AML Blasts and Bone Marrow Mesenchymal Stromal Cells to Accurately Predict the Clinical Efficacy of Cytarabine-Daunorubicin Treatment. Blood. 132 (suppl. 1): 2636. **(American Society of Hematology [ASH] conference abstract)**
2. O' Reilly E*, **Dhami SPS***, Baev DV, Ortutay C, Halpin-McCormick A, Morrell R, Santocanale C, Samali A, Quinn J, O'Dwyer ME, Szegezdi E. (2018). Repression of Mcl-1 expression by the CDC7/CDK9 inhibitor PHA-767491 overcomes bone marrow stroma-mediated drug resistance in AML. **Scientific Reports. 8(1): 15752.** (* equal contribution)
3. **Dhami SPS**, Kappala SS, Thompson A, Szegezdi E. (2016). Three-dimensional *ex vivo* co-culture models of the leukaemic bone marrow niche for functional drug testing. **Drug Discovery Today. 21(9): 1464-1471.**
5. **Dhami SPS**, Tirincsi A, Baev DV, Krawczyk J, Quinn J, Szegezdi E. (2019). *Ex vivo* culture modeling the bone marrow microenvironment can accurately predict the clinical efficacy of chemotherapy **(under review).**
6. **Dhami SPS**, Reidy M, Krawczyk J, Quinn J, Benes V, Szegezdi E. (2019). Induction of Proteostatic stress abrogates the bone marrow microenvironment-leukaemia communication and increases drug sensitivity to FLT3-ITD cells **(under preparation).**

Appendix B: List of Presentations and Awards

Oral Presentations

- **Irish Association for Cancer Research (IACR) conference** at Dublin, Ireland on 22nd February 2018. "Proteostatic stress reverts the leukemia-supporting bone marrow microenvironment to a leukemia rejecting microenvironment." **Dhami SPS**., Reidy M., O'Dwyer M., Szegezdi E. (2018)
- **Haematology Association of Ireland conference** at Galway, Ireland on 15th October 2015. "Inhibition of cullin-ring ligases abrogates the leukemia supporting function of the bone marrow microenvironment." **Dhami SPS**., Szegezdi E. (2015)

Poster Presentations

1. **European School of Haematology (ESH) 3rd scientific workshop,** Francis Crick Institute, London, UK, February 2019.

   A) *"Ex vivo* co-culture of AML blasts and bone marrow mesenchymal stromal cells to accurately predict the clinical efficacy of cytarabine-daunorubicin treatment." **Dhami SPS**., Tirincsi A., Baev DV., Krawcyzk J., Quinn J., Szegezdi E. (2019)

   B) "Repression of Mcl-1 expression by CDC7/CDK9 inhibitor PHA-767491 overcomes bone marrow stroma mediated drug resistance in AML." O'Reilly E*., **Dhami SPS***., Baev DV., Ortutay C., Halpin A., Morrell R., Santocanale C., Samali A., Quinn J., O'Dwyer M., Szegezdi E. (2019)

2. **American Society of Hematology (ASH) 60th Annual meeting and conference**, San Diego, CA, USA, December 2018. "*Ex vivo* co-culture of AML-bone marrow mesenchymal stromal cells to accurately predict the clinical efficacy of cytarabine-daunorubicin treatment." **Dhami SPS**., Tirincsi A., Baev DV., Krawcyzk J., Quinn J., Szegezdi E. (2018)
3. **Irish Association for Cancer Research (IACR) Conference**, Dublin, Ireland, February 2018. "Proteostatic stress reverts the leukemia-supporting bone marrow microenvironment to a leukemia rejecting microenvironment." **Dhami SPS**., Reidy M., O'Dwyer M., Szegezdi E. (2018)
4. **Science Foundation of Ireland annual review meeting**, October 2018. "Targeting the leukemia-bone marrow interaction to enhance the AML drug sensitivity." **Dhami SPS**, Reidy M, Szegezdi E. (2018).

5. **Blood Cancer Network of Ireland Annual meeting and Conference**, June 2018. “Effect of CDK7 inhibition and BH3- mimetics as therapeutic agents against acute myeloid leukemia.” Phillips W, **Dhami SPS**, Alizadeh H, Cichocka T, Szegezdi E. (2018).
6. **European School of Haematology conference**, Berlin, Germany on 8th April 2017. “Systems biology approach to decipher the bone marrow microenvironment mediated resistance to FLT3-ITD AML cells.” **Dhami SPS**., Szegezdi E. (2017)
7. **European School of Hematology (ESH) Conference** in Budapest, Hungary, October 2015. “The NEDD8 activating enzyme inhibitor MLN4924 diminishes the paracrine bone marrow stroma-leukemia communication and increases leukaemia drug sensitivity.” **Dhami SPS.**, Reidy M., O’Dwyer M., Szegezdi E. (2015)
8. **Irish Area Section of Biochemical Society (IASBS) conference**, Galway, Ireland, June 2015. “Proteostatic stress blocks the bone marrow microenvironment mediated resistance to FLT3-ITD AML cells.” **Dhami SPS**, Reidy M, O’Dwyer M, Krawczyk J and Szegezdi E. (2015).

Awards

1. **Discover RISE-Marie Sklodowska-Curie and EU Horizon 2020 fellowship**, PhD Student exchange program placed in Institute of Pathology, Murtenstrasse 31, Universitat Bern, Bern, Switzerland from April 2019 to September 2019.
2. **General Travel Grant** (£450) awarded by Biochemical Society, UK to attend the American Society of Hematology (ASH) 60th Annual meeting and conference in San Diego, CA, USA in December 2018.
3. **Thomas Crawford Hayes research award** of €5000 by National University of Ireland, Galway, Ireland in 2017.
4. **Thomas Crawford Hayes research award** of €4000 by National University of Ireland, Galway, Ireland in 2015.

Appendix C: Study Funding and Acknowledgements

- The work presented in this thesis is primarily funded by College of Science Scholarship for PhD from National University of Ireland, Galway.
- Chapter 2 study was partly funded by Thomas Crawford Hayes research award from National University of Ireland, Galway and Science Foundation Ireland (SFI) and the Irish Cancer Society (BCNI,14/ICS/B3042), SFI (12/TIDA/B2388).
- Chapter 3 study was partly funded by Thomas Crawford Hayes research award from National University of Ireland, Galway and Science Foundation Ireland (SFI) and the Irish Cancer Society (BCNI,14/ICS/B3042), SFI (12/TIDA/B2388).
- Chapter 4 study was partly funded by Thomas Crawford Hayes research award from National University of Ireland, Galway, Millenium Takeda research grant and Science Foundation Ireland (SFI) and the Irish Cancer Society (BCNI,14/ICS/B3042), SFI (12/TIDA/B2388).

Thanks to all the patients and healthy volunteers for providing the blood samples and BCBI staff of University Hospital Galway, Galway and Beaumont Hospital, Dublin, Ireland for contributing towards patient sample collection, handling and biobanking activities.

Appendix D: Additional Article (not included in thesis)

Oncogene (2016) **35,** 1261–1270

www.nature.com/onc

ORIGINAL ARTICLE

Decoy receptors block TRAIL sensitivity at a supracellular level: the role of stromal cells in controlling tumour TRAIL sensitivity

L O'Leary[1,9], AM van der Sloot[2,3], CR Reis[4,10], S Deegan[1], AE Ryan[5], SPS Dhami[1], LS Murillo[6], RH Cool[4], P Correa de Sampaio[7,11], K Thompson[8], G Murphy[7], WJ Quax[4], L Serrano[2], A Samali[1] and E Szegezdi[1]

Tumour necrosis factor-related apoptosis-inducing ligand (TRAIL) is a death ligand cytokine known for its cytotoxic activity against malignantly transformed cells. TRAIL induces cell death through binding to death receptors DR4 and DR5. The inhibitory decoy receptors (DcR1 and DcR2) co-expressed with death receptor 4 (DR4)/DR5 on the same cell can block the transmission of the apoptotic signal. Here, we show that DcRs also regulate TRAIL sensitivity at a supracellular level and thus represent a mechanism by which the microenvironment can diminish tumour TRAIL sensitivity. Mathematical modelling and layered or spheroid stroma–extracellular matrix–tumour cultures were used to model the tumour microenvironment. By engineering TRAIL to escape binding by DcRs, we found that DcRs do not only act in a cell-autonomous or cis-regulatory manner, but also exert trans-cellular regulation originating from stromal cells and affect tumour cells, highlighting the potent inhibitory effect of DcRs in the tumour tissue and the necessity of selective targeting of the two death-inducing TRAIL receptors to maximise efficacy.

Oncogene (2016) **35,** 1261–1270; doi:10.1038/onc.2015.180; published online 8 June 2015

INTRODUCTION

Tumour necrosis factor (TNF)-related apoptosis-inducing ligand (TRAIL) is a key effector molecule in tumour immune surveillance. It is expressed by natural killer cells and natural killer-T cells when they encounter malignantly transformed cells. TRAIL kills target cells by binding to death receptor 4 (DR4) or DR5 on their surface.[1,2] Activation of DR4 and/or DR5 by TRAIL is controlled by two other membrane-bound TRAIL receptors, decoy receptor 1 (DcR1) and DcR2[3] and a soluble receptor, osteoprotegerin.[4] These receptors lack a functional death domain, thus cannot trigger apoptosis.[3,4]

Recombinant soluble human TRAIL (rhTRAIL, Dulanermin) showed very high potency against a broad range of tumours *in vitro* and in pre-clinical studies. However, despite being well tolerated, clinical trials testing rhTRAIL both as a monotherapy or in combination with other chemotherapeutics have failed to exhibit the same potency.[5] One major shortcoming of the pre-clinical models was the lack of assessment of the contribution of the tumour microenvironment (TME). The TME consists of various cell types, soluble factors and signals from the extracellular matrix, which is in a reciprocal interaction with the tumour cells. To date, only one study indicated that the efficacy of TRAIL could be influenced by the TME where the sensitivity of patient mesothelioma fragments grown *ex vivo* as spheroids to TRAIL-induced apoptosis was tested.[6]

Interestingly, high level of TRAIL expression in the tumour stroma (but not in tumour cells) was found to strongly correlate with longer overall survival and relapse-free survival of prostate cancer patients.[7] TRAIL has been found to be secreted by irradiated tumour cells to mediate the bystander effect that propagates post-irradiation cell death throughout the treated tissue.[8,9] In addition, Ashkenazi and co-workers have recently shown that the endothelial cells in the tumour vasculature express DR5, the targeting of which destructs tumour vasculature and reduces tumour growth[10] indicating that the tumour stroma may have a role in controlling TRAIL response, although currently it is very poorly understood.

The first line of regulation of TRAIL-induced apoptosis is provided by the TRAIL DcRs[11] by either sequestering TRAIL from the death receptors or by forming inactive, heteromeric DcR1/2–DR4/5 complexes.[12,13] TRAIL has the highest receptor promiscuity within the TNF cytokine family with five receptors out of which three are regulatory (decoy) receptors, indicating that activation of DR4 and DR5 is a key regulatory point of TRAIL sensitivity. Indeed, DcRs have been shown to be highly expressed in a number of tumour tissues such as acute myeloid leukaemia, prostate cancer and breast cancer and their expression is linked with poor

[1]Apoptosis Research Centre, National University of Ireland, Galway, Ireland; [2]EMBL/CRG Systems Biology Research Unit, Centre for Genomic Regulation (CRG), Barcelona, Spain; [3]Institute for Research in Immunology and Cancer, University of Montreal, 2950, Chemin de Polytechnique Pavillon Marcelle-Coutu, Dock 20, Montréal, Québec, Canada; [4]Department of Pharmaceutical Biology, University of Groningen, Antonius Deusinglaan 1, 9713 AV, Groningen, The Netherlands; [5]Discipline of Pharmacology and Therapeutics, School of Medicine, National University of Ireland, Galway, Ireland; [6]National Centre for Biomedical Engineering Science, National University of Ireland, Galway, Ireland; [7]Department of Oncology, University of Cambridge, Cancer Research UK Cambridge Research Institute, Li Ka Shing Centre, Cambridge, UK and [8]Centre for Microscopy and Imaging, National University of Ireland, Galway, Ireland. Correspondence: A Samali or Dr E Szegezdi, Apoptosis Research Centre, Discipline Biochemistry, National University of Ireland, University Road, Galway, Ireland.
E-mail: afshin.samali@nuigalway.ie or eva.szegezdi@nuigalway.ie
[9]Present address: The Breakthrough Breast Cancer Research Centre, The Institute of Cancer Research, 237 Fulham Road, London SW3 6JB, UK.
[10]Present address: Department of Cell Biology, University of Texas Southwestern Medical Centre, Dallas, TX 75390-9039, USA.
[11]Present address: Department of Cancer Biology, Metastasis Research Centre, The University of Texas MD Anderson Cancer Center, Houston, TX 77030, USA.
Received 24 September 2014; revised 2 March 2015; accepted 27 March 2015; published online 8 June 2015

prognosis.[14–16] For example, DcR1 was found to be the strongest single predictor of overall survival in AML[17] and *in vitro* over-expression of DcRs protected tumour cells from TRAIL-induced apoptosis. On the contrary, DcR expression in the tumour does not correlate with TRAIL sensitivity[18,19] and non-transformed cells do not require DcRs to be protected from TRAIL-induced apoptosis,[20] suggesting that the *in vivo* role of the DcRs may be more complex than originally thought. In this study, we examined the hypothesis that DcRs exert a 'tissue-level control' of TRAIL sensitivity rather than simply regulating TRAIL resistance at a cell autonomous level.

We used mathematical modelling in conjunction with layered and spheroid mixed-cell type tumour plus stromal cell cultures to assess the ability of DcRs expressed in the TME to regulate TRAIL sensitivity of adjacent tumour cells. By mutating glycine at position 160 to glutamate and threonine at position 261 to leucine (G160E/T261L) in TRAIL, we generated a TRAIL mutant that does not bind to DcRs without affecting its binding toward DR4 and DR5. Using this TRAIL variant, we present evidence here that DcRs do not only act in a cell-autonomous or cis-regulatory manner (that is, acting on the same cell), but are also able to exert trans-cellular regulation by acting from stromal cells and affecting tumour cells. These results clearly illustrate the potent inhibitory effect DcRs can have *in vivo* in the tumour and its surrounding tissue and highlight the necessity of selective targeting of the two death-inducing TRAIL receptors for an efficient TRAIL-based therapy.

RESULTS

DcR1 and DcR2 are commonly expressed in tissues, whereas tissue stroma only expresses DcR1

The effect of DcR1/2 expression on TRAIL efficacy *in vivo*, such as DcR expression by normal somatic cells, is poorly explored largely due to the limited value of animal models. Rodents have one death-inducing TRAIL receptor gene, mTRAIL-R, which is homologous to human DR4/DR5[21] and two TRAIL DcRs, however, their homology to human DcR1 and DcR2 is very low and their biological function is poorly understood.[21,22]

In order to better understand the role of DcR1 and DcR2 *in vivo*, we determined their expression in tumour cells, tumour stroma and in non-malignant, tumour-adjacent tissues with immunohistochemistry in breast, prostate, liver, urinary bladder, pancreas and ovarian cancer (118 tissue cores in total, intensity scoring images at Supplementary Figure 1; Figure 1). Analysis of the tumour tissue cores showed that DcR1 and DcR2 were both expressed in all tumour types and their expression level varied on a broad scale (Figure 1 and Supplementary Figures 2 and 3). DcR1 was abundant both in the tumour cells and in the tumour stroma, whereas expression of DcR2 was restricted to the tissue cells (that is, epithelial, glandular and so on) and it showed no expression in the stroma (Figure 1). Tumour-adjacent normal tissues showed a similar expression pattern and intensity scale as the tumour tissues. We have also analysed a restricted number of normal tissues from non-cancer patients. Although we had no access to

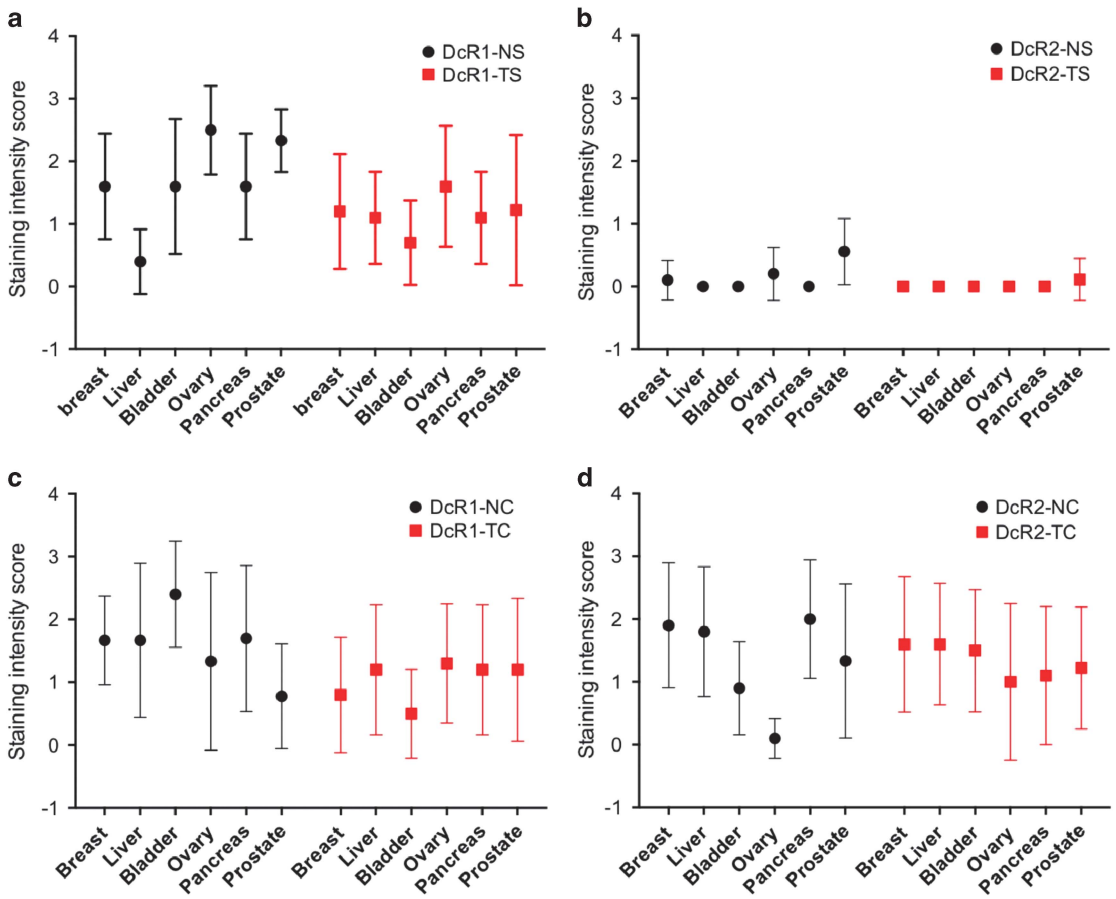

Figure 1. Expression of DcR1 and DcR2 in tumour tissues and tumour-adjacent normal tissues. Tissue cores of tumours and adjacent normal tissues on tissue microarrays (59 samples each) were immunostained for DcR1 and DcR2 expression. The expression of the DcRs was evaluated by scoring the percentage of positive cells and staining intensity within cells. The graphs show the mean expression with s.d. in the different tissue types examined for DcR1 (**a** and **c**) and DcR2 (**b** and **d**) in stromal cells in tumour-adjacent normal tissue (normal stroma (NS)) and stromal cells within the tumour tissue (tumour stroma (TS)) (**a** and **b**), as well as in non-transformed tissue cells (NC) and tumour cells (TC) (**c** and **d**).

sufficient number of tissues for statistical analysis, we confirmed that the distribution of expression of both DcRs was very similar as in the tumours (Supplementary Figure 4). Of note, DcR1 expression in the stroma was the highest in the fibro-muscular compartment, whereas it is typically low in the non-muscular fibroblasts indicating a cell type-specific regulation of expression. Significantly, DcR2 was not expressed in the stroma of any tissue except a weak expression in a restricted number of cores, regardless of disease status (malignant tissue, tumour adjacent or normal).

Design and characterisation of decoy-insensitive TRAIL mutants

In order to determine the potential of stromal-expressed DcRs to block TRAIL-induced apoptosis, we generated DcR-insensitive TRAIL mutants. Using the FoldX protein design algorithm,[23–26] amino-acid residues that form the ligand receptor-binding interface of TRAIL were mutated *in silico* to all possible natural amino-acid permutations and the change in the binding energy to all four TRAIL receptors was calculated as described previously.[24–27] Amino-acid substitutions that increased the energy of interaction between TRAIL-DcR1/DcR2 (that is, reduced binding affinity, positive $\Delta\Delta G_i$) and mutations that decreased the energy of interaction between TRAIL and DR4/DR5 have been identified (Supplementary Figure 5).

The *in silico* identified amino-acid substitutions were introduced in TRAIL by site-directed mutagenesis and the rhTRAIL mutant proteins were produced and purified.[24] DR4 and/or DR5 agonistic activity of the mutants was determined using the TRAIL-sensitive Colo205 cell line[24] by measuring the percentage of cells with exposed phosphatidylserine after 3-h treatment using Annexin V (Supplementary Figure 3) or measuring cell viability (MTT assay) after 24-h treatment from which the dose inducing 50% cell death (ED_{50}) was determined (Table 1).

Table 1. ED_{50} ratios of decoy-insensitive TRAIL single mutants to WT TRAIL ($ED50_{WT}$/ $ED50_{mutant}$)

Mutants with increased activity (ED50 ratio ⩾ 2.0)		*Mutants with unchanged activity (ED50 ratio 2.0–0.5)*		*Mutants with reduced activity (ED50 ratio ⩽ 0.5)*	
T200H	10.3	L147K	1.4	L147P	0.2
T261L	94.5	G160D	1.6	S159E	0.3
H270D	5.1	G160E	0.96	H161E	0.3
		H161F	0.8	I220M	0.4
		H161I	2.0	T261H	0.1
		H161M	1.4	D267Y	0.4
		Q193N	2.0		
		K197E	0.7		

Abbreviation: TRAIL, tumour necrosis factor-related apoptosis-inducing ligand.

Mutants T261L (threonine at position 261 replaced with leucine), T200H (threonine to histidine mutation at position 200), H270D (histidine to aspartate mutation at position 270) displayed a minimum 2-fold increased cytotoxic activity. (Table 1; Supplementary Figure 6). Although mutation of glycine at position 160 to glutamate (G160E) did not show increased cytotoxic activity, this mutant was retained for further analysis because of its robust effect on DcR-binding predicted with FoldX. Based on these mutations, combination variants containing two or more single mutations were generated to create a more potent and selective molecule (Table 2).

DR4/DR5 agonistic activity of the combination variants was tested in Colo205 cells as described for the single mutants. TRAIL45-c and TRAIL45-d showed activity similar to that of WT TRAIL, whereas TRAIL45-a and TRAIL45-b displayed an increased activity, with an $ED_{50\text{-}WT\ TRAIL}$:$ED_{50\text{-}TRAIL45}$ ratio of 5.2 and 3.9, respectively (Figure 2b). Receptor binding of the combination TRAIL variants to the four membrane-bound TRAIL receptors was assessed in real-time by surface plasmon resonance (SPR) and apparent dissociation constants (K_D) were calculated based on pre-steady-state response values (Table 2). TRAIL45-a and TRAIL45-b showed a large reduction in binding to both DcR1 and DcR2, whereas their binding to DR4 and DR5 was only slightly reduced. TRAIL45-c and TRAIL45-d showed the largest reduction in binding to DcR1 and DcR2, but this was accompanied by a significant reduction in DR4 and DR5 binding (Table 2). Enzyme-linked immunosorbent assays corroborated the SPR measurements (Supplementary Figure 7). Importantly, the binding profile confirms that the increased pro-apoptotic potential of the TRAIL45 mutants (Figure 2) is not due to an increased DR4/DR5 affinity, but to increased specificity through their diminished binding to the DcRs.

The ability of the combination mutants to activate both DR4 and DR5 was tested and confirmed in ML-1 cells (DR4-responsive cells) and Jurkat (DR5-sensitive cells[24,25]; Figures 2c and d). All mutants could induce cell death in both ML-1 and Jurkat cells with TRAIL45-a being the most potent inducer of apoptosis. Finally, the ability of the TRAIL45 mutants to avoid DcR-mediated inhibition was tested. We used Colo205 cells where we have previously shown that neutralisation of DcR1 and DcR2 enhanced WT TRAIL-induced apoptosis.[27] Colo205 cells were treated with neutralising antibodies against DcR1 and DcR2 for 1 h before treatment with TRAIL45 mutants for 3 h. The percentage of apoptotic cells was determined using Annexin V. As expected, neutralisation of DcR1 and DcR2 significantly enhanced WT TRAIL-mediated apoptosis, but it had no effect on the pro-apoptotic potency of TRAIL45-a, TRAIL45-c and TRAIL45-d confirming that these mutants have lost the ability to bind to the DcRs and thus provided us with a valuable tool to test the role of DcRs in tissue-level/trans-regulation of TRAIL sensitivity (Figure 2e).

To determine if the loss of DcR-binding enabled faster DR4/DR5 activation by TRAIL45 mutants, DR4/DR5 activation kinetics was determined as described previously.[27] Briefly, Colo205 cells were

Table 2. Relative binding affinity of TRAIL45 mutants to DR4, DR5, DcR1 and DcR2 measured by surface plasmon resonance

	K_D ratio (mutant/WT)			
	DR4-Fc	*DR5-Fc*	*DcR1-Fc*	*DcR2-Fc*
TRAIL45-a (T261L/G160E)	1.3 ± 0.2	1.4 ± 0.1	5.0 ± 1.2	10.7 ± 4.5
TRAIL45-b (T261L/H270D)	1.9 ± 0.8	1.7 ± 0.5	4.7 ± 0.3	8.5 ± 2.8
TRAIL45-c (T261L/G160E/H270D)	6.5 ± 0.3	7.4 ± 2.0	13.3 ± 4.6	35.4 ± 13.4
TRAIL45-d (T261L/G160E/H270D/T200H)	8.1 ± 2.6	12.7 ± 1.2	15.4 ± 5.2	33.5 ± 1.6

Abbreviations: DcR1, decoy receptor 1; DR4, death receptor 4; TRAIL, tumour necrosis factor-related apoptosis-inducing ligand. K_D ratios were calculated relative to WT TRAIL.

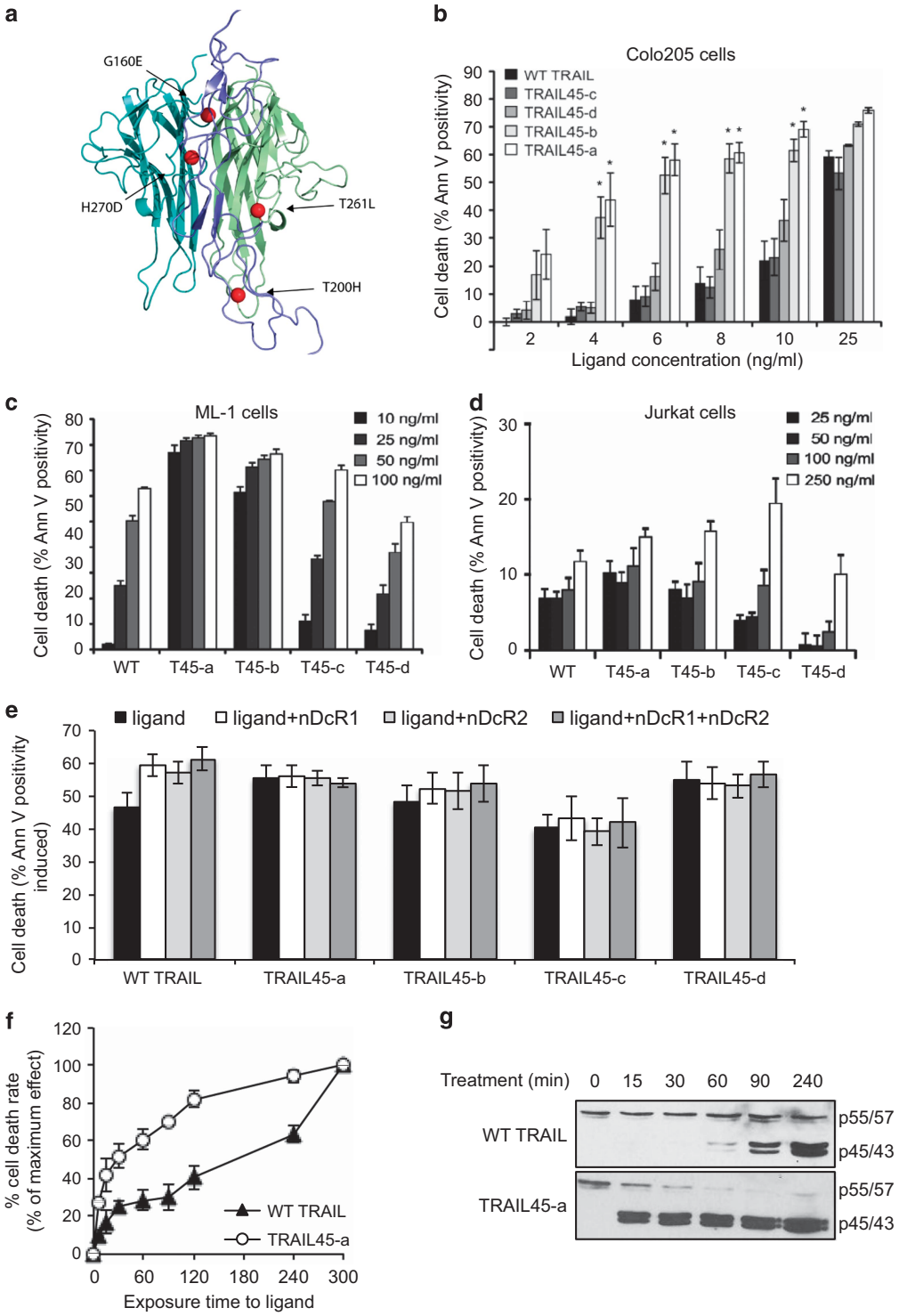

Figure 2. TRAIL45-a and TRAIL45-b do not bind to DcR1/2 and show strong cytotoxic activity. (**a**) Positions of mutations introduced in TRAIL. The image shows two TRAIL monomers (light and dark green) binding a monomer of DR5 (purple). The positions of the mutated amino-acid residues are indicated with red balls. (**b**) Biological activity of WT TRAIL and TRAIL45 mutants. Cytotoxic potency of the TRAIL45 mutants was tested in Colo205 cells. Induction of cell death was quantified by measuring percentage annexin V positivity following a 3- h incubation period. TRAIL45-a and TRAIL45-b mutants retain DR4 and DR5 agonistic activity and lost DcR1/2 binding. DR4 and DR5 agonistic activity of TRAIL45 mutants was measured in (**c**) ML-1 cells and (**d**) Jurkat cells, respectively. Cells were treated with the indicated doses of WT TRAIL or TRAIL45 mutants for 24 h and induction of cell death was determined using Annexin V staining. (**e**) Effect of DcRs neutralisation on the apoptosis-inducing activity of TRAIL45 mutants. Colo205 cells were treated with 2 μg/ml of DcR1 and/or DcR2 receptor-neutralising antibodies for 1 h before treatment with the ED50 dose of WT TRAIL or TRAIL45 mutants for 3 h after which cell death induction was quantified with annexin V. Error bars indicate s.e.m.; $*P < 0.05$ (**f** and **g**) Kinetics of DR4/DR5 activation by TRAIL45-a. Colo205 cells were treated with 100 ng/ml of WT TRAIL or TRAIL45-a for increasing times after which the ligand was washed out to terminate receptor activation. The cells were incubated for a total length of 3 h for quantification of apoptotic cells with annexin V assay (**f**) and 2 h for analysis of pro-caspase-8 processing (**g**) with western blotting as measures of DR4/DR5 activation.

treated with WT TRAIL or TRAIL45-a for increasing time (15–180 min), at the end of which the ligand was washed out and receptor activation was monitored by detecting induction of cell death and processing of pro-caspase-8. The TRAIL45-a mutant induced DR4/DR5 activation significantly faster than WT TRAIL (Figures 2f and g).

Stromal DcRs provide protection to tumour cells against TRAIL

Mathematical modelling was used to assess the potential of DcR1/2 expressed by tumour-surrounding stromal cells to protect cancer cells from TRAIL-induced apoptosis. Our previously published model that described TRAIL receptor activation on a single cell (cis-effect)[27] was adapted to include DcR-expressing stromal cells. Stromal cell-expressed DcRs were defined as additional species, which in contrast to the tumour cell-expressed DcRs, could not participate in the formation of DcR-DR heteromeric receptor complexes with TRAIL. Diffusion of TRAIL was modelled with a fast diffusion term within the bulk solution (that is, culture media; diffusion coefficient D = 60 $\mu m^2 \times s^{-1}$) and a slow diffusion term from the bulk solution to the cell surface ($D = 5\ \mu m^2 \times s^{-1}$). The receptor-binding affinities of TRAIL45-a determined by SPR were used to model the decoy-insensitive TRAIL variant (Table 2) by attributing the measured K_d values equally to the rate constants k_{on} and k_{off}. When taking the number of homotrimeric TRAIL-3DR5 or TRAIL-3DR4 complexes as a measure of their activation in the simulation model, it could be observed that as the proportion of stromal DcRs increased over tumour-DRs (plotted as stromal-DcR1+2:tumour-DR4+5 ratio), the kinetics of DR4 and DR5 activation slowed down. This suggests that kinetic regulation of TRAIL-death receptor activation exists not only at the level of individual tumour cells (cis-effect) as we have reported it previously, but also at the level of the tissue (trans-effect), which at high DcR/DR ratios completely blocks DR4/DR5 activation (Figures 3a and d).[27] The effect can be attributed to TRAIL sequestration by stromal DcRs and to mass transport limitations of TRAIL from the bulk solution to the cell surface. Of note, this model incorporated DcRs on the surface of Colo205 cells (that they normally express), however, to better assess the potential effect of stromal DcRs, DcRs were removed from the Colo205 cell surface in the simulation and a stronger effect of

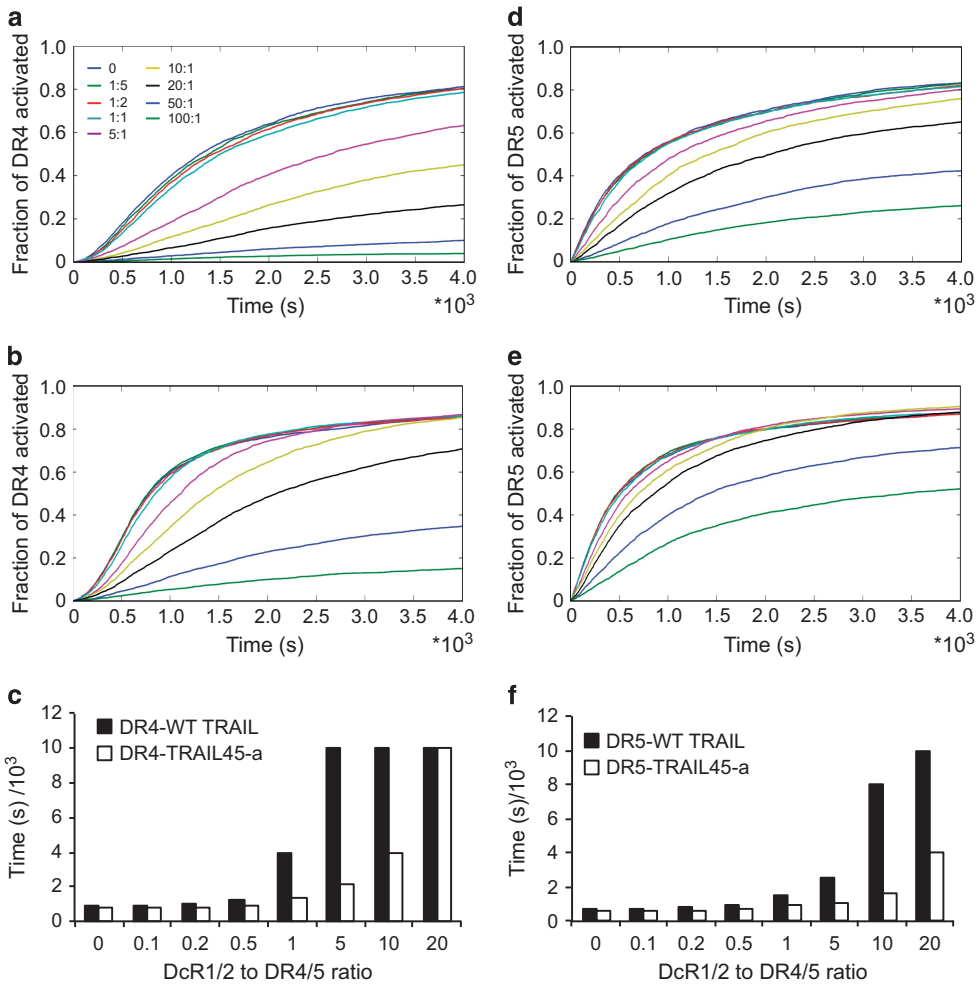

Figure 3. Stromal-expressed DcRs reduce TRAIL-induced DR4/DR5 homotrimerisation and activation in tumour cells. The effect of increasing amounts of DcRs expressed on the surface of fibroblasts surrounding Colo205 tumour cells on the kinetics of TRAIL-mediated DR4 and DR5 activation was simulated using settings described in Materials and methods section. The fraction (1 = 100% of DRs) of homotrimerised DR4 and DR5 receptors over time was used as a measure of death receptor activation. The amount of DcRs is represented as the ratio of stromal-DcR to tumour-DR in the range of DcR/DR of 0.2–100. In the absence or low DcR/DR ratio, the fraction of activated DR4 and DR5 rapidly plateaus (top blue, green, red and turquoise lines). The left and right panels show activation of DR4 (**a**, **b** and **c**) and DR5 (**d**, **e** and **f**), respectively. The top graphs (**a** and **d**) show DR-activation kinetics by WT TRAIL, the middle graphs (**b** and **e**) show the same simulation for TRAIL45-a and the bottom graphs (**c** and **f**) show the time required by WT TRAIL versus TRAIL45-a to activate 75% of DR4 (**c**) and DR5 (**f**).

stromal DcRs could be seen, highlighting the importance of DcR expression in the tumour's milieu (Supplementary Figure 8).

The DcR-insensitive TRAIL variant was able to maintain fast DR4/DR5 activation even at high DcR:DR ratio despite its lower affinity for DR4 and DR5 compared to that of WT TRAIL (Figures 3b, c, e and f). To better simulate DR4/DR5 activation in a tissue setting, a simplified three-dimensional (3D) model consisting of transport of TRAIL from bulk (via diffusion, $D = 5\,\mu m^2 \times s^{-1}$) to the cell surface of Colo205 cells through an 'interstitial' space of fibroblasts expressing DcRs has been set up. This 3D model showed an increased effect of stromal-expressed DcRs on TRAIL-induced DR4/DR5 activation, which again was caused by mass transport limitations of TRAIL from the bulk solution to the tumour interior (Supplementary Figure 9).

Reduced efficacy of TRAIL in a stromal/tumour co-culture system

To assess whether DcRs can reduce TRAIL-induced apoptosis in a trans-acting manner by being only expressed on tumour-adjacent non-transformed cells, primary human dermal fibroblasts (hFbs) were labelled with a red cell tracker (CM-DiI) and transduced with DcR1- or DcR2-expressing lentiviruses at a low MOI to achieve low, close to *in vivo*-level DcR expression (Figure 4a) and cultured together with Colo205 cells. The co-culture of cells was treated with a dosage of WT TRAIL or TRAIL45 mutant and induction of cell death in the tumour cells was determined by Annexin V (Figure 4b). Expression of DcR1 reduced the efficacy of WT TRAIL by fivefold, whereas DcR2 expression caused a twofold reduction in the efficacy of WT TRAIL (Figure 4b). On the other hand, the

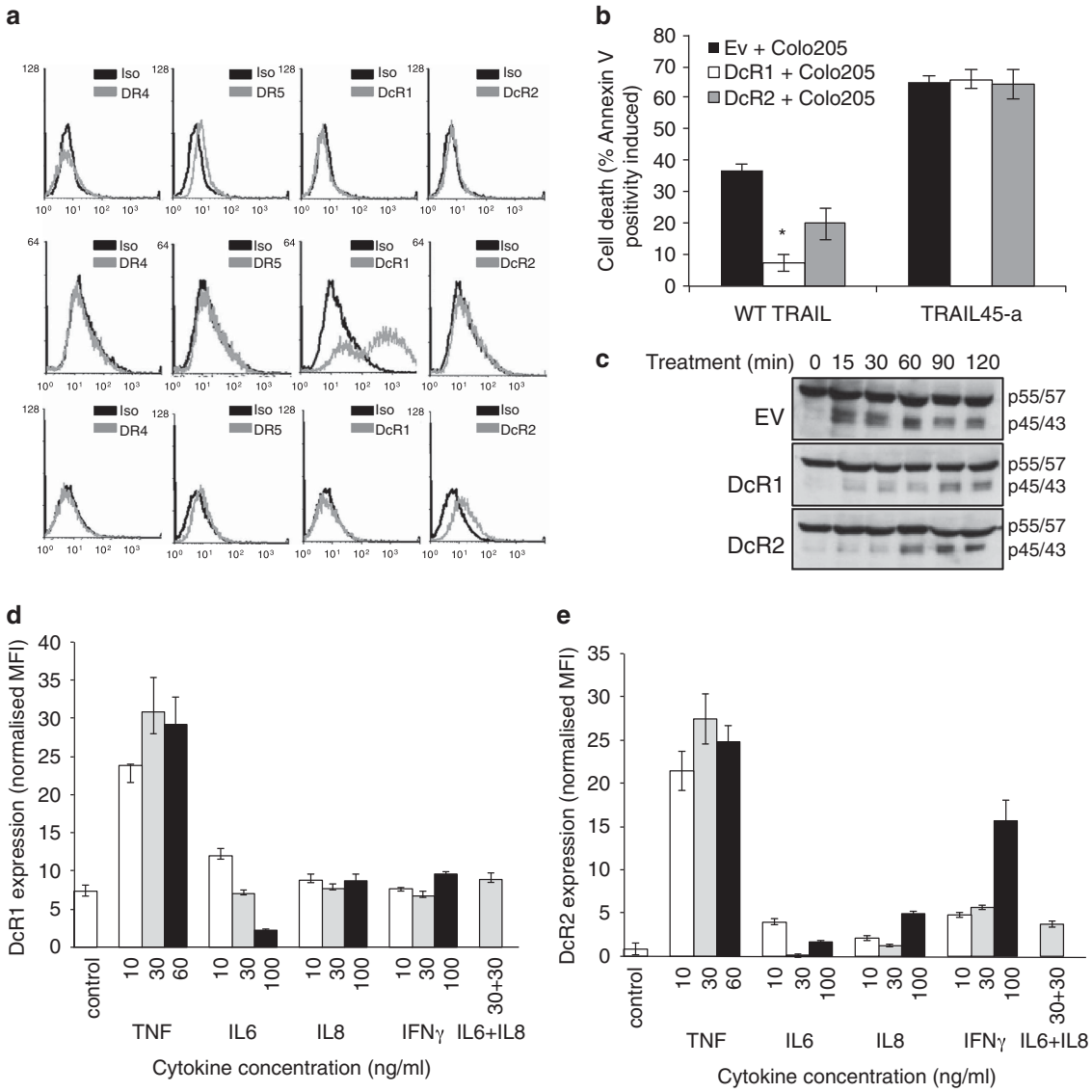

Figure 4. Expression of DcRs by neighbouring stromal cells diminishes TRAIL-mediated cytotoxicity. (**a**) TRAIL receptor expression in primary human fibroblasts overexpressing moderate levels of DcR1 or DcR2. Fibroblasts were transduced with lentiviral vectors expressing only RFP (RFP, EV), DcR1 and RFP(DcR1) or DcR2 and RFP (DcR2). Surface expression of the four membrane-bound TRAIL receptors were quantified after immunofluorescent labelling by flow cytometry. (**b**) Stromal-expressed DcRs diminish TRAIL-induced apoptosis in neighbouring tumour cells. Colo205 cells were cultured together with hFb expressing an empty vector (EV), DcR1 or DcR2. Cells were treated with WT TRAIL or TRAIL45-a at 25 ng/ml for 3 h and induction of cell death was measured in the RFP-negative Colo205 cells by Annexin V. Graph shows percentage of cell death induced ± s.e.m. $^*P < 0.05$. (**c**) Colo205 cells were cultured with hFb as for (**b**) and treated with 25 ng/ml of WT TRAIL for the indicated times after which the ligand was washed out and the level of pro-caspase-8 processing determined as a measure of DR4/DR5 activation. (**d** and **e**) Fibroblasts induce DcR1 (**c**) and DcR2 (**d**) expression in response to TNF. Fibroblasts were exposed to a dosage of inflammatory or immunoregulatory cytokines for 48 h after which cell surface expression of DcR1 and DcR2 were determined. The graphs show normalised mean fluorescence intensity (MFI; corrected with MFI of isotype control) ± s.e.m.

TRAIL45 mutant retained full efficacy, confirming that the reduced efficacy of WT TRAIL was caused by DcR expressed by tumour-neighbouring cells. In the same culture, we measured DR4/DR5 activation kinetics by treating the cells with WT TRAIL for increasing time (15–180 min) after which it was washed out and pro-caspase-8 processing determined as a measure of DR4/DR5 activation (Figure 4c). Presence of either DcR1 or DcR2 on the hFb significantly delayed TRAIL-induced pro-caspase-8 activation.

DcR expression can vary on a broad scale in the stroma. Mining of curated published data and predicted regulatory elements on the DECODE database (SABiosciences' Text Mining Application and UCSC Genome Browser; Qiagene, Sussex, UK) for DcR1 and DcR2, revealed that the promoter region of both receptors contain nuclear factor-kB-binding sites, whereas DcR1 also contains STAT3 sites indicating that inflammatory or immunoregulatory cytokines, such as interleukin-6 (IL-6) may control their expression. As these cytokines are known regulators of the TME, we treated the hFb with IL-6, IL-8, interferon gamma or TNF for 48 h and measured the expression of DcR1 and DcR2. The surface expression of both DcRs increased subtantially in response to TNF, but not with any of the other cytokines, highlighting the possibility that an inflammatory environment may induce DcR expression and tumour TRAIL resistance (Figures 4d and e).

To further demonstrate the potential of the DcRs to regulate the *in vivo* efficacy of WT TRAIL, we used a 3D mixed-cell type spheroid tumour model.[28] The spheroids comprises endothelial cells (human umbilical vein endothelial cell, labelled with CMTPX-red cell tracker), stromal cells (hFB, expressing red fluorescent protein (RFP)) and MDA-MB-231 breast cancer cells, embedded in an extracellular matrix (Figure 5a).

The spheroids were treated with either WT TRAIL or TRAIL45-a for 24 h after which the nuclei of the cells with caspase activity or all dying cells were labelled with a fluorescent caspase substrate (NucView or Sytox green, respectively) (Figure 5c, Supplementary Figure 10). The minitumours were then imaged in full depth and the percentage of cells with caspase activity was quantified (Figures 5b and c). Cell death induced by WT TRAIL was markedly reduced when hFB in the spheroid expressed either DcR1 or DcR2 (Figure 5b). On the other hand, expression of DcR1 or DcR2 did not reduce the efficacy of TRAIL45-a and efficient killing of the tumour cells could only be achieved with the DcR-insensitive TRAIL variant.

DISCUSSION

TRAIL is best known as a mediator of tumour immuno-surveillance.[29] Preclinical studies have found that TRAIL can induce apoptosis in a broad range of tumour types, and approximately 30–40% of tumour cell lines are sensitive to TRAIL-induced apoptosis.[18,30] On the other hand, healthy non-transformed cells are typically resistant to TRAIL.[20,31] In addition to being an immune effector molecule, TRAIL is also emerging as a paracrine factor controlling cell proliferation and differentiation. TRAIL is induced in intestinal cells stimulated to differentiate by inhibiting phosphatidylinositol-3 kinase. Tumour cells were also found to induce TRAIL expression and initiate an autocrine, TRAIL-mediated suicide programme when they lose Erk and Akt activity.[32,33]

The classical view of apoptotic cell death depicts this pathway as a 'quiet', cell-restricted suicide programme that selectively eliminates individual cells without influencing the surrounding cells in the tissue. This view is, however, beginning to change. Paracrine factors released by apoptotic cells can promote tissue recovery or remodelling by triggering cell proliferation or wide-spread apoptosis, respectively.[34,35] As an example, the report by Boland *et al*.[34] shows that apoptotic cells promote the survival and proliferation of neighbouring cells by releasing pro-inflammatory cytokines and thus promote tissue regeneration. Alternatively, apoptotic cells can promote widespread apoptosis in tissues as it has been detected during tissue morphogenesis.[36] In a *Drosophila* model studied by Perez-Garijo *et al*., the apoptotic cells were found to secrete Eiger, the *Drosophila* homologue of TNF. Eiger acted as a long-distance pro-apoptotic factor to propagate the apoptotic signal through the tissue.

Widespread apoptosis has also been known to occur upon viral infection,[37] or remodelling of the breast tissue during mammary gland involution after weaning.[38] These results indicate that as immune effectors, the effect of death ligands may not be targeted to individual cells but rather to control the function of whole tissues. Supporting this, a recent study by the Ashkenazi lab showed that similar to TNF, TRAIL does not only target the tumour cells, but is also able to disrupt the tumour vasculature by killing the DR5-expressing endothelial cells in the tumour tissue.[10] Similarly, irradiation of breast cancer cells induces death receptor and death ligand expression (FasL, TNF as well as TRAIL) in the cancer cells and it is responsible for the delayed cell death observed after gamma-irradiation. The bystander effect of irradiation on neural stem cells has also been found to be due to TRAIL secretion. Finally, the drastic drop in surviving bystander fibroblasts has been linked to TRAIL-mediated apoptosis due to suppression of the IGF-1R-AKT-IL-33 signalling cascade in both directly irradiated and bystander cells.[39]

Although death ligands are being assessed for cancer therapy, their effect either alone or as part of a drug combination is predominantly studied at the level of individual tumour cells and not on the tissue in all its complexity. It is also becoming evident that although induction of death of tumour cells is a key mechanism in cancer chemotherapy, in the absence of a feed-forward mechanism that could propel the initiated death signal throughout the tumour tissue, it is unlikely to eradicate the tumour entirely.

Although this phenomenon may be exploitable for the treatment of cancer, the mechanisms that limit the spread of the apoptotic signal through the tissue has to be considered. In the case of TRAIL, the DcRs may serve this purpose in tissues. TRAIL is a promiscuous cytokine with three regulatory receptors. However, despite initial indications, normal somatic cells do not rely on DcRs to maintain TRAIL resistance.[31] Instead, expression of cFLIP and Bcl-2 and/or XIAP that act in a redundant manner block propagation of the TRAIL-induced caspase cascade.[20] DcR expression in tumour cells does not correlate with TRAIL resistance either[19] (also unpublished observation from a study of 40 cell lines by ES), indicating that the cell-autonomous regulation of TRAIL sensitivity is normally achieved via intracellular regulators, such as cFLIP or XIAP expression (for review, see Mahalingam *et al*.[5]).

Here, we showed that tissues adjacent to the tumour, as well as the tumour stroma express DcRs. DcR1 and DcR2 are both abundant in tumour-adjacent normal tissues, and DcR1 is typically present within the tumour stroma. The blood vessels in the tumours are also positive for both DcR1 and DcR2. To address the potential effect of these DcRs, we have altered the receptor specificity of WT TRAIL to block its binding to the DcRs. Mutating the threonine residue at position 261 in TRAIL to leucine and the glycine at position 160 to glutamate achieved these characteristics (TRAIL45-a mutant). The mutations in TRAIL45-a did not increase, rather slightly reduced the affinity toward DR4 and DR5, highlighting that the detected increased pro-apoptotic potential was due to a reduced binding to DcR1 and DcR2. Using this TRAIL45 variant, we found that DcRs expressed by tumour-surrounding fibroblasts can reduce the efficacy of TRAIL by 80%.

Utilising death ligands, such as TRAIL for cancer therapy still holds promise, however, the signalling in the tumour has to be set to 'tissue-destruction mode' rather than 'tissue-recovery mode', for example, by utilising decoy-insensitive TRAIL mutants or agonistic antibodies and by combining the treatment with other agents, such as the TRAIL-inducing compound 10 or other phosphatidylinositol-3 kinase/Akt and/or Erk inhibitors.[32]

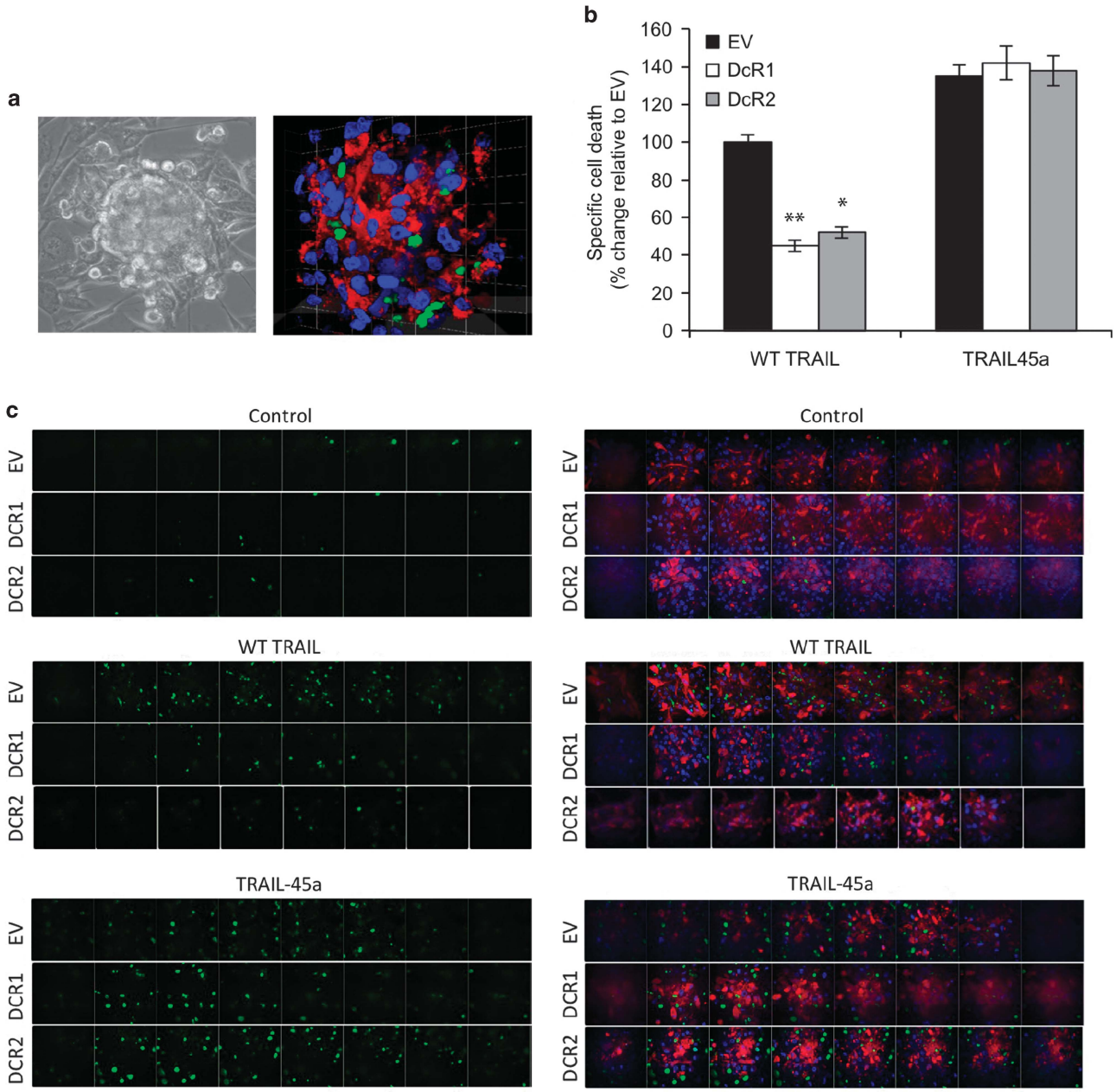

Figure 5. TRAIL45-a retains its cytotoxic efficacy in 3D spheroids expressing empty vector (EV), DcR1 and DcR2. Spheroids expressing either EV, DcR1 or DcR2 were treated with 250 ng/ml of either WT TRAIL or TRAIL45-a for 24 h, after which 1 μM of SYTOX green was added for 1 h to visualise cells with compromised plasma membranes. All cells were also stained with 1 μg/ml of Hoechst33342 (blue) and non-malignant cells (endothelial cells and fibroblasts) were labelled with a red cell tracker (CMTPX). Images are representative of four independent experiments and were generated on the Andor Revolution Spinning Disk Confocal system at x200 and x400 magnification. Z-stacks were taken to image the spheroid in its entirety, with an image captured every 2 μm. (**a**) Phase contrast image of a tumour spheroid and the 3D reconstitution of the middle 10 μm section of a spheroid treated with TRAIL45-a for 24 h. Image analysis (**b**) was carried out using ImageJ software (National Institutes of Health, Bethesda, MD, USA). All samples were normalised and all three cell populations were found to be comparable between spheroid samples. % Area occupied by a particular population was calculated, cell death was then expressed as percentage of cell death relative to WT TRAIL treated EV sample ± s.e.m. from four independent experiments. *$P < 0.05$, **$P < 0.005$. (**c**) Serial images of the tumour spheroid cross sections showing all nuclei (blue), dying cells (green), hFb and endothelial cells (red) and merged channels.

MATERIALS AND METHODS

Statistical analysis

Statistical analysis was carried out using the statistical software Minitab 15 (Coventry, UK). Significant differences between treatments were determined using a paired Student's *t*-test and $P < 0.05$ was deemed significant. All *in vitro* experiments were repeated a minimum of three times unless otherwise stated. In the case of the minitumour experiment, this was repeated independently four times and counting five minitumours per treatment group. All error bars represent s.e.m.

Reagents

All reagents were of analytical grade. All chemicals were from Sigma-Aldrich (Gillingham, UK) unless otherwise stated. All buffers used in SPR, enzyme-linked

immunosorbent assays and biological activity assays were of physiological pH and ionic strength.

Immunohistochemical staining for DcR1 and DcR2

Tissue microarrays (common cancers and matching normal adjacent tissue microarrays, Imgenex, Cambridge, UK) were deparaffinized and rehydrated. Antigen retrieval was performed at 95 °C for 20 min in 0.01 M sodium citrate (pH 6.0) and once cooled to 40 °C the slides were incubated with 3% H_2O_2 in methanol for 30 min at room temperature. Blocking was carried out for 1 h at room temperature with blocking solution from ImmPRESS HRP Universal Antibody Detection Kit (Vector Labs, Peterborough, UK). Slides were then incubated with DcR1 (1:50) or DcR2 (1:300) antibodies (Enzo Life Sciences, Exeter, UK) overnight at 4 °C, followed by incubation with ImmPRESS Universal reagent anti-mouse secondary antibody for 1 h at room temperature. Immunostaining was developed using ImmPACT DAB (Vector Labs) as per suppliers instructions and Gills Hematoxylin no.2 was used to counterstain. Analysis of the tissues were carried out by two people independently. The tissues were scored for the percentage of cells expressing DcRs (score 0 or 1 for expression in less, or $>50\%$ of cells) and for the intensity of expression (scores 0–3; Supplementary Figure 1) separately for stromal cells and tissue cells.[40]

Computational design of TRAIL variants

TRAIL receptor complexes were modelled based on the known TRAIL-DR5 crystal structure as described before.[24] A detailed description of the empirical force field FoldX and the FoldX executable (version 3.0) is available at (http://foldx.crg.es).

Cell culture

Colon carcinoma Colo205 cells, acute myeloid leukaemia cells ML-1 and acute T-cell leukaemia Jurkat cells were maintained in RPMI1640 medium, supplemented with 10% foetal bovine serum, 2 mM glutamine, 1 mM pyruvate, 50 U/ml penicillin and 50 ug/ml streptomycin. ML-1 cells were a kind gift from Dr Heinz-Peter Nasheuer (National University of Ireland, Galway, Ireland), Colo205 and Jurkat cells were obtained from ATCC (LGC Standards, Middlesex, UK). Human umbilical vein endothelial cells were procured from PromoCell (Heidelberg, Germany), and cultured in endothelial cell growth medium-2 (PromoCell). hFbs were a kind gift Dr Linda Howard (REMEDI, National University of Ireland) and cultured in low glucose Dulbecco's modified Eagle's medium, with 10% foetal bovine serum and 50 U/ml penicillin, 50 ug/ml streptomycin.

Detection of cell death with Annexin V

Cells were seeded 24 h before treatment in 24-well plates (0.5 ml per well) at 2×10^5, 3×10^5 and 5×10^5 cells/ml density for Colo205, ML-1 and Jurkat cells, respectively, and stained with Annexin V as described before.[20]

MTT cell viability assay

Cell viability was determined using MTT (3-(4,5-dimethylthiazol-2-yl)-2,5-diphenyltetrazolium bromide) viability assay as described before.[41]

TRAIL receptor immunocytochemistry

Expression level of DR4, DR5, DcR1 and DcR2 on the surface of hFB were determined using immunofluorescence coupled with flow cytometry as described before.[42]

Cloning, expression and purification of TRAIL variants and receptor-binding studies with SPR

Cloning, expression and purification of TRAIL variants, as well as the SPR measurements have been carried out as as described previously.[43]

Generation of DcR-overexpressing cell lines

Full-length complementary DNA clones for DcR1 (IRCMp5012H1033D) and DcR2 (IRAUp969C08104D; Imagene, Berlin, Germany) were cloned into the lentiviral vector pCDH-RFP (Vector map for pCDH-RFP can be found at Systems Biosciences, Cambridge, UK, cat # CD512A-1). Lentiviral particles were generated by co-transfecting the pCDH-DcR1-RFP or pCDH-DcR2-RFP lentiviral vectors with a second-generation lentivirus packaging system (Addgene, Middlesex, UK pMD2.G cat # 12259, psPAX2 cat # 12260, pRSV-Rev cat # 12253) using JET-PEI transfection reagent (Polyplus Transfection, Dublin, Ireland cat # 101-01N) into HEK293T cells. Virus supernatant was harvested at 24- and 48-h posttransfection and filtered via a 0.45 μm nalgene filter. hFb were transduced in a six-well plate at ~30% confluency. The virus was incubated with 5 μg/ml of polybrene per ml of virus at 37 °C for 5 min, added on the hFB cells then the plates were centrifuged at 1500 r.p.m. for 90 min at 37 °C. Transduction efficiency was $>90\%$, which was monitored by detecting lentivirus-expressed RFP using flow cytometry (FACS-CantoII, BD BioSciences, Dublin, Ireland).

Mathematical modelling of DR4 and DR5 activation

Mathematical modelling of Receptor binding of WT TRAIL or TRAIL45-a was performed as described before[42] using SmartCell[44,45] (http://software.crg.es/smartcell/). Receptor-binding rate constants for WT TRAIL were as described before,[42] and receptor-binding rate constants for TRAIL45-a were assigned based on the measured K_d ratios as depicted ins Table 2, by equally decreasing the k_{on} and increasing the k_{off} of WT TRAIL in accordance with the measured ratio (Supplementary Table 1). Stromal cell-derived DcRs were defined as additional DcR species that were only able to interact with themselves or with TRAIL, but not with tumour cell-expressed DR4/DR5 in the same stepwise manner as the Colo205-expressed receptors.[42] The number of stromal-derived DcRs in the calculations was expressed relative to the number of Colo205-expressed DR4 and DR5 receptors together. Diffusion reactions were used to describe diffusion of TRAIL within the bulk solution and from bulk solution to the cell surface to allow depletion and mass transport limitations to occur. Diffusion coefficients were taken from the Bionumbers database for a ~60 kDa protein in a dilute aqueous solution and in cytoplasm, respectively.[46] Dependence of the modelling calculation results on a particular value for the diffusion coefficient, TRAIL concentration and the number of DcRs (Supplementary Table 2) was estimated by scanning a range of values around the value used in the calculation.

Layered co-culture of primary hFbs with Colo205 cells

Primary hFbs containing empty vector pCDH or overexpressing DcR1 and DcR2 were trypsinised and labelled with 5 μM CellTracker red CMTPX (Molecular Probes, Paisley, UK) in serum-free medium for 45 min and then mixed with Colo205 cells in Colo205 growth medium in a 1:1 ratio ($1*10^5$ cells/ml each) and cultured in 24-well plates.

3D minitumour generation

Spheroid cultures were generated as described by Correa de Sampaio *et al*[28] with a modification for inclusion of hFb in the spheroids as described below. hFbs and human umbilical vein endothelial cells were trypsinized, counted and mixed in a 2:1 cell ratio. The cells were labelled with the red cell tracker CMTPX (Invitrogen, Dublin, Ireland) at a concentration of 5 μM for 45 min at 37 °C shaking every 5–10 min. In all, 7.5×10^4 human umbilical vein endothelial cell and $3.75\text{x}10^4$ hFb were spun down, resuspended in 12 ml of endothelial cell growth medium-2 (PromoCell) containing 7.5×10^4 MDA-MB-231, 3 ml of 1.2% methocellulose solution in endothelial cell growth medium-2 was added to the cell mixture and then divided by 150 μl into wells of a 96 U-shaped well suspension plate (Greiner BioOne, Stonehouse, UK). The plate was incubated for 24 h at 37 °C to allow for spheroid formation.

CONFLICT OF INTEREST

A Samali is a scientific founding member and Director of Aquila Ltd.

ACKNOWLEDGEMENTS

We thank Teresa McHale (University College Hospital, Galway) for scoring the tissue microarrays and Paul Lohan for immunohistochemical assistance. We acknowledge the facilities and scientific and technical assistance of the Centre for Microscopy and Imaging at National University of Ireland, Galway (NUIG), a facility that is funded by NUIG and the Irish Government's Programme for Research in Third Level Institutions, Cycles 4 and 5, National Development Plan. AMS was partially supported by a Juan de la Cierva grant of the Spanish ministry of Science and Education. Financial Support: The project was funded by Enterprise Ireland, National Development Plan of Ireland, Commercialisation Fund to AS and ES (CFTD/06/112), SFI SIRG award to ES (09/SIRG /B1575) and Millennium Grant to ES from the NUIG.

REFERENCES

1 Bodmer JL, Holler N, Reynard S, Vinciguerra P, Schneider P, Juo P *et al.* TRAIL receptor-2 signals apoptosis through FADD and caspase-8. *Nat Cell Biol* 2000; **2**: 241–243.
2 Kischkel FC, Lawrence DA, Chuntharapai A, Schow P, Kim KJ, Ashkenazi A. Apo2L/TRAIL-dependent recruitment of endogenous FADD and caspase-8 to death receptors 4 and 5. *Immunity* 2000; **12**: 611–620.
3 LeBlanc HN, Ashkenazi A. Apo2L/TRAIL and its death and decoy receptors. *Cell Death Differ* 2003; **10**: 66–75.
4 Emery JG, McDonnell P, Burke MB, Deen KC, Lyn S, Silverman C *et al.* Osteoprotegerin is a receptor for the cytotoxic ligand TRAIL. *J Biol Chem* 1998; **273**: 14363–14367.
5 Mahalingam D, Szegezdi E, Keane M, de Jong S, Samali A. TRAIL receptor signalling and modulation: are we on the right TRAIL? *Cancer Treat Rev* 2009; **35**: 280–288.
6 Kim K, Wilson SM, Abayasiriwardana KS, Collins R, Fjellbirkeland L, Xu Z *et al.* A novel *in vitro* model of human mesothelioma for studying tumor biology and apoptotic resistance. *Am J Respir Cell Mol Biol* 2005; **33**: 541–548.
7 Anees M, Horak P, El-Gazzar A, Susani M, Heinze G, Perco P *et al.* Recurrence-free survival in prostate cancer is related to increased stromal TRAIL expression. *Cancer* 2011; **117**: 1172–1182.
8 Luce A, Courtin A, Levalois C, Altmeyer-Morel S, Romeo PH, Chevillard S *et al.* Death receptor pathways mediate targeted and non-targeted effects of ionizing radiations in breast cancer cells. *Carcinogenesis* 2009; **30**: 432–439.
9 Shareef MM, Cui N, Burikhanov R, Gupta S, Satishkumar S, Shajahan S *et al.* Role of tumor necrosis factor-alpha and TRAIL in high-dose radiation-induced bystander signaling in lung adenocarcinoma. *Cancer Res* 2007; **67**: 11811–11820.
10 Wilson NS, Yang A, Yang B, Couto S, Stern H, Gogineni A *et al.* Proapoptotic activation of death receptor 5 on tumor endothelial cells disrupts the vasculature and reduces tumor growth. *Cancer Cell* 2012; **22**: 80–90.
11 Shirley S, Morizot A, Micheau O. Regulating TRAIL receptor-induced cell death at the membrane: a deadly discussion. *Recent Pat Anticancer Drug Discov* 2011; **6**: 311–323.
12 Merino D, Lalaoui N, Morizot A, Schneider P, Solary E, Micheau O. Differential inhibition of TRAIL-mediated DR5-DISC formation by decoy receptors 1 and 2. *Mol Cell Biol* 2006; **26**: 7046–7055.
13 Clancy L, Mruk K, Archer K, Woelfel M, Mongkolsapaya J, Screaton G *et al.* Preligand assembly domain-mediated ligand-independent association between TRAIL receptor 4 (TR4) and TR2 regulates TRAIL-induced apoptosis. *Proc Natl Acad Sci USA* 2005; **102**: 18099–18104.
14 Ganten TM, Sykora J, Koschny R, Batke E, Aulmann S, Mansmann U *et al.* Prognostic significance of tumour necrosis factor-related apoptosis-inducing ligand (TRAIL) receptor expression in patients with breast cancer. *J Mol Med* 2009; **87**: 995–1007.
15 Koksal IT, Sanlioglu AD, Karacay B, Griffith TS, Sanlioglu S. Tumor necrosis factor-related apoptosis inducing ligand-R4 decoy receptor expression is correlated with high Gleason scores, prostate-specific antigen recurrence, and decreased survival in patients with prostate carcinoma. *Urol Oncol* 2008; **26**: 158–165.
16 Riccioni R, Pasquini L, Mariani G, Saulle E, Rossini A, Diverio D *et al.* TRAIL decoy receptors mediate resistance of acute myeloid leukemia cells to TRAIL. *Haematologica* 2005; **90**: 612–624.
17 Chamuleau ME, Ossenkoppele GJ, van Dreunen L, Jirka SM, Zevenbergen A, Schuurhuis GJ *et al.* High TRAIL-R3 expression on leukemic blasts is associated with poor outcome and induces apoptosis-resistance which can be overcome by targeting TRAIL-R2. *Leuk Res* 2011; **35**: 741–749.
18 Dyer MJ, MacFarlane M, Cohen GM. Barriers to effective TRAIL-targeted therapy of malignancy. *J Clin Oncol* 2007; **25**: 4505–4506.
19 Zhang XD, Franco A, Myers K, Gray C, Nguyen T, Hersey P. Relation of TNF-related apoptosis-inducing ligand (TRAIL) receptor and FLICE-inhibitory protein expression to TRAIL-induced apoptosis of melanoma. *Cancer Res* 1999; **59**: 2747–2753.
20 van Dijk M, Halpin-McCormick A, Sessler T, Samali A, Szegezdi E. Resistance to TRAIL in non-transformed cells is due to multiple redundant pathways. *Cell Death Dis* 2013. 4.
21 Wu GS, Burns TF, Zhan Y, Alnemri ES, El-Deiry WS. Molecular cloning and functional analysis of the mouse homologue of the KILLER/DR5 tumor necrosis factor-related apoptosis-inducing ligand (TRAIL) death receptor. *Cancer Res* 1999; **59**: 2770–2775.
22 Schneider P, Olson D, Tardivel A, Browning B, Lugovskoy A, Gong D *et al.* Identification of a new murine tumor necrosis factor receptor locus that contains two novel murine receptors for tumor necrosis factor-related apoptosis-inducing ligand (TRAIL). *J Biol Chem* 2003; **278**: 5444–5454.
23 Tur V, van der Sloot AM, Reis CR, Szegezdi E, Cool RH, Samali A *et al.* DR4-selective tumor necrosis factor-related apoptosis-inducing ligand (TRAIL) variants obtained by structure-based design. *J Biol Chem* 2008; **283**: 20560–20568.
24 van der Sloot AM, Tur V, Szegezdi E, Mullally MM, Cool RH, Samali A *et al.* Designed tumor necrosis factor-related apoptosis-inducing ligand variants initiating apoptosis exclusively via the DR5 receptor. *Proc Natl Acad Sci USA* 2006; **103**: 8634–8639.
25 Reis CR, Van der Sloot AM, Natoni A, Szegezdi E, Setroikromo R, Meijer M *et al.* Rapid and efficient cancer cell killing mediated by high-affinity death receptor homotrimerizing TRAIL variants. *Cell Death Dis* 2010; ;**1**: e83.
26 Schymkowitz J, Borg J, Stricher F, Nys R, Rousseau F, Serrano L. The FoldX web server: an online force field. *Nucleic Acids Res* 2005; **33**: 382–388.
27 Szegezdi E, Van der Sloot AM, Mahalingam D, O' Leary L, Cool RH, Munoz IG *et al.* Kinetics in signal transduction pathways involving promiscuous oligomerizing receptors can be determined by receptor specificity: apoptosis induction by TRAIL. *Mol Cell Proteomics* 2012. 11.
28 Correa de Sampaio P, Auslaender D, Krubasik D, Failla AV, Skepper JN, Murphy G *et al.* A heterogeneous *in vitro* three dimensional model of tumour-stroma interactions regulating sprouting angiogenesis. *PLoS One* 2012; **7**: e30753.
29 Finnberg N, Klein-Szanto AJP, E-D. WS. TRAIL-R deficiency in mice promotes susceptibility to chronic inflammation and tumorigenesis. *J Clin Invest* 2008; **118**: 111–123.
30 Lemke J, von Karstedt S, Zinngrebe J, Walczak H. Getting TRAIL back on track for cancer therapy. *Cell Death Differ* 2014; **21**: 1350–1364.
31 Ashkenazi A, Pai RC, Fong S, Leung S, Lawrence DA, Marsters SA *et al.* Safety and antitumor activity of recombinant soluble Apo2 ligand. *J Clin Invest* 1999; **104**: 155–162.
32 Allen JE, Krigsfeld G, Mayes PA, Patel L, Dicker DT, Patel AS *et al.* Dual inactivation of Akt and ERK by TIC10 signals Foxo3a nuclear translocation, TRAIL gene induction, and potent antitumor effects. *Sci Transl Med* 2013; **5**: 171ra17.
33 Wang Q, Wang X, Hernandez A, Hellmich MR, Gatalica Z, Evers BM. Regulation of TRAIL expression by the phosphatidylinositol 3-kinase/Akt/GSK-3 pathway in human colon cancer cells. *J Biol Chem* 2002; **277**: 36602–36610.
34 Boland K, Flanagan L, Prehn JHM. Paracrine control of tissue regeneration and cell proliferation by caspase-3. *Cell Death Dis* 2013; **4**: e725.
35 Cullen SP, Henry CM, Kearney CJ, Logue SE, Feoktistova M, Tynan GA *et al.* Fas/CD95-induced chemokines can serve as "find-me" signals for apoptotic cells. *Mol Cell* 2013; **49**: 1034–1048.
36 Perez-Garijo A, Fuchs Y, Steller H. Apoptotic cells can induce non-autonomous apoptosis through the TNF pathway. *Elife* 2013; **2**: e01004.
37 Roulston A, Marcellus RC, Branton PE. Viruses and apoptosis. *Annu Rev Microbiol* 1999; **53**: 577–628.
38 Furth PA, Bar-Peled U, Li M. Apoptosis and mammary gland involution: reviewing the process. *Apoptosis* 1997; **2**: 19–24.
39 Ivanov VN, Hei TK. A role for TRAIL/TRAIL-R2 in radiation-induced apoptosis and radiation-induced bystander response of human neural stem cells. *Apoptosis* 2014; **19**: 399–413.
40 Sanlioglu AD, Korcum AF, Pestereli E, Erdogan G, Karaveli S, Savas B *et al.* TRAIL death receptor-4 expression positively correlates with the tumor grade in breast cancer patients with invasive ductal carcinoma. *Int J Radiat Oncol Biol Phys* 2007; **69**: 716–723.
41 Mahalingam D, Natoni A, Keane M, Samali A, Szegezdi E. Early growth response-1 is a regulator of DR5-induced apoptosis in colon cancer cells. *Br J Cancer* 2010; **102**: 754–764.
42 Szegezdi E, van der Sloot AM, Mahalingam D, O'Leary L, Cool RH, Munoz IG *et al.* Kinetics in signal transduction pathways involving promiscuous oligomerizing receptors can be determined by receptor specificity: apoptosis induction by TRAIL. *Mol Cell Proteomics* 2012; **11**: 013730.
43 Szegezdi E, Reis CR, van der Sloot AM, Natoni A, O'Reilly A, Reeve J *et al.* Targeting AML through DR4 with a novel variant of rhTRAIL. *J Cell Mol Med* 2011; **15**: 2216–2231.
44 Ander M, Beltrao P, Di Ventura B, Ferkinghoff-Borg J, Foglierini M, Kaplan A *et al.* SmartCell, a framework to simulate cellular processes that combines stochastic approximation with diffusion and localisation: analysis of simple networks. *Syst Biol (Stevenage)* 2004; **1**: 129–138.
45 Dublanche Y, Michalodimitrakis K, Kummerer N, Foglierini M, Serrano L. Noise in transcription negative feedback loops: simulation and experimental analysis. *Mol Syst Biol* 2006; **2**: 41.
46 Milo R, Jorgensen P, Moran U, Weber G, Springer M. BioNumbers--the database of key numbers in molecular and cell biology. *Nucleic Acids Res* 2010; **38**: D750–D753.

Supplementary Information accompanies this paper on the Oncogene website (http://www.nature.com/onc)